Generation of an Immunocompetent B-cell Repertoire

Het opbouwen van een immunocompetent B-cel repertoire

Generation of an Immunocompetent B-cell Repertoire

Het opbouwen van een immunocompetent B-cel repertoire

Thesis

To obtain the degree of Doctor from the Erasmus University Rotterdam
by command of the rector magnificus Prof.dr. H.G. Schmidt
and in accordance with the decision of the Doctorate Board

The public defense shall be held on
Wednesday 28 November 2012 at 13.30 hours by

Magdalena Agnieszka Berkowska
born in Jaworzno, Poland

ERASMUS UNIVERSITEIT ROTTERDAM

DOCTORAL COMMITTEE

Promoter: Prof.dr. J.J.M. van Dongen

Other members: Prof.dr. R.W. Hendriks
Prof.dr. E.R.F. Meffre
Prof.dr. T. Szczepański

Co-promoter   Dr. M.C. van Zelm

Generation of an Immunocompetent B-cell Repertoire

Het opbouwen van een immunocompetent B-cel repertoire

CONTENTS

I

General Introduction

The immune system of higher vertebrates, such as humans, has multiple lines of defense against invading microorganisms. The first line is a physical and chemical barrier formed by the skin, mucous membranes and their secretions to prevent the entrance of microorganisms into the body.[1-3] The second line consists of proteins (e.g. complement)[4] and immune cells (e.g. macrophages, granulocytes, natural killer cells) which are the components of the innate immune system.[5-6] Finally, the third line concerns the adaptive immune system with T and B lymphocytes specifically interacting with the invading pathogen. These cells do not only recognize pathogen with a specific antigen receptor, they also adapt their response during an infection to improve recognition of the pathogen and they generate long-term immunological memory.

The adaptive capabilities of T and B cells are the result of two independent stages of development. First, each lymphocyte creates a unique receptor for recognition of pathogens during precursor differentiation in bone marrow (B cells) or thymus (T cells). As a consequence, a large repertoire of antigen receptors is generated with the potential to specifically recognize many different pathogens.[7-8] Second, the lymphocytes that actually recognize antigen in peripheral lymphoid organs are selected to undergo enormous clonal proliferation of ~6 to 10 cell cycles, thereby generating a huge numbers of daughter cells with the potential to recognize the same pathogen.[9-10] This clonal expansion generates effector cells for a strong response and long term memory in the form of memory B- and T-cells and immunoglobulin (Ig)-producing plasma cells. Consequently, a renewed encounter with the same antigen results in a faster and stronger response, which can be visualized by the antigen-specific serum Ig levels (Figure 1).

The generation of an immunocompetent T and B-cell repertoire requires a tight balance between the production of a large repertoire of cells with unique receptors and a strong immune response of groups of cells with an antigen-specific and thereby a more limited (selected) repertoire. Impairment of this balance can have major implications and contributes to the development of immune disorders such as immunodeficiency, autoimmunity, allergy, leukemia and lymphoma.

This thesis is focused on understanding how a broad B-cell repertoire is created in bone marrow, and how immunological memory is generated via distinct types of antigen responses.

1. ANTIGEN INDEPENDENT B-CELL DIFFERENTIATION IN BONE MARROW

Commitment of hematopoietic progenitors to the B-cell lineage

Hematopoietic stem cells (HSC) in bone marrow are long-lived and self-renewing. They generate multilineage progenitors that are capable of developing into erythroid, myeloid and lymphoid cells, but do not self-renew (Figure 2). Thus, every single multilineage progenitor will only differentiate and commit itself to only one of the many specific blood cell types. Extensive studies in mouse models have supported our understanding of their progressive restriction in developmental potential through intermediate steps (reviewed in [11-12]). A multilineage progenitor will become restricted to either a lymphoid or myeloid cell fate depending on the levels of transcription factors PU.1 and Ikaros (Figure 2).[13-16] Myeloid
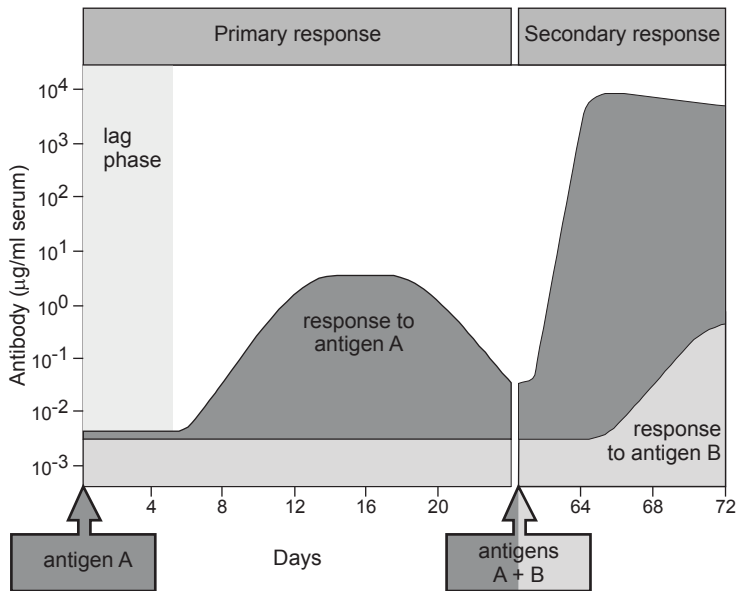
Figure 1. The course of a typical Ig response.
The first encounter with antigen A initiates a primary immune response. After a lag phase of several days the level of antigen-specific antibodies gradually increases and reaches a plateau level followed by a slow decrease. The second challenge with the same antigen results in a faster and stronger immune response, which is the hallmark of immunological memory. Still, encounter of the unrelated antigen B *de novo* induces a primary immune response. Figure adapted from Janeway *et al.* Immunobiology, 2008, Garland Science.

progenitors can develop into erythrocytes and myeloid cells, including monocytes and granulocytes. The myeloid fate is inhibited by upregulation or E2A and expression of IL7R and the resulting lymphoid progenitor can only give rise to NK cells, T cells and B cells. Upon induction of RAG1, the fate is further specified to the T- or B-cell lineage, while NK-cell potential is lost. These cells can be identified in the mouse based on Ly6D expression.[17] Subsequent expression of EBF1 specifies the B-cell fate. These pre-pro-B cells can be identified by intracellular λ5, a component of the surrogate light chain.[17] Still, these cells are not yet fully committed to the B-cell lineage and can still be directed to the T-cell lineage.[18] Only upon expression of Pax5, the cell is fully committed. This pro-B cell can be identified based on membrane CD19 expression.

Ordered Ig gene rearrangements during stepwise precursor B-cell differentiation
The primary objective of every precursor B-cell in bone marrow is to generate a unique B-cell antigen receptor (BCR). Each BCR is composed of two identical heavy chains (IgH) and light chains (Igκ or Igλ isotype). In contrast to nearly all other proteins, the constituents of Ig molecules are not encoded by germline DNA. As discovered by Susumu Tonegawa, genetic elements in Ig loci, Variable (V), Diversity (D)
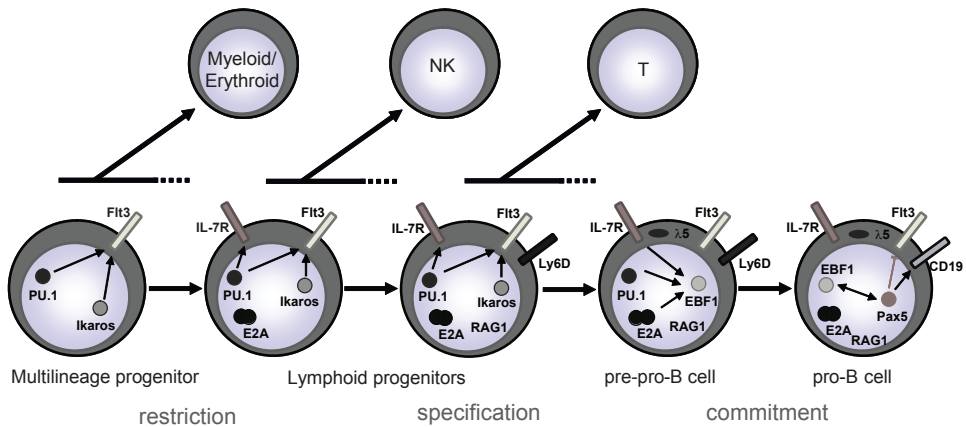
Figure 2. Stepwise control of B cell commitment from hematopoietic stem cells (HSC) in bone marrow.
HSC generate multilineage progenitors that have the potential to differentiate into all blood cell lineages. Stepwise specification and commitment processes take place as a result of tight balances between transcription factors. Ikaros and low PU.1 expression levels restrict towards a lymphoid cell fate. Subsequently, E2A and IL7R signaling specify the B cell program to which the cell becomes committed upon expression of Pax5. Figure adapted from Kee *et al*. J. Exp. Med., 1998[164] and Zandi *et al.* Immunol. Rev. 2010[12]

and Joining (J) genes, need to be rearranged to encode a functional protein through a process named V(D)J recombination.[7-8] In the *IGH* locus, one of each V, D and J genes are randomly coupled to form a functional exon (Figure 3). Similar rearrangements are initiated between one V and one J gene segment in the *IGK* and *IGL* loci.

Rearrangement between two genes depends on their spatial co-localization. Since Ig loci can span over 1Mb in size and genes poised to rearrange can be in genomically distant locations, this requires large-scale DNA contraction. Indeed, spatial co-localization of genes in the *IGH* locus in cells poised to rearrange,[19-20] and large scale compaction and looping of distant *IGH* regions [21-22] were previously demonstrated in mouse models using 3D fluorescence *in situ* hybridization techniques.

The first Ig gene rearrangements that occur during precursor B-cell differentiation are D to J rearrangements in the *IGH* locus.[23-24] These rearrangements are generally initiated on both *IGH* alleles.[25-26a] Subsequently, only one allele starts complete V to DJ rearrangements, and the second allele rearranges only when the first is not successful, e.g. if there is no functional protein. In the majority of precursor B cells, V to J gene rearrangements in the *IGK* and *IGL* loci are initiated only after a functional IgH protein is formed. Still, it has been demonstrated that both in man and mice a minor fraction of pro-B cells can rearrange IgL genes before the assembly of a productive IgH.[26b,c]

The order of Ig gene rearrangements became the basis of precursor B-cell nomenclature (Figure 4). The two most commonly used precursor B-cell nomenclature systems are by Melchers and Rolink[27] and by Osmond,[28-29] the second of which is followed in this thesis. Thus, according to this nomenclature, cells which initiate D to J rearrangements in the *IGH* are pre-pro-B cells and continue with the V to DJ rearrangement at the pro-B cell stage.

A

DNA: *IGH* locus (14q32.3)
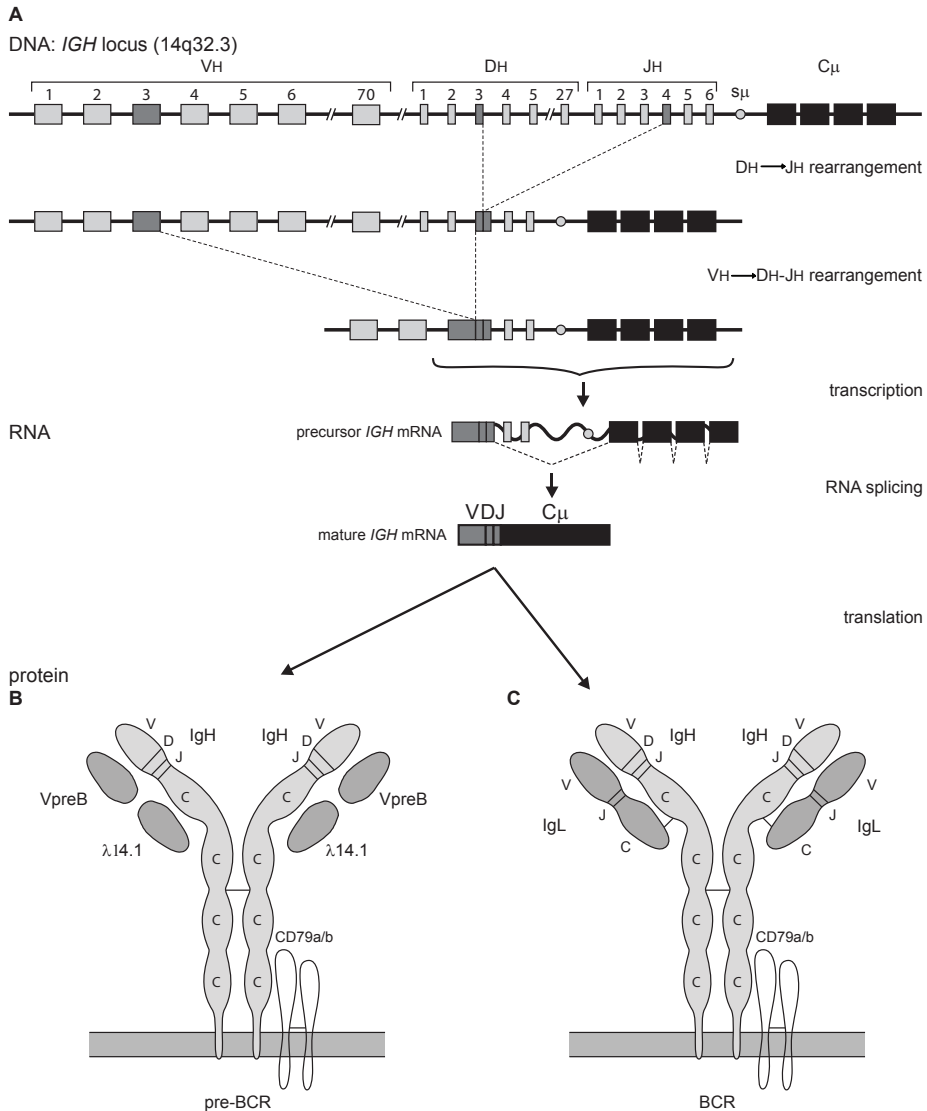
Figure 3. Schematic representation of *IGH* gene rearrangement.
(A) In the first step of V(D)J recombination in the *IGH* a D gene is coupled to a J gene. Subsequently, a V gene is coupled to the DJ joint. The VDJ exon is transcribed and spliced to the *IGHM* exons. **(B) (C)** A functional IgM protein is transported to the plasma membrane with anchoring molecules CD79a and CD79b, and surrogate light chain molecules λ14.1 and VpreB (pre-BCR) in pre-B large cells, or a functional Ig light chain protein in immature and mature B cells.

Pre-B cells have a functional IgH protein and start rearranging V-J in the *IGK* or *IGL*. Finally, immature B cells express a functional BCR.
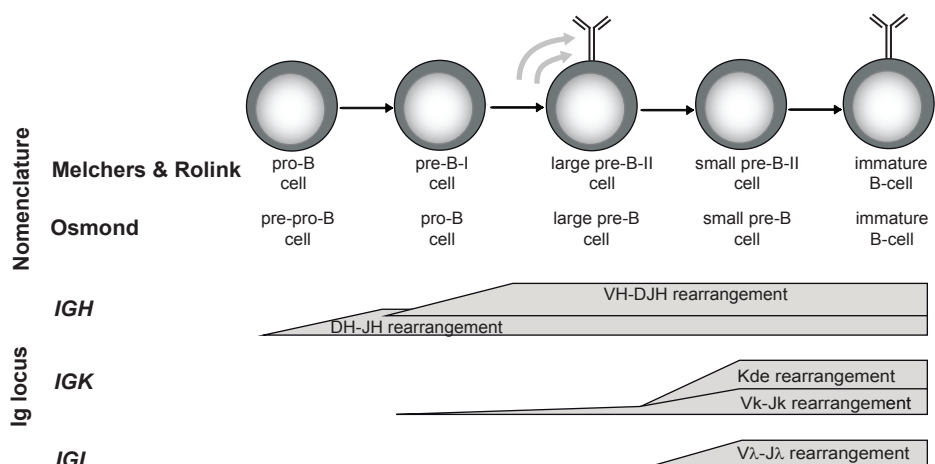
Figure 4. Antigen-independent B-cell differentiation in bone marrow.
Precursor B-cell development takes place in discrete stages based on ordered Ig gene rearrangements.[24,55] A highly hierarchical process of V(D)J recombinations is initiated by D to J rearrangements and followed by V to DJ rearrangements in the *IGH* loci. While a functional Ig heavy chain is formed and expressed on the surface together with the pre-BCR, cells intensively proliferate and start rearranging Ig light chains: first *IGK* and then *IGL*. Two commonly used precursor B-cell nomenclature systems are these by Melchers and Rolink,[27] and by Osmond.[28-29] Figure adapted from van Zelm *et al*. J. Immunol. 2005[55]

Each Ig molecule is composed of one Ig variable domain and one (Igκ, Igλ) or multiple (IgH) Ig constant domains. The Ig variable domain is a barrel structure composed of framework regions (FR) separated by three complementarity determinig region (CDR) in a form of loops recognizing an antigen (Figure 5). Two of the CDR loops are encoded by V gene (CDR1 and CDR2) and one, the most polymorphic, by the junction between rearranged V, (D) and J genes.

Molecular mechanisms of V(D)J recombination
Double stranded (ds)DNA breaks at V, D and J genes are induced by the recombinase activating gene protein products RAG1 and RAG2 that specifically recognize conserved DNA sequences: recombination signal sequence (RSS) (Figure 6A). The RAG-dimers juxtapose the two gene segments poised to rearrange and nick the DNA at the border of both gene segments and their flanking RSS.[30-32] The 3´OH at each nick attacks the antiparallel strand to create a DNA hairpin at the gene segment. Blunt ends remain on the RSS sequences and are directly joined to each other

Figure 5. IgH variable domain structure. (facing page)
The antigen-binding Ig variable domain has a barrel structure which is composed of three complementarity determinig regions (CDR) in a form of loops separated by framework regions (FR). Two of the CDR loops are encoded by the V gene (CDR1 and CDR2) and one (CDR3) by the junction between rearranged V, (D) and J genes in the *IGH*. Together these three CDRs form the antigen-bonding site of each Ig chain.

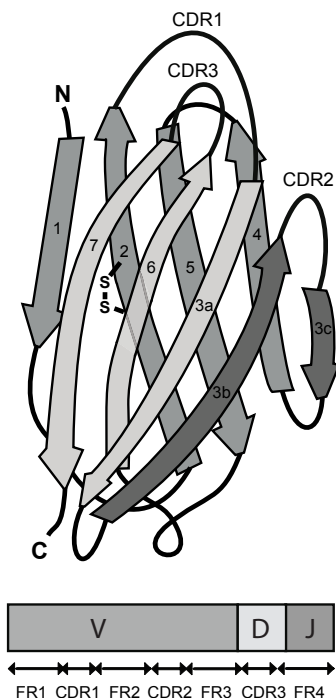by non-homologous end joining (NHEJ) to create a circular excision product. A protein complex consisting of NBN, MRE11 and RAD50 holds the coding ends together for processing prior to ligation by NHEJ components.[33-36] The proteins Ku70 and Ku80 first bind the coding ends and recruit the catalytic subunit of DNA-dependent protein kinase (DNA-PKcs) and Artemis.[37-38] The protein Artemis nicks the hairpin preferentially at the tip or 1-2 bp 5' of the tip, [39-40] which results in a 3' overhang. Complementary nucleotides can be inserted from the 5' end to generate a blunt end, resulting in the generation of palindromic (P-) nucleotides (Figure 6B). Furthermore, exonucleases can delete nucleotides, whereas terminal deoxynucleotidyl transferase (TdT) can add random (N-) nucleotides.[41-42] Finally, the Ku heterodimer recruits a protein complex, including XRCC4, DNA ligase IV and XLF, that ligates the coding ends.[43-45]

A crucial role of individual molecules in the process of V(D)J recombination is reflected by its defects in the immunodeficient patients. Genetic defects in the RAG proteins result in strongly reduced mature B cell (and T cell) numbers. Still, incomplete D-J rearrangements in *IGH*, which can be found in precursor B cells in some patients, show normal patterns of nucleotide deletions, additions and P-nucleotides (Figure 6C).[36] Apparently, the initiation of the break is impaired, but subsequent processing occurs normally. In contrast, impaired hairpin processing due to Artemis or DNA-PKcs deficiency, results in longer P-nucleotide stretches due to aberrant hairpin opening.[46-47] Finally, defects in ligation of the coding ends due to *LIG4* mutations leads to increased nucleotide deletion as compared to controls, caused by prolonged exonuclease exposure due to delayed and/or aberrant ligation.[48] While patients with genetic defects in the NBN-encoding gene *NBS* have mature B and T cells with seemingly normal rearrangement patterns,[49] these numbers are decreased due to impaired juxtapositioning of coding ends.[34] Thus, in healthy individuals the junctional region is formed by combined action of these proteins.

Control of stepwise Ig gene rearrangement by IL-7 and pre-BCR signaling
Once rearrangements of the *IGH* locus are complete, the *VDJ* exon is transcribed and spliced to the *IGHM* encoding exons. Once the functionally rearranged *IGH* gene is transcribed and translated into an IgH protein, the precursor B cell will express IgM chain on the membrane in a complex with signaling proteins CD79A and CD79B and with surrogate light chain proteins VpreB and λ14.1, forming the pre-B cell antigen receptor (pre-BCR; Figures 3, 7). Expression of a functional pre-BCR is an important checkpoint in precursor-B cell differentiation, because downstream signaling pathways are required for further maturation. First, V(D)J recombination at the *IGH* loci is terminated, followed by induction of proliferation and subsequently by induction of Ig light chain gene rearrangements (Figure 4).

One of the major unresolved questions regarding B-cell differentiation concerns the controlled order in which Ig gene rearrangements are induced. While a common machinery is responsible for V(D)J recombination of three Ig and four T-cell
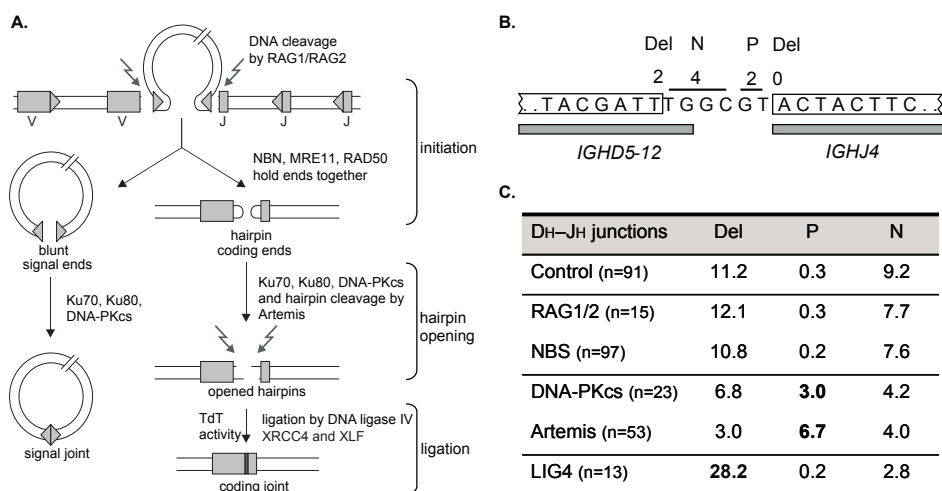
Figure 6. Ig repertoire formation by V(D)J recombination.
(A) Schematic representation of V(D)J recombination. The RAG proteins initiate DNA break formation in two gene segments at the border of the RSSs. This results in two hairpinned coding ends and two blunt signal ends. The blunt signal ends are directly joined by a complex of Ku70, Ku80 and DNA-PKcs. The coding ends are held together by NBN, MRE1 and RAD50, while Ku70, Ku80 and DNA-PKcs recruit Artemis that cleaves the hairpins. Subsequently, the coding ends are processed by endonuclease and TdT activity. Finally, a complex of DNA ligase IV, XRCC4 and XLF is required to ligate the ends into a coding joint. **(B)** Schematic representation of deleted, palindromic (P) and randomly inserted non-templated (N) nucleotides in a hypothetical *IGHD5-12* to *IGHJ4* gene rearrangement. **(C)** Junctional region characteristics of *IGHD* to *IGHJ* gene rearrangements in healthy controls and in patients with defects in the initiation, processing or ligation processes of V(D)J recombination.[36,46-49]

receptor (TCR) loci, nearly all precursor B cells only rearrange their Ig receptor loci in a strict order: D to J and V to DJ on *IGH*, and only after pre-BCR signaling *IGK* is rearranged prior to *IGL*.

A role for stromal cell-derived IL-7 in regulation of V to DJ rearrangements in *IGH* via signaling through IL-7R and STAT5 is currently under debate. STAT5 binds to elements in the V gene in *IGH* and distal V to J gene rearrangements are severely impaired in STAT5 deficient mouse precursor-B cells.[50] However, STAT5 activation is also important for precursor-B cell survival and the recombination defects could be rescued by overexpression of the prosurvival gene *BCL2*.[51] In contrast, in mice inhibition of IL-7 signaling was found to induce premature *IGK* rearrangements in pro-B cells that lack functional *IGH* gene rearrangements implying an important role in controlling the order of Ig gene rearrangements.[51] Still, since SCID patients with mutations in genes encoding the IL-7Rα (CD127) or the common γ subunit (CD132) have normal numbers of circulating B cells at 3-6 months of age, the role of IL-7/IL-7R signaling in the precursor-B cell development in human remains unclear.[52-53]

Ig light chain gene rearrangements and BCR selection in bone marrow
Signaling from the pre-BCR induces Ig light chain rearrangements (Figure 8). Similar to
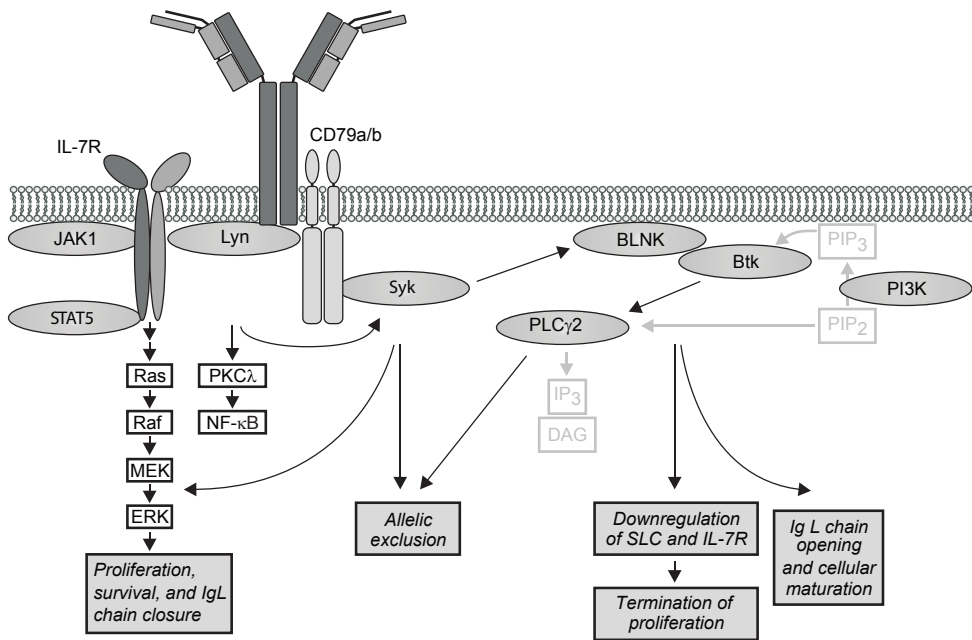
Figure 7. Pre-BCR signaling is required for precursor B cell differentiation.
The pre-BCR and the IL-7R signal via Lyn, Syk, Stat5 and the Ras-Raf-MEK-ERK pathway for proliferation, survival and IgL closure. Signaling of the pre-BCR via Syk is also required for allelic exclusion. Furthermore, the pre-BCR signals via BLNK and Btk to limit proliferation and induce Ig light chain rearrangements.

V to J rearrangements in *IGH*, the initiation of V to J rearrangements in the *IGK* and *IGL* light chain loci appears to be highly regulated.[54] The initiation of *IGL* gene rearrangements seemingly coincides with *IGK* rearrangements in small pre-B cells.[55] Still, single cell analysis revealed that *IGK* rearrangements precede *IGL* rearrangements: Igκ⁺ B cells rarely contain *IGL* rearrangements, while Igλ⁺ B cells are abundant in *IGK* rearrangements.[56-57]

In addition to subsequent V-J rearrangements, the *IGK* locus can initiate rearrangements between *IGKV* gene and the kappa-deleting element (Kde), which is located downstream of the *IGKC* exons (Figure 8).[58] These rearrangements remove the rearrangement and the *IGKC* from the genome. The Kde element can also rearrange with the RSS located downstream of the J genes in the *IGK* and upstream of the *IGKC* exons. This rearrangement removes the *IGKC* exons from the genome. Both types of *IGK*-deleting rearrangements are found in ~70% of mature B lymphocytes of healthy individuals.[55]

Once an Ig light chain protein is generated that can pair with the Ig heavy chain to form a functional Ig receptor, the cell will be positively selected and become an immature B cell. Still, immature B cells frequently carry autoreactive or polyreactive receptors, which need to be removed from the repertoire in a process of negative selection. These cells are assumed either undergo apoptosis,[59] become anergic and unresponsive to Ig receptor crosslinking,[60] or modify
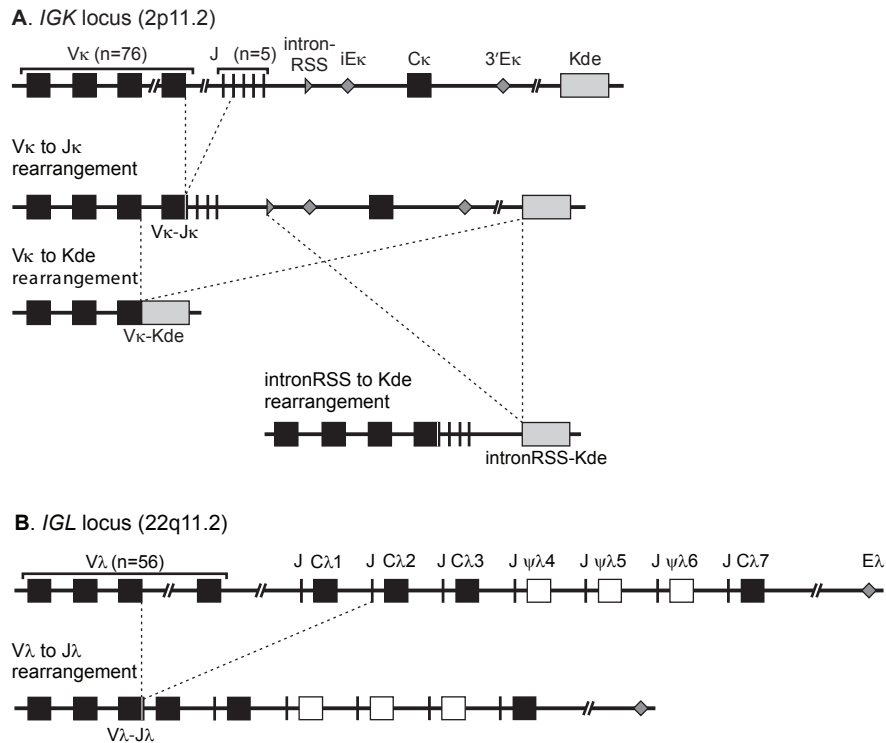
Figure 8. Schematic overview of Ig light chain gene rearrangements.
IGK contains 76 functional V genes and 5 functional J genes that can be rearranged to form a functional *IGKVJ* exon. In addition *IGKV* genes and an intron-RSS can rearrange with the kappa-deleting element (Kde). These kappa-deleting rearrangements remove the enhancer and the *IGKC* region, thereby making the allele non-functional. The *IGL* locus contains 56 functional V and 4 functional J-C clusters (black squares).

Ig receptor reactivity by initiation of secondary Ig gene rearrangement. This process is called receptor editing[61-62]

Counterselection of cells with polyreactive and autoreactive BCRs takes place during two checkpoints. The first or central checkpoint occurs in the bone marrow and results in the removal of cells with both autoreactive and polyreactive BCRs. Consequently, the frequencies of autoreactive (~75%) and polyreactive (~55%) BCRs in early immature B-cells decreases to ~45% and <10% in immature B cells, respectively (Figure 9).[63] The second or peripheral checkpoint occurs upon B-cell migration from the bone marrow to the periphery, and is mainly directed against remaining autoreactive BCRs, reducing their frequency to ~20% in naive mature B cells. Since, autoreactive BCRs often display long (> 20 amino acids) and positively charged IGH-CDR3 regions,[63] the removal of B cells with these sequences from the B-cell repertoire can be used to demonstrate ongoing selection.
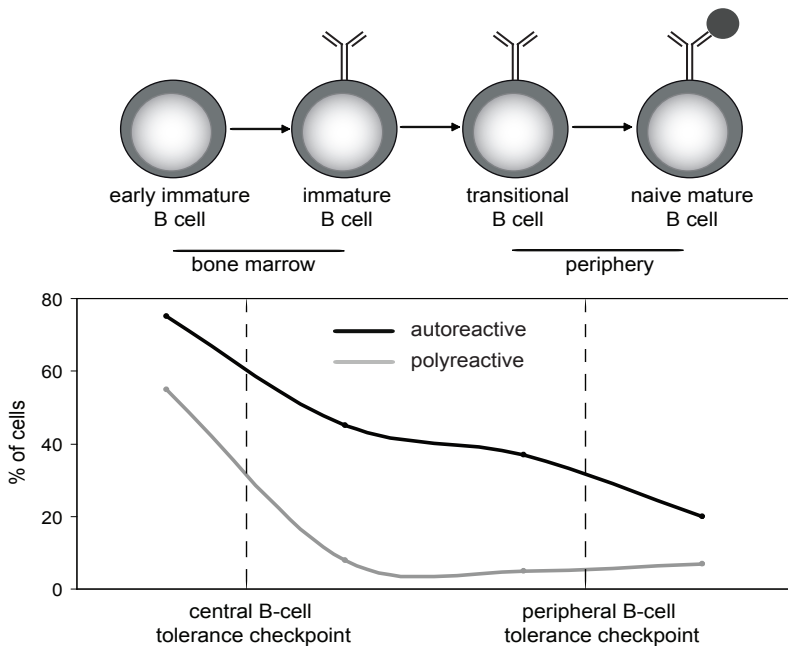
Figure 9. Early B-cell tolerance checkpoints.
B cells carrying autoreactive and polyreactive BCRs are removed from the repertoire during two selection checkpoints. The first or central checkpoint takes place in the bone marrow prior to development of immature B cells, and results in removal of cells with both autoreactive and polyreactive BCRs. The second of peripheral checkpoint occurs upon B-cell migration from the bone marrow to the periphery, and is mainly directed against remaining autoreactive BCRs. Figure adapted from Meffre E, 2011. Ann N Y Acad Sci.[165]

2. ANTIGEN DEPENDENT B-CELL MATURATION IN THE PERIPHERY

Following successful antigen-independent differentiation in bone marrow, B cells migrate to peripheral lymphoid organs and recirculate in blood. The cells require external signals for survival by rate-limiting factors, which thereby ensure stable homeostasis of the total B-cell pool. Furthermore, only those cells that recognize their cognate antigen initiate further differentiation and generate memory B cells and antibody-producing plasma cells. The maturation pathways differ depending on the anatomic location of the response (e.g. lymph node vs. gut, lung or splenic marginal zone) and the type of antigen (e.g. protein vs. polysaccharide).

Survival and maturation of naive B cells
Recent bone marrow emigrants are functionally immature, i.e. they do not respond to Ig

receptor stimulation. These transitional B cells constitute ~5-10% of total B cells in blood of healthy adults and have a characteristic phenotype that includes expression of CD5 and high expression levels of CD24 and CD38.[64-65] Maturation into pre-naive B cells is accompanied by downregulation of CD38 and CD24 which makes them partially responsive to BCR receptor stimulation and CD40 ligation.[66] Finally, upon subsequent downregulation of CD5, pre-naive B cells become naive mature B cells, which are fully responsive to antigen. Development of transitional B cells into naive mature B cells is accompanied by homeostatic proliferation of ~2 cell cycles.[10]

The size of the mature B-cell pool is tightly regulated by B-cell activating factor (BAFF). Similar to proliferation-inducing ligand (APRIL), BAFF is member of the tumor necrosis factor (TNF) family that is implicated in several aspects of B-cell survival and Ig isotype switching and production.[67-68] BAFF and APRIL can both bind the BCMA (B-cell maturation antigen) and TACI (transmembrane activator and CAML interactor) receptors,[69-73] whereas BAFF also specifically binds to a third receptor, BAFF-R,[74-75] and APRIL can interact with proteoglycans.[76-77] BAFF-R is quite specifically expressed on B cells and the BAFF – BAFF-R interaction is crucial for survival of naive B cells,[67,78] and genetic ablation of BAFF or BAFF-R in mice and mutations in the human *BAFFR* result in a dramatic reduction of naive mature B cells.[79-81]

T-cell dependent and T-cell independent B-cell responses to antigen
B cells respond to antigens, which are specifically recognized by their BCR. Upon binding to its cognate antigen, the BCR induces downstream signaling using the same pathways as the pre-BCR, to initiate target gene transcription (Figures 7 and 10). The CD19-complex, consisting of CD19, CD21, CD81 and CD225, is necessary for sufficiently strong signaling (Figure 10A).[82-84]

In addition to antigen recognition via the BCR, B cells need a second signal to become activated.[85] Activated T cells can provide such a signal via CD40L that interacts with CD40 on B cells (Figure 10A). T cell-dependent (TD) B-cell responses are characterized by germinal center (GC) formation. Germinal center B cells undergo extensive proliferation, affinity maturation and Ig class switch recombination (CSR).[9] Thus, high-affinity memory B cells and Ig-producing plasma cells are formed.

Additionally, B cells can respond to T cell-independent (TI) antigens that either activate them via the Ig receptor and another (innate) receptor (TI-1) or via extensive cross-linking of the BCR due to the repetitive nature of the antigen (TI-2) (Figure 10B).[86] These antigens can be both lipid and carbohydrate structures.[87] TI responses are directed against blood-borne pathogens in the splenic marginal zone and in mucosal tissues. (reviewed in [88-89]) B cells express many different pattern recognition receptors, including Toll-like receptors (TLRs) and nucleotide oligomerization domain-like receptors (NLRs) that have been implicated in TI responses.[90-91] Furthermore, BAFF and APRIL likely support TD and TI through binding with TACI and induction of affinity maturation and Ig CSR.[92-93]

Introduction and selection of somatic hypermutation
The Ig variable regions of activated B cells are targets for somatic hypermutation (SHM). Key player in the molecular process of SHM is the activation-induced cytidine deaminase

I
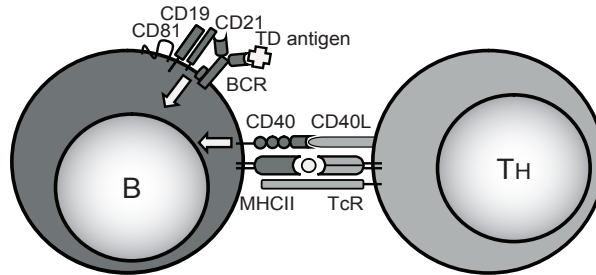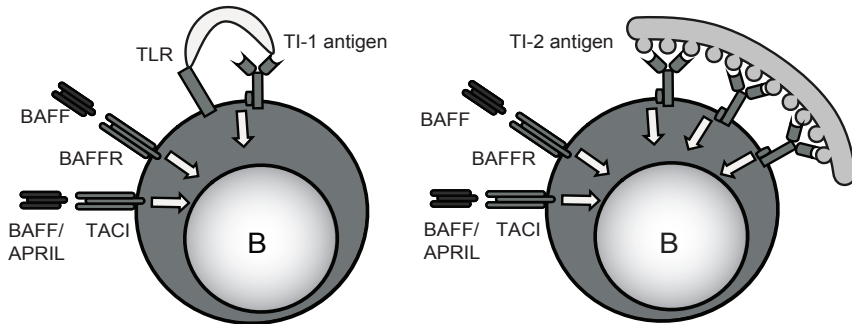
Figure 10. B cell activation signals. (A) T-cell dependent B-cell activation.
The first B cell activation signal is provided by cognate BCR–antigen interactions and requires the CD19, CD21, CD81 complex for optimal signaling. The second signal is provided by CD40 – CD40L interactions following presentation of antigenic peptides in MHC class II by the B cell to helper T cells. (B) T-cell independent B-cell activation. B cells can also be activated independent of T-cell help following binding of TI-1 antigen to the Ig receptor and another innate receptor (i.e. Toll-like receptors, TLR; left panel) or binding TI-2 antigen which causes extensive cross-linking of the BCR due to its repetitive nature (right panel). B cell can receive additional signals via BAFF–BAFF-R or BAFF/APRIL–TACI interactions.

(AID).[94] AID initiates deamination of cytidine to uracil (U) on single-stranded DNA and shows preferential targeting of RGYW and WRCY DNA motifs (R = purine, Y = pyrimidine, and W = A or T).[95-96]

Deamination of cytidine generates a mismatch between the newly formed uracil (U) and guanine (G) on the complementary DNA strand. In proliferating cells, the U residue can be recognized as thymine (T) by high-fidelity polymerase resulting in a cytosine (C) to T transition mutation (Figure 11). Alternatively, the uracil is removed by uracil-N-glycosylase (UNG) to create an abasic site.[97] This abasic site can attract the members of the base excision repair (BER) machinery.

The BER machinery induces replication over the abasic site, which results in insertion of a random nucleotide by the error-prone polymerases. Thus, this process only generates mutations at G•C bases, which reflect direct targets of AID. Still, nearly half of the mutations introduced during SHM target adenine (A) and T residues.[96] The A•T mutation spectrum is associated with mismatch repair (MMR) using MutS homology proteins MSH2-MSH6[98-101] and exonuclease 1,[102] which normally provides high-fidelity repair that presumably becomes mutagenic in GC
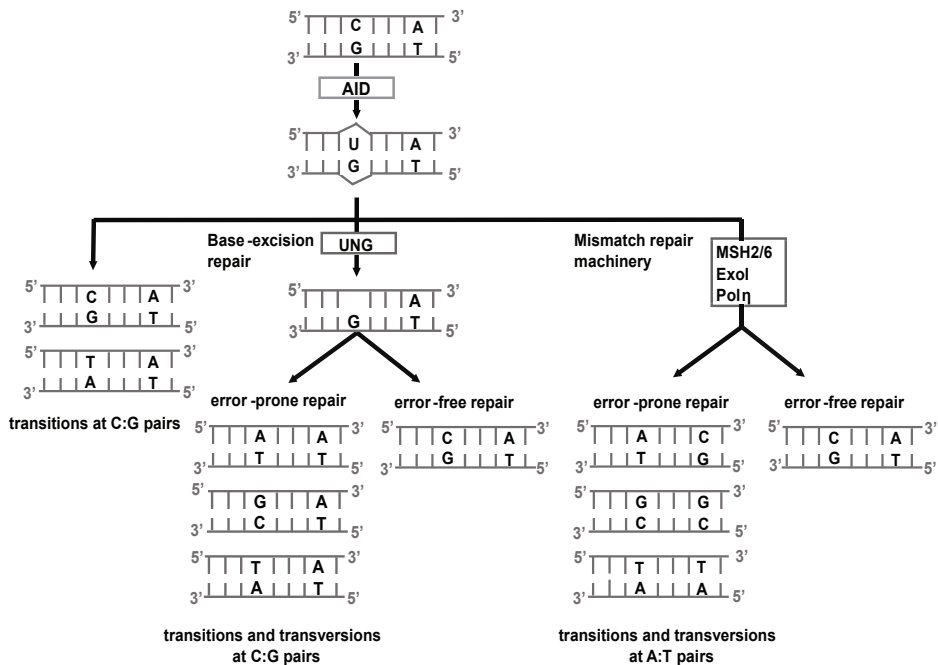
Figure 11. Introduction of SHM by the error-prone repair of AID-induced lesions.
AID initiates SHM by the deamination of a cytidine (C) residue to a uracil (U) residue on the transcriptionally active or non-transcribed DNA strain. In the resulting U•G mismatch, U can be recognized as a thymine (T) by high-fidelity polymerase in proliferating cells, which leads to the cytosine (C) to T transition mutations. Alternatively, the uracil is removed by the uracil-N-glycosylase (UNG) to create an abasic site, which attracts the members of the base-excision repair (BER) machinery. BER initiates replication over the abasic site, which can generate both transition and transversion mutations. Finally, the U•G mismatch can be sensed by the mismatch repair molecules. MMR creates mutations at the adenine (A)•T pair closest to the U•G mismach; Exo1, exonuclease 1; MSH, homologue of *Escherichia coli* MusS; polη,polymerase (DNA-directed) η. or the mismatch repair (MMR) machinery.

B cells with the recruitment of error-prone translesional polymerase eta (POLη)[103-104] targeting WA and TW motifs. First, the G•U mismatches are recognized by MSH2-MSH6 heterodimer, which recruits additional MMR proteins, e.g. exonuclease 1 that excise the DNA containing G•U mismatch. This strand is newly synthesized by POLη which can result in generation of mutations in A•T bases that were not original targets of AID. Repair process initiated by the formation of the abasic site can lead to either transition or transversion mutations.[105]

Although SHM can be introduced throughout entire Ig variable regions, mutations in post-GC cells are preferentially found in CDRs. This partially reflects the overrepresentation of AID-targeted RGYW and WRCY DNA motifs in Ig CDRs,[106-107] and their low frequency in FR regions,[108-109] but is mainly the result of ongoing selection in GC B cells. Mutations in the DNA can either be silent (S) with no effect on the amino acid composition or replacement (R) leading to amino acid substitutions. R mutations in the FR regions are likely to impair the Ig structure and cells that acquired these mutations are removed from the repertoire. R mutations in the CDR regions can have either positive or negative effects on antigen recognition and affinity. B cells that cannot recognize antigen

undergo apoptosis, while these with mutations increasing their affinity for antigen survive and proliferate. Generally, a high ratio of replacement versus silent mutations (R/S) in IGHV-CDRs is regarded as a molecular sign of affinity maturation. However, a clear cut-off value is difficult to determine.[110]

Ig class-switch recombination

In addition to the crucial role of AID in generation of SHM, it is also involved in the process of CSR, which changes Ig receptor effector functions.[94] The *IGH* locus contains multiple constant region-encoding genes (*IGHC*) downstream of *IGHM*. In precursor and naive mature B cells, these regions are not used, and rearranged VDJ exons are spliced to the *IGHM* exons. In the GC response, the B cell is capable of rearranging the Ig switch region upstream of *IGHM* with one of the switch regions upstream another constant region. This results in deleting the intervening DNA, and splicing of VDJ exons to the exons of another *IGHC*.

The Ig switch regions upstream of each *IGHC* consist of multiple tandem repeats of 20-80bp (total length from ~2kb in Sε to ~10kb in Sγ1),[111] which contain multiple AID hotspot motifs. Similar to the process of SHM, AID deaminates cytidine to uracil, which can be later removed by UNG and subjected to mismatch repair (Figure 12).[112-113] The high density of AID hotspots within switch regions can induce two abasic sites within a close proximity on opposite strands resulting in a dsDNA break. These dsDNA breaks recruit NHEJ proteins. If dsDNA breaks are induced simultaneously in the *IGHM* switch region and one of the other switch regions, they can lead to rearrangement. Since the intervening DNA is excised, the process of CRS is irreversible. Still, cells can undergo successive CSR to more downstream *IGHC*, which can be visualized by the presence of the primary switch region-remnants in the newly formed switch regions. Since some of the primary switch regions can be completely removed during the consecutive CSR, the frequency of indirect class-switching calculated based of the presence of their remnant is always underestimated.

The human *IGH* locus contains 9 *IGHC* genes encoding 5 Ig classes: IgM, IgD, IgG, IgA and IgE. Among these four IgG and two IgA subclasses can be identified. CSR is not a random process, but is regulated by cytokines, which control the accessibility of particular *IGHC* and switch regions, [114-115] e.g. IL-4 is required for formation of IgG;[116] TGFβ and IL-10 for IgA;[117-118] and IL-4 and IL-13 for IgE.[119-122]

The process of CSR does not affect the antigen specificity of the Ig molecule, but it influences its effector functions. This is due to the differential recognition of Ig (sub)classes by Fc receptors on immune cells and soluble proteins. Furthermore, the ability of IgM and IgA antibodies to form polymers increases their avidity.[123-125]

IgG is the predominant Ig class in human serum, and can act locally in the tissue. All IgG subclasses are involved in neutralization of pathogens, but only IgG1 and IgG3 are potent activators of the complement system and inducers of antibody-dependent cell-mediated cytotoxicity.[126] Complement activation is also the predominant function of IgM.[127] Two IgA subclasses have different susceptibility to digestion by bacterial proteases.[128] This is mainly the result of a shorter and more protease-resistant hinge region in IgA2. Therefore, while IgA1 production dominates in the systemic immune system, IgA2 is commonly found in the lower intestinal tract, where it is involved in interactions with local microflora.[129] Finally, IgE is involved in mast cell sensitization and is the mediator of allergic responses and parasitic infections.[130]
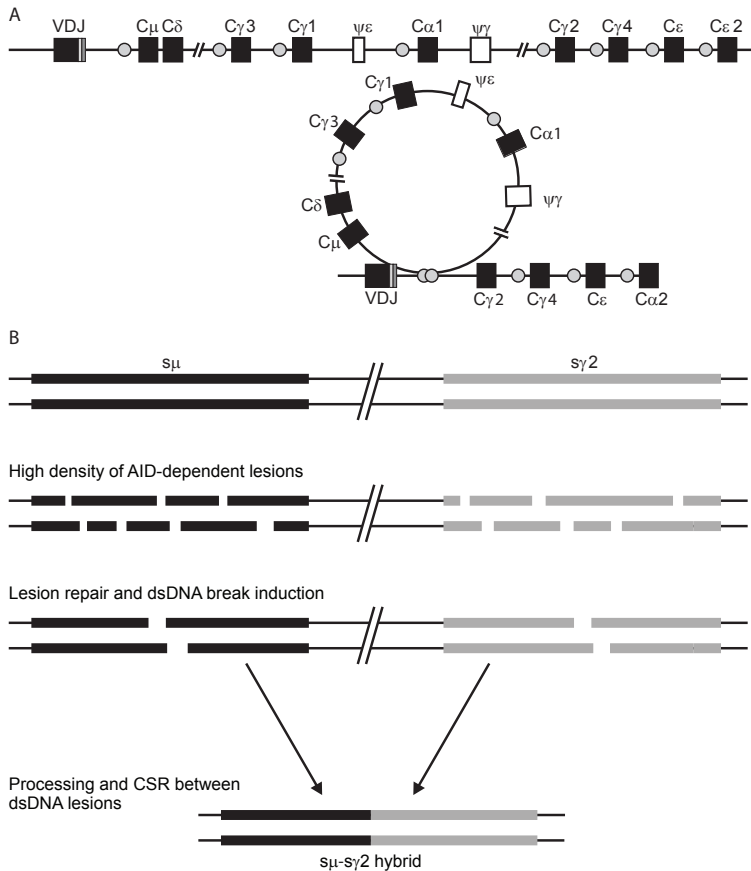
Figure 12. Molecular processes of CSR.
(A) The human *IGH* locus contains 9 functional constant (*IGHC*) regions (black squares). Besides IgD, each of these regions is preceded by repetitive DNA stretches of 20-80bp forming Ig switch regions (s). **(B)** The Ig switch regions contain multiple hot-spots for AID targeting. Consequently, multiple single-stranded DNA lesions can occur in close proximity. These can result in double-stranded DNA breaks and when two Ig switch regions are brought into close proximity, they can be recombined. Thus, a hybrid switch region is formed and the intervening DNA is excised as a circular product.

Diversity of B-cell memory

A substantial fraction of B cells in human has experienced antigen and shows hallmarks of B-cell memory. One of these hallmarks is an increased responsiveness which results from upregulation of co-stimulatory and activation molecules (i.e. CD80, CD86, CD180, TACI),[131] and downregulation of Ig signaling inhibitors (i.e. CD72, LAIR1).[132-134] Until recently, also expression of CD27 was considered to be a memory B-cell hallmark,[131] but recent studies have demonstrated that also CD27- cells can present with an activated phenotype and molecular signs of antigen experience, suggesting that they are memory cells.[135-137]

The majority of circulating memory B cells in healthy adults is derived from TD responses in GCs (Figure 13). GC cells (centroblasts and centrocytes) and memory B cells in childhood

tonsils were shown to undergo ~8 cell divisions.[10] Upon secondary antigen challenge, memory B cells generated during primary immune responses can re-circulate to GCs and undergo additional rounds of proliferation which results in an increase of >10 cell divisions in circulating memory B cells in adults.[10]

The earliest GC responses generate IgM^{+} cells. It had been demonstrated that these cells can undergo subsequent class switching towards IgG,[138] and clonally related IgM[+] and IgG^{+} cells can be found in human GCs and blood.[139-140] IgA[+] and IgG[+] GC-derived memory B cells occur later in the course of an immune response and carry high loads of SHM.[10,141] Until recently, presumably due to their scarcity, IgE[+] memory B cells have not been successfully identified in human.

Systemic TI memory B-cell responses have been described in the marginal zone of the spleen (Figure 13). Human marginal zone B lymphocytes carry a memory phenotype (CD27^{+}), and mutated Ig genes, but do not undergo CSR.[142-143] Their extra-splenic counterparts 'natural effector' B cells are found in lymph nodes, tonsils, Peyer's patches and blood.[144-147] Still, these natural effector B cells have a limited replication history (~6 cell divisions), and a lower SHM level as compared to class-switched memory B cells.[10,144,148]

The local microenvironment of gut, the presence of dendritic cells (DC) and DC-derived cytokines, supports the TI class-switching towards IgA (Figure 13).[92,149-150] Especially, large amounts of IgA2 are produced in this way in the lower gastrointestinal tract.[93] IgA2^{+} cells can be derived either from naive mature B cells, or from IgA1^{+} cells via sequential class-switching.[88] Still, although local TI formation of Ig-secreting plasma cells is well established, it is unknown whether IgA[+] memory B cells can be generated in the same way in human.

Terminal differentiation and survival of plasma cells

Plasma cells are derived from activated B cells through a different transcriptional program than memory B cells, mainly involving BLIMP1, XBP-1 and IRF-4 (Figure 14; reviewed in [151]). Furthermore, IL-21, produced by follicular T$_H$ cells in the GC, is a potent cytokine involved in induction and maintenance of Ig responses. IL-21 signals through STAT3 to upregulate both BLIMP-1 and an inhibitor of plasma cell differentiation, BCL6.[152-154] Still, the duration of IL-21 stimulation and subsequent differential kinetics of STAT3 activation will determine whether plasma cell fate is induced.[155]

Since plasma cells progressively loose membrane BCR expression while maturing, they depend on other mechanisms for survival. Recent studies implicate CD28 for long-term maintenance of plasma cells in bone marrow.[156] The survival signals are provided by the ligands CD80 and CD86 on bone marrow dendritic cells and induce PI3K and NF-κB signaling,[157-158] thereby potentially compensating for the lack of BCR signaling.

While most plasma cells are generated in lymphoid organs and long-lived plasma cells reside in bone marrow, small numbers can be found circulating in blood of healthy adults and have high CD38, CD27 and CD43 expression levels.[159-162]

Despite their low numbers in blood (1-5 cells/μl),[163] plasma cells display large phenotypic heterogeneity. The total blood plasma cell compartment spans from immature cells that resemble lymph node plasmablasts (CD20^{+}sIg^{+}CD138^{-}) to bone marrow plasma cells (CD20[-]sIg^{-}CD138^{+}).[159,163] Moreover, the plasma cells can express one of the various Ig classes. Interestingly, circulating IgA^{+} plasma cells are more frequent than IgM[+] or IgG[+].[160,163] These IgA^{+} plasma cells display characteristics suggestive of a mucosal origin.[160]
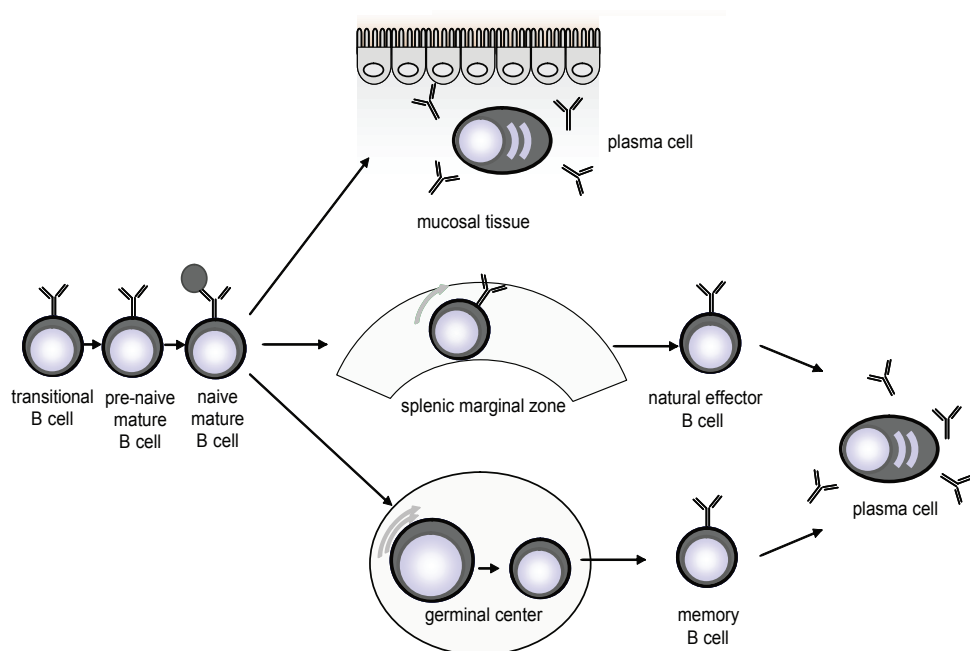
Figure 13. Antigen-dependent B-cell differentiation in the periphery.
The earliest bone marrow emigrants, transitional B cells, are unable to respond to antigen, but mature via the pre-naive B-cell stage into naive mature cells. These naive mature B cells that recognize antigen migrate to the lymphoid follicles and start a GC. In the GC, activated B cells undergo intensive proliferation, acquire SHM in Ig encoding genes and can change the Ig effector function in the process of CSR. The germinal center reaction generates memory B cells and Ig-secreting plasma cells. Alternatively, memory B cells can be generated outside of germinal centers. TI immune responses have been described in spleen where they generate CD27^{+}IgM^{+}IgD^{+} 'natural effector' cells, and in the mucosa of the gastrointestinal tract where they generate IgA-producing plasma cells.
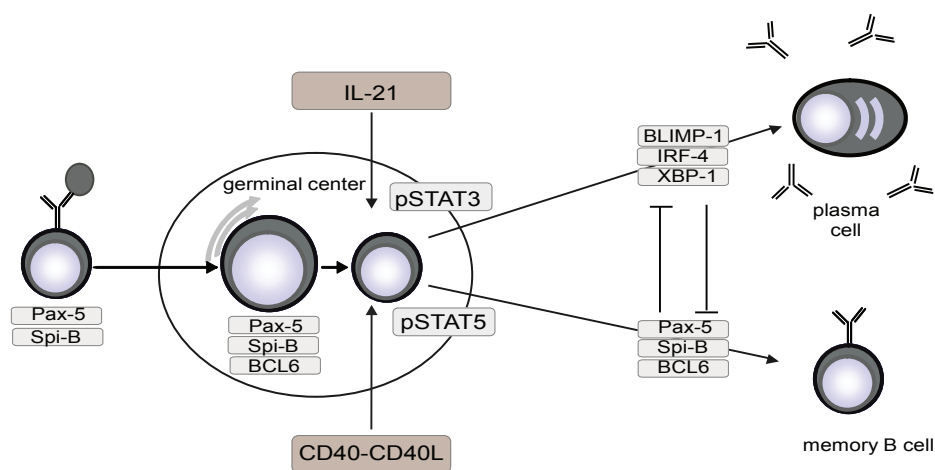
Figure 14. Commitement into the memory B cell and plasma cell fate. (facing page)
Activated B cells in the GC can either differentiate into memory B cells or antibody-secreting plasma cells. The B-cell fate is determined by the interplay between IL-21 and CD40 signaling pathways, which act via STAT3 and STAT5, respectively. B cells which have high levels of phosphorylated (p)STAT3 specify to become plasma cells, by upregulating BLIMP-1, IRF-4 and XBP-1, while B cells with increased levels of pSTAT3 become memory B cells with high levels of Pax-5, Spi-B and BCL6. Once expression of the transcription factors associated with one of the B-cell fates reaches high levels, the cell becomes committed. Figure adapted from Schmidlin H. *et al.* 2009. Trends Immunol.[151]

I

4. AIMS OF THE THESIS

B lymphocytes are critical components of the adaptive immune system, and their most import role is to recognize an antigen via their specific BCR and respond to this antigen by production of soluble Igs and generation of memory cells. The great diversity of potential pathogens encountered by the immune system requires a broad B-cell repertoire. This broad repertoire is first generated during precursor B-cell differentiation in the bone marrow in a process of V(D)J recombination, and then further specified upon antigen encounter in the peripheral lymphoid system. The studies described in this thesis are aimed at understanding how a broad B-cell repertoire is generated in bone marrow, and how immunological memory is generated via distinct types of antigen responses.

In contrast to mice, IL-7/IL-7R signaling in man seems to be redundant for precursor B-cell survival and proliferation, and IL-7R-deficient patients carry mature B cells in blood. Still, it is unknown whether IL-7 exerts any other effect on human B-cell development. The aim of **Chapter II** was to elucidate the role of IL-7/IL-7R signaling in Ig gene rearrangement in man.

Multiple distinct memory B-cell subsets have been identified in humans, but it remains unclear how their phenotypic diversity corresponds to the type of responses from which they originate. The main goal of **Chapter III** was to characterize these circulating memory B-cell subsets and to determine their origin and maturation pathways through analysis of their molecular characteristics.

In **Chapter IV**, knowledge about the memory B-cell characteristics in health was applied to unravel the origin and potential repertoire defects in persistent polyclonal B-cell lymphocytosis (PPBL), a benign condition characterized by an expansion of $CD27^+IgM^+IgD^+$ cells. Furthermore, extensive immunophenotyping of PPBL cells was aimed to find cell-surface markers which would be of value in the flow cytometric diagnostic of PPBL.

In **Chapter V** $CD27^+IgA^+$ and $CD27^-IgA^+$ B cells were studied to dissect the nature of TD and TI IgA B-cell memory through gene expression profiling and detailed immunophenotyping of naive and memory B-cell subsets. Also the reactivity patterns of monoclonal antibodies obtained from single-cell sorted IgA^+ cells were analyzed to determine how these correspond to the physiological function of the subsets.

Chapter VI describes the first phenotypic and molecular characterization of IgE^+ plasma cells and two IgE^+ memory B-cell subsets. This study was aimed to determine the origin of IgE^+ cells in human and their involvement in IgE-mediated disease.

The implications of the studies described in this thesis and the directions for future research are presented in the **General Discussion**.

REFERENCES

1. Turner JR. Intestinal mucosal barrier function in health and disease. *Nat Rev Immunol*. 2009;9:799-809.
2. Marchiando AM, Graham WV, Turner JR. Epithelial barriers in homeostasis and disease. *Annu Rev Pathol*. 2010;5:119-144.
3. Gallo RL, Murakami M, Ohtake T, Zaiou M. Biology and clinical relevance of naturally occurring antimicrobial peptides. *J Allergy Clin Immunol*. 2002;110:823-831.
4. Tomlinson S. Complement defense mechanisms. *Curr Opin Immunol*. 1993;5:83-89.
5. Janeway CA, Jr., Medzhitov R. Innate immune recognition. *Annu Rev Immunol*. 2002;20:197-216.
6. Fearon DT, Locksley RM. The instructive role of innate immunity in the acquired immune response. *Science*. 1996;272:50-53.
7. Hozumi N, Tonegawa S. Evidence for somatic rearrangement of immunoglobulin genes coding for variable and constant regions. *Proc Natl Acad Sci U S A*. 1976;73:3628-3632
8. Tonegawa S. Somatic generation of antibody diversity. *Nature*. 1983;302:575-581.
9. MacLennan IC. Germinal centers. *Annu Rev Immunol*. 1994;12:117-139.
10. van Zelm MC, Szczepanski T, van der Burg M, van Dongen JJ. Replication history of B lymphocytes reveals homeostatic proliferation and extensive antigen-induced B cell expansion. *J Exp Med*. 2007;204:645-655.
11. Nutt SL, Kee BL. The transcriptional regulation of B cell lineage commitment. *Immunity*. 2007;26:715-725.
12. Zandi S, Bryder D, Sigvardsson M. Load and lock: the molecular mechanisms of B-lymphocyte commitment. *Immunol Rev*. 2010;238:47-62.
13. Kondo M, Weissman IL, Akashi K. Identification of clonogenic common lymphoid progenitors in mouse bone marrow. *Cell*. 1997;91:661-672.
14. Akashi K, Traver D, Miyamoto T, Weissman IL. A clonogenic common myeloid progenitor that gives rise to all myeloid lineages. *Nature*. 2000;404:193-197.
15. DeKoter RP, Singh H. Regulation of B lymphocyte and macrophage development by graded expression of PU.1. *Science*. 2000;288:1439-1441.
16. Nichogiannopoulou A, Trevisan M, Neben S, Friedrich C, Georgopoulos K. Defects in hemopoietic stem cell activity in Ikaros mutant mice. *J Exp Med*. 1999;190:1201-1214.
17. Mansson R, Zandi S, Anderson K, et al. B-lineage commitment prior to surface expression of B220 and CD19 on hematopoietic progenitor cells. *Blood*. 2008;112:1048-1055.
18. Rumfelt LL, Zhou Y, Rowley BM, Shinton SA, Hardy RR. Lineage specification and plasticity in CD19- early B cell precursors. *J Exp Med*. 2006;203:675-687.
19. Roldan E, Fuxa M, Chong W, et al. Locus 'decontraction' and centromeric recruitment contribute to allelic exclusion of the immunoglobulin heavy-chain gene. *Nat Immunol*. 2005;6:31-41.
20. Sayegh C, Jhunjhunwala S, Riblet R, Murre C. Visualization of looping involving the immunoglobulin heavy-chain locus in developing B cells. *Genes Dev*. 2005;19:322-327.
21. Jhunjhunwala S, van Zelm MC, Peak MM, et al. The 3D structure of the immunoglobulin heavy-chain locus: implications for long-range genomic interactions. *Cell*. 2008;133:265-279.
22. Jhunjhunwala S, van Zelm MC, Peak MM, Murre C. Chromatin architecture and the generation of antigen receptor diversity. *Cell*. 2009;138:435-448.
23. Ghia P, ten Boekel E, Sanz E, de la Hera A, Rolink A, Melchers F. Ordering of human bone marrow B lymphocyte precursors by single-cell polymerase chain reaction analyses of the rearrangement status of the immunoglobulin H and L chain gene loci. *J Exp Med*. 1996;184:2217-2229.
24. Ghia P, ten Boekel E, Rolink AG, Melchers F. B-cell development: a comparison between mouse and man. *Immunol Today*. 1998;19:480-485.
25. Ehlich A, Schaal S, Gu H, Kitamura D, Muller W, Rajewsky K. Immunoglobulin heavy and light chain genes rearrange independently at early stages of B cell development. *Cell*. 1993;72:695-704.
26a. Alt FW, Yancopoulos GD, Blackwell TK, et al. Ordered rearrangement of immunoglobulin heavy chain variable region segments. *Embo J*. 1984;3:1209-1219.
26b. Novobrantseva TI, Martin VM, Pelanda R, Muller W, Rajewsky K, Ehlich A. Rearrangement and expression of immunoglobulin light chain genes can precede heavy chain expression during normal B cell development in mice. J.Exp.Med. 1999; 1:75-87.
26c. Meffre E, Milili M, Blanco-Betancourt C, Antunes H, Nussenzweig MC, Schiff C. Immunoglobulin heavy chain

expression shapes the B cell receptor repertoire in human B cell development. *J.Clin. Invest*. 2001; 108:879-886

27. Melchers F, Strasser A, Bauer SR, Kudo A, Thalmann P, Rolink A. B cell development in fetal liver. *Adv Exp Med Biol*. 1991;292:201-205.

28. Osmond DG. Population dynamics of bone marrow B lymphocytes. *Immunol Rev*. 1986;93:103-124.

29. Osmond DG, Rolink A, Melchers F. Murine B lymphopoiesis: towards a unified model. *Immunol Today*. 1998;19:65-68.

30. van Gent DC, Hiom K, Paull TT, Gellert M. Stimulation of V(D)J cleavage by high mobility group proteins. *Embo J*. 1997;16:2665-2670.

31. McBlane JF, van Gent DC, Ramsden DA, et al. Cleavage at a V(D)J recombination signal requires only RAG1 and RAG2 proteins and occurs in two steps. *Cell*. 1995;83:387-395.

32. Hiom K, Gellert M. A stable RAG1-RAG2-DNA complex that is active in V(D)J cleavage. *Cell*. 1997;88:65-72.

33. Helmink BA, Bredemeyer AL, Lee BS, et al. MRN complex function in the repair of chromosomal Rag-mediated DNA double-strand breaks. *J Exp Med*. 2009;206:669-679.

34. van der Burg M, Pac M, Berkowska MA, et al. Loss of juxtaposition of RAG-induced immunoglobulin DNA ends is implicated in the precursor B-cell differentiation defect in NBS patients. *Blood*. 2010;115:4770-4777.

35. Grawunder U, Harfst E. How to make ends meet in V(D)J recombination. *Curr Opin Immunol*. 2001;13:186-194.

36. van Gent DC, van der Burg M. Non-homologous end-joining, a sticky affair. *Oncogene*. 2007;26:7731-7740.

37. Gottlieb TM, Jackson SP. The DNA-dependent protein kinase: requirement for DNA ends and association with Ku antigen. *Cell*. 1993;72:131-142.

38. Nussenzweig A, Chen C, da Costa Soares V, et al. Requirement for Ku80 in growth and immunoglobulin V(D)J recombination. *Nature*. 1996;382:551-555.

39. Moshous D, Callebaut I, de Chasseval R, et al. Artemis, a novel DNA double-strand break repair/V(D)J recombination protein, is mutated in human severe combined immune deficiency. *Cell*. 2001;105:177-186.

40. Schlissel MS. Structure of nonhairpin coding-end DNA breaks in cells undergoing V(D)J recombination. *Mol Cell Biol*. 1998;18:2029-2037.

41. Benedict CL, Gilfillan S, Thai TH, Kearney JF. Terminal deoxynucleotidyl transferase and repertoire development. *Immunol Rev*. 2000;175:150-157.

42. Benedict CL, Gilfillan S, Kearney JF. The long isoform of terminal deoxynucleotidyl transferase enters the nucleus and, rather than catalyzing nontemplated nucleotide addition, modulates the catalytic activity of the short isoform. *J Exp Med*. 2001;193:89-99.

43. Critchlow SE, Bowater RP, Jackson SP. Mammalian DNA double-strand break repair protein XRCC4 interacts with DNA ligase IV. *Curr Biol*. 1997;7:588-598.

44. Grawunder U, Wilm M, Wu X, et al. Activity of DNA ligase IV stimulated by complex formation with XRCC4 protein in mammalian cells. *Nature*. 1997;388:492-495.

45. Ahnesorg P, Smith P, Jackson SP. XLF interacts with the XRCC4-DNA ligase IV complex to promote DNA nonhomologous end-joining. *Cell*. 2006;124:301-313.

46. van der Burg M, Ijspeert H, Verkaik NS, et al. A DNA-PKcs mutation in a radiosensitive T-B- SCID patient inhibits Artemis activation and nonhomologous end-joining. *J Clin Invest*. 2009;119:91-98.

47. van der Burg M, Verkaik NS, den Dekker AT, et al. Defective Artemis nuclease is characterized by coding joints with microhomology in long palindromic-nucleotide stretches. *Eur J Immunol*. 2007;37:3522-3528.

48. van der Burg M, van Veelen LR, Verkaik NS, et al. A new type of radiosensitive T-B-NK+ severe combined immunodeficiency caused by a LIG4 mutation. *J Clin Invest*. 2006;116:137-145.

49. Harfst E, Cooper S, Neubauer S, Distel L, Grawunder U. Normal V(D)J recombination in cells from patients with Nijmegen breakage syndrome. *Mol Immunol*. 2000;37:915-929.

50. Bertolino E, Reddy K, Medina KL, Parganas E, Ihle J, Singh H. Regulation of interleukin 7-dependent immunoglobulin heavy-chain variable gene rearrangements by transcription factor STAT5. *Nat Immunol*. 2005;6:836-843.

51. Malin S, McManus S, Cobaleda C, et al. Role of STAT5 in controlling cell survival and immunoglobulin gene recombination during pro-B cell development. *Nat Immunol*. 2010;11:171-179.

52. Buckley RH. Molecular defects in human severe combined immunodeficiency and approaches to immune reconstitution. *Annu Rev Immunol*. 2004;22:625-655.

53. Giliani S, Mori L, de Saint Basile G, et al. Interleukin-7 receptor alpha (IL-7Ralpha) deficiency: cellular and

molecular bases. Analysis of clinical, immunological, and molecular features in 16 novel patients. *Immunol Rev*. 2005;203:110-126.

54. Korsmeyer SJ, Hieter PA, Sharrow SO, Goldman CK, Leder P, Waldmann TA. Normal human B cells display ordered light chain gene rearrangements and deletions. *J Exp Med*. 1982;156:975-985.

55. van Zelm MC, van der Burg M, de Ridder D, et al. Ig gene rearrangement steps are initiated in early human precursor B cell subsets and correlate with specific transcription factor expression. *J Immunol*. 2005;175:5912-5922.

56. Engel H, Rolink A, Weiss S. B cells are programmed to activate kappa and lambda for rearrangement at consecutive developmental stages. *Eur J Immunol*. 1999;29:2167-2176.

57. van der Burg M, Tumkaya T, Boerma M, de Bruin-Versteeg S, Langerak AW, van Dongen JJ. Ordered recombination of immunoglobulin light chain genes occurs at the IGK locus but seems less strict at the IGL locus. *Blood*. 2001;97:1001-1008.

58. Siminovitch KA, Bakhshi A, Goldman P, Korsmeyer SJ. A uniform deleting element mediates the loss of kappa genes in human B cells. *Nature*. 1985;316:260-262.

59. Nemazee D, Buerki K. Clonal deletion of autoreactive B lymphocytes in bone marrow chimeras. *Proc Natl Acad Sci U S A*. 1989;86:8039-8043.

60. Nossal GJ, Pike BL. Clonal anergy: persistence in tolerant mice of antigen-binding B lymphocytes incapable of responding to antigen or mitogen. *Proc Natl Acad Sci U S A*. 1980;77:1602-1606.

61. Gay D, Saunders T, Camper S, Weigert M. Receptor editing: an approach by autoreactive B cells to escape tolerance. *J Exp Med*. 1993;177:999-1008.

62. Tiegs SL, Russell DM, Nemazee D. Receptor editing in self-reactive bone marrow B cells. *J Exp Med*. 1993;177:1009-1020.

63. Wardemann H, Yurasov S, Schaefer A, Young JW, Meffre E, Nussenzweig MC. Predominant autoantibody production by early human B cell precursors. *Science*. 2003;301:1374-1377.

64. Cuss AK, Avery DT, Cannons JL, et al. Expansion of functionally immature transitional B cells is associated with human-immunodeficient states characterized by impaired humoral immunity. *J Immunol*. 2006;176:1506-1516.

65. Sims GP, Ettinger R, Shirota Y, Yarboro CH, Illei GG, Lipsky PE. Identification and characterization of circulating human transitional B cells. *Blood*. 2005;105:4390-4398.

66. Lee J, Kuchen S, Fischer R, Chang S, Lipsky PE. Identification and characterization of a human CD5+ pre-naive B cell population. *J Immunol*. 2009;182:4116-4126.

67. Mackay F, Schneider P, Rennert P, Browning J. BAFF AND APRIL: a tutorial on B cell survival. Annu Rev Immunol. 2003;21:231-264.

68. Dillon SR, Gross JA, Ansell SM, Novak AJ. An APRIL to remember: novel TNF ligands as therapeutic targets. *Nat Rev Drug Discov*. 2006;5:235-246.

69. Gross JA, Johnston J, Mudri S, et al. TACI and BCMA are receptors for a TNF homologue implicated in B-cell autoimmune disease. *Nature*. 2000;404:995-999.

0. Marsters SA, Yan M, Pitti RM, Haas PE, Dixit VM, Ashkenazi A. Interaction of the TNF homologues BLyS and APRIL with the TNF receptor homologues BCMA and TACI. *Curr Biol*. 2000;10:785-788.

71. Thompson JS, Schneider P, Kalled SL, et al. BAFF binds to the tumor necrosis factor receptor-like molecule B cell maturation antigen and is important for maintaining the peripheral B cell population. *J Exp Med*. 72000;192:129-135.

72. Wu Y, Bressette D, Carrell JA, et al. Tumor necrosis factor (TNF) receptor superfamily member TACI is a high affinity receptor for TNF family members APRIL and BLyS. *J Biol Chem*. 2000;275:35478-35485.

73. Yu G, Boone T, Delaney J, et al. APRIL and TALL-I and receptors BCMA and TACI: system for regulating humoral immunity. *Nat Immunol*. 2000;1:252-256.

74. Thompson JS, Bixler SA, Qian F, et al. BAFF-R, a newly identified TNF receptor that specifically interacts with BAFF. *Science*. 2001;293:2108-2111.

75. Yan M, Brady JR, Chan B, et al. Identification of a novel receptor for B lymphocyte stimulator that is mutated in a mouse strain with severe B cell deficiency. *Curr Biol*. 2001;11:1547-1552.

76. Hendriks J, Planelles L, de Jong-Odding J, et al. Heparan sulfate proteoglycan binding promotes APRIL-induced tumor cell proliferation. *Cell Death Differ*. 2005;12:637-648.

77. Ingold K, Zumsteg A, Tardivel A, et al. Identification of proteoglycans as the APRIL-specific binding partners. *J Exp Med*. 2005;201:1375-1383.

78. Schneider P. The role of APRIL and BAFF in lymphocyte activation. *Curr Opin Immunol*. 2005;17:282-289.

79. Gross JA, Dillon SR, Mudri S, et al. TACI-Ig neutralizes molecules critical for B cell development and autoimmune disease. impaired B cell maturation in mice lacking BLyS. *Immunity*. 2001;15:289-302.

80. Schiemann B, Gommerman JL, Vora K, et al. An essential role for BAFF in the normal development of B cells through a BCMA-independent pathway. *Science*. 2001;293:2111-2114.

81. Warnatz K, Salzer U, Rizzi M, et al. B-cell activating factor receptor deficiency is associated with an adult-onset antibody deficiency syndrome in humans. *Proc Natl Acad Sci U S A*. 2009;106:13945-13950.

82. Carter RH, Fearon DT. CD19: lowering the threshold for antigen receptor stimulation of B lymphocytes. *Science*. 1992;256:105-107.

83. van Noesel CJ, Lankester AC, van Lier RA. Dual antigen recognition by B cells. *Immunol Today*. 1993;14:8-11.

84. Fearon DT, Carroll MC. Regulation of B lymphocyte responses to foreign and self-antigens by the CD19/CD21 complex. *Annu Rev Immunol*. 2000;18:393-422.

85. Bretscher P, Cohn M. A theory of self-nonself discrimination. Science. 1970;169:1042-1049.

86. Mond JJ, Vos Q, Lees A, Snapper CM. T cell independent antigens. *Curr Opin Immunol*. 1995;7:349-354.

87. Fagarasan S, Honjo T. T-Independent immune response: new aspects of B cell biology. *Science*. 2000;290:89-92.

88. Cerutti A. The regulation of IgA class switching. *Nat Rev Immunol*. 2008;8:421-434.

89. Weill JC, Weller S, Reynaud CA. Human marginal zone B cells. *Annu Rev Immunol*. 2009;27:267- 285.

90. Delgado MF, Coviello S, Monsalvo AC, et al. Lack of antibody affinity maturation due to poor Toll-like receptor stimulation leads to enhanced respiratory syncytial virus disease. *Nat Med*. 2009;15:34-41.

91. Weller S, Faili A, Garcia C, et al. CD40-CD40L independent Ig gene hypermutation suggests a second B cell diversification pathway in humans. *Proc Natl Acad Sci U S A*. 2001;98:1166-1170.

92. He B, Santamaria R, Xu W, et al. The transmembrane activator TACI triggers immunoglobulin class switching by activating B cells through the adaptor MyD88. *Nat Immunol*. 2010;11:836-845.

93. He B, Xu W, Santini PA, et al. Intestinal bacteria trigger T cell-independent immunoglobulin A(2) class switching by inducing epithelial-cell secretion of the cytokine APRIL. *Immunity*. 2007;26:812-826.

94. Muramatsu M, Kinoshita K, Fagarasan S, Yamada S, Shinkai Y, Honjo T. Class switch recombination and hypermutation require activation-induced cytidine deaminase (AID), a potential RNA editing enzyme. *Cell*. 2000;102:553-563.

95. Rogozin IB, Kolchanov NA. Somatic hypermutagenesis in immunoglobulin genes. II. Influence of neighbouring base sequences on mutagenesis. *Biochim Biophys Acta*. 1992;1171:11-18.

96. Dorner T, Foster SJ, Farner NL, Lipsky PE. Somatic hypermutation of human immunoglobulin heavy chain genes: targeting of RGYW motifs on both DNA strands. *Eur J Immunol*. 1998;28:3384-3396.

97. Odegard VH, Schatz DG. Targeting of somatic hypermutation. Nat Rev Immunol. 2006;6:573-583.

98. Phung QH, Winter DB, Cranston A, et al. Increased hypermutation at G and C nucleotides in immunoglobulin variable genes from mice deficient in the MSH2 mismatch repair protein. *J Exp Med*. 1998;187:1745-1751.

99. Rada C, Ehrenstein MR, Neuberger MS, Milstein C. Hot spot focusing of somatic hypermutation in MSH2-deficient mice suggests two stages of mutational targeting. *Immunity*. 1998;9:135-141.

100. Wiesendanger M, Kneitz B, Edelmann W, Scharff MD. Somatic hypermutation in MutS homologue (MSH)3-, MSH6-, and MSH3/MSH6-deficient mice reveals a role for the MSH2-MSH6 heterodimer in modulating the base substitution pattern. *J Exp Med*. 2000;191:579-584.

101. Delbos F, Aoufouchi S, Faili A, Weill JC, Reynaud CA. DNA polymerase eta is the sole contributor of A/T modifications during immunoglobulin gene hypermutation in the mouse. *J Exp Med*. 2007;204:17-23.

102. Bardwell PD, Woo CJ, Wei K, et al. Altered somatic hypermutation and reduced class-switch recombination in exonuclease 1-mutant mice. *Nat Immunol*. 2004;5:224-229.

103. Wilson TM, Vaisman A, Martomo SA, et al. MSH2-MSH6 stimulates DNA polymerase eta, suggesting a role for A:T mutations in antibody genes. *J Exp Med*. 2005;201:637-645.

104. Martomo SA, Yang WW, Wersto RP, et al. Different mutation signatures in DNA polymerase eta- and MSH6-deficient mice suggest separate roles in antibody diversification. *Proc Natl Acad* Sci   *U S A*. 2005;102:8656-

8661.

105. Casali P, Pal Z, Xu Z, Zan H. DNA repair in antibody somatic hypermutation. *Trends Immunol*. 2006;27:313-321.

106. Pham P, Bransteitter R, Petruska J, Goodman MF. Processive AID-catalysed cytosine deamination on single-stranded DNA simulates somatic hypermutation. *Nature*. 2003;424:103-107.

107. Yu K, Huang FT, Lieber MR. DNA substrate length and surrounding sequence affect the activation-induced deaminase activity at cytidine. *J Biol Chem*. 2004;279:6496-6500.

108. Kepler TB. Codon bias and plasticity in immunoglobulins. *Mol Biol Evol*. 1997;14:637-643.

109. Shapiro GS, Wysocki LJ. DNA target motifs of somatic mutagenesis in antibody genes. *Crit Rev Immunol*. 2002;22:183-200.

110. Bose B, Sinha S. Problems in using statistical analysis of replacement and silent mutations in antibody genes for determining antigen-driven affinity selection. *Immunology*. 2005;116:172-183.

111. Kataoka T, Miyata T, Honjo T. Repetitive sequences in class-switch recombination regions of immunoglobulin heavy chain genes. *Cell*. 1981;23:357-368.

112. Storb U, Stavnezer J. Immunoglobulin genes: generating diversity with AID and UNG. *Curr Biol*. 2002;12:R725-727.

113. Kenter AL. Class-switch recombination: after the dawn of AID. *Curr Opin Immunol*. 2003;15:190-198.

114. Stavnezer J, Radcliffe G, Lin YC, et al. Immunoglobulin heavy-chain switching may be directed by prior induction of transcripts from constant-region genes. *Proc Natl Acad Sci U S A*. 1988;85:7704-7708.

115. Stavnezer J. Molecular processes that regulate class switching. *Curr Top Microbiol Immunol*. 2000;245:127-168.

116. Fujieda S, Zhang K, Saxon A. IL-4 plus CD40 monoclonal antibody induces human B cells gamma subclass-specific isotype switch: switching to gamma 1, gamma 3, and gamma 4, but not gamma 2. *J Immunol*. 1995;155:2318-2328.

117. Defrance T, Vanbervliet B, Briere F, Durand I, Rousset F, Banchereau J. Interleukin 10 and transforming growth factor beta cooperate to induce anti-CD40-activated naive human B cells to secrete immunoglobulin A. *J Exp Med*. 1992;175:671-682.

118. Zan H, Cerutti A, Dramitinos P, Schaffer A, Casali P. CD40 engagement triggers switching to IgA1 and IgA2 in human B cells through induction of endogenous TGF-beta: evidence for TGF-beta but not IL-10-dependent direct S mu-->S alpha and sequential S mu-->S gamma, S gamma-->S alpha DNA recombination. *J Immunol*. 1998;161:5217-5225.

119. Gascan H, Gauchat JF, Aversa G, Van Vlasselaer P, de Vries JE. Anti-CD40 monoclonal antibodies or CD4+ T cell clones and IL-4 induce IgG4 and IgE switching in purified human B cells via different signaling pathways. *J Immunol*. 1991;147:8-13.

120. Gascan H, Gauchat JF, Roncarolo MG, Yssel H, Spits H, de Vries JE. Human B cell clones can be induced to proliferate and to switch to IgE and IgG4 synthesis by interleukin 4 and a signal provided by activated CD4+ T cell clones. *J Exp Med*. 1991;173:747-750.

121. Cocks BG, de Waal Malefyt R, Galizzi JP, de Vries JE, Aversa G. IL-13 induces proliferation and differentiation of human B cells activated by the CD40 ligand. *Int Immunol*. 1993;5:657-663.

122. Punnonen J, Aversa G, Cocks BG, et al. Interleukin 13 induces interleukin 4-independent IgG4 and IgE synthesis and CD23 expression by human B cells. *Proc Natl Acad Sci U S A*. 1993;90:3730-3734.

123. Hendrickson BA, Conner DA, Ladd DJ, et al. Altered hepatic transport of immunoglobulin A in mice lacking the J chain. *J Exp Med*. 1995;182:1905-1911.

124. Niles MJ, Matsuuchi L, Koshland ME. Polymer IgM assembly and secretion in lymphoid and nonlymphoid cell lines: evidence that J chain is required for pentamer IgM synthesis. *Proc Natl Acad Sci U S A*. 1995;92:2884-2888.

125. Brewer JW, Randall TD, Parkhouse RM, Corley RB. IgM hexamers? *Immunol Today*. 1994;15:165-168.

126. Bruggemann M, Williams GT, Bindon CI, et al. Comparison of the effector functions of human immunoglobulins using a matched set of chimeric antibodies. *J Exp Med*. 1987;166:1351-1361.

127. Brewer JW, Randall TD, Parkhouse RM, Corley RB. Mechanism and subcellular localization of secretory IgM polymer assembly. *J Biol Chem*. 1994;269:17338-17348.

128. Mistry D, Stockley RA. IgA1 protease. *Int J Biochem Cell Biol*. 2006;38:1244-1248.

129. Brandtzaeg P, Johansen FE. Mucosal B cells: phenotypic characteristics, transcriptional regulation, and homing

properties. *Immunol Rev*. 2005;206:32-63.

130. Kawakami T, Galli SJ. Regulation of mast-cell and basophil function and survival by IgE. *Nat Rev Immunol*. 2002;2:773-786.

131. Agematsu K, Nagumo H, Yang FC, et al. B cell subpopulations separated by CD27 and crucial collaboration of CD27+ B cells and helper T cells in immunoglobulin production. *Eur J Immunol*. 1997;27:2073-2079.

132. Pritchard NR, Smith KG. B cell inhibitory receptors and autoimmunity. *Immunology*. 2003;108:263-273.

133. van der Vuurst de Vries AR, Clevers H, Logtenberg T, Meyaard L. Leukocyte-associated immunoglobulin-like receptor-1 (LAIR-1) is differentially expressed during human B cell differentiation and inhibits B cell receptor-mediated signaling. *Eur J Immunol*. 1999;29:3160-3167.

134. Yamazaki T, Nagumo H, Hayashi T, Sugane K, Agematsu K. CD72-mediated suppression of human naive B cell differentiation by down-regulating X-box binding protein 1. *Eur J Immunol*. 2005;35:2325-2334.

135. Fecteau JF, Cote G, Neron S. A new memory CD27-IgG+ B cell population in peripheral blood expressing VH genes with low frequency of somatic mutation. *J Immunol*. 2006;177:3728-3736.

136. Wei C, Anolik J, Cappione A, et al. A new population of cells lacking expression of CD27 represents a notable component of the B cell memory compartment in systemic lupus erythematosus. *J Immunol*. 2007;178:6624-6633.

137. Cagigi A, Du L, Dang LV, et al. CD27(-) B-cells produce class switched and somatically hyper- mutated antibodies during chronic HIV-1 infection. *PLoS One*. 2009;4:e5427.

138. Dogan I, Bertocci B, Vilmont V, et al. Multiple layers of B cell memory with different effector functions. *Nat Immunol*. 2009;10:1292-1299.

139. Seifert M, Kuppers R. Molecular footprints of a germinal center derivation of human IgM+(IgD+)CD27+ B cells and the dynamics of memory B cell generation. *J Exp Med*. 2009;206:2659-2669.

140. Bende RJ, van Maldegem F, Triesscheijn M, Wormhoudt TA, Guijt R, van Noesel CJ. Germinal enters in human lymph nodes contain reactivated memory B cells. *J Exp Med*. 2007;204:2655-2665.

141. Pascual V, Liu YJ, Magalski A, de Bouteiller O, Banchereau J, Capra JD. Analysis of somatic mutation in five B cell subsets of human tonsil. *J Exp Med*. 1994;180:329-339.

142. Spencer J, Perry ME, Dunn-Walters DK. Human marginal-zone B cells. *Immunol Today*. 1998;19:421-426.

143. Martin F, Kearney JF. Marginal-zone B cells. *Nat Rev Immunol*. 2002;2:323-335.

144. Weller S, Braun MC, Tan BK, et al. Human blood IgM "memory" B cells are circulating splenic marginal zone B cells harboring a prediversified immunoglobulin repertoire. *Blood*. 2004;104:3647-3654.

145. van den Oord JJ, de Wolf-Peeters C, Desmet VJ. The marginal zone in the human reactive lymph node. *Am J Clin Pathol*. 1986;86:475-479.

146. Dono M, Zupo S, Augliera A, et al. Subepithelial B cells in the human palatine tonsil. II. Functional characterization. *Eur J Immunol*. 1996;26:2043-2049.

147. Spencer J, Finn T, Pulford KA, Mason DY, Isaacson PG. The human gut contains a novel population of B lymphocytes which resemble marginal zone cells. *Clin Exp Immunol*. 1985;62:607-612.

148. Tian C, Luskin GK, Dischert KM, Higginbotham JN, Shepherd BE, Crowe JE, Jr. Evidence for preferential Ig gene usage and differential TdT and exonuclease activities in human naive and memory B cells. *Mol Immunol*. 2007;44:2173-2183.

149. Castigli E, Wilson SA, Scott S, et al. TACI and BAFF-R mediate isotype switching in B cells. *J Exp Med*. 2005;201:35-39.

150. Litinskiy MB, Nardelli B, Hilbert DM, et al. DCs induce CD40-independent immunoglobulin class switching through BLyS and APRIL. *Nat Immunol*. 2002;3:822-829.

151. Schmidlin H, Diehl SA, Blom B. New insights into the regulation of human B-cell differentiation. *Trends Immunol*. 2009;30:277-285.

152. Avery DT, Deenick EK, Ma CS, et al. B cell-intrinsic signaling through IL-21 receptor and STAT3 is required for establishing long-lived antibody responses in humans. *J Exp Med*. 2010;207:155-171.

153. Ettinger R, Sims GP, Fairhurst AM, et al. IL-21 induces differentiation of human naive and memory B cells into antibody-secreting plasma cells. *J Immunol*. 2005;175:7867-7879.

154. Ozaki K, Spolski R, Ettinger R, et al. Regulation of B cell differentiation and plasma cell generation by IL-21, a novel inducer of Blimp-1 and Bcl-6. *J Immunol*. 2004;173:5361-5371.

155. Diehl SA, Schmidlin H, Nagasawa M, et al. STAT3-mediated up-regulation of BLIMP1 Is coordinated with BCL6 down-regulation to control human plasma cell differentiation. *J Immunol*. 2008;180:4805-4815.

156. Rozanski CH, Arens R, Carlson LM, et al. Sustained antibody responses depend on CD28 function in bone marrow-resident plasma cells. *J Exp Med*. 2011;208:1435-1446.

157. Bahlis NJ, King AM, Kolonias D, et al. CD28-mediated regulation of multiple myeloma cell proliferation and survival. *Blood*. 2007;109:5002-5010.

158. Tu Y, Gardner A, Lichtenstein A. The phosphatidylinositol 3-kinase/AKT kinase pathway in multiple myeloma plasma cells: roles in cytokine-dependent survival and proliferative responses. *Cancer Res*. 2000;60:6763-6770.

159. Caraux A, Klein B, Paiva B, et al. Circulating human B and plasma cells. Age-associated changes in counts and detailed characterization of circulating normal CD138- and CD138+ plasma cells. Haematologica. 2010;95:1016-1020.

160. Mei HE, Yoshida T, Sime W, et al. Blood-borne human plasma cells in steady state are derived from mucosal immune responses. *Blood*. 2009;113:2461-2469.

161. Odendahl M, Mei H, Hoyer BF, et al. Generation of migratory antigen-specific plasma blasts and mobilization of resident plasma cells in a secondary immune response. *Blood*. 2005;105:1614-1621.

162. Perez-Andres M, Grosserichter-Wagener C, Teodosio C, van Dongen JJ, Orfao A, van Zelm MC. The nature of circulating CD27+CD43+ B cells. *J Exp Med*. 2011;208:2565-2566

163. Perez-Andres M, Paiva B, Nieto WG, et al. Human peripheral blood B-cell compartments: a crossroad in B-cell traffic. *Cytometry B Clin Cytom*. 2010;78 Suppl 1:S47-60.

164. Kee BL, Murre C. Induction of early B cell factor (EBF) and multiple B lineage genes by the basic helix-loop-helix transcription factor E12. *J Exp Med*. 1998;188:699-713.

165. Meffre E. The establishment of early B cell tolerance in humans: lessons from primary immunodeficiency diseases. *Ann N Y Acad Sci*. 2011;1246:1-10.

II

IL-7R expression and IL-7 signaling confer a distinct phenotype on developing human B-lineage cells

Sonja E. Nodland[1], Magdalena A. Berkowska[2], Anna A. Bajer[1], Nisha Shah[1], Dick de Ridder[3], Jacques J.M. van Dongen[2], Tucker W. LeBien[1],* and Menno C. van Zelm[2],*

[1]Masonic Cancer Center, University of Minnesota, Minneapolis, MN; [2]Department of Immunology, Erasmus MC, University Medical Center, Rotterdam, The Netherlands; and [3]The Delft Bioinformatics Lab, Faculty of Electrical Engineering, Mathematics and Computer Science, Delft University of Technology, Delft, The Netherlands

*T.W.L. and M.C.v.Z. are joint senior authors of this study.

ABSTRACT

IL-7 is an important cytokine for lymphocyte differentiation. Similar to what occurs in vivo, human CD19$^+$ cells developing in human/murine xenogeneic cultures show differential expression of the IL-7 receptor α (IL-7Rα) chain (CD127). We now describe the relationship between CD127 expression/signaling and Ig gene rearrangement. In the present study, < 10% of CD19$^+$CD127$^+$ and CD19$^+$CD127$^-$ populations had complete VDJ$_H$ rearrangements. *IGH* locus conformation measurements by 3D FISH revealed that CD127$^+$ and CD127$^-$ cells were less contracted than pediatric BM pro-B cells that actively rearrange the *IGH* locus. Complete *IGH* rearrangements in CD127$^+$ and CD127$^-$ cells had smaller CDR3 lengths and fewer N-nucleotide insertions than pediatric BM B-lineage cells. Despite the paucity of VDJ$_H$ rearrangements, microarray analysis indicated that CD127$^+$ cells resembled large pre-B cells, which is consistent with their low level of Ig light-chain rearrangements. Unexpectedly, CD127$^-$ cells showed extensive Ig light-chain rearrangements in the absence of *IGH* rearrangements and resembled small pre-B cells. Neutralization of IL-7 in xenogeneic cultures led to an increase in Ig light-chain rearrangements in CD127$^+$ cells, but no change in complete *IGH* rearrangements. We conclude that IL-7–mediated suppression of premature Ig light-chain rearrangement is the most definitive function yet described for IL-7 in human B-cell development.

The online version of this article contains supplemental material.

INTRODUCTION

Mammalian B-lineage cells develop from hematopoietic stem cells in fetal liver and adult BM, and differentiate through well-characterized stages before migrating to secondary lymphoid tissues as naive B lymphocytes.[1,2] Successful development of a broad Ig repertoire is accomplished by selection of cells with functional rearrangements at the Ig heavy- and light-chain loci. Ig gene rearrangement generally proceeds through an ordered process that is initiated at the *IGH* locus, with D$_H$ to J$_H$ rearrangements occurring in pro-B cells[3,4] and mediated by RAG1 and RAG2 proteins.[5,6] Distinct V$_H$ segments then rearrange to the DJ$_H$ element, and in-frame VDJ$_H$ rearrangements are expressed as Igμ heavy chains, which can then pair with the surrogate light-chain components VpreB and λ5[7] to form the pre-BCR. Expression of the pre-BCR initiates several cycles of proliferation at the large pre-B-cell stage, at which time the Ig light-chain loci are epigenetically silenced. After this proliferation phase, Ig light-chain rearrangement is initiated in small pre-B cells. If a functional Ig light chain (Igκ or Igλ) is able to assemble with Igμ, then the cell expresses surface Ig as a BCR$^+$ immature B cell.

The role of transcription factors in regulating Ig gene rearrangement and the expression/ function of RAG1 and RAG2 is well chronicled.[8] Cytokine signaling also plays a regulatory role. Mice lacking a functional IL-7 receptor (IL-7R) pathway by virtue of targeted deletion of genes encoding the IL-7Rα (IL-7Rα) chain[9] or signal transducer and activator of transcription 5 (STAT5)[10] exhibit reductions in *IGH* locus germline transcription and rearrangement of distal V$_H$ genes. STAT5-mediated IL-7 signaling can also influence Ig rearrangement via induction of the early B-cell transcription factor (EBF)[11] and by germline transcription of distal V$_H$ genes.[12] Recent studies using a *Stat5* conditional deletion mutant mouse showed that IL-7 signaling served to repress premature *Igk* rearrangement in pro-B cells, thereby maintaining the Ig heavy chain to light-chain rearrangement hierarchy in developing B-lineage cells.[13]

Efforts to elucidate the role of IL-7 in human B-cell development date back to the mid-1990s.[14] Interestingly, SCID patients with mutations in genes encoding the IL-7Rα (CD127) or the common γ subunit (CD132) have normal numbers of circulating B cells at 3-6 months of age.[15,16] These experiments of nature have been the basis for arguments that human B-cell development is IL-7 independent. Although CD127 is expressed on human B-lineage cells at several stages of differentiation, its function has remained elusive. We[17,18] and others[19–22] have used the human cord blood/murine MS-5 stromal cell xenogeneic culture as a model to study human B-cell development and as a resource for generating sufficient numbers of B-lineage cells for biochemical and molecular studies. We previously identified 2 populations of CD19$^+$ B-lineage cells that could be distinguished by expression of CD127. CD127$^+$ cells were more blastic than CD127$^-$ cells,[17] and the former responded to IL-7 by induction of pSTAT5 and pERK1/2.[18] However, whether CD127$^+$ and CD127$^-$ cells differ by other characteristics, suggesting different stages or pathways in B-cell development, is unknown. To characterize the role of IL-7 signaling in human B-cell lymphopoiesis in greater detail, we examined the Ig gene rearrangement patterns and gene-expression profiles of these IL-7R signaling competent and incompetent B-lineage populations in the MS-5 xenogeneic model. Our results provide new insight into the consequences of IL-7R expression and IL-7 signaling on Ig gene rearrangement and expression in human B-lineage cells.

METHODS

Isolation and culture of cells

Cord blood CD34^{+} hematopoietic progenitor cells (HPCs) were isolated and plated on the murine MS-5 stromal cell line as described previously.[17,18] Pediatric BM was obtained from allogeneic transplantation donors.[23] Thymic specimens were obtained from children requiring surgery for congenital heart disease. All tissues were obtained following protocols approved by the institutional review board at the University of Minnesota and the medical ethics committee at the Erasmus MC Rotterdam.

Neutralization experiments

Xenogeneic cultures were maintained as described previously.[17] After 3 weeks of culture, goat anti–murine IL-7–neutralizing antibody (AB-407-NA; R&D Systems) was added to a final concentration of 10 μg/mL, and cultures were maintained for 1 additional week without medium changes. After 4 or 7 days, cells were harvested by anti-CD19 bead–positive selection[19] and sorted into CD127^{+}Igμ^{−} and CD127^{−}Igμ^{−} populations to > 95% purity. For short-term neutralizing cultures, 0.5-1 × 10^{5} CD19^{+} cells were sorted to be CD98^{hi}/sIgμ^{−} and plated on confluent monolayers of MS-5 in 96-well plates, as described previously.[17] Neutralizing anti-murine IL-7 was added to a final concentration of 10 μg/mL. Cells were harvested at day 3 or 6 for surface phenotyping and quantitation as described previously.[17]

Other

Details for flow cytometry, cell sorting, probe preparation, 3D FISH, image acquisition, distance calculations, statistics, quantitation of Ig gene rearrangements, junctional region analysis, quantitative RT-PCR, and gene-expression profiling are provided in supplemental Methods (available on the *Blood* Web site; see the Supplemental Materials link at the top of the online article). All microarray data are available in ArrayExpress under accession number E-MEXP-384.

RESULTS

Biologic characteristics of CD19^{+}CD127^{+} and CD19^{+}CD127^{−} cells

Previous studies of freshly isolated human B-lineage cells from fetal[24] and adult[25,26] BM have revealed that the IL-7Rα chain (CD127) is expressed on multiple stages of B-cell development. We extended this analysis to pediatric BM and, as shown in Figure 1A, CD127 was expressed on ∼ 30% of pro-, pre-, and immature/naive B-lineage cells. This pattern of expression is consistent with our previous study of fetal BM24 and a recent study using adult BM.[26] Therefore, in normal BM, CD127 expression may confer distinct functions within the pro-B and pre-B compartments. Alternatively, CD127 expression may discriminate populations independently of the historical definition of CD19^{+}CD34^{+} pro-B and CD19^{+}CD34^{−} pre-B cells. We tested the latter possibility using a human/murine xenogeneic culture system to generate CD19^{+}CD127^{+}IgM^{−} and CD19^{+}CD127^{−}IgM^{−} cells (hereafter

referred to as CD127^{+} and CD127^{−}). We reported previously that CD19^{+}CD127^{−}IgM^{−} cells from xenogeneic cultures were small cells with low forward light-scattering characteristics, whereas CD19^{+}CD127^{+}IgM^{−} cells were more blastic.[17] To determine whether these properties affected survival, we enriched the 2 populations from xenogeneic cultures and replated them in the absence of exogenous cytokines and MS-5 stromal cells. Both populations underwent gradual cell death over 7 days, with CD127^{+} cells showing slightly greater survival capability (data not shown). We next determined whether CD127^{+} and CD127^{−} populations harbored differences in Ig protein expression. As shown in Figure 1B, FACS-purified CD127^{+} and CD127^{−} populations both contained < 5% Igμ^{+} cells. The frequency of Igμ^{+}, Igμ^{+}Igκ^{+}, and Igμ^{+}Igλ^{+} cells in the CD127^{+} and CD127− populations were similar when the cells were examined by cell-surface staining and after fixation and permeabilization (Figure 1C and data not shown). Although xenogeneic cultures generally undergo a loss of stromal cell integrity and lymphoid cell survival between 4 and 6 weeks, a minority can survive longer. An example of B-cell differentiation occurring in a 7-week culture is shown in Figure 1D, where well-defined populations of Igμ[+]Igδ[−] immature B cells and Igμ[+]Igδ[+] naive B cells can be seen. Therefore, xenogeneic cultures can support a full range of B-cell development that occurs in normal human BM.

Ig gene rearrangement patterns in CD127^{+} and CD127^{−} cells
We next determined whether competency to respond to IL-7 was correlated with differences in Ig gene rearrangement patterns. Sorted CD19^{+}CD127^{+}Igμ^{−} and CD19^{+}CD127^{−}Igμ^{−} populations were assessed for *IGH*, *IGK*, and *IGL* rearrangements by quantitative RT-PCR. Rearrangements were quantified relative to monoallelically rearranged control cell lines, which were defined as "100% rearranged." In both populations, approximately 150% of *IGH* alleles (ie, three-fourths of the total alleles) had undergone DJ$_H$ rearrangement, and similar D$_H$ gene family usage profiles were present (Figure 2A). However, complete V$_H$ to DJ$_H$ gene rearrangements were low, occurring in only ~10% of cells from both populations (Figure 2B), similar to the frequency of cells in each population expressing the Igμ protein (Figure 1B). These rearrangements largely used the V$_H$1-3 gene families (4.6%-7.6% compared with V$_H$4-7 at 0.01%-0.02%). This was somewhat unexpected, because V$_H$4 is one of the most commonly used families in fetal BM[27] and pediatric BM CD19[+]CD34[+] pro-B cells.[23] However, although not visible in the bar graph shown in Figure 2B, V$_H$4-DJ rearrangements were detectable. GeneScan size analysis of V$_H$-DJ$_H$ rearrangements showed large size variations (Figure 2G). Therefore, both cell populations have their *IGH* loci in immature configuration with high levels of D$_H$-J$_H$ rearrangements and low levels of V$_H$-DJ$_H$ rearrangements that do not demonstrate in-frame selection.

Multiple types of Ig light-chain rearrangements were assayed, including the Vκ-Jκ and Vλ-Jλ rearrangements, which can yield functional Ig light chains, as well as Ig κ–deleting (Kde) rearrangements that render an *IGK* allele nonfunctional (Vκ-Kde and IntronRSS-Kde). Vκ-Kde rearrangements delete Jκ gene segments, thereby removing the previously formed Vκ-Jκ rearrangements from the genome. In contrast, IntronRSS-Kde rearrangements do not delete Jκ gene segments, allowing for the detection of both IntronRSS-Kde and Vκ-Jκ joints on the same allele.[23,28] The majority of Ig light-chain gene rearrangements are induced in small pre-B cells,[23] with Vκ-Jκ rearrangements preceding Kde and Vλ-Jλ rearrangements.[29] Very few Ig light-chain
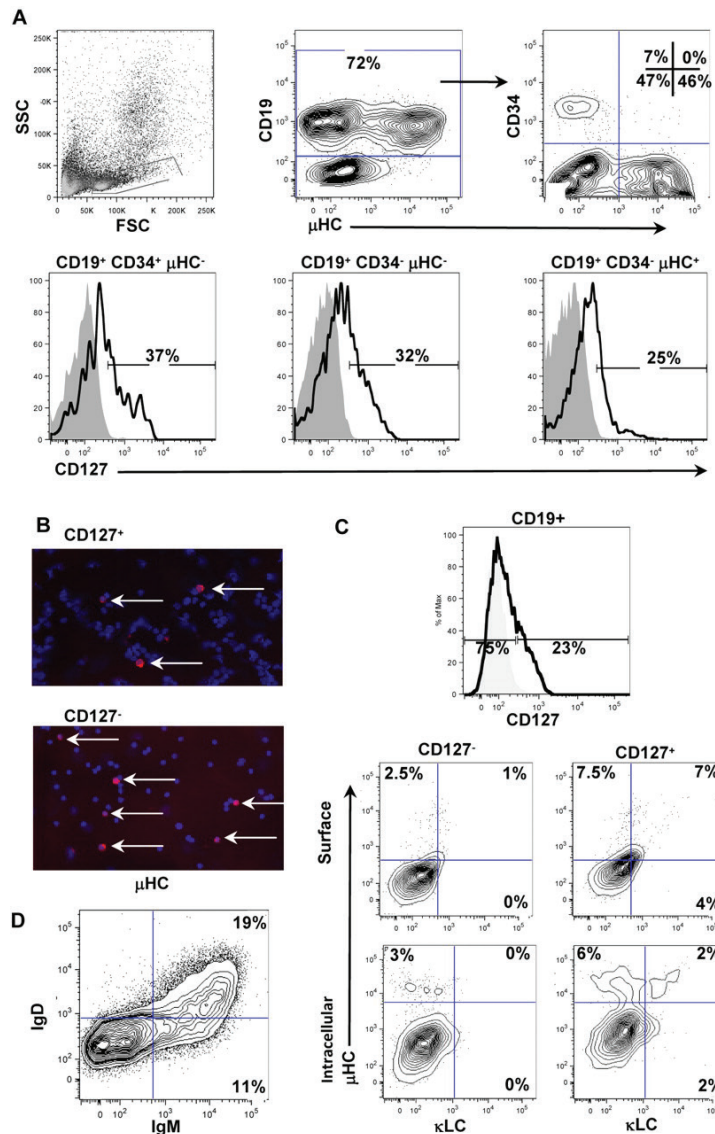
Figure 1. Expression of CD127 and Ig proteins on normal pediatric BM B-lineage cells and CD19$^+$ cells from xenogeneic cultures. (A) CD127 expression was assayed on normal pediatric BM by flow cytometry. Total CD19$^+$ cells in the lymphoid light-scatter gate were analyzed for surface μHC and CD34 expression (top right contour plot). CD127 expression was then analyzed and plotted on the 3 major populations of B-lineage cells in human BM: pro-B cells (CD19$^+$/CD34$^+$/μHC$^-$), pre-B cells (CD19$^+$/CD34$^-$/μHC$^-$), and immature/naive B cells (CD19$^+$/CD34$^-$/μHC$^+$). CD127 expression was detected on all 3 subpopulations of B-lineage cells in human BM. (B) Cytocentrifuge slides of FACS-purified CD127$^+$ and CD127$^-$ cells from xenogeneic cultures were stained for expression of Igμ heavy chains using goat anti–human IgM TRITC (red) and counterstained with DAPI (blue). Mounting medium

(2.3% wt/vol DABCO; Sigma D-2522/10% 1× PBS/87.7% glycerol) was used to cover the stained slides and slides were stored at 4°C and visualized at room temperature. Images were acquired using the Plan-Apochromat 10×/0.45 numerical aperture (NA) objective on an Axiovert 2 fluorescent microscope (Carl Zeiss) equipped with a Spot CCD camera (Diagnostic Instruments) and Spot Advanced 4.6 acquisition software. Adobe Photoshop 7.0 was used to create image overlays. Approximately 5% of cells in each population expressed Igμ. (C) CD19^{+} cells were isolated from 4-week xenogeneic cultures and stained for expression of CD127, Igμ, Igκ, and Igλ. (D) CD19^{+} cells were isolated from a 7-week xenogeneic cultures and stained for expression of Igμ and Igδ heavy chains.

rearrangements were detected in CD127^{+} cells (Figure 2C-F). Interestingly, CD127^{−} cells had extensive rearrangement activity at the Ig light-chain loci despite the paucity of VDJH rearrangements. Abundant Vκ-Jκ rearrangements were present (Figure 2C), exceeding the 200% level that corresponds to 2 rearranged alleles per cell. The levels of Kde (Figure 2D-E) and Vλ-Jλ rearrangements (Figure 2F) were comparable to those found in freshly isolated small pre-B cells, but were dramatically higher than in CD127^{+} cells. GeneScan analysis of Vκ-Jκ and Vλ-Jλ rearrangements showed size distributions similar to those detected in small pre-B cells.[23] Despite the high levels of gene rearrangements in CD127^{−} cells, this analysis did not reveal uniform triplet peaks, indicating that in-frame selection had not occurred. These results show that CD127^{−} cells have high levels of Ig light-chain gene rearrangements in the absence of complete VDJH rearrangements.

Limited TdT activity in cultured human B-lineage cells

We next analyzed coding joint formation in CD127^{+} and CD127^{−} cells. The results were compared with *IGH* and *IGK* rearrangements occurring in pro- and pre-B cells from pediatric BM and B cells from cord blood. CD127^{+} and CD127^{−} cells had significantly lower N-nucleotide insertions at VH-DH and DH-JH junctions compared with pediatric BM pro-B and pre-B cells (Figure 3A-B), resulting in shorter CDR3 lengths (Table 1). In addition, their junctions had significantly more nucleotides deleted from the 5′ end of the JH segment than did pro-B and pre-B cells (Table 1). These results suggest that *IGH* gene rearrangements were formed in the presence of less TdT compared with B-lineage cells from normal pediatric BM. Cord blood B cells (that represent a mixture of immature, transitional, and mature populations[30]) had CDR3 lengths comparable to CD127^{+} and CD127^{−} cells (Table 1). The number of N-nucleotide insertions in cord blood B-cell DJH and VDJH junctions was significantly larger than CD127^{+} and CD127^{−} cells (Figure 3A-B), but smaller than pediatric BM.

Analysis of Vκ-Jκ junctions showed that pediatric BM pro-B cells had longer CDR3 lengths than pre-B cells (Table 2), mainly due to the inclusion of N-nucleotides (Figure 3C). This finding is consistent with the lower TdT expression in normal pre-B cells, as shown in quantitative RT-PCR and microarray analysis (Table 3). In addition, pre-B cells showed more deletions and fewer P-nucleotides than pro-B cells at the Vκ site of the Vκ-Jκ junction (Table 2). The Vκ-Jκ junctions in CD127^{+} and CD127^{−} cells were indistinguishable from those in pre-B cells (Figure 3C), but were significantly different from pro-B cells with respect to CDR3 lengths, addition of N-nucleotides (Figure 3C), formation of P-nucleotides, and deletions at the Vκ site of the junction (Table 2).
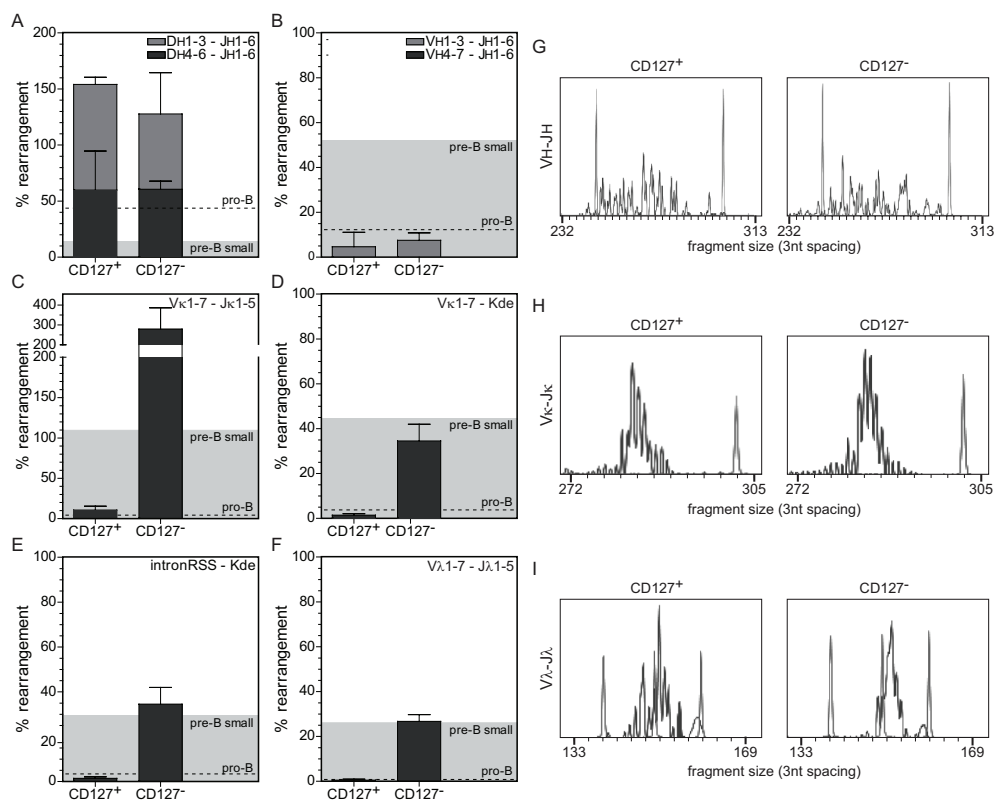
Figure 2. Unique Ig rearrangement patterns in purified CD19⁺CD127⁺ and CD19⁺CD127⁻ populations.
(A-F) The levels of DH-JH, VH-DJH, Vκ-Jκ, Vκ-Kde, IntronRSS-Kde, and Vλ-Jλ rearrangements were quantified in FACS-purified CD127⁺ and CD127⁻ populations and compared with freshly isolated pediatric BM pro-B cells (dotted line) and small pre-B cells (gray shaded area). The quantitative standards used to determine the percentage of rearranged alleles were a mixture of leukemic cell lines with monoallelic rearrangements set at 100%. All data were obtained from triplicate experiments using cells isolated from 3 separate xenogeneic cultures. (G-I) The size distributions of complete VH-DJH, Vκ-Jκ, and Vλ-Jλ were assessed using GeneScan analysis. These patterns are not consistent with in-frame selection, which would be indicated by a characteristic trinucleotide spacing (triplet peaks) shown on the x-axis of each plot. Size standard peaks are shown in light gray at positions 139, 160, 246, and 300.

3D architecture of the *IGH* locus in human B-lineage cells

The *IGH* locus undergoes contraction before VH to DJH recombination in murine pro-B cells.[31–34] Subsequent differentiation to pre-B cells leads to *IGH* locus decontraction, which is thought to prevent further rearrangements and contribute to allelic exclusion.[34] To determine whether the relative paucity of VH-DJH rearrangements in CD19⁺ cells from 4-week xenogeneic cultures resulted from impaired contraction, we measured the spatial distances between 3 probe sets recognizing distal VH, proximal VH, and CH regions (Figure 4A). Similar analyses were conducted on pediatric BM B-lineage cells and CD8⁺ thymocytes (the latter serving as a control for maximum decontraction of the *IGH* locus). Spatial distances between distal VH and CH regions, distal VH and proximal VH regions, and proximal VH and CH regions were the shortest in pediatric BM pro-B cells (Figure 4B-D). The distances

II

Table 1. *IGH* junction characteristics.

sequence	CDR3 length		del	P	N	P	del	del	P	N	P	del
	no	aa	nt	V_H	V_H	V_H-D_H	5'D_H	5'D_H	3'D_H	3'D_H	D_H-J_H	J_H	J_H
pro-B	92	20.41	60.55	2.53	0.34	8.68	0.18	4.47	4.89	0.11	10.21	0.14	5.34
pre-B	53	19.91	59.81	2.15	0.11	8.83	0.11	4.62	5.21	0.04	7.42	0.08	6.08
CD127$^+$	43	15.43	45.65	1.22	0.24	3.16	0.05	5.76	5.16	0.08	1.46	0.05	3.08
CD127$^-$	37	14.91	44.12	1.53	0.16	3.02	0.00	6.35	4.44	0.19	1.91	0.11	3.30
NCB	65	16.02	47.97	1.41	0.25	5.88	0.03	5.57	5.26	0.08	3.52	0.14	3.52

The data shown are the means ± SD from 2-3 donors. Bolded values indicate significantly different values compared to all freshly isolated BM and NCB cells.

Table 2. *IGK* junction characteristics.

sequence	CDR3 length		del	P	N	P	del
	no	aa	nt	V_K	V_K	V_K-DJ_K	J_K	J_K
pro-B	92	20.41	60.55	2.53	0.34	8.68	0.18	4.47
pre-B	53	19.91	59.81	2.15	0.11	8.83	0.11	4.62
CD127$^+$	43	15.43	45.65	1.22	0.24	3.16	0.05	5.76
CD127$^-$	37	14.91	44.12	1.53	0.16	3.02	0.00	6.35
NCB	65	16.02	47.97	1.41	0.25	5.88	0.03	5.57

The data shown are the means ± SD of 2-3 donors. Bolded values indicate significantly different values compared to all freshly isolated BM and NCB cells.
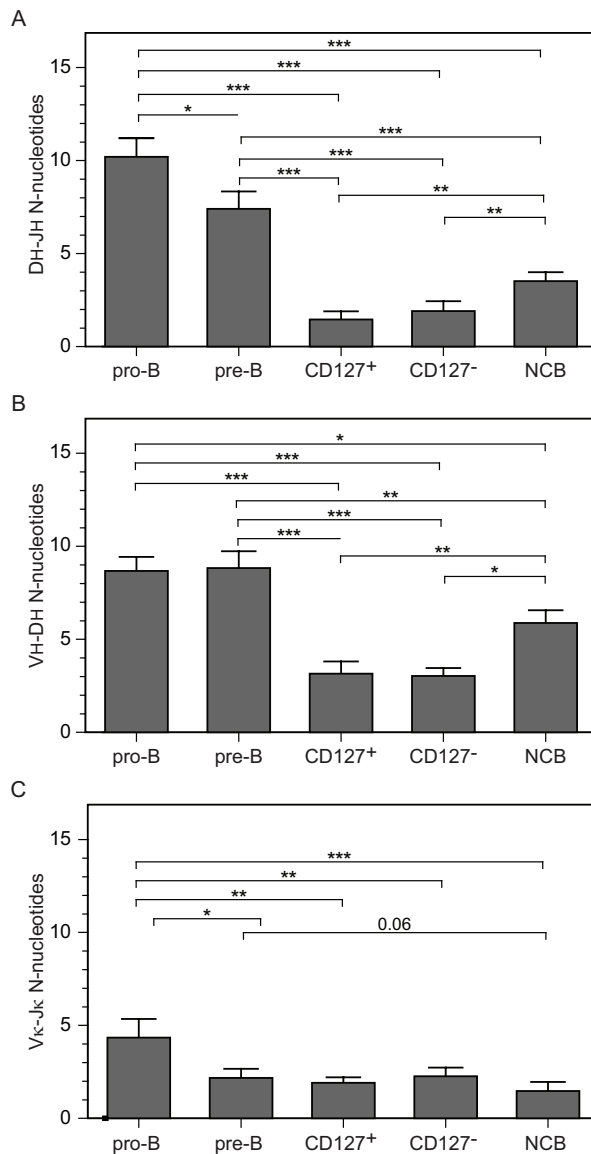
Figure 3. Limited N-nucleotide insertions in complete V$_H$-DJ$_H$ and Vκ-Jκ gene rearrangements of cultured CD19$^+$CD127$^+$ and CD19$^+$CD127$^-$ cells.

Bar graphs show the number of N-nucleotides (y-axis) in D$_H$-J$_H$ (A), V$_H$-D$_H$ (B), and Vκ-Jκ (C) junctions. Values represent the means ± SD of multiple sequences from FACS-purified CD127$^+$ and CD127$^-$ populations from 3 donors, normal cord blood B cells (NCB) from 2 donors, and FACS-purified pediatric pro-B and pre-B-cell populations from 2-3 donors. The nonparametric Mann-Whitney test was used to calculate significance levels between paired populations (horizontal bars). *P < .05; **P < .01; ***P < .001.

between distal V_H and proximal V_H probes (Figure 4C), as well as distal V_H and C_H probes (Figure 4B), were significantly shorter in pre-B cells compared with CD8^{+} thymocytes. However, distances between proximal V_H and C_H probes were similar between pre-B and CD8^{+} thymocytes (Figure 4D), indicating that this region is close to or fully decontracted in pre-B cells. Contraction distances in CD127^{+} cells were identical to pre-B cells, but significantly longer than pro-B cells (Figure 4B-D). Contraction of the *IGH* locus in CD127^{−} cells was intermediate between pro-B and pre-B cells (Figure 4B-D).

Figure 4 Impaired *IGH* locus compaction in cultured CD19^{+}CD127^{+} and CD19^{+}CD127^{−} cells.
(A) Schematic representation of the human *IGH* locus and the combinations of bacterial artificial chromosome clones used as 3D FISH probes are shown. The distance separating each of the 3 probes and their positions within the *IGH* locus were determined from the IMGT database[35] Distal V_H probes were labeled with Alexa Fluor 568 (red), proximal V_H probes with Cy5 (blue), and C_H probes with Alexa Fluor 488 (green). Numbers in the rectangles represent the size of the regions recognized by the probes and the numbers below the arrows represent genomic distances between probe sets. (B-D) Scatter plots showing the distances in micrometers (y-axis) separating distal V_H, proximal V_H, and C_H regions in FACS-purified pediatric BM pro-B and small pre-B cells, CD8^{+} thymocytes, and FACS-purified CD19^{+}CD127^{+} and CD19^{+}CD127^{−} populations from xenogeneic cultures. Except for pro-B cells (1 donor) at least 2 different donors and at least 100 alleles were analyzed per population. Red horizontal lines represent median distances between indicated probes in each population. The nonparametric Mann-Whitney test was used to calculate significance levels between paired populations (horizontal bars). [*]$P < .05$; [**]$P < .01$; [***]$P < .001$. (E) Representative images of *IGH* loci in the primary and cultured cells populations captured with an SP5 confocal microscope (Leica Microsystems). Using a 63×/1.4 NA lens, images of ~70 serial optical sections spaced by 0.148 μm were acquired at room temperature using LAS AF 1.8.2 software (Leica Microsystems). The datasets were deconvolved and analyzed with Huygens Professional software (Scientific Volume Imaging).

Gene-expression profiling of CD19⁺CD127⁺ and CD19⁺CD127⁻ cells

The data presented above revealed some prominent differences in Ig gene rearrangement and expression in CD127⁺ and CD127⁻ cells. To identify additional differences, we performed gene-expression profiling on the 2 populations and compared them with each other and with pediatric BM B-lineage cell subsets.[23] Unbiased clustering analysis was performed based on probe sets that best discriminated between cultured cells and the 4 most mature B-lineage cell stages from BM (Figure 5). This analysis showed that the cultured cells were most comparable to each other and to the later stages of precursor-B-cell development. Specifically, CD127⁺ cells showed the highest correlation with pro-B and large pre-B cells, whereas CD127⁻ cells showed the highest correlation with small pre-B cells (Figure 5).

In addition to unbiased clustering analysis, expression patterns for specific sets of well-studied genes in B-cell differentiation were determined. Table 3 shows the gene-array results for selected genes and the confirmation by quantitative RT-PCR (the last column in Table 3). As expected based on membrane protein expression, CD127 transcripts were dramatically higher in CD127⁺ cells than in CD127⁻ cells. These levels were still higher than those in pediatric BM B-lineage subsets, of which large pre-B cells showed the highest *IL7R* expression. *STAT5A* and *STAT5B*, which encode transcription factors in the CD127 pathway, did not differ in expression between CD127⁺ cells and CD127⁻ cells. The increased expression of *CCND2* and *MKI67* in CD127⁺ cells was correlated with the more blastic characteristics reported previously for these cells.[17] Furthermore, CD127⁺ cells showed higher expression of BCL2, but not MCL1, which is consistent with the Western blotting analysis of sorted CDl27⁺ and CD127⁻ cells (data not shown). Finally, CD127⁻ cells showed higher BCL6 expression than CD127+ cells, which is consistent with the findings that IL-7R signaling negatively regulates BCL6.[36]

Analysis of genes involved in V(D)J recombination revealed that CD127⁻ cells had increased expression of *RAG1*, *RAG2*, and *LIG4*, which is consistent with increased rearrangement at the Ig L chain loci in these cells (Figure 2). Furthermore, these cells contained increased levels of *IGH*, *IGK*, and *IGL* transcripts. The probes for these transcripts are specific for constant regions and therefore likely represent transcripts from both rearranged alleles and germline (sterile) transcripts. Finally, several genes encoding transcription factors involved in the regulation of Ig gene rearrangement were up-regulated in CD127⁻ cells, including *TCF3*, *EBF1*, *FOXO1*, and *IRF4*. *PAX5*, *FOXO3*, *IKZF1*, and IRF8 were not differentially expressed, and *EZH2* and *ID2* (inhibitor of E2A) were down-regulated in CD127⁻ cells compared with CD127⁺ cells.

IL-7R signaling inhibits Ig light-chain gene rearrangements in human precursor B cells

IL-7 signaling has been shown to repress premature Igk rearrangements in murine pro-B cells.[13] We have demonstrated previously that MS-5–derived IL-7 mediates effects on CD19⁺ cells in our xenogeneic model.[17] Given the paucity of *IGK* rearrangements in CD127⁺ cells (Figure 2), in the present study, we investigated whether suppression of IL-7 signaling would initiate the onset of *IGK* rearrangements in CD127⁺ cells.

To initially exclude the possibility that suppressing an IL-7 signal would lead to selective cell death of a subpopulation of CD127⁺ cells or induction of B-cell differentiation, we determined the effect of neutralizing mIL-7 on the viability and maturity of sorted CD127⁺ cells. To eliminate any contribution that the anti-CD127 used in a sorting protocol could have
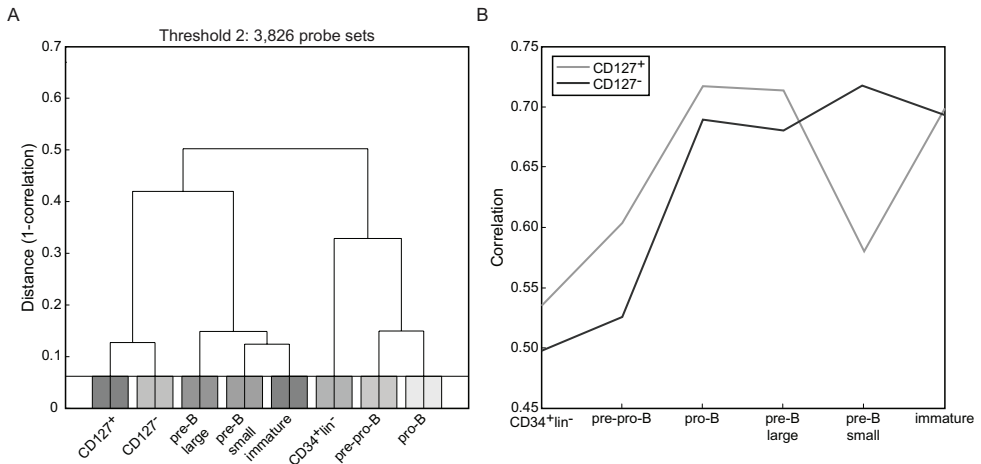
Figure 5. Unbiased clustering analysis of genome-wide expression profiles indicate that CD19+CD127+ and CD19+CD127− cells are most similar to pro-B and large pre-B cells and small pre-B cells, respectively. Clustering analysis was performed without bias for known genes or subsets. All probe sets were ranked based on the maximum difference in expression that was observed between any 2 arrays (excluding the CD34+Lin− and pre-pro-B cells). (A) Hierarchical clustering (complete linkage) using $1 - \rho$ as a distance measure based on the 3826 (threshold at $\log_2$ value 2) probe sets that showed the most variation between any 2 samples. (B) Correlation of the CD127+ and CD127− cells with each of the freshly isolated cord blood CD34+Lin− cells and pediatric BM B-lineage cell subsets.

on recultured CD127+ cells (via either a positive agonistic signal or blocking access to IL-7 binding), we used an antibody to CD98 for purification. The rationale was based on the fact that our gene microarray data revealed that CD98 was more highly expressed on CD127+ cells compared with CD127− cells (Table 3). Although CD98 was expressed on all CD19+ B-lineage cells from xenogeneic cultures, CD127+ cells segregated into the CD98hi fraction (Figure 6A). Therefore, by sorting CD19+CD98hi cells, we could obtain a population highly enriched for CD127+ cells (Figure 6B). Using this strategy, we showed that the IL-7 signal did not induce acquisition of cell-surface Igμ (Figure 6C) or the development of CD127− cells from CD127+ cells (Figure 6D). Neutralization of mIL-7 had no effect on the survival of CD127+ cells when assayed at 3-6 days after plating of sorted cells (data not shown).

To address directly whether IL-7 signaling suppresses Ig light-chain rearrangements, anti–mIL-7 was added to xenogeneic cultures at 3 weeks and CD127+ and CD127− cells were sorted 4-7 days later. As shown in Figure 7, the frequency of all types of rearrangements in the *IGK* locus increased in CD127+ cells as the duration of mIL-7 neutralization increased. The frequency of Vκ-Kde and IntronRSS-Kde rearrangements was significantly greater after 7 days of IL-7 neutralization, whereas the increase in Vκ-Jκ rearrangements was close to significant (P = .064). *IGL* locus rearrangements showed a trending increase in CD127+ cells in the presence of neutralizing anti–mIL-7. There was no change in VH to DJH rearrangements. Rearrangements in CD127− cells are shown for comparison, and demonstrate high levels of rearrangements at the L-chain loci, as shown in Figure 2. Therefore, inhibition of IL-7R signaling initiates Ig light-chain rearrangements in human precursor B cells.

Table 3. Gene expression in freshly isolated B-lineage cell subsets from pediatric BM* and sorted CD19⁺CD127⁺ and CD19⁺CD127⁻ cells from 4-week xenogeneic cultures

Gene	Probe set	CD34⁺ lin−	Pre-pro-B	Pro-B	Pre-B large	Pre-B small	imma-ture B	CD127⁺	CD127⁻	CD127⁺ vs CD127⁺, fold difference	CD127⁺ vs CD127⁺, fold difference
Survival/proliferation											
CD127 (IL7R)	226218_at	114.5	681.6	377.1	919.8	706.5	630.8	5242.1	2074.0	-2.5‡	-5.6#
STAT5A	203010_at	1085.3	1201.7	693.3	456.5	523.2	375.9	468.4	448.5	1.0	ND
STAT5B	205026_at	76.2	116.1	158.1	128.5	99.5	109.6	97.2	82.4	-1.2	ND
CCND2	200951_s_at	332.5	377.9	167.5	130.9	99.0	117.1	334.5	135.9	-2.5‡	-5.0¶
SLC2A1	201250_s_at	263.0	255.5	295.3	409.3	370.1	458.3	376.9	244.8	-1.5	-1.4§
BCL2	203685_at	117.8	283.9	144.5	143.7	76.4	110.3	796.7	283.7	-2.8‡	ND
BCL6	203140_at	383.8	1006.1	367.7	759.3	798.0	1292.0	470.6	645.0	1.4‡	ND
MCL1	200797_s_at	4372.5	5049.2	3264.3	4421.2	5347.8	4184.0	1786.4	1538.9	-1.2	ND
MKI67	212021_s_at	134.1	533.0	1082.9	1562.2	578.9	1025.0	900.0	460.9	-2.0‡	ND
Ig rearrangement											
IGH	209374_s_at	2814.2	5512.7	7720.9	13182.0	14308.4	14294.9	4709.9	8866.8	1.9	ND
IGKC	224795_x_at	437.2	320.3	4931.0	12559.6	12982.2	11829.2	1698.8	5090.4	3.0‡	1.8§
IGLC	234764_x_at	106.3	63.6	93.0	150.9	383.6	269.6	86.1	208.2	2.4‡	ND
RAG1	206591_at	38.1	99.7	780.6	146.0	534.5	51.8	898.9	3160.0	3.5‡	6.7#
RAG2	215117_at	24.6	70.9	389.9	219.2	289.8	58.7	657.1	1186.5	1.8‡	1.9§
LIG4	227766_at	52.4	37.6	253.7	93.3	215.0	120.5	269.2	780.6	2.9‡	ND
XRCC4	210813_s_at	40.6	45.9	66.5	75.3	53.3	61.6	199.2	133.6	-1.5‡	ND
EZH2	203358_s_at	216.6	1094.0	1627.9	1503.6	1046.8	1175.2	2763.2	2056.0	-1.3‡	-2.5
DNTT	210487_at	117.9	9204.1	14100.0	1860.8	2970.3	943.7	2728.3	4067.0	1.5	2.2§
IGLL	206660_at	413.9	2378.5	6067.5	5344.0	3150.2	2447.8	2330.3	2730.3	1.2	1
VPREB1	221349_at	60.6	1365.2	4780.5	3257.6	3175.3	1882.2	1793.3	3753.6	2.1	1.8§

Transcription factors

TCF3	209153_s_at	648.9	1599.9	3078.6	3917.8	3805.8	1805.9	2259.9	4272.3	1.9‡ 1.5§
EBF1	229487_at	134.2	980.4	1124.6	1072.3	946.3	744.0	1389.4	2245.7	1.6‡ 1.3
FOXO1	202723_s_at	2784.6	1108.4	4723.5	3275.3	3672.9	985.0	2758.4		2.8‡ 2.7¶
FOXO3	204131_s_at	4404.1	4002.6	2646.4	691.8	1026.1	686.4	541.2	643.4	1.2 1.1
ID2	201565_s_at	1738.6	384.3	727.1	1071.5	761.5	864.9	1461.3	787.4	-1.9‡ -2.9§
IKZF1	227346_at	676.3	760.0	988.7	1139.8	885.1	1152.6	2956.7	3374.2	1.1 -1.1
IRF4	204562_at	120.8	280.4	1068.1	4161.9	5581.8	3580.5	1179.8	2652.8	2.2‡ 4.3§
IRF8	204057_at	530.5	911.0	560.4	729.6	543.7	2693.6	795.4	559.2	-1.4 -1.2
PAX5	221969_at	83.6	2709.9	4850.0	6006.2	7351.0	6083.7	4152.5	5177.0	1.2 1.2
Other										
CD19	206398_s_at	100.1	310.3	2104.5	5010.5	6853.9	4997.7	3469.2	3621.7	1.0 -1.5
CD22	38521_at	255.3	2038.1	1316.3	2086.9	1833.0	1841.4	732.3	958.5	1.3 ND
CD79a	205049_s_at	190.4	3114.3	2194.5	5099.8	2450.2	3802.6	1748.8	1445.9	-1.2 1
CD79b	205297_s_at	154.3	2338.0	6444.1	8468.3	9375.5	4908.8	3257.4	7916.3	2.4‡ ND
CD98 (SLC3A2)	200924_s_at	413.0	636.1	555.7	696.8	414.0	774.2	494.5	275.9	-1.8 ND
CD98 (SLC7A5)	201195_s_at	1215.8	1733.8	876.9	1697.9	1375.3	2014.7	968.1	151.0	-6.4‡ ND

- ND indicates not determined.
- * The results for CD34+Lin−, pre-pro-B, pro-B, pre-B large, pre-B small, and immature B were obtained from a new analysis on previously published data.[25]
- † The -fold difference was calculated by determining the absolute value of the ratio of transcript expression between each population. Values were assigned a negative value if gene expression was higher in CD127+ compared with CD127− and values were assigned a positive value if gene expression was higher in CD127− compared with CD127+. Left column is microarray data and right column is quantitative RT-PCR data.
- ‡ Statistically significant difference between CD127+ and CD127− cells based on DNA microarray data.
- § P < .05 as determined by Student t test on quantitative RT-PCR data.; ¶ P < .01 as determined by Student t test on quantitative RT-PCR data.
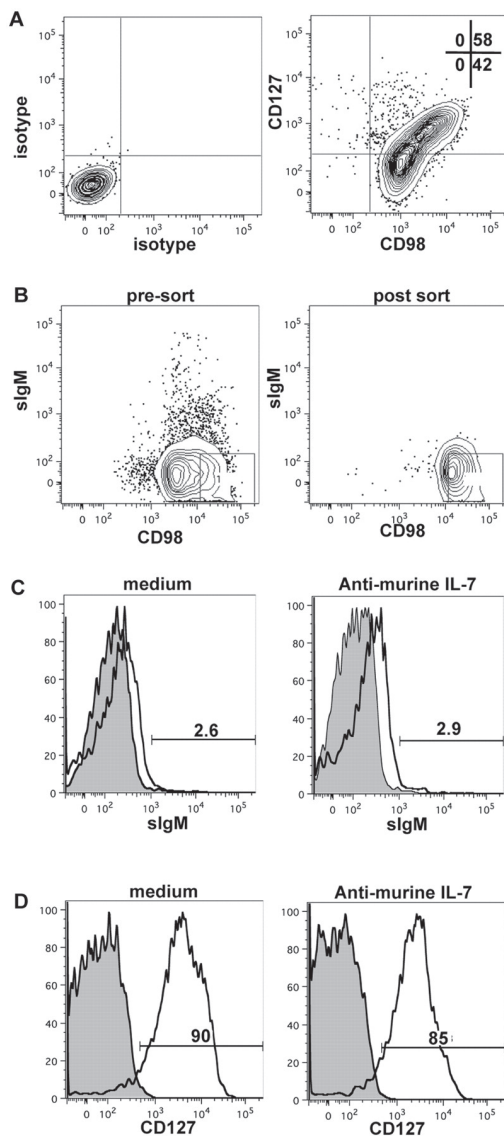- # P < .001 as determined by Student t test on quantitative RT-PCR data.

Figure 6. Effect of neutralizing murine IL-7 on CD127 and surface IgM expression on sorted CD98hi (CD127+) cells.
(A) CD19+ cells from MS-5 xenogeneic cultures were stained for expression of CD98 and CD127; the expression of CD127 is correlated with high CD98 expression. (B) Pre-sort sIgM and CD98 phenotype (left), post-sort analysis of sorted sIgM-CD98hi cells (middle), and CD127 expression on sorted sIgM-CD98hi (right). (C-D) Surface IgM (C) and CD127 (D) expression on CD19+CD98hisIgM− cells after 6 days of culture on MS-5 in the absence or presence of neutralizing anti–mIL-7. Filled histograms indicate unstained control cells (B-D).
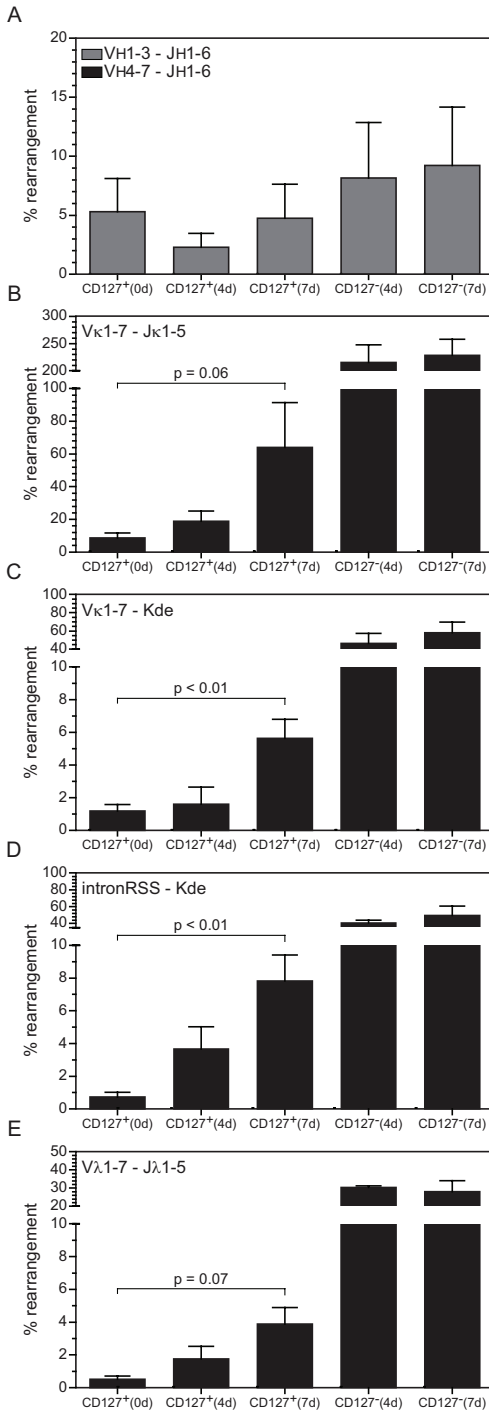
A

B

C

D

E

II

Figure 7. IL-7R signaling and complete Ig gene rearrangements.

(A-E) The levels of VH-DJH, Vκ-Jκ, Vκ-Kde, IntronRSS-Kde, and Vλ-Jλ rearrangements were quantified as in Figure 2 in FACS-purified CD127$^+$ and CD127$^-$ populations from cultures in which endogenous IL-7 was neutralized for either 4 or 7 days. Each bar represents the mean $\pm$ SD of triplicate experiments except CD127$^+$ (0 days), which represents quadruplicate values (the triplicate values from Figure 2 plus 1 additional experiment donor matched to one of the experiments in which IL-7 was neutralized).

DISCUSSION

We embarked on this study with the expectation that evaluating human B-lineage cells that are competent versus incompetent to respond to IL-7 would facilitate our understanding of how development of the human immune system is regulated. The MS-5 murine stromal cell line[17–22] and human BM mesenchymal stromal cells[24,26] have both been useful for analyzing the development of human B-lineage cells. However, an advantage of the MS-5 xenogeneic model is the opportunity to analyze the contribution of stromal cell–derived IL-7 to the developmental biology of human B-lineage cells. Such an analysis requires that IL-7 signaling can be controlled, and the efficiency of neutralizing anti–IL-7 in the xenogeneic model fulfills this important criterion. The goals of the current study were: (1) to undertake a comprehensive analysis of Ig gene rearrangements in CD127$^+$ and CD127$^-$ cells present in MS-5 xenogeneic cultures, and (2) to determine whether CD127 expression and/or IL-7 signaling conferred functional consequences on Ig gene rearrangement and global gene expression in B-cell precursors.

The MS-5 xenogeneic model can support up to 30% of CD19$^+$ B-lineage cells expressing cell-surface Igμ (Figure 1D). This is similar to the frequency of CD19$^+$/cell-surface Igμ$^+$ B-lineage cells in normal human BM and comparable to results using human BM mesenchymal stromal cells.[26,37] However, we focused on earlier time points in the xenogeneic model: 4 weeks, at which time the cultures are enriched for cells that do not express cell-surface Igμ. CD127$^+$ and CD127$^-$ populations derived from 4-week cultures both have a small fraction of cells expressing Igμ, in agreement with the low frequency of complete VDJ$_H$ rearrangements determined by quantitative RT-PCR (Figure 2B). However, it is unclear why V$_H$ to DJ$_H$ rearrangements exist at low frequency (Figure 2B), when the frequency of DJ$_H$ rearrangements is much higher (Figure 2A). One approach to answering this question was to use 3D FISH to assess the nuclear topography of the *IGH* locus. Murine studies have shown that the entire repertoire of V$_H$ genes juxtaposes to D$_H$ elements at the pro-B-cell stage,[32] which means that the locus undergoes contraction. A comparable analysis of *IGH* locus topography has not been reported for human B-lineage cells. Therefore, we initially addressed whether freshly isolated pediatric pro-B and pre-B cells show differences in *IGH* locus contraction. As shown in Figure 4B-D, pro-B cells exhibit significantly greater *IGH* locus contraction than pre-B cells, as measured by the 3 probe sets. Analysis of *IGH* locus contraction showed that CD127$^+$ cells are less contracted than normal pediatric BM pro-B cells (Figure 4B-D), providing at least one potential explanation for the low frequency of VDJ$_H$ rearrangements in CD127$^+$ cells. In the case of CD127$^-$ cells, only one probe set (distal V$_H$-proximal V$_H$; Figure 4C) showed a significant difference compared with normal pro-B cells. Pax5 gene–targeted mice harbor early B-lineage cells that are severely impaired in their capacity to undergo V$_H$ to DJ$_H$ rearrangement,[38] and Pax5 also promotes IGH locus contraction[39] and transactivates the RAG complex.[40] PAX5 expression in CD127$^+$ and CD127$^-$ cells from xenogeneic cultures was comparable to expression in normal pro-B cells (Table 3), suggesting that simple differences in PAX5 expression do not explain why complete VDJ$_H$ rearrangements occur at low frequency in cells from 4-week xenogeneic cultures. It remains possible that the subcellular distribution of Pax5, expression of different Pax5 isoforms, or Pax5 transcriptional activity differ in CD127$^+$ and CD127$^-$ cells in 4-week xenogeneic

cultures compared with normal BM pro-B cells.

Both CD127^{+} and CD127^{−} populations have a small number of cells expressing cell-surface Igμ/κ or Igμ/λ (Figure 1C). Surprisingly, analysis of Ig light-chain locus recombination revealed extensive rearrangements in CD127^{−} cells that greatly exceeded CD127^{+} cells (Figure 2C). There are several possible explanations for the existence of CD19^{+}CD127^{−} cells with extensive Ig light-chain rearrangements but few VDJ$_H$ rearrangements, including heightened recombinatorial flexibility[41,42] and Igμ$_H$ chain deficiency.[43] However, Ig light-chain rearrangement before Ig heavy chain rearrangement still appears to be a rare event. CD19^{+}CD127^{−} cells may be normally destined to die in the BM because of the absence of a functional V$_H$ to DJ$_H$ rearrangement. In this scenario, they would likely be eliminated (after cell death) by macrophages and would be difficult to detect in vivo. Their presence in xenogeneic cultures may reflect the absence of a normal clearing mechanism.

The high level of Vκ-Jκ rearrangements present in CD127^{−} cells (Figure 2C) may have been due to amplification of Vκ-Jκ rearrangements present on excision circles formed by ongoing rearrangements between upstream Vκ and downstream Jκ gene segments. It is also possible that the elevated number of Vκ-Jκ rearrangements included in-frame *IGK* rearrangements, which would predict that cytoplasmic Igκ protein should be present (and in a larger fraction of cells than those expressing the BCR; Figure 1B). However, efforts to detect cytoplasmic Igκ protein by flow cytometry or Western blotting were inconclusive, suggesting that Igκ protein levels may be beneath the sensitivity of the assays we used. This could be a consequence of a low rate of transcription and/or translation of Igκ in these small, resting cells, or Igκ proteins may have a short half-life in the absence of pairing with Igμ.

Figure 1D shows that xenogeneic cultures can support the development of immature (Igμ[+]Igδ[−]) and naive mature (Igμ[+]Igδ[+])populations. CD127 expression and IL-7 signaling are generally assumed to be restricted to cells that have not reached the immature/naive mature B-cell stage.[44,45] However, we found that ~ 25% of peripheral blood B cells expressd CD127 (Figure 1A), as did cord blood transitional (CD10^{+}IgM^{+}IgD^{+}) and naive mature (CD10^{−} IgM^{+}IgD^{+}) B cells (S.E.N. and T.W.L, unpublished data, March 2010). The detection of CD127 on immature/naive B cells was unexpected, and the functional significance is under investigation. Therefore, the CD127^{+}BCR^{+} cells that develop in xenogeneic cultures (Figure 1C) could be developmentally similar to the CD127^{+}BCR^{+} cells we detect in peripheral and cord blood.

IGH rearrangements in pediatric BM pro-B cells occur in the presence of high levels of TdT.[23] These rearrangements therefore have a high content of N-nucleotides, which are retained in pre-B cells (Figure 3A-B). The rare Vκ-Jκ rearrangements present in pro-B cells contain several N-nucleotides, whereas the high levels of Vκ-Jκ rearrangements in pre-B cells contain significantly fewer N-nucleotides (Figure 3C). In contrast to pediatric BM, cord blood B cells contain fewer N-nucleotides in *IGH* gene rearrangements (Figure 3A-B). CD127^{+} and CD127^{−} cells showed few N-nucleotides, resulting in junctions that were significantly smaller than the *IGH* junctions formed in pediatric BM pro-B cells and in cord blood B cells. Therefore, the B cells that develop from cord blood CD34^{+} HPCs plated on MS-5 may have a more restricted V$_H$ repertoire, likely reflecting the lower expression of TdT.

Gene-array analysis using unbiased hierarchical clustering indicated was further used to characterize CD127^{+} and CD127^{−} populations. The blastic features of CD127^{+} cells—

the absence of VDJ$_H$ rearrangements and decreased expression of genes associated with VDJ$_H$ rearrangement—suggests a resemblance to pro-B cells/large pre-B cells. By contrast, CD127⁻ cells are morphologically small cells[17] and have a high frequency of Ig light-chain gene rearrangements and increased expression of RAG1 and RAG2. Excluding the absence of complete VDJH rearrangements in the majority of CD127⁻ cells, this population most closely resembles small pre-B cells. Pro-B and pre-B populations in normal pediatric BM contain both CD127⁺ and CD127⁻ subpopulations (Figure 1A). Future studies comparing CD19⁺CD127⁺ and CD19⁺CD127⁻ cells from xenogeneic cultures with subpopulations isolated from normal pediatric BM will be informative, and these complementary approaches will yield deeper insights into the developmental biology of the human immune system.

E2A proteins have been shown to promote access to the Jκ1 RSS by RAG1 and RAG2,[46] and can induce recombination at the Igκ locus when coexpressed with RAG proteins in nonlymphoid cells. In the present study, increased levels of E2A transcripts were detected in CD127⁻ cells compared with CD127⁺ cells (Table 3), but whether this is an instructive or permissive event for Ig light-chain rearrangement before complete *IGH* rearrangement is unknown. The increased expression of Foxo1 in CD127⁻ cells could reflect the heightened expression of RAG1 and RAG2, because Foxo1 is known to regulate expression of these genes in the mouse.[47,48]

Several studies have reported that IL-7 signaling leads to changes in chromatin accessibility at the *Igh* locus via induction of histone acetylation at distal V$_H$ genes.[9,10,12,49] Malin et al readdressed the role of STAT5 and IL-7 signaling using murine pro-B cells with a conditional deletion in the *Stat5* gene,[15] and found that IL-7 signaling did not regulate V$_H$ expression, but rather functioned to suppress rearrangement at the Igk locus in pro-B cells that had not completed a functional V$_H$ to DJ$_H$ rearrangement. This represents a change in our mechanistic understanding of how IL-7 functions in regulating Ig rearrangement in the mouse. Given that human B-cell development in the murine MS-5 xenogeneic culture depends on IL-7 signaling,[17,18] we exploited this model to determine whether IL-7 might function to suppress human *IGK* rearrangements. The results shown in Figure 7 reveal that CD127⁺ cells isolated from IL-7–neutralized cultures had increased *IGK* rearrangements but no change in *IGH* rearrangements. Furthermore, results shown in Figure 6 reveal that the increase in *IGK* rearrangements is not (1) likely to be explained by a simple loss of CD127⁺ cells and concomitant enrichment of CD127⁻ cells, and (2) accompanied by an increase in cell-surface Igμ or differentiation of CD127⁺ cells into CD127⁻ cells. This may be the most definitive function yet ascribed to a role for IL-7 signaling in human B-cell development and appears to be conserved between mice and humans.

Despite the widely cited T⁻/B⁺/NK⁺ phenotype in SCID patients with mutations in *IL2RG*, *IL7R*, and *JAK3*[15,16] as evidence that human B-cell development does not require IL-7 signaling, evidence supporting a role for IL-7 signaling in BM B-lineage cell proliferation in vivo has been described. In a phase 1 trial of recombinant human IL-7 therapy for T-cell reconstitution in 16 cancer patients, a statistically significant increase in the frequency of BM CD19⁺CD45^{dim} and CD19⁺CD10⁺ cells was observed after treatment in approximately 80% of patients.[50] Based on the results in the present study, it is possible that these SCID patients have promiscuous *IGK* rearrangements in cells with incompletely rearranged *IGH* loci because of the absence of IL-7 signaling. Future studies

investigating the rearrangement status of the Ig loci in B-lineage cells from these SCID patients will be important to validate the consequences of IL-7 signaling described herein.

In conclusion, we report unappreciated functional relationships between the expression of the IL-7R, IL-7 signaling, and Ig gene rearrangement in human B-lineage cells. These relationships were delineated using a model wherein CD127^{+} and CD127^{−} B-lineage cells develop from CD34^{+} HPCs and B-cell development is IL-7 dependent. The emergence of CD19^{+}CD127^{+} cells provided the means to examine the role of IL-7 signaling and led to the revelation that suppression of *IGK* rearrangement before the onset of VDJ[H] rearrangement is the most specific function yet attributable to IL-7 in human B-cell development. Similarly, the absence of IL-7 signaling in CD127^{−} B-lineage cells was associated with extensive *IGK* and some *IGL* gene rearrangements, and this was independent of *IGH* gene rearrangements. Stochastic differences in this regulatory network at the single-cell level could lead to asynchronous (premature) *IGK* and *IGL* rearrangements and thereby to dysfunctional rearrangements. The xenogeneic model was invaluable for the generation of the new results reported herein, but further studies will be necessary to validate and extend its physiologic relevance. Future studies will be needed to explore the network position of IL-7 signaling in the suppression of *IGK* rearrangement in mice and in humans to determine differences in the effect of IL-7 on proliferation.

II

ACKNOWLEDGMENTS

REFERENCES

1. Hardy RR, Kincade PW, Dorshkind K. The protean nature of cells in the B lymphocyte lineage.*Immunity*. 2007;26(6):703-714.
2. LeBien TW, Tedder TF. 2008. B lymphocytes: how they develop and function. *Blood*. 2008; 112(5):1570-1580.
3. Chowdhury D, Sen R. Regulation of immunoglobulin heavy chain rearrangements. *Immunol Rev*. 2004;200:182-196.
4. Jung D, Giallourakis C, Mostoslavsky R, Alt FW. Mechanism and control of V(D)J recombination at the immunoglobulin heavy chain locus. *Annu Rev Immunol*. 2006;24:541-570.
5. Fugmann FD, Lee AI, Shockett PE, Villey IJ, Schatz DG. The RAG proteins and V(D)J recombination: complexes, ends, and transposition. *Annu Rev Immunol*. 2000;18:495-527.
6. Gellert M. V(D)J recombination: RAG proteins, repair factors and regulation. *Annu Rev Biochem*. 2002;71:101-132.
7. Herzog S, Reth M, Jumaa H. Regulation of B-cell proliferation and differentiation by pre-B-cell receptor signaling. *Nat Rev Immunol*. 2009;9(3):195-205.

8. Nutt SL, Kee BL. The transcriptional regulation of B cell lineage commitment. *Immunity*. 2007;26(6):715-725.

9. Corcoran AE, Riddell A, Krooshoop D, Venkitaraman AR. Impaired immunoglobulin gene rearrangement in mice lacking the IL-7 receptor. *Nature*. 1998;391(6670):904-907.

10. Bertolino E, Reddy K, Medina KL, Parganas E, Ihle J, Singh H. Regulation of interleukin 7-dependent immunoglobulin heavy-chain variable gene rearrangements by transcription factor STAT5. *Nat Immunol*. 2005;6(8):836-843.

11. Kikuchi K, Lai AY, Hsu C-L, Kondo M. IL-7 receptor signaling is necessary for stage transition in adult B cell development through up-regulation of EBF. *J Exp Med*. 2005;201(8):1197-1203.

12. Stanton ML, Brodeur PH. 2005. Cutting Edge: Stat5 mediates the IL-7-induced accessibility of a representative D-distal VH gene. *J Immunol*. 2005;174(6):3164-3168.

13. Malin S, McManus S, Cobaleda C, et al. Role of STAT5 in controlling cell survival and immunoglobulin gene recombination during pro-B cell development. *Nat Immuno*l. 2010;11(2):171-179.

14. LeBien TW. Fates of human B-cell precursors. *Blood*. 2000;96(1):9-23.

15. Buckley RH. Molecular defects in human severe combined immunodeficiency and approaches to immune reconstitution. *Annu Rev Immunol*. 2004; 22:625-655.

16. Giliani S, Mori L, Basile GS, et al. Interleukin-7 receptor (IL-7Ralpha) deficiency; cellular and molecular bases: analysis of clinical, immunological, and molecular features in 16 novel patients. *Immunol Rev*. 2005;203:110-126.

17. Johnson SE, Shah N, Panoskaltsis-Mortari A, LeBien TW. Murine and human IL-7 activate STAT5 and induce proliferation of normal human pro-B cells. *J Immunol*. 2005;175(11):7325-7331.

18. Johnson SE, Shah N, Bajer AA, LeBien TW. IL-7 activates the phosphatidylinositol 3-kinase/AKT pathway in normal human thymocytes but not normal human B cell precursors. *J Immunol*. 2008;180(12):8109-8117.

19. Berardi AC, Meffre EF, Pflumio F, et al. Individual CD34+CD38lowCD19-CD10- progenitor cells from human cord blood generate B-lymphocytes and granulocytes. *Blood*. 1997;89(10):3554-3564.

20. Nishihara M, Wada Y, Ogami K, et al. A combination of stem cell factor and granulocyte colonystimulating factor enhances the growth of human progenitor B cells supported by murine stromal cell line MS-5. *Eur J Immunol*. 1998;28(3):855-864.

21. Ohkawara JI, Ikebuchi K, Fujihara M, et al. Culture system for extensive production of CD19+IgM+ cells by human cord blood CD34+ progenitors. *Leukemia*. 1998;12(5):764-771.

22. Rossi MI, Yokota T, Medina KL, et al. B lymphopoiesis is active throughout human life, but there are developmental age-related changes. *Blood*. 2003;101(2):576-584.

23. van Zelm MC, van der Burg M, de Ridder D, et al. Ig gene rearrangement steps are initiated in early human B cell precursor subsets and correlate with specific transcription factor expression. *J Immunol.* 2005;175(9):5912-5922.

24. Dittel BN, LeBien TW. The growth response to IL-7 during normal human B cell ontogeny is restricted to B-lineage cells expressing CD34. *J Immunol*. 1995;154(1):58-67.

25. Hystad ME, Myklebust JH, Bo TH, et al. Characterization of early stages of human B cell development by gene expression profiling. *J Immunol.* 2007;179(6):3662-3671.

26. Parrish YK, Baez I, Milford T-A, et al. IL-7 dependence in human B lymphopoiesis increases during progression of ontogeny from cord blood to bone marrow. *J Immunol*. 2009;182(7):4255-4266.

27. Rao SP, Riggs JM, Friedman DF, Scully MS, LeBien TW, Silberstein LE. Biased VH usage in early lineage human B cells: evidence for preferential Ig gene rearrangement in the absence of selection. *J Immunol*. 1999;163(5):2732-2740.

28. Langerak AW, Nadel B, De Torbal A, et al. Unraveling the consecutive recombination events in the human IGK locus. *J Immunol*. 2004;173(6):3878-3888.

29. van der Burg M, Tumkaya T, Boerma M, de Bruin-Versteeg S, Langerak AW, van Dongen JJ. Ordered recombination of immunoglobulin light chain genes occurs at the IGK locus but seems less strict at the IGL locus. *Blood*. 2001;97(4):1001-1008.

30. Sims GP, Ettinger R, Shirota Y, Yarboro CH, Illei GG, Lipsky PE. Identification and characterization of circulating human transitional B cells. *Blood*. 2005;105(11):4390-4398.

31. Sayegh T, Jhunjhunwala S, Riblet R, Murre C. Visualization of looping involving the immunoglobulin heavy-chain locus in developing B cells. *Genes Dev*. 2005;19(3):322-327.

32. Jhunjhunwala S, van Zelm MC, Peak MM, et al. 3D-Architecture of the immunoglobulin heavy chain locus: implications for long-range genomic interactions. Cell. 2008;133(2):265-279.

33. Kosak ST, Skok JA, Medina KL, et al. Subnuclear compartmentalization of immunoglobulin loci during lymphocyte development. *Science*. 2002; 296(5565):158-162.
34. Rolda´n E, Fuxa M, Chong W, et al. Locus 'decontraction' and centromeric recruitment contribute to allelic exclusion of the immunoglobulin heavychain gene. *Nat Immunol*. 2005;6(1):31-41.
35. Poulsen TS, Silahtaroglu AN, Gisselø CG, et al. Detection of illegitimate rearrangement within the immunoglobulin locus on 14q32.3 in B-cell malignancies using end-sequenced probes. *Genes Chromosomes Cancer*. 2001;32(3):265-274
36. Duy C, Yu JJ, Nahar R, et al. Bcl-6 is critical for the development of a diverse primary B cell repertoire. *J Exp Med*. 2010;207(6):1209-1221.
37. Prieyl JA, LeBien TW. Interleukin 7 independent development of human B cells. *Proc Natl Acad Sci U S A*. 1996;93(19):10348-10353.
38. Urba´nek P, Wang ZQ, Fetka I, Wagner EF, Busslinger M. Complete block of early B cell differentiation and altered patterning of the posterior midbrain in mice lacking Pax5/BSAP. *Cel*l. 1994; 79(5):901-912.
39. Fuxa M, Slok J, Souabni A, Salvagiotto G, Roldan E, Busslinger M. Pax5 induces V-to-DJ rearrangements and locus contraction of the immunoglobulin heavy-chain gene. *Genes Dev*. 2004;18(4):411-422.
40. Zhang Z, Espinoza CR, Yu Z et al. Transcription factor Pax5 (BSAP) transactivates the RAG-mediated VH-to-DJH rearrangement of immunoglobulin genes. Nat Immunol. 2006;7(6):616-624.
41. Kubagawa H, Cooper MD, Carroll AJ, Burrows PD. Light chain gene expression before heavy chain gene rearrangement in pre-B cells transformed by Epstein-Barr virus. *Proc Natl Acad Sci U S A*. 1989;86(7):2356-2360.
42. Novobrantseva TI, Martin VM, Pelanda R, Muller W, Rajewsky K, Ehlich A. Rearrangement and expression of immunoglobulin light chain genes can precede heavy chain expression during normal B cell development in mice. *J Exp Med*. 1999;189(1):75-88.
43. Meffre E, Milili M, Blanco-Betancourt C, Antunes H, Nussenzweig MC, Schiff C. Immunoglobulin heavy chain expression shapes the B cell repertoire in human B cell development. *J Clin Invest*. 2001;108(6):879-886.
44. Milne CD, Paige CJ. IL-7: a key regulator of B lymphopoiesis. Semin Immunol. 2006;18(1):20-30.
45. Mazzucchelli R, Durum SK. Interleukin-7 receptor expression: intelligent design. *Nat Rev Immunol*.2007;7(2):144-154.
46. Romanow WJ, Langerak AW, Goebel P, et al. E2A and EBF act in synergy with the V (D) J recombinase to generate a diverse immunoglobulin repertoire in nonlymphoid cells. *Mol Cell*. 2000; 5(2):343-353.
47. Dengler HS, Barocho GV, Omori SA, et al. Distinct functions for the transcription factor Foxo1 at various stages of B cell differentiation. *Nat Immunol*. 2008;9(12):1388-1398.
48. Amin RH, Schlissel MS. Foxo1 directly regulates the transcription of recombination activating genes during B cell development. *Nat Immunol*. 2008;9(6):613-622.
49. Chowdhury D, Sen R. Stepwise activation of the immunoglobulin mu heavy chain gene locus. *EMBO J*. 2001;20(22):6394-6403.
50. Sporte`s C, Babb RR, Krumlauf MC, et al. Phase I study of recombinant human interleukin-7 administration in subjects with refractory malignancy. *Clin Cancer Res*. 2010;16(2):727-735.

II

III

Human memory B cells originate from three distinct germinal center-dependent and -independent maturation pathways

Magdalena A. Berkowska[1], Gertjan J.A. Driessen[1,2], Vasilis Bikos[3], Christina Grosserichter-Wagener[1], Kostas Stamatopoulos[3,4], Andrea Cerutti[5,6], Bing He[6], Katharina Biermann[7], Johan F. Lange[8], Mirjam van der Burg[1], Jacques J.M. van Dongen[1], and Menno C. van Zelm[1]

Departments of [1]Immunology and [2]Pediatrics, Erasmus MC, Rotterdam, The Netherlands; [3]Hematology Department and HCT Unit, G. Papanicolaou Hospital, Thessaloniki, Greece; [4]Institute of Agrobiotechnology, Center for Research and Technology, Thessaloniki, Greece; [5]Catalan Institute for Research and Advanced Studies, Municipal Institute of Medical Research (IMIM)–Hospital del Mar, Barcelona, Spain; [6]The Immunology Institute, Department of Medicine, Mount Sinai School of Medicine, New York, NY; and Departments of [7]Pathology and [8]Surgery, Erasmus MC, Rotterdam, The Netherlands

ABSTRACT

Multiple distinct memory B-cell subsets have been identified in humans, but it remains unclear how their phenotypic diversity corresponds to the type of responses from which they originate. Especially, the contribution of germinal center-independent responses in humans remains controversial. We defined 6 memory B-cell subsets based on their antigen-experienced phenotype and differential expression of CD27 and IgH isotypes. Molecular characterization of their replication history, Ig somatic hypermutation, and class-switch profiles demonstrated their origin from 3 different pathways. CD27$^-$IgG$^+$ and CD27$^+$IgM$^+$ B cells are derived from primary germinal center reactions, and CD27$^+$IgA$^+$ and CD27$^+$IgG$^+$ B cells are from consecutive germinal center responses (pathway 1). In contrast, natural effector and CD27$^-$IgA$^+$ memory B cells have limited proliferation and are also present in CD40L-deficient patients, reflecting a germinal center-independent origin. Natural effector cells at least in part originate from systemic responses in the splenic marginal zone (pathway 2). CD27$^-$IgA$^+$ cells share low replication history and dominant Igλ and IgA2 use with gut lamina propria IgA$^+$ B cells, suggesting their common origin from local germinal center-independent responses (pathway 3). Our findings shed light on human germinal center-dependent and -independent B-cell memory formation and provide new opportunities to study these processes in immunologic diseases.

The online version of this article contains supplemental material.

INTRODUCTION

Antigen-specific memory formation after a primary infection contributes greatly to human health. Immunologic memory lies in long-lived T and B cells derived from the initial immune response. Precursor B cells develop from hematopoietic stem cells in the bone marrow and create a unique receptor by V(D)J recombination in their immunoglobulin (Ig) loci.[1–3] After antigen recognition, mature B cells proliferate and can further optimize antigen-binding by the introduction of point mutations in the V(D)J exons of their Ig heavy and light chains (somatic hypermutations; SHMs) and the subsequent selection for high-affinity mutants.[4] Furthermore, the antibody effector functions can be modified by changing the isotype of the *IGH* constant region from μ to α, δ, ϵ, or γ (Ig class-switch recombination; CSR).[5] Both processes are mediated by activation-induced cytidine deaminase (AID), which preferentially targets specific DNA motifs.[6,7]

In addition to antigen recognition via the B-cell antigen receptor (BCR), B cells need a second signal to become activated.[8] Activated T cells can provide such a signal via CD40L that interacts with CD40 on B cells. T cell–dependent B-cell responses are characterized by germinal center (GC) formation, extensive B-cell proliferation, affinity maturation, and Ig CSR.[9] Thus, high-affinity memory B cells and Ig-producing plasma cells are formed. In addition, B cells can respond to T cell–independent (TI) antigens that either activate via the BCR and another (innate) receptor (TI-1) or via extensive cross-linking of the BCR because of the repetitive nature of the antigen (TI-2).[10] TI responses are directed against blood-borne pathogens in the splenic marginal zone and in mucosal tissues (reviewed in Cerutti *et al*[11] and Weill *et al*[12]).

A substantial fraction of B cells in blood of human subjects has experienced antigen and shows hallmarks of memory B cells: SHMs of rearranged Ig genes and fast recall responses to antigen.[13] Initially, human memory B cells were identified based on the expression of CD27.[14,15] IgA and IgG class-switched CD27+ B cells are derived from T cell–dependent responses in the GC and contain high loads of SHMs in their Ig genes.[16–18] CD27+IgM+ B cells contain less SHMs but show molecular footprints of (early) GC generation.[19] Interestingly, in contrast to CD27+IgM+IgD− "IgM-only" cells, CD27+IgM+IgD+ "natural effector" B cells are present in patients with CD40 or CD40L deficiency, indicating that at least part of this subset can be generated independently of T-cell help.[17,20,21] Furthermore, natural effector B cells resemble splenic marginal zone B cells and have a limited replication history compared with GC B cells (both centroblasts and centrocytes) and CD27+IgD− memory B cells.[17,18]

More recently, CD27− IgG and IgA class-switched B cells have been CD27−IgG+ B cells contain fewer SHMs in their Ig genes and have increased IgG3 use compared with their CD27+ counterparts.[22,23] Thus, 6 B-cell subsets have been described to contain genetic hallmarks of B-cell memory. This raises the question whether all these subsets show functional characteristics of memory B cells[25] and whether the phenotypic diversity reflects functional diversity or an origin from different maturation pathways.

We performed detailed analyses on 6 phenotypically distinct memory B-cell subsets, which all seem to display an activated phenotype and molecular signs of antigen recognition. The comparative analyses of replication history, SHM, and CSR profiles of these subsets enabled us to trace their origins to 3 different germinal center-dependent and -independent maturation pathways.

METHODS

Flow cytometric immunophenotyping and purification of B-cell subsets from human peripheral blood, tonsils, and colon

Peripheral blood, tonsil, and colon samples were obtained with informed consent following the Declaration of Helsinki and according to the guidelines of the Medical Ethics Committee of Erasmus MC and the Institutional Review Board of Weill Medical College of Cornell University.

Immunophenotyping and cell sorting details are provided in supplemental Methods (available on the *Blood* Web site; see the Supplemental Materials link at the top of the online article).

Hematoxylin and eosin staining

Up to 30 000 cells from each sorted population were applied to poly-l-lysine–coated slides and stained with Diff-Quik staining set (Medion Diagnostics). Pictures were acquired on an Axioskop microscope using a Plan-NEOFLUAR 63/1.25 oil objective, MRc5 digital camera, and Axio Vision Release 4.8.1 software (Carl Zeiss).

CD40L-deficient patients

All 5 CD40L-deficient patients lacked expression of CD40L protein on activated T cells as shown after 5-hour stimulation with phorbol 12-myristate 13-acetate (Sigma-Aldrich) and calcium ionophore (Sigma-Aldrich). Mutations were detected by exon sequencing of the *CD40L* gene. Details of the patients are shown in supplemental Table 3.

Sequence analysis of complete *IGH* gene rearrangements and Ig switch regions

DNA was isolated from each sorted subset with the GenElute Mammalian Total DNA Miniprep kit, and RNA was isolated from Ig class-switched B-cell subsets using the GeneElute Mammalian Total RNA Miniprep kit (Sigma-Aldrich). Complete *IGH* gene rearrangements and hybrid switch regions were amplified and analyzed as described in supplemental Methods.

Replication history analysis using the KREC assay

The replication history of sorted B-cell subsets was determined with the Igκ-deleting recombination excision circles (KREC) assay as described previously.[18] In brief, the amounts of coding and signal joints of the *IGK*-deleting rearrangement were measured by real-time quantitative-PCR in DNA from sorted B-cell populations on an ABI Prism 7000 sequence detection system (Applied Biosystems). Signal joints, but not coding joints are diluted 2-fold with every cell division.[18] To measure the number of cell divisions undergone by each population, we calculated the ratio between the number of coding joints and signal joints. The previously established control cell line U698 DB01 (InVivoScribe) contains 1 coding and 1 signal joint per genome and was used to correct for minor differences in efficiency of both real-time quantitative-PCR assays.

IgκREHMA

The frequency of mutated *IGK* alleles was determined with the Igκ restriction enzyme hot-

spot mutation assay (IgκREHMA) as described previously.[18,26] In brief, PCR was performed on genomic DNA using a hexachlorofluorescein phosphoramidite (HEX)–coupled *IGKV3-20* intron forward primer and two 5-carboxyfluorescein–coupled *IGKJ* reverse primers recognizing all 5 *IGKJ* genes. The PCR products were digested by the KpnI and Fnu4HI restriction enzymes and run on an ABI Prism 3130 XL genetic analyzer. Fnu4HI recognizes 2 adjacent sites in the unmutated gene product in the hot-spot region of IGKV-complementarity-determining region (CDR) 1. Unmutated gene products can therefore be visualized as 244- or 247-bp HEX-coupled fragments. KpnI cuts the gene product in FR2 downstream of the Fnu4HI sites, resulting in a 262-bp HEX-coupled mutated fragment. The unmutated B cell line CLL-1 was used as a positive control for complete digestion with Fnu4HI. The digests hardly contained undigested gene products of 481 bp, indicating complete digestion by KpnI.

Statistical analyses
Statistical analyses were performed with the Mann-Whitney U test, or χ^2 test as indicated in details in figure legends. P values < .05 were considered statistically significant.

RESULTS

Phenotypic characterization of memory B-cell subsets in healthy individuals
To study the diversity in the human B-cell compartment, we defined and purified 2 naive and 6 memory B-cell subsets (Figure 1A). Within the CD19+ B-cell compartment, we defined CD38hiCD24hi transitional B cells. CD38dimCD24dim B cells were subdivided based on the expression of IgM and CD27. Naive mature B cells were defined as CD27−IgM+. CD27+IgM+ B cells were separated into IgD+ "natural effector" B cells and IgD− "IgM-only" B cells. Finally, IgM-negative B cells were separated into 4 class-switched B cell populations based on the expression of IgA, IgG, and CD27.

All 8 purified subsets had a typical lymphocytic morphology with a large nucleus and little cytoplasm as observed after hematoxylin and eosin staining (Figure 1B). Furthermore, all 6 memory B-cell subsets showed an immunophenotype that was characteristic for activated cells; with increased expression of the B7 family member CD80, TLR-related CD180, and TNF receptor superfamily member TACI compared with naive B-cell subsets (Figure 1C).[25,27] In addition, all B-cell subsets highly expressed BAFFR, and all memory B-cell subsets showed bimodal expression of inhibitory collagen receptor CD305 and were dimly positive for CD95 (data not shown).[25,28] Thus, all 6 subsets we studied had the phenotype that was reported to be important for fast and powerful memory responses.

Ig repertoire selection in memory B-cell subsets
To study whether the memory B-cell subsets showed molecular signs of antibody selection, we sequenced *IGH* gene rearrangements from sorted fractions of healthy adult donors and compared these with naive B-cell subsets from adult blood as well as with GC B cells from childhood tonsils. We analyzed gene use for the most frequent *IGHV* subgroups: *IGHV3* and *IGHV4*.[29,30] All subsets showed diverse usage of *IGHV3* subgroup genes with *IGHV3-23*, *IGHV3-21*, and *IGHV3-30* predominating (Figure 2A). Naive mature B cells showed

III

dominant use of the *IGHV4-34* and *IGHV4-59* genes (Figure 2B), probably resulting from increased recombination frequency because of highly efficient recombination signal sequences.[31,32] Importantly, *IGHV4-34* was hardly used in memory B-cell subsets, indicating selection against this inherently autoreactive gene.[33,34]

Of the 3 CDRs, the VDJ-junction encoded CDR3 region is the most dominant in establishment of antigen binding specificity. Long IGH-CDR3s are associated with auto- and polyreactivity.[35] We observed diverse IGH-CDR3 sizes in transitional and naive mature B cells, with a median of 17 amino acids (Figure 2C). The median size was slightly reduced to 16 in both centroblasts and centrocytes. All memory B-cell subsets had significantly (P < .05) shorter IGH-CDR3s (median of 14-15 amino acids) compared with naive mature B cells. Thus, all 6 memory B-cell subsets showed comparable signs of Ig repertoire selection.

Distinct degrees of replication history and SHMs in memory B-cell subsets

Typical hallmarks of memory B cells are extensive antigen-induced proliferation and SHMs. We showed previously that GC B cells in tonsils from young children have undergone ~8 cell cycles, by calculating the ratio between genomic coding joints and signal joints on KREC of the *IGK*-deleting rearrangement.[18] This replication history was similar in childhood CD27+IgD− B cells but clearly higher in adulthood CD27+IgD− cells, probably because of consecutive GC reactions. Proliferation of GC B cells was accompanied by SHMs in their Ig loci and further enrichment of mutated *IGKV3-20* alleles in memory B cells, both in children and adults.[18] We quantified the replication history, the frequency of mutated nucleotides in rearranged *IGHV* genes, and the frequency of mutated *IGKV3-20* alleles in 2 naive and all 6 memory B-cell subsets. As shown before, transitional B cells did not undergo proliferation since their release from bone marrow, whereas naive mature B cells underwent ~2 cell cycles in absence of SHMs (Figure 3).[18] Conventional adult CD27+IgG+ and CD27+IgA+ B cells underwent the highest number of cell divisions (~10) with high levels of SHMs. Both proliferation and SHM levels were clearly higher than in GC B cells from childhood tonsils. This might suggest additional proliferation and mutation in consecutive GC reactions.

IgM-only and CD27−IgG+ B cells underwent ~9 cell divisions and had similar SHM levels in rearranged *IGHV* genes as GC B cells but increased frequencies of mutated *IGKV3-20* alleles. The characteristics of both subsets suggest an origin from primary GC responses followed by selection for mutated *IGKV3-20*.

Finally, natural effector and CD27−IgA+ B-cell subsets showed less proliferation compared with GC B cells (Figure 3A). Natural effector B cells showed only 7 cell cycles, whereas the *IGHV* mutation loads were similar to GC B cells, and these cells were enriched for mutated *IGKV3-20* alleles. These proliferation and SHM levels were clearly higher than those observed for natural effector cells in childhood tonsils.[18] Still, these results indicate that a substantial fraction of this population had been generated independently from a GC. Finally, we observed only 4 cell divisions for CD27−IgA+ B cells. Interestingly, the *IGHV* gene mutation loads were increased as compared with GC B cells, although the frequency of mutated *IGKV3-20* alleles was similar. These results indicate a GC-independent origin of CD27−IgA+ B cells but with high AID activity generating high SHM levels and IgA class switching. Still, these cells lacked selection for mutated *IGKV3-20* alleles.

Targeting and selection of SHMs in rearranged *IGHV* genes

We analyzed type and targeting of SHMs in the memory B-cell subsets to obtain insight into the activity of AID, POLη, and UNG. Neither the SHM targeting nor the nucleotide substitution spectra and transition/transversion ratios were significantly different between the memory B-cell subsets and centrocytes (supplemental Table 1 and supplemental Figure 1). Furthermore, the targeting of specific nucleotides in motifs was largely similar between subsets (supplemental Table 2). Thus, we conclude that the differences in mutation frequencies did not result from altered AID, UNG, and Polη activities; rather, they probably reflect the   duration of exposure to these enzymes.

Generally, a high ratio of replacement versus silent mutations (R/S) in IGHV-CDRs is regarded as a molecular sign of affinity maturation. Nevertheless, a clear cut-off value, which would reflect antigenic selection, remains difficult or even impossible to define.[36] We found accumulation of replacement mutations in CDR1 and CDR2 of rearranged *IGHV* genes in all analyzed subsets (supplemental Figure 2). IGHV-CDR R/S ratios were similar between all memory B-cell subsets, ranging between 3.3 and 4.0, except for CD27⁻IgG⁺ B cells that had a slightly lower IGHV-CDR R/S ratio of 2.3 (supplemental Table 1).

Alignment of rearranged *IGHV* genes revealed the existence of recurrent amino acid changes (ie, the same amino acid replacement at the same position) in all except the natural effector, transitional, and naive mature B-cell subsets. In centrocytes, we identified a cluster of 5 sequences with identical VDJ gene use and closely similar if not identical IGH-CDR3s (always of identical length), pointing to their common ancestry. In addition to recurrent mutations, the sequences exhibited a different number and distribution of SHMs, indicating that the process of antigen-driven clonal expansion also was accompanied by intraclonal diversification.

IgG and IgA subclass distribution in class-switched memory B-cell subsets

In addition to differential CD27 expression, both IgG⁺ and both IgA⁺ memory B-cell subsets varied in their replication history and SHM levels (Figure 3). This suggests different origins and functions for the CD27⁺ and CD27⁻ B-cell subsets. Because the constant region of an antibody molecule is important for its function and the human *IGH* locus contains 4 *IGHG* and 2 *IGHA* constant genes (Figure 4A), we studied the Ig subclass use in sequenced *IGH* transcripts. We found a dominant use of *IGHG2* (51%) and *IGHG1* (40%) and low *IGHG3* and *IGHG4* in CD27⁺IgG⁺ cells (Figure 4B). In contrast, CD27⁻IgG⁺ cells showed a dominant use of *IGHG1* (63%) and *IGHG3* (31%) with little *IGHG2* and no *IGHG4*.[22,37] Thus, the CD27⁻IgG⁺ cells showed a dominant use of *IGHM*-proximal *IGHG3* and *IGHG1* regions (94%), whereas this was reduced to only 47% in CD27⁺IgG⁺ cells (P < .0001). Ig CSR to distal constant genes can occur indirectly via an *IGHM*-proximal gene. Analysis of hybrid switch regions (Sμ-Sγ2) in genomic DNA of sorted populations indeed revealed that 24% of junctions had remnants of Sγ3, Sγ1, or Sα1, whereas only 9% of Sμ-Sγ1 junctions had Sγ3 remnants (Figure 4C-D). Furthermore, the *IGHV* genes in *IGHG2* and *IGHG4* transcripts contained higher SHM loads than *IGHG1* and *IGHG3* (supplemental Figure 3A). The (indirect) switching to downstream *IGHG* genes accompanied by increased SHM frequencies suggests more prolonged AID activity in CD27⁺IgG⁺ cells, potentially reflecting multiple GC reactions.
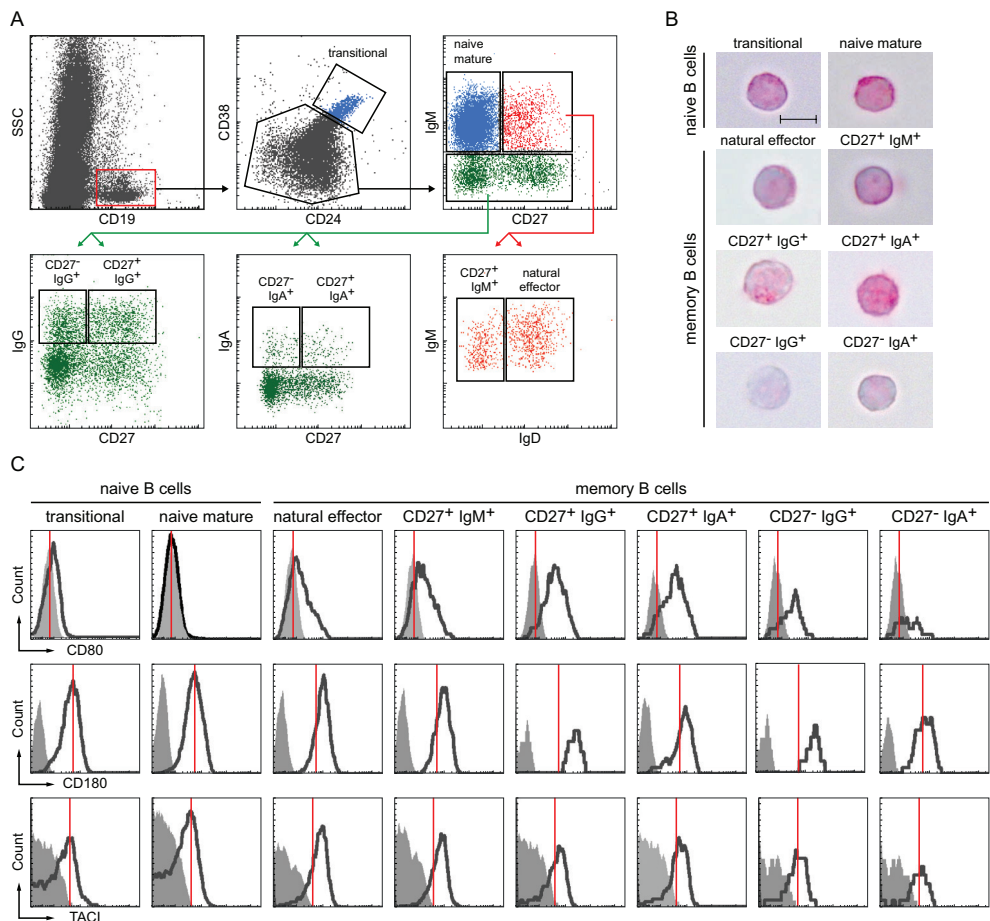
III

Figure 1. Isolation and phenotypic characterization of peripheral blood memory B-cell subsets.
(A) Gating strategy to identify 2 naive and 6 memory B-cell subsets based on expression of CD24, CD38, CD27, and IgH isotypes. (B) H&E staining of sorted subsets revealed a typical lymphocytic morphology with large nucleus (purple) and little cytoplasm (pink; ×63, original magnification; bars represent 5 μm). (C) All 6 memory B cell subsets showed up-regulation of CD80, CD180 and TACI as compared with naive B cells. Expression levels are shown in black and isotype controls as filled, gray histograms. Red lines indicate mode expression levels for each molecule on naive mature B cells.

The IgA$^+$ memory B-cell subsets also showed differential subclass use: CD27$^-$IgA$^+$ memory B cells contained significantly more *IGHA2* transcripts (33%) than CD27$^+$IgA$^+$ memory B cells (19%; Figure 4B; P < .05). Even though *IGHA2* is the most downstream constant gene in the human *IGH* locus (Figure 4A), only 4% of hybrid Sμ-Sα2 regions contained remnants of more proximal S regions (Figure 4C-D), suggesting that most of the switching toward *IGHA2* occurred directly from Sμ. No evidence for indirect class switching was found in Sμ-Sα hybrid switch regions. Furthermore, there was no difference in the mutation frequencies between *IGHA1* and *IGHA2* transcripts (supplemental Figure
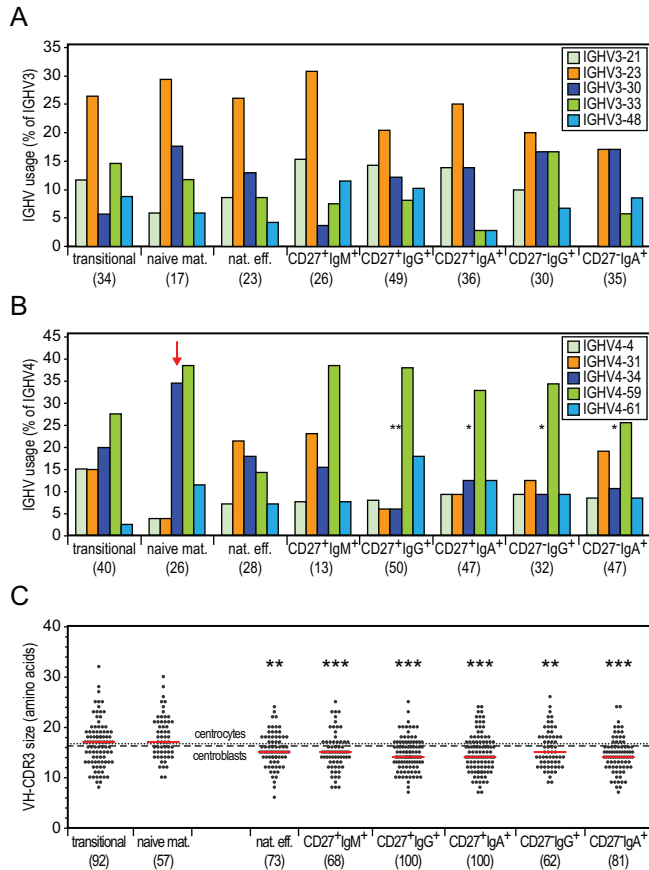
Figure 2. Selection against the *IGHV4-34* gene and long IGH-CDR3s in all 6 memory B-cell subsets.
(A) Frequencies of the most commonly used *IGHV3* genes in cloned *IGH* gene rearrangements. Differences between each memory B-cell subset compared with naive mature B cells were statistically analyzed with the χ^2 test. (B) Frequencies of the most commonly used *IGHV4* genes in cloned *IGH* gene rearrangements. An arrow indicates *IGHV4-34* gene use in naive mature B cells. Differences between each memory B-cell subset compared with naive mature B cells were statistically analyzed with the χ^2 test. $^*P < .05$, $^{**}P < .01$. (C) IGH-CDR3 size distributions. All individual sizes are indicated for each subset as gray dots, with red lines representing the median values. The dashed and dotted lines represent median values for centroblasts (n = 67) and centrocytes (n = 55), respectively. Differences between each memory B-cell subset compared with naive mature B cells were statistically analyzed with the Mann-Whitney test. $^{**}P < .01$, $^{***}P < .001$.

3B). These results imply that switching toward *IGHA2* occurs mainly directly from Sμ and the molecular differences between CD27$^+$IgA$^+$ and CD27$^-$IgA$^-$ memory B cells most likely reflects their generation via separate response pathways, rather than consecutive GC reactions as observed for CD27$^-$IgG$^+$ versus CD27$^+$IgG$^+$ memory B cells.

T cell–independent generation of B-cell memory in CD40L-deficient patients

Replication history analyses indicated a GC-independent origin of natural effector and CD27⁻IgA⁺ B cells. To demonstrate that these subsets can be generated in the absence of the T-cell help, we analyzed their presence in 5 CD40L-deficient patients (supplemental Table 3). We found a clear population of natural effector B cells in CD40L-deficient patients, confirming previous observations that at least part of the blood natural effector B-cell population can be generated independently from T-cell help.[17,20,21,38] Still, this subset was ~3 times reduced in number compared with age-matched healthy controls (Figure 5), highlighting the fact that in healthy controls a major part of this subset has a germinal center origin. More importantly, blood of CD40L-deficient patients also contained CD27⁻IgA⁺ memory B cells, and their numbers were similar compared with healthy controls (Figure 5). Thus, in addition to natural effector cells, T cell–independent humoral responses in human can generate IgA class-switched memory B cells.

CD27⁻IgA⁺ memory B cells resemble colon *lamina propria* IgA⁺ B cells

T cell–independent responses have been demonstrated to generate IgA-producing B cells in the *lamina propria* of human gut.[39,40] Furthermore, these IgA⁺ B cells showed predominant use of *IGHA2*.[41] These similarities with blood CD27⁻IgA⁺ memory B cells encouraged us to study whether these cells had been generated in similar responses. First, we analyzed the replication history of IgA2⁺ B cells isolated from colon *lamina propria*. Similar to CD27⁻IgA⁺ B cells, these cells had proliferated less than GC B cells in childhood tonsils and significantly less than GC-derived CD27⁺IgA⁺ memory B cells in adult blood (Figure 6A). In addition, because it was suggested previously that a broad Igλ repertoire may be beneficial for responses in the human gastrointestinal tract,[42] we analyzed the κ/λ light chain isotype ratios of blood B-cell subsets by flow cytometry. We found a high frequency of Igλ⁺ cells (80%) within the CD27⁻ IgA⁺ B-cell subset compared with both CD27⁺IgA⁺ cells (55%) and naive mature B cells (45%; Figure 6B). Sequence analysis of *IGLV-IGLJ* rearrangements revealed fewer mutations in CD27⁻IgA⁺ than in CD27⁺IgA⁺ memory B cells, despite similar *IGLV* and *IGLJ* gene use and IGL-CDR3 size and composition (Figure 6C; supplemental Table 4). The molecular similarities between CD27⁻IgA⁺ B cells and gut lamina propria IgA-producing B cells suggest a common origin of these cells from local responses in the gastrointestinal tract.

Model of memory B-cell generation from 3 distinct pathways

Here, we demonstrate by molecular analysis of Ig genes that 6 distinct memory B-cell subsets can be identified based on their IgH isotype and expression of CD27. To recapitulate our findings, we propose a modified scheme of memory B-cell generation (Figure 7): CD27⁻IgA⁺ B cells and natural effector B cells (at least in part) are derived from local and systemic GC-independent responses, respectively; CD27⁻IgG⁺ and CD27⁺IgM⁺ B cells are derived from primary GC responses and CD27⁺IgG⁺ and CD27⁺IgA⁺ B cells (at least in part) from secondary GC responses.

DISCUSSION

In this study, we set out to relate distinct memory B-cell subsets to the diverse humoral response types that have been documented in the literature. We defined 6 memory B-cell subsets with phenotypic and molecular signs of antigen encounter. Detailed comparative analysis of their Ig genes, comparison with tissue-derived B-cell subsets, and analysis of memory B-cell subsets in CD40L-deficient patients allowed us to distinguish 3 unique maturation pathways: GC-independent local and systemic responses and GC-dependent responses. Furthermore, we delineated primary and consecutive phases of GC responses.

The CD27+IgA+ and CD27+IgG+ subsets are generally regarded as true B-cell memory.[25] Whereas this qualification is somewhat controversial for CD27+IgM+ subsets and CD27− class-switched subsets, our results strongly support these to be true memory B cells based on the (1) high expression of activation and costimulatory molecules; (2) selection against inherently autoreactive VH domain characteristics; (3) extensive replication history compared with naive B cells; and (4) SHM profiles of Ig heavy and light variable genes with high R/S ratios in IGH-CDRs. Despite these common features of B-cell memory, we found clear quantitative differences in proliferation, SHM, and CSR processes among these subsets. We conclude that these differences reflect different origins and maturation pathways before becoming memory B cells. Consequently, these differences justify dividing the memory B-cell compartment into subsets.

Of the 6 memory B-cell subsets, the CD27+IgG+ and CD27+IgA+ B cells had the highest degrees of proliferation and SHMs. Interestingly, these levels were higher than those of GC B cells from childhood tonsils. We previously observed increased proliferation and SHMs in CD27+IgD− cells from adults compared with children and concluded that in adults at least part of these cells had undergone additional immune responses on secondary or tertiary antigen encounter.[18] Our current results showed similar additional proliferation and SHMs for both CD27+IgA+ and CD27+IgG+ B cells. Furthermore, the increased proliferation was accompanied by increased use of distally located *IGHG2* and *IGHG4* genes with signs of indirect CSR. Thus, these results support the concept that at least part of the CD27+IgA+ and CD27+IgG+ B-cell subsets in healthy adults has undergone multiple immune responses.

Interestingly, the *IGHV* gene mutation frequency was clearly higher in CD27+IgA+ compared with CD27+IgG+ B cells. Because the targeting of mutations was similar, AID and UNG activities seemed unaffected. Rather, CD27+IgA+ B cells might have experienced prolonged AID and UNG activities. Because IgA class switching mostly occurs in mucosa-associated lymphoid tissues, this difference might reflect the location of the immune response. Still, despite these higher mutation loads, we found no differences in replacement mutation patterns in *IGHV* genes or the frequency of mutated *IGK* alleles, suggesting similar selection mechanisms for both CD27+IgA+ and CD27+IgG+ B cells.

We conclude that IgM-only and CD27−IgG+ B cells are derived from primary GC responses. This was based on their highly similar replication history and *IGHV* gene mutation loads compared with GC B cells from childhood tonsils and is further supported by the dominant use (> 90%) of the *IGHM*-proximal *IGHG1* and *IGHG3* genes in CD27−IgG+ B cells. In contrast to *IGHV* gene mutation loads, the frequencies of mutated *IGKV* alleles were increased in both subsets compared with GC B cells. We previously found this increased
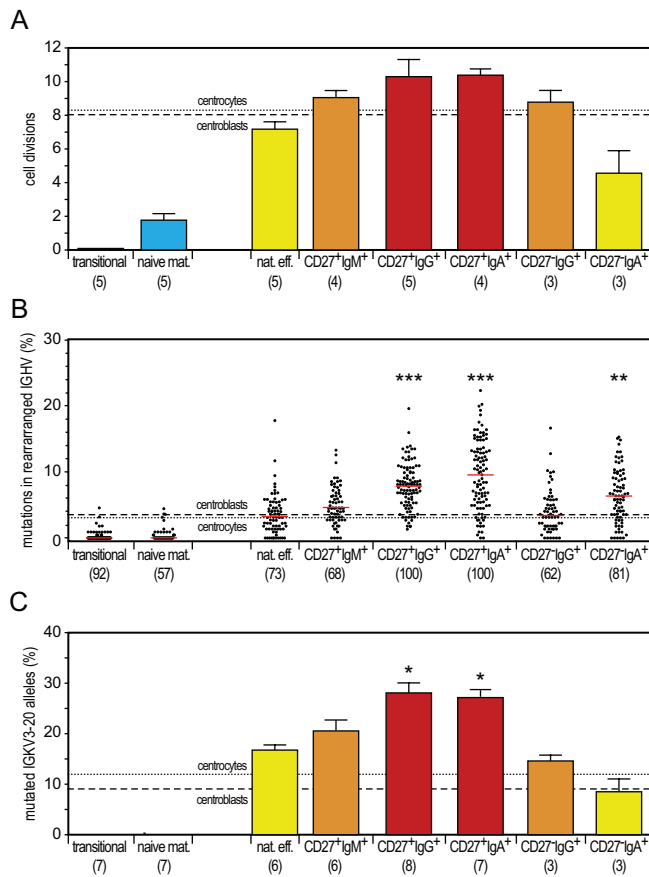
Figure 3. Discrimination of GC-dependent and -independent B-cell maturation pathways based on quantitative analysis of the replication history and SHM levels.
(A) Replication history of 2 naive and 6 memory B-cell subsets as measured with the KREC assay.[18] Three different levels of extensive proliferation in memory B-cell subsets in contrast to naive B cells (blue) could be identified: lower than GC (yellow bars), similar to GC (orange bars) and increased compared with GC (red bars). Bars represent mean values with SEM. In the whole figure, dashed and dotted lines represent values for centroblasts and centrocytes, respectively. Differences between each memory B-cell subset compared with centrocytes were statistically analyzed with the Mann-Whitney test. (B) Frequency of mutated nucleotides in rearranged *IGHV* genes. All individual data points are shown as gray dots, with red lines indicating the median value. Differences between each memory B-cell subset compared with centrocytes were statistically analyzed with the Mann-Whitney test. **P < .01, ***P < .001. (C) Frequency of mutated *IGKV3-20* genes as measured with the IgκREHMA assay. Bars represent mean values with SEM. Differences between each memory B-cell subset compared with centrocytes were statistically analyzed with the Mann-Whitney test. *P < .05.
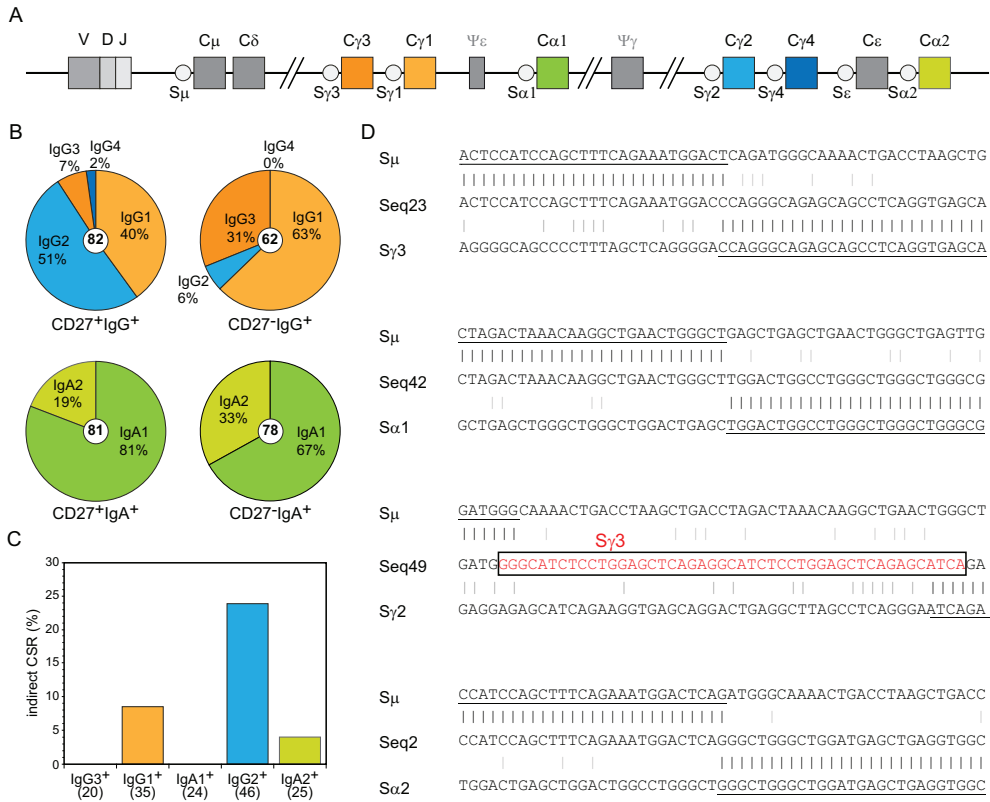
Figure 4. Molecular analysis of Ig class switching in IgA⁺ and IgG⁺ memory B-cell subsets.
(A) Schematic representation of the constant region of the human *IGH* locus. (B) Distribution of IgA and IgG receptor subclass use in *IGH* rearrangements of class-switched memory B-cell subsets. Total number of analyzed sequences is indicated in the center of each plot. Differences in the distribution were statistically analyzed with the χ^2 test and were found significant for both CD27⁺IgG⁺ vs CD27⁻IgG⁺ (P < .0001) and CD27⁺IgA⁺ vs CD27⁻IgA⁺ (P < .05) B-cell subsets. (C) Frequency of Sμ-Sα and Sμ-Sγ rearrangements bearing remnants of indirect class switching. Number of analyzed sequences is given in brackets. (D) Examples of direct and sequential class switching; a piece of Sγ3 sequence in the Sμ-Sγ2 junction is indicated boxed in red font.

frequency in tonsillar CD27⁺IgD⁻ memory B cells.[18] Because this occurred in the absence of additional proliferation, it probably reflects positive selection for the mutated hot-spot in memory B cells rather than additional mutations.

IgM responses are initiated early in primary infection. Dogan et al[43] described that following primary immunization of mice, IgM⁺ memory B cells were formed that on secondary challenge could class switch toward IgG1⁺ cells. Furthermore, clonally related IgM⁺ and IgG⁺ B cells were found in human GCs and peripheral blood.[19,44] Thus, compared with CD27⁺IgA⁺ and CD27⁺IgG⁺ memory B cells, CD27⁺IgM⁺ memory B cells are early GC
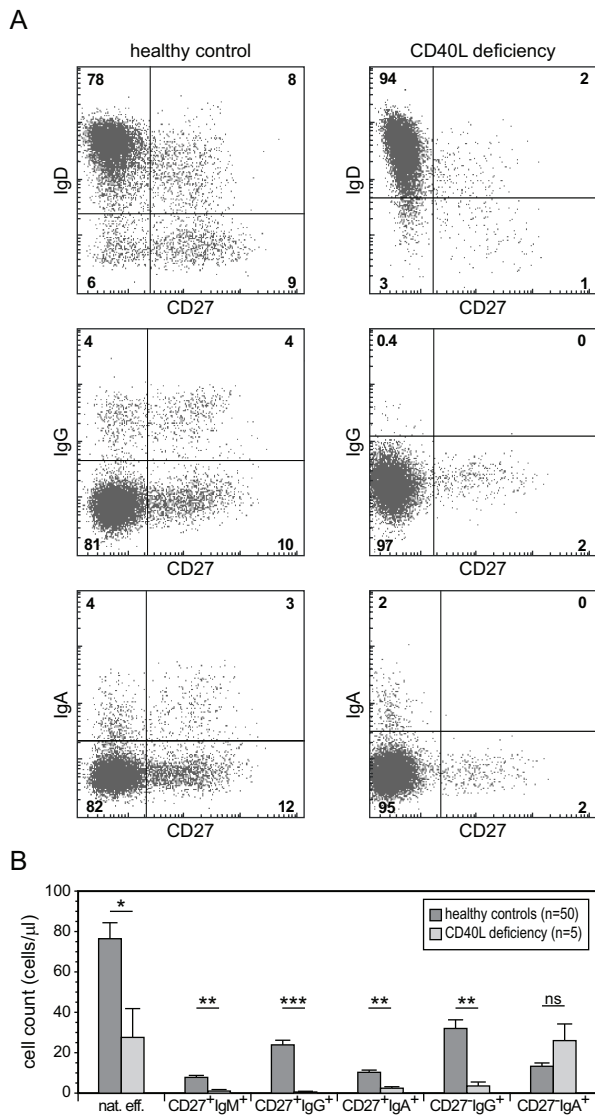
Figure 5. GC-independent generation of natural effector and CD27⁻IgA⁺ memory B cells.
(A) Memory B-cell subset distribution was analyzed in 5 CD40L-deficient patients (age, 1-13 years) and 50 healthy controls (age, 1-5 years). Representative FACS plots of B-cell subsets. (B) Absolute cell numbers of 6 memory B-cell subsets. Bars represent mean values with SEM. Statistical significance was calculated with the Mann-Whitney test. * P < .05, **P < .01, ***P < .001.

emigrants that did not undergo class switching.[45] Still, 2 issues have hampered proper studies on IgM^{+} memory B cells in recent years. First, the CD27^{+}IgM^{+}IgD^{−} and CD27^{+}IgM^{+}IgD^{+} subsets have not always been separated, despite evidence that only the CD27^{+}IgM^{+}IgD^{+} subset contains cells that have been generated independently from GCs (Figure 5B).[17,21] Second, often the CD27^{+}IgD^{−} population is not further subdivided. As a consequence, this is a mixed population of Ig class-switched and IgM^{+} memory B cells. Our results demonstrate that this has no major implications, because these subsets all seem GC dependent. However, it should be noted that the CD27^{+}IgD^{−} subsets contain a substantial fraction of IgM^{+} memory B cells, particularly in young children; therefore, it should be avoided to address these as "Ig class-switched memory."

The low SHM loads in CD27^{−}IgG^{+} B cells compared with CD27^{+}IgG^{+} B cells have lead to speculations on the origin of these cells: from T cell-independent responses or first wave from a GC reaction.[22,23] We found that the replication history and SHM levels of CD27^{−}IgG^{+} B cells highly resemble GC B cells. Furthermore, CD27^{−}IgG^{+} B cells were hardly detectable in CD40L-deficient patients and they have dominant use of IgM-proximal IgG3 and IgG1 subclasses. Thus, we conclude that similarly to CD27^{+}IgM^{+} cells, CD27^{−}IgG^{+} cells are derived from primary GC-dependent responses.

Several studies have shown an expansion of both CD27^{+}IgM^{+}IgD^{−} and CD27^{−}IgG^{+} memory B cells in autoimmune diseases.[17,22,23] Interestingly, CD27^{−}IgG^{+} B cells dominantly use IgG1 and IgG3, which are potent activators of the complement system and inducers of antibody-dependent cell-mediated cytotoxicity.[46] Thus, our observations of the different IgG subclass use in CD27^{+}IgG^{+} versus CD27^{−}IgG^{+} B cells suggest a potential role of CD27^{−}IgG^{+} cells in autoimmunity. Still, additional studies need to address whether many CD27^{−}IgG^{+} B cells carry an autoreactive BCR or whether other mechanisms result in deregulation of CD27^{−}IgG^{+} B cells in patients with an autoimmune disease.

In contrast to the other memory B-cell subsets, natural effector and CD27^{−}IgA^{+} B cells showed limited proliferation compared with GC B cells and were present in CD40L-deficient patients. Thus, we concluded that these cells can be generated independent from T-cell help. It is debated whether CD27^{+}IgM^{+}IgD^{+} natural effector B cells in healthy adults are generated from germinal center responses or independently of T-cell help in the splenic marginal zone.[17,19–21] We describe reduced replication history and SHM levels in natural effector B cells compared with IgM-only memory B cells. Because IgM-only memory B cells highly resemble germinal center B cells on the molecular level, we conclude that in healthy adults part of the natural effector B cells can be generated outside of a GC. Thus, the natural effector B-cell subset in healthy individuals is probably a mixed population of GC-derived and splenic marginal zone-derived memory B cells. Interestingly, a recent study described the presence of CD27^{+}CD43^{+}CD20^{+} B1 cells in umbilical cord blood and in adult peripheral blood.[47] It is possible that the T cell–independent characteristics ascribed to CD27^{+}IgM^{+}IgD^{+} natural effector B cells are specific for the CD43^{+} fraction. This should be further investigated.

The CD27^{−}IgA^{+} memory B-cell subset was the smallest population we studied and, to our knowledge, we showed for the first time that these cells can be derived independent from T-cell help. TI IgA responses have been observed both in human and mouse, both systemically in the splenic marginal zone and locally in the gastrointestinal system.[40,48–49] Potential mediators of CD40-independent IgA CSR are BAFF and APRIL.[39] Because
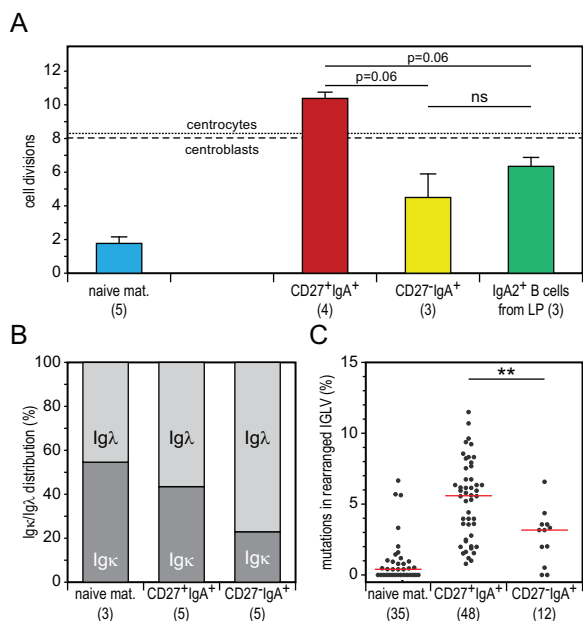
III

Figure 6. CD27⁻IgA⁺ memory B cells resemble colon lamina propria IgA⁺ B cells.

(A) Replication history in naive mature, IgA⁺ memory B-cell subsets and CD19⁺IgA2⁺ B cells isolated from human colon *lamina propria* as measured with the KREC assay. Bars represent mean values with SEM. Statistical significance was calculated with the Mann-Whitney test. (B) Igκ and Igλ isotype distribution of naive mature and IgA⁺ memory B cell subsets as determined with flow cytometric analysis. (C) Frequency of mutated nucleotides in rearranged *IGLV* gene segments. All individual data points are showed as gray dots, with red lines indicating the median value. Statistical significance was calculated with the Mann-Whitney test. **P < .01.
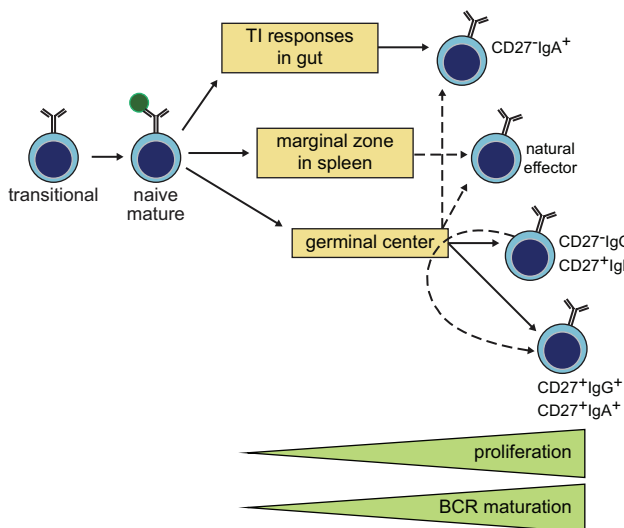
Figure 7. Model of human memory B-cell generation from GC-dependent and -independent pathways.

Six purified memory B-cell subsets showed differential levels of proliferation and BCR maturation. Ig class-switching profiles and immunophenotyping of blood of CD40L-deficient patients supported delineation of these 6 subsets from T cell-dependent and -independent maturation pathways. CD27⁻IgA⁺ and natural effector B cells can be derived independently from T-cell help, probably locally in the gastrointestinal tract and from systemic responses in splenic marginal zone, respectively. The molecular profiles of CD27⁻IgG⁺ and CD27⁺IgM⁺ memory B cells resembled those of primary GC cells, whereas CD27⁺IgG⁺ and CD27⁺IgA⁺ memory B cells has increased proliferation and SHM levels suggestive of further maturation in consecutive GC response.

blood CD27⁻IgA⁺ B cells and gut *lamina propria* IgA-producing B cells were highly similar in their limited replication history, and dominant IgA2 and Igλ light chain isotypes, we conclude that these cells have been generated in similar responses. Although the anatomic location of TI CSR toward IgA in human gut remains controversial,[40,50] on the basis of our findings, we can state that CD27⁻IgA⁺ memory B cells resemble IgA⁺ cells from the gut *lamina propria* and seem to be a blood counterpart of this IgA-producing population. Even though analysis of the memory B-cell compartment showed that CD27⁻IgA⁺ B cells seem completely TI, we cannot exclude that in physiologic conditions a minor fraction of CD27⁻IgA⁺ B cells is generated in a primary immune response analogous to CD27⁻IgG⁺ B cells.

The human memory B-cell compartment is more complex than originally thought and actually consists of diverse subsets that have originated from functionally distinct responses. Interestingly, differential expression of CD27 was the key to identification of the diverse subsets. The function of CD27 on B cells remains unclear. CD27-CD70 interactions can trigger plasma cell differentiation and provide negative feedback signals. Thus, CD27⁺ and CD27⁻ memory B cells might function differently. Still, the similar up-regulation of many other costimulatory molecules on these cells might compensate for the lack of CD27. Alternatively, the differential CD27 expression might reflect the different types of responses in which the cells have been generated and thus represents a useful marker to discriminate between these subsets.

Different levels of memory B-cell responses seem to reflect the phylogenetic evolution of the immune system from local TI responses, via systemic TI responses to most advanced T cell–dependent responses in the GC. These different origins suggest unique physiologic functions in protection against pathogens.

In this study, we dissected the human memory B-cell compartment into 6 distinct subsets. Molecular analysis of these memory B cells in healthy controls and comparison with memory B cells from CD40L-deficient patients and colon *lamina propria* B cells enabled us to delineate their origin from 3 different maturation pathways: local and systemic TI responses and primary or secondary GC responses. Because these B-cell subsets are present in blood, our study provides new opportunities to analyze these processes in patients with (auto)inflammatory conditions, B-cell immunodeficiencies, and nodal and extranodal B-cell malignancies.

REFERENCES

1. Alt FW, Yancopoulos GD, Blackwell TK, et al. Ordered rearrangement of immunoglobulin heavy chain variable region segments. *EMBO J*. 1984;3(6):1209-1219.
2. Ghia P, ten Boekel E, Rolink AG, Melchers F. B-cell development: a comparison between mouse and man. *Immunol Today*. 1998;19(10):480-485.
3. LeBien TW, Tedder TF. B lymphocytes: how they develop and function. *Blood*. 2008;112(5):1570- 1580.
4. Odegard VH, Schatz DG. Targeting of somatic hypermutation. *Nat Rev Immunol*. 2006;6(8):573- 583.
5. Chaudhuri J, Alt FW. Class-switch recombination:interplay of transcription, DNA deamination and DNA repair. *Nat Rev Immunol*. 2004;4(7):541-552.
6. Muramatsu M, Kinoshita K, Fagarasan S, Yamada S, Shinkai Y, Honjo T. Class switch recombination and hypermutation require activationinduced cytidine deaminase (AID), a potential RNA editing enzyme. *Cell*. 2000;102(5):553-563.
7. Rogozin IB, Kolchanov NA. Somatic hypermutagenesis in immunoglobulin genes. II. Influence of neighbouring base sequences on mutagenesis. *Biochim Biophys Acta*. 1992;1171(1):11-18.
8. Bretscher P, Cohn M. A theory of self-nonself discrimination. Science. 1970;169(950):1042-1049.
9. MacLennan IC. Germinal centers. *Annu Rev Immunol*. 1994;12:117-139.
10. Mond JJ, Vos Q, Lees A, Snapper CM. T cell independent antigens. *Curr Opin Immunol*. 1995; 7(3):349-354.
11. Cerutti A, Rescigno M. The biology of intestinal immunoglobulin A responses. *Immunity*. 2008; 28(6):740-750.
12. Weill JC, Weller S, Reynaud CA. Human marginal zone B cells. *Annu Rev Immunol*. 2009;27: 267-285.
13. Ahmed R, Gray D. Immunological memory and protective immunity: understanding their relation. *Science*. 1996;272(5258):54-60.
14. Agematsu K, Nagumo H, Yang FC, et al. B cell subpopulations separated by CD27 and crucial collaboration of CD27 B cells and helper T cells in immunoglobulin production. *Eur J Immunol*. 1997;27(8):2073-2079.
15. Tangye SG, Liu YJ, Aversa G, Phillips JH, de Vries JE. Identification of functional human splenic memory B cells by expression of CD148 and CD27. *J Exp Med*. 1998;188(9):1691-1703.
16. Pascual V, Liu YJ, Magalski A, de Bouteiller O, Banchereau J, Capra JD. Analysis of somatic mutation in five B cell subsets of human tonsil. *J Exp Med*. 1994;180(1):329-339.
17. Weller S, Braun MC, Tan BK, et al. Human blood IgM "memory" B cells are circulating splenic marginal zone B cells harboring a prediversified immunoglobulin repertoire. *Blood*. 2004;104(12):3647-3654.
18. van Zelm MC, Szczepanski T, van der Burg M, van Dongen JJ. Replication history of B lymphocytes reveals homeostatic proliferation and extensive antigen-induced B cell expansion. *J Exp Med*. 2007;204(3):645-655.
19. Seifert M, Kuppers R. Molecular footprints of a germinal center derivation of human IgM(IgD)CD27 B cells and the dynamics of memory B cell generation. *J Exp Med*. 2009; 206(12):2659-2669.
20. Agematsu K, Nagumo H, Shinozaki K, et al. Absence of IgD-CD27() memory B cell population in X-linked hyper-IgM syndrome. *J Clin Invest*. 1998;102(4):853-860
21. Weller S, Faili A, Garcia C, et al. CD40-CD40L independent Ig gene hypermutation suggests a second B cell diversification pathway in humans. *Proc Natl Acad Sci U S A*. 2001;98(3):1166-1170.
22. Fecteau JF, Cote G, Neron S. A new memory CD27IgG B cell population in peripheral blood expressing VH genes with low frequency of somatic mutation. *J Immunol*. 2006;177(6):3728-3736.
23. Wei C, Anolik J, Cappione A, et al. A new population of cells lacking expression of CD27 represents a notable component of the B cell memory compartment in systemic lupus erythematosus. *J Immunol*. 2007;178(10):6624-6633.
24. Cagigi A, Du L, Dang LV, et al. CD27(-) B-cells produce class switched and somatically hypermutated antibodies during chronic HIV-1 infection. *PLoS ONE*. 2009;4(5):e5427.
25. Good KL, Avery DT, Tangye SG. Resting human memory B cells are intrinsically programmed for enhanced survival and responsiveness to diverse stimuli compared to naive B cells. *J Immunol.* 2009;182(2):890-901.
26. Andersen P, Permin H, Andersen V, et al. Deficiency of somatic hypermutation of the antibody light chain is associated with increased frequency of severe respiratory tract infection in common variable immunodeficiency. *Blood*. 2005;105(2):511-517.
27. Novak AJ, Darce JR, Arendt BK, et al. Expression of BCMA, TACI, and BAFF-R in multiple myeloma: a mechanism for growth and survival. *Blood*. 2004;103(2):689-694.

28. van der Vuurst de Vries AR, Clevers H, Logtenberg T, Meyaard L. Leukocyte-associated immunoglobulin-like receptor-1 (LAIR-1) is differentially expressed during human B cell differentiation and inhibits B cell receptor-mediated signaling. *Eur J Immunol*. 1999;29(10):3160-3167.

29. Brezinschek HP, Brezinschek RI, Lipsky PE. Analysis of the heavy chain repertoire of human peripheral B cells using single-cell polymerase chain reaction. *J Immunol*. 1995;155(1):190-202.

30. Suzuki I, Pfister L, Glas A, Nottenburg C, Milner EC. Representation of rearranged VH gene segments in the human adult antibody repertoire. *J Immunol*. 1995;154(8):3902-3911.

31. Rao SP, Riggs JM, Friedman DF, Scully MS, LeBien TW, Silberstein LE. Biased VH gene usage in early lineage human B cells: evidence for preferential Ig gene rearrangement in the absence of selection. *J Immunol*. 1999;163(5):2732-2740.

32. Yu K, Taghva A, Lieber MR. The cleavage efficiency of the human immunoglobulin heavy chain VH elements by the RAG complex: implications for the immune repertoire. *J Biol Chem*. 2002; 277(7):5040-5046.

33. Pascual V, Victor K, Lelsz D, et al. Nucleotide sequence analysis of the V regions of two IgM cold agglutinins. Evidence that the VH4–21 gene segment is responsible for the major cross-reactive idiotype. *J Immunol*. 1991;146(12):4385-4391.

34. Pugh-Bernard AE, Silverman GJ, Cappione AJ, et al. Regulation of inherently autoreactive VH4–34 B cells in the maintenance of human B cell tolerance. *J Clin Invest*. 2001;108(7):1061-1070.

35. Wardemann H, Yurasov S, Schaefer A, Young JW, Meffre E, Nussenzweig MC. Predominant autoantibody production by early human B cell precursors. *Science*. 2003;301(5638):1374-1377.

36. Bose B, Sinha S. Problems in using statistical analysis of replacement and silent mutations in antibody genes for determining antigen-driven affinity selection. *Immunology*. 2005;116(2):172-183.

37. Wirths S, Lanzavecchia A. ABCB1 transporter discriminates human resting naive B cells from cycling transitional and memory B cells. *Eur J Immunol*. 2005;35(12):3433-3441.

38. Ma CS, Pittaluga S, Avery DT, et al. Selective generation of functional somatically mutated IgM+CD27+, but not Ig isotype-switched, memory B cells in X-linked lymphoproliferative disease. *J Clin Invest*. 2006;116(2):322-333.

39. Litinskiy MB, Nardelli B, Hilbert DM, et al. DCs induce CD40-independent immunoglobulin class switching through BLyS and APRIL. *Nat Immunol*. 2002;3(9):822-829.

40. He B, Xu W, Santini PA, et al. Intestinal bacteria trigger T cell-independent immunoglobulin A(2) class switching by inducing epithelial-cell secretion of the cytokine APRIL. *Immunity*. 2007;26(6): 812-826.

41. Kett K, Brandtzaeg P, Radl J, Haaijman JJ. Different subclass distribution of IgA-producing cells in human lymphoid organs and various secretory tissues. *J Immunol*. 1986;136(10):3631-3635.

42. Su W, Gordon JN, Barone F, et al. Lambda light chain revision in the human intestinal IgA response. *J Immunol*. 2008;181(2):1264-1271.

43. Dogan I, Bertocci B, Vilmont V, et al. Multiple layers of B cell memory with different effector functions. *Nat Immunol*. 2009;10(12):1292-1299.

44. Bende RJ, van Maldegem F, Triesscheijn M, Wormhoudt TA, Guijt R, van Noesel CJ. Germinal centers in human lymph nodes contain reactivated memory B cells. *J Exp Med*. 2007;204(11): 2655-2665.

45. Klein U, Kuppers R, Rajewsky K. Evidence for a large compartment of IgM-expressing memory B cells in humans. *Blood*. 1997;89(4):1288-1298.

46. Bru̇ggemann M, Williams GT, Bindon CI, et al. Comparison of the effector functions of human immunoglobulins using a matched set of chimeric antibodies. *J Exp Med*. 1987;166(5):1351-1361.

47. Griffin DO, Holodick NE, Rothstein TL. Human B1 cells in umbilical cord and adult peripheral blood express the novel phenotype CD20+CD27+CD43+CD70. *J Exp Med*. 2011; 208(1):67-80.

48. Fagarasan S, Kinoshita K, Muramatsu M, Ikuta K, Honjo T. In situ class switching and differentiation to IgA-producing cells in the gut lamina propria. *Nature*. 2001;413(6856):639-643.

49. Bergqvist P, Gardby E, Stensson A, Bemark M, Lycke NY. Gut IgA class switch recombination in the absence of CD40 does not occur in the lamina propria and is independent of germinal centers. *J Immunol*. 2006;177(11):7772-7783.

50. Boursier L, Gordon JN, Thiagamoorthy S, Edgeworth JD, Spencer J. Human intestinal IgA response is generated in the organized gutassociated lymphoid tissue but not in the lamina propria. *Gastroenterology*. 2005;128(7):1879-1889.

III

IV

CD27^{+}IgM^{+}IgD^{+} B cells in Persistent Polyclonal B-cell Lymphocytosis are hyperproliferated memory B cells with limited somatic mutations and a distinct immunophenotype

Magdalena A. Berkowska[1], Henk J. Adriaansen[2], Dick de Ridder[3], Karin Pagano Mirani-Oostdijk[4], Hendrik J. Agteresch[5], Sebastian Böttcher[6], Alberto Orfao[7], Jacques J.M. van Dongen[1], Menno C. van Zelm[1]

[1]Dept. Immunology, Erasmus MC, Rotterdam, the Netherlands; [2]Dept. Clinical Chemistry and Laboratory Hematology, Gelre ziekenhuizen, Apeldoorn/Zutphen, the Netherlands; [3]The Delft Bioinformatics Lab, Faculty of Electrical Engineering, Mathematics and Computer Science, Delft University of Technology, Delft, the Netherlands; [4]Dept. Clinical Chemistry, Franciscus Hospital, Roosendaal, the Netherlands; [5]Dept. Internal Medicine, Admiral De Ruyter Ziekenhuis, Goes, the Netherlands; [6]Second Dept. of Medicine, University Hospital of Schleswig-Holstein, Campus Kiel, Germany; [7]Service of Cytometry, Dept. of Medicine, University of Salamanca, Spain

ABSTRACT

Persistent polyclonal B-cell lymphocytosis (PPBL) is a rare benign disorder characterized by an expansion of CD27$^+$IgM$^+$IgD$^+$ cells. Despite an increasing number of described cases, the nature of the persistent lymphocytosis and its relation to mature B-cell malignancies remain poorly understood. Therefore, we subjected PPBL patients and healthy controls to gene expression profiling, immunoglobulin (Ig) repertoire and replication history analyses. In addition, we compared the immunophenotype of PPBL cells with B-cell malignancies and B-cell subsets from controls. PPBL cells displayed hyperproliferation and somatic hypermutations (SHM) in their *IGHV* genes. Still, the IgH repertoire was highly diverse without evidence for stereotypy. Despite the low SHM frequency, *IGHV* genes showed selection for replacement mutations in complementarity determining regions, similar to memory B cells. PPBL cells showed a gene expression profile reminiscent of memory B cells and accompanied by heterogeneous deregulation of oncogenes. Furthermore, we identified cell surface markers to discriminate PPBL cells from control B-cell subsets: IgD, CD38, CD73 and CD62L. These combined insights, especially the newly identified cell surface markers, can prove valuable for diagnosis of PPBL and might contribute to prognostic classification of patients at risk for developing a lymphoid malignancy.

INTRODUCTION

Persistent polyclonal B-cell lymphocytosis (PPBL) is a rare disorder, which mostly affects middle-aged women and is associated with smoking.[1-2] It is characterized by the persistent expansion of CD27^{+}IgM^{+}IgD^{+} B cells, the presence of circulating binucleated lymphocytes and increased IgM serum levels.[1-3] The course of PPBL is usually benign with affected individuals either remaining asymptomatic or having minor and nonspecific complaints.[4] Still, approximately 10% of patients present with mild splenomegaly and a few patients have been described to subsequently develop a mature B-cell malignancy, such as diffuse large B-cell lymphoma (DLBCL) or splenic marginal zone lymphoma (MZL).[4-5] The idea that PPBL might be a pre-malignant stage is further supported by the presence of t(14;18) translocations resulting in *BCL2-IGH* gene rearrangements in most of the patients.[2,6-9] However, the polyclonal nature of the B-cell expansion in PPBL and the presence of *BCL2-IGH* translocations in healthy elderly and smoking individuals, put this hypothesis into question.[10-12]

The initial trigger and subsequent mechanisms that result in the persistent lymphocytosis are currently unknown. Polyclonal B-cell proliferation triggers such as Epstein-Barr virus infection and tobacco smoke are potential stimuli.[13-14] Still, the circulating B cells are resting and display deregulation of genes encoding adhesion molecules and apoptosis regulators, suggesting that their accumulation in blood results from impaired extravasation and/or aberrant apoptosis.[15-16]

In healthy individuals, the IgM[+] B-cell fraction is phenotypically diverse (Figure 1A). Recent bone marrow emigrants – transitional B cells – express IgM and IgD as well as CD5 and high levels of CD38 and CD24.[17] Pre-naive B cells have downregulated CD38 and CD24 levels, but are still CD5^{+},[18] while naive mature B cells lack CD5 expression. These three naive B-cell subsets lack expression of CD27. CD27 is present on two IgM^{+} memory B-cell subsets in blood: CD27^{+}IgM^{+}IgD^{-} (IgM-only) cells, which are formed in germinal centers in response to T cell-dependent (TD) antigens, and CD27^{+}IgM^{+}IgD^{+} (natural effector) cells, which can be generated from the splenic marginal zone following response to T cell-independent (TI) antigens.[19-21] Both of these IgM[+] memory B cells show typical signs of antibody maturation with accumulation of somatic hypermutations (SHM) in complementarity determining regions (CDR) of rearranged immunoglobulin (Ig) encoding genes.[19,22] While multiple studies have reported the presence of mutated Ig genes in CD27^{+}IgM^{+}IgD^{+} PPBL cells, the numbers of analyzed sequences was too small to determine if and where these cells underwent selection processes.[23-24]

Here we performed in depth molecular and flow cytometric analysis of CD27^{+}IgM^{+}IgD^{+} B cells from PPBL patients, IgM^{+} B-cell subsets in healthy controls and leukemia/lymphoma patients. These detailed comparisons provided new insights into the nature of the persistent B-cell proliferation and the identification of membrane markers to distinguish PPBL from controls and B-cell malignancies.

METHODS

Flow cytometric immunophenotyping and cell sorting

All peripheral blood samples from 5 PPBL patients, multiple healthy age-matched donors, and childhood tonsils were obtained with informed consent and according to the guidelines of the Medical Ethics Committee of Erasmus MC.

Absolute counts of blood CD4^{+} and CD8^{+} T cells, CD16^{+}/56^{+} NK cells and CD19^{+} B cells were obtained with a lyse-no-wash protocol. Furthermore, 8-color flow cytometric immunophenotyping was performed using monoclonal antibodies against CD24-FITC (gran-B-ly-1), CD5-FITC (C12) (both from Sanquin), CD24-PB (SN3; Exbio), CD38-APC, CD38-APC-H7 (both HB7), CD19-PerCP-Cy5.5, CD19-PE-Cy7 (both SJ25C1), CD20-PerCP (L27), CD27-APC (L128), IgD-biotin (IA6-2) CD1d-PE (CD1d42), CD47-FITC (IAP), CD58-FITC (1C3), CD62L-FITC (SK11), CD73-PE (AD2), CD74-FITC (M-B741), CD200 (OX2) (all from BD Biosciences), IgM-FITC, IgM-PE, IgD-PE (all goat polyclonal from SBA), Igλ-PE (rabbit polyclonal; SBA), Igκ-FITC (rabbit polyclonal; Dako), CD119-PE (GIR-94), IgM-HorV450 (G20-127; both from BD Pharmingen), CD37-PE (BL14; Beckman Coulter). Biotinylated antibodies were detected with Streptavidin PE-Cy7 (eBioscience) or Streptavidin PO (Invitrogen). Mouse IgG1-FITC and IgG1-PE (BD Biosciences) were used as isotype controls. In addition, PPBL samples were stained with the recently described B-CLPD antibody panel from the EuroFlow Consortium.[25]

CD27^{+}IgM^{+}IgD^{+} cells from PPBL samples were directly high-speed cell-sorted from post-Ficoll mononuclear cells. Mononuclear cells from healthy donors were enriched for B cells by magnetic separation with CD19 beads (Miltenyi Biotech) prior to purification of transitional, pre-naive, naive mature, natural effector and IgM-only B cells. CD19^{+}CD38^{+}IgD^{-}CD77^{-} centrocytes were isolated from childhood tonsil described previously.[26]

All cell sorting experiments were performed on a FACSAriaII (BD Biosciences) with a purity of >95% as determined by post-sort analysis.

Replication history analysis using the KREC assay

DNA was isolated from each sorted subset with the GenElute Mammalian Total DNA Miniprep Kit (Sigma-Aldrich). The replication history of sorted B-cell subsets was determined with the Kappa-deleting Recombination Excision Circles (KREC) assay as described previously.[26] Briefly, the amounts of coding and signal joints of the *IGK*-deleting rearrangement were measured by realtime-quantitative (RQ-)PCR in DNA from sorted B-cell populations on an ABI Prism 7000 (Applied Biosystems). Signal joints, but not coding joints are diluted two-fold with every cell division.[26] To measure the number of cell divisions undergone by each population, we calculated the ratio between the number of coding joints and signal joints. The previously established control cell line U698 DB01 (InVivoScribe) contains one coding and one signal joint per genome and was used to correct for minor differences in efficiency of both RQ-PCR assays.[26]

IgκREHMA

The frequency of mutated *IGK* alleles was determined with the Igκ restriction enzyme hot-spot mutation assay (IgκREHMA) as described previously.[26-27] The frequently used *IGKV3-*

20 gene contains a mutation hotspot in IGKV-CDR1, which can be cut by restriction enzyme Fnu4HI. IGKV3-20–IGKJ rearrangements were amplified with a HEX-labeled forward primer from genomic DNA of sorted B-cell subsets, subjected to restriction enzyme digestion with KpnI and Fnu4HI and run on the ABI Prism 3130 XL (Applied Biosystems). Unmutated gene products were cut by Fnu4HI and visualized as 244 or 247-bp HEX-coupled fragments. KpnI cuts all products in FR2 downstream of the Fnu4HI sites, resulting in a 262-bp HEX-coupled mutated fragment. The unmutated B-cell line CLL-1 was used as a positive control for complete digestion with Fnu4HI. The digests hardly contained undigested gene products of 481bp, indicating complete digestion by KpnI.

IGH-CDR3 immunospectratyping and sequence analysis

Complete *IGH* rearrangements were amplified from sorted B-cell populations with a previously described set of 6 VH-FR1 forward primers and one FAM-labeled JH consensus reverse primer.[28] IGH-CDR3 immunospectratyping was performed on an ABI Prism 7000 (Applied Biosystems).

In addition, PCR products were cloned into the pGEM-T easy vector (Promega, Madison, WI) and prepared for sequencing on the ABI Prism 3130 XL fluorescent sequencer (Applied Biosystems). Obtained sequences were analyzed using the IMGT database (http://imgt.cines. fr) to assign the *IGHV*, *IGHD* and *IGHJ* gene, and to identify somatic mutations.[29] Of each unique clone, the position and frequency of mutations was determined within the *IGHV* gene, as was the length of the IGH-CDR3.

Targeting and selection of SHM in framework regions (FR) 1, 2 and 3 and CDR1 and 2 in rearranged *IGHV* genes were analyzed with the JoinSolver program.[30-31] The following parameters were examined: (1) targeting of SHM to RGYW/WRCY, WA/TW motifs and (2) to individual nucleotides within these motifs; (3) frequencies of transition and transversion mutations; (4) replacement/silent mutation ratios in FR and CDR; (5) nucleotide substitution frequencies and patterns in rearranged *IGHV* genes.

Gene expression profiling

RNA was isolated from each sorted subset with the RNeasy Mini Kit (Qiagen). Gene expression was quantified using Affymetrix HG-U133 Plus 2.0 GeneChip arrays (containing 54,675 probe sets), as previously described.[32-33] Expression profiles of PPBL cells and B-cell subsets from healthy donors were compared based on the perfect match probe intensity levels. Robust Multi-array Average (RMA) background removal and quantile normalization was performed, followed by a per-probe set two-way ANOVA (with factors probe and subset). This resulted in average expression levels for each probe set in each cell type, as well as p values for the significance of the difference between cell types. The p values were adjusted for multiple testing using Šidák stepdown adjustment and all differences with adjusted p values < .05 were considered significant.

The maximum difference in expression between any two subsets was calculated for each probe set that showed a signal. Only probe sets that showed larger differences than a certain threshold were selected for clustering. Tested thresholds were 8-fold, 16-fold, 32-fold and 64 fold (i.e. $\log_2$ values of 3, 4, 5 and 6). Correlation ρ between samples was then calculated based on only these selected probe sets, and the data was hierarchically clustered (complete linkage) using 1-ρ as a distance measure.[33]

Multiparameter flow cytometric analysis

Flow cytometric data on cell surface expression of markers discriminative between PPBL cells and IgM$^+$ memory B cells from healthy donors were analyzed with INFINICYT software (Cytognos SL, Salamanca, Spain).[25] Upon defining populations of interest, data files corresponding to different aliquots of each individual sample were merged and flow cytometry data were calculated as previously described in detail.[34] The same software was used for principal component analysis of flow cytometric data obtained for PPBL cells, IgM$^+$ memory B cells from healthy donors, and previously published mature B-cell malignancies.[25,35]

Detection of t(14; 18) *BCL2-IGH* rearrangements

BCL2-IGH translocations were studied with three separate PCR reactions using primer sets designed to detect breakpoints within the MBR, 3'MBR and mcr regions of *BCL2* as described previously.[28] The detected *BCL2-IGH* translocations were subsequently amplified with RQ-PCR reactions containing the MBR1 primer, six JH family-specific primers and three JH-specific TaqMan probes as described previously.[28,36] Analyses were performed on PPBL cells from 5 patients, natural effector cells from 5 healthy donors and 9 t(14;18)-negative mature human B-cell lines: L428, DG75, CA-46, KCA, Ramos, U698, Namalwa, ROS15, CLL-1. Quantification of *BCL2-IGH* translocations was performed using the ΔΔCT method relative to the albumin gene. The t(14;18)-positive DoHH2 cell line was used as a positive control.[37]

Statistical analyses

Statistical analyses were performed with the Mann-Whitney U test. p values < .05 were considered statistically significant.

RESULTS

Persistent polyclonal expansion of CD27$^+$IgM$^+$IgD$^+$ B cells

Five middle-aged patients (4 female, 1 male) with a history of smoking presented with moderate lymphocytosis (mean, 6.8 x10^9 cells/l) due to increased absolute B-cell numbers (mean, 4.2 x10^9 cells/l). These B cells showed a normal Igκ/Igλ ratio ranging from 0.9 to 1.3. T cell numbers were slightly increased or within the normal range (mean, 2.2 x10^9 cells/l), and NK cell numbers were within the normal range (mean, 0.26 x10^9 cells/l). IgM serum levels were increased (mean, 6.9 g/l). On average, lymphocytosis had been persistently present for 3.8 years (range 1-5; Table 1).

Detailed flow cytometric analysis of patients' blood B cells revealed the complete absence of transitional B cells and an expansion of CD27$^+$IgM$^+$IgD$^+$ B cells, which constituted on average 79% of total B cells (Figure 1B). The polyclonal character of the expanded population was confirmed by IGH-CDR3 immunospectratyping. In all patients, amplified *IGH* rearrangements showed a normal length distribution and in frame selection (Figure 1C). Based on these characteristics the patients were diagnosed with PPBL.

Table 1. Baseline characteristics and laboratory findings in 5 PPBL patients.

	patient 1	patient 2	patient 3	patient 4	patient 5	normal range
Age of diagnosis (years)	48	34	41	36	40	-
Age of analysis (years)	52	39	45	37	45	-
Sex	F	F	F	M	F	-
Splenomegaly	yes	no	no	yes	yes	-
Serum IgM (g/l)	**7.6**	**2.7**	**6.6**	**5.7**	**12.1**	0.4-2.3
Lymphocytes (x10^9 cells/l)	**10.3**	**6.6**	**5.9**	**5.4**	**6.0**	1.1-2.5
T cells (x10^9 cells/l)	1.3	**2.9**	**2.7**	**2.1**	**2.1**	0.7-1.9
NK cells (x10^9 cells/l)	0.2	0.3	0.4	0.3	0.2	0.1-0.4
B cells (x10^9 cells/l)	**8.7**	**3.2**	**2.7**	**2.9**	**3.7**	0.1-0.4
Igκ/Igλ ratio	1.2	1.1	1.3	1.0	0.9	0.8-2.8

Cell counts or Ig serum levels above the normal range are shown in bold font.[73]

Ig repertoire diversity

To obtain more insight into the Ig repertoire diversity in PPBL cells, we performed in-depth sequence analyses of amplified *IGH* gene rearrangements from sorted CD27$^+$IgM$^+$IgD$^+$ cells of PPBL patients and from natural effector and IgM-only memory B cells from controls. We focused on rearrangements utilizing two most frequent *IGHV* subgroups: *IGHV3* and *IGHV4*.[38-39] Similar to healthy controls, each clone yielded a unique sequence, implying a broad Ig repertoire. *IGHV3-23* and *IGHV4-59* were the most frequently used *IGHV* genes in PPBL (data not shown).

To further assess combinational diversity, we analyzed pairing of the 12 mostly utilized *IGHV* genes with *IGHD* genes. Both memory B-cell subsets from healthy donors and the PPBL cells showed similarly high repertoire diversity and no preferential pairing between individual *IGHV* and *IGHD* genes (Figure 2A). Furthermore, the *IGHJ* gene usage was diverse with the most frequent usage of *IGHJ4* and *IGHJ6* (not shown).

High replication history, but low levels of SHM in PPBL cells

To study the nature of the expanded B-cell population in PPBL, we studied their replication history and SHM profiles and compared these with IgM$^+$ B-cell subsets from healthy controls. The replication history was calculated as the ratio between genomic coding joints and signal joints on kappa-deleting recombination excision circles (KREC) of the *IGK*-deleting rearrangement.[26] Three out of 5 analyzed PPBL samples showed a mean replication history of ~15 cell divisions. The replication histories for the 2 remaining samples were beyond the detection limit (18) of the assay. The observed proliferation was significantly higher (p< .05) than the 7 cell divisions in natural effector and 9 cell divisions in IgM-only cells of controls (Figure 2B). Despite the increased number of cell divisions, only ~4% of *IGKV3-20* alleles of PPBL cells were mutated in a hotspot region in CDR1 (Figure 2C). This frequency was significantly lower (p< .05) than 16% in natural effector cells and 20% in IgM-only cells from controls. Furthermore, the frequency of mutated nucleotides in
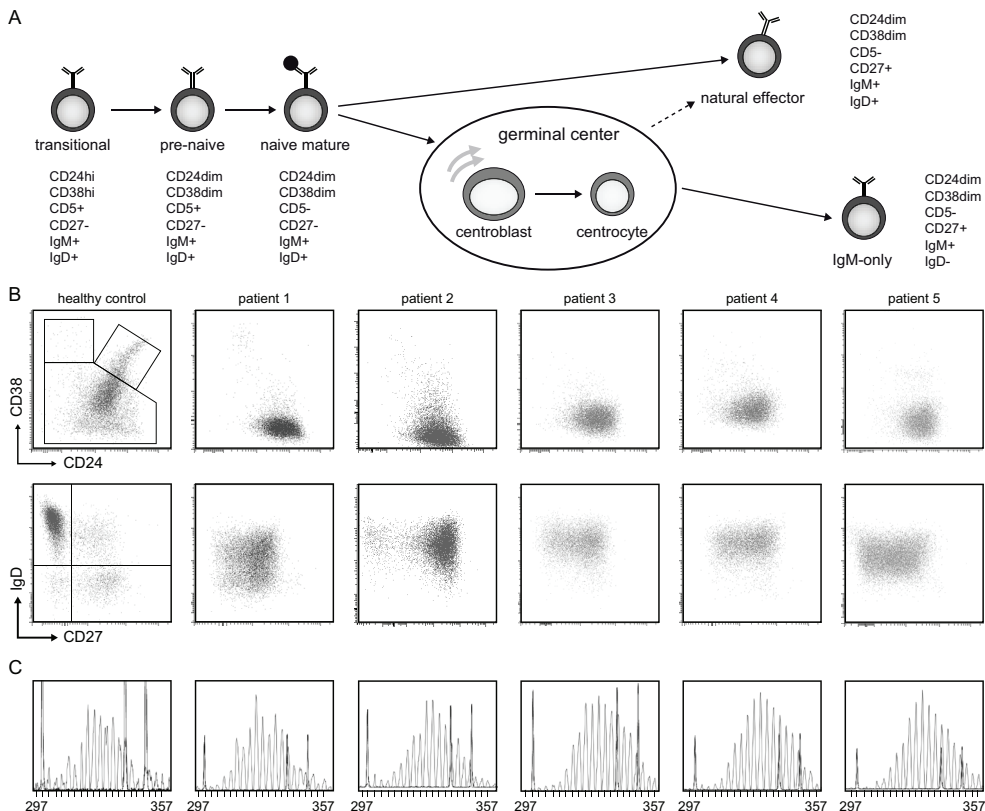
IV

Figure 1. Polyclonal expansion of CD27$^+$IgM$^+$IgD$^+$ cells and lack of transitional B cells in 5 PPBL patients.
(A) Differentiation scheme of naive and IgM$^+$ memory B cells. Naive B cells are IgM$^+$IgD$^+$. Within this population, early bone marrow emigrants, transitional B cells, express CD5 and high levels of CD38 and CD24. Pre-naive B cells are CD5$^+$CD38^{dim}CD24^{dim}, while naive mature B cells are CD5-CD38^{dim}CD24^{dim}. IgM-only memory B cells are derived from germinal center responses and express CD27, but not IgD. Natural effector B cells are CD27$^+$IgM$^+$IgD$^+$ and are at least in part derived from T-cell independent responses. (B) Immunophenotyping of B cells in blood of a representative healthy donor and 5 PPBL patients. Diverse subsets can be identified in healthy controls: CD38^{high}CD24^{high} transitional B cells and CD38^{high}CD24^{dim} plasmablasts (upper panel). CD38^{dim}CD24^{dim} cells are subdivided into CD27$^-$IgD$^+$ naive B cells, CD27$^+$IgD$^+$ natural effector B cells and CD27$^+$IgD$^-$ memory B cells (lower panel). PPBL patients show a dominant population that is negative for CD38 and CD27$^+$IgD$^+$. (C) IGH-CDR3 immunospectratyping of complete rearrangements amplified from CD27$^+$IgM$^+$IgD$^+$ cells in a representative healthy donor and 5 PPBL patients. Positions of triplet peaks indicating in-frame selection of rearrangements are indicated at the bottom of each panel. Internal size standard peaks are shown at positions 300, 340 and 350.

rearranged *IGHV* genes was only 1.4% in PPBL cells as compared to 2.7% in natural effector (p< .01) and 4.5% in IgM-only cells from controls (p< .0001; Figure 2D). Thus, PPBL cells showed unusually low SHM frequencies in relation to their high replication histories.

To study whether these differences were the result of altered SHM targeting, we analyzed

mutations in hypermutable motifs. RGYW/WRCY and WA/TW DNA sequence motifs are preferentially targeted by Activation Induced Cytidine Deaminase (AID) and the error-prone Polymerase η (Polη), respectively.[30] *IGHV* genes of PPBL patients accumulated less SHM in RGYW motifs and more mutations in TW motifs than healthy controls (data not shown). While no difference was observed in targeting of hypermutable nucleotides in RGYW/WRCY motifs, PPBL patients showed an increased targeting of A within WA motifs, and increased targeting of T in TW motifs as compared to controls (not shown). The latter likely contributed to the overall more frequent T→ C transitions in patients than in controls (not shown). Still, the overall frequencies of transition and transversion mutations in PPBL and controls were not significantly different, suggestive of similar uracil-N-glycosylase (UNG) activity.[40]

In conclusion, PPBL cells displayed hyperproliferation with unusually low SHM levels per cell cycle that displayed preferential repair by Polη, which did not reflect the physiological antigen-dependent B-cell maturation observed in IgM⁺ memory B-cells subsets of healthy controls.

Normal selection against long IGH-CDR3s and replacement mutations in FRs

Memory B cells in healthy controls show molecular signs of selection in their Ig genes: short IGH-CDR3 regions and accumulation of SHM in CDR regions.[19,41] To study whether PPBL cells had undergone similar selection, we analyzed IGH-CDR3 size distributions and *IGHV* SHM patterns. PPBL cells and both IgM⁺ memory B-cell subsets from controls had a median IGH-CDR3 length of 15 amino acids. These were significantly shorter than the 17 amino acids in naive mature B cells (p< .001; data not shown). Thus, PPBL cells showed selection against long IGH-CDR3 regions.

To study whether despite the low mutation frequency, replacement mutations in PPBL accumulated in CDR regions, we calculated the frequencies of amino acid substitutions for each position in rearranged *IGHV* genes. Similar to both IgM⁺ memory B-cell subsets from controls, the amino acids in CDR1 and CDR2 regions of PPBL cells were more frequently mutated than in FR regions. Moreover, PPBL cells and control IgM⁺ memory B-cell subsets had a similarly high ratio between replacement and silent mutations in CDRs (data not shown). Thus, the molecular characteristics of *IGH* transcripts in PPBL cells are suggestive of a memory B-cell origin, despite the low levels of SHM.

Gene expression profiling of purified PPBL cells and control B-cell subsets

Detailed analysis of Ig gene rearrangements revealed molecular signs of antigen maturation in PPBL. Still, their replication history, SHM levels and SHM targeting were significantly different from those in marginal zone-like natural effector and GC-derived IgM-only memory B cells. To obtain more insight into the origin and maturation status of PPBL cells, we performed genome-wide gene expression profiling of purified PPBL cells, and 3 naive and 2 memory B-cell subsets from controls. All 6 analyzed subsets showed high expression of genes encoding pan-B markers, including CD19, CD20, CD22, CD79A, CD79B and BAFF-R (data not shown), and the gene expression patterns for markers used to isolate the subsets (CD5, CD38, IgM, IgD) correlated well with their protein expression. Moreover, PPBL and control B cell subsets were out of cell cycle as revealed by low *MKI67* gene expression and absence of nuclear Ki67 protein (not shown). Of the entire gene expression profile of PPBL cells,

IV
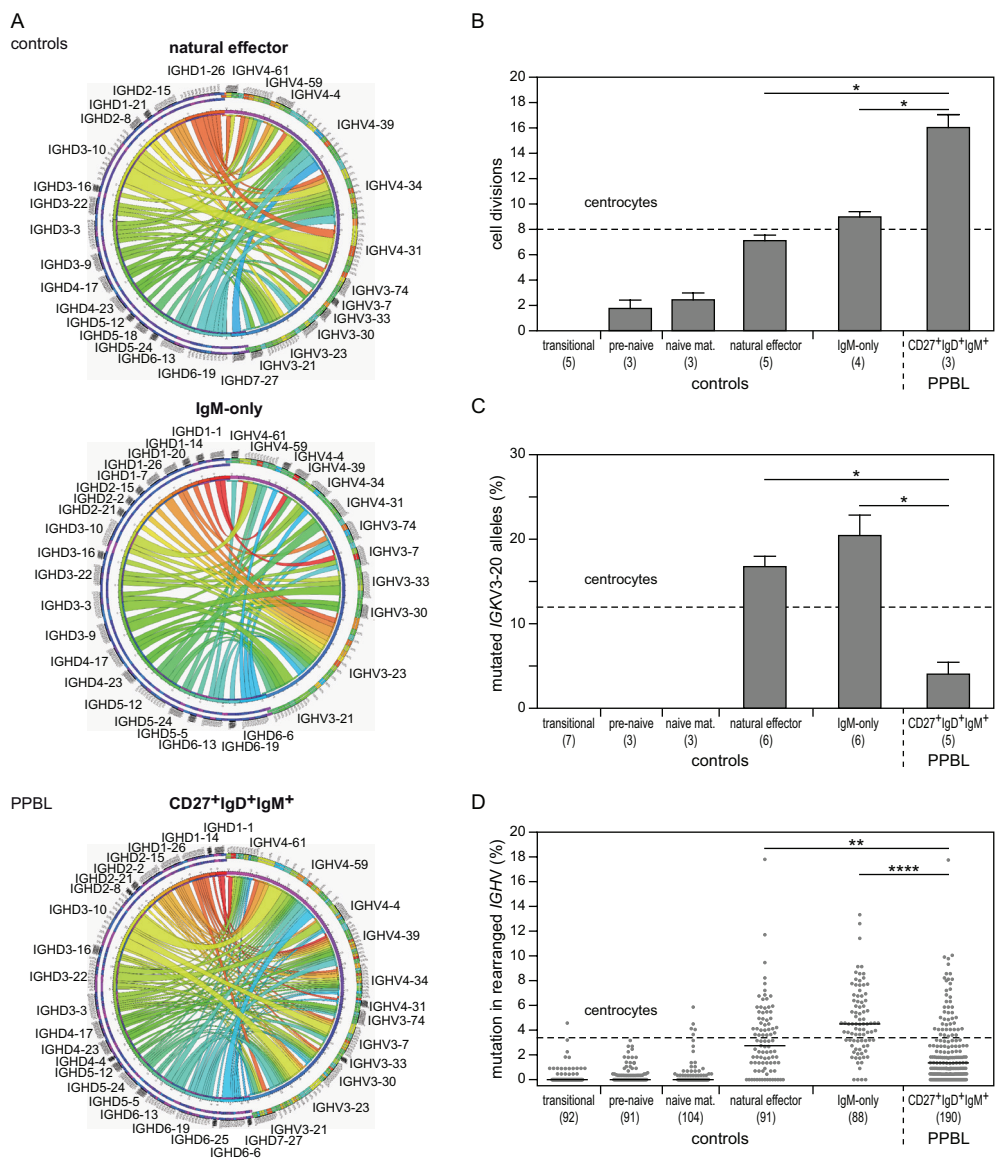
Figure 2. Ig repertoire diversity, replication history and SHM levels.
(A) The 12 predominantly used *IGHV3* and *IGHV4* genes are recombined with diverse *IGHD* genes as visualized with the Circos software package (http://mkweb.bcgsc.ca/circos). (B) Replication history in PPBL cells and control naive and IgM[+] memory B cells, as measured with the KREC assay.[19,26] Here and in panel C, bars represent mean values with SEM, and dashed lines represent values for tonsil–derived centrocytes.[19,26] In 2 out of 5 analyzed patients replication history of PPBL cells was above the detection limit of the assay. Differences between subsets were statistically analyzed with the Mann-Whitney test. [*], p< .05; [**], p< .01; [****], p< .0001 (C) Frequency of mutated *IGKV3-20* genes as measured with the IgκREHMA assay. (D) Frequency of mutated nucleotides in rearranged *IGHV* genes. All individual data points are shown as grey dots with black lines indicating median values.
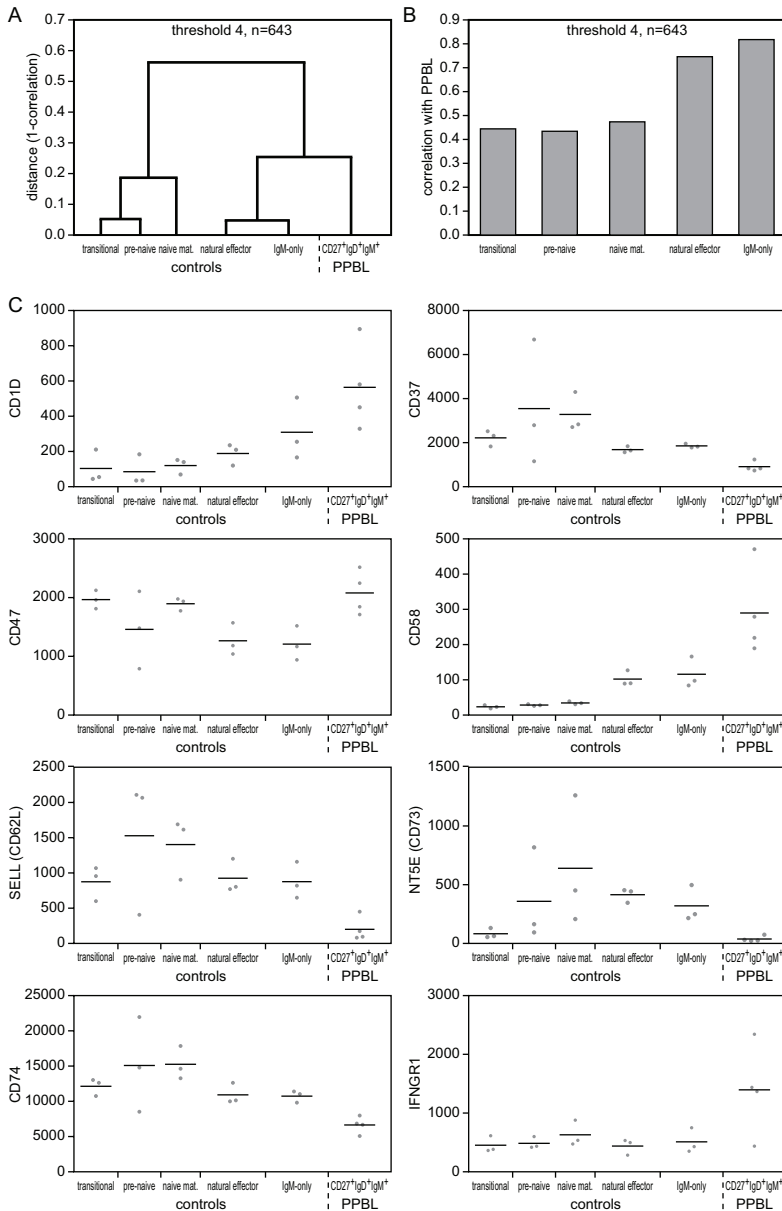
Figure 3. Gene expression profiling of PPBL B cells and control IgM⁺ B-cell subsets.
(A) Hierarchical clustering (complete linkage) using 1-correlation as a distance measure based on the 643 (threshold at $\log_2$ value 4) probe sets that showed the most variation between any two samples. Clustering analyses was performed without bias for known genes or subsets. (B) Correlation of the PPBL cells with each of the healthy naive and memory B-cell subsets. (C) Expression of selected genes encoding cell surface proteins that were significantly differentially expressed between PPBL cells and IgM⁺ memory B cells from healthy donors. All individual data points are shown as grey dots with black lines indicating mean values.

1,850 genes were significantly differentially expressed from transitional B cells, 1,468 from pre-naive B cells, 1,656 from naive mature B cells, 1,439 from natural effector B cells, and 1,129 from IgM-only B cells. Interestingly, the differences in gene expression levels of these genes were larger for the naive B-cell subsets than the memory B-cell subsets. Furthermore, PPBL cells showed high expression of the genes encoding CD27, CD80, CD86, CD180 and TACI fitting with an activated memory B-cell profile.[19,42]

To study which B-cell subset PPBL resembles best, we performed unsupervised clustering based on the probe sets that showed signal variation over all arrays. Maximum separation was observed with threshold 4 utilizing the 643 most informative probe sets (Figure 3A). Irrespective of the clustering threshold selected, naive B-cell subsets clustered separately from PPBL and memory B-cells (clustering distance 0.55). Control IgM[+] memory B cells were more similar to each other (clustering distance 0.05) than to PPBL cells (clustering distance 0.25) (Figure 3A). Thus, the expression patterns of these 643 genes in PPBL showed high correlation with both IgM[+] memory B-cell subsets (0.75-0.8), while hardly any correlation was found with naive B-cell subsets (~0.45).

Apoptosis and migration defects in PPBL

Previously, upregulation of the activator protein-1 (AP-1) transcription complex acting downstream the TGFβ signaling pathway, and downregulation of the Fas signaling pathway were described to underlie apoptosis defects in PPBL.[16] Therefore, we analyzed expression of genes involved in both pathways. While *FAS* was normally expressed in PPBL, multiple genes acting downstream in this pathway, such as *FADD*, *CASP8*, *BID*, *HTRA2* and *CYCS*, were upregulated in PPBL (data not shown). Several genes in the TGFβ signaling pathway (*SMURF2*, *SMAD2*, *SMAD4*, *MAPK8*, *RUNX3*) were differentially expressed in PPBL, but their overall pattern did not reflect upregulation of downregulation of the whole pathway. Genes of the AP-1 complex were normally expressed (*JUN*, *JUNB*, *JUND*) or downregulated (*FOS*, *FOSB*) (not shown). Moreover, there was no clear pattern in deregulation of BCL2-family genes, since both pro-apoptotic *BAD* and anti-apoptotic *BCL2* were downregulated. Interestingly, PPBL cells showed downregulation of *BACH2*, which is a B-cell specific pro-apoptotic transcription factor commonly downregulated in non-Hodgkin's lymphoma.[16,43] Thus, our gene expression studies did not confirm previous findings on global defects in apoptosis pathways. Still, downregulation of individual pro-apoptotic genes might tip the balance towards increased survival of PPBL cells.

Feugier *et al*. reported downregulation of lymphocyte adhesion molecules (CD11a, CD62L, CD29, CD49d, CD31) on PPBL cells in bone marrow, and suggested that these resulted in migration abnormalities and accumulation of cells in bone marrow and blood.[15] We found reduced expression of the genes encoding CD62L and CD31 in PPBL as compared to controls, but normal expression of CD11a, CD29 and CD49d (not shown). Additionally, we found that CD18, ICAM3 and CD73 were reduced in PPBL. These observations support previous indications of cell adhesion defects in PPBL cells.

Novel markers for immunophenotyping of PPBL

To identify novel immunophenotyping markers for identification of PPBL cells, we studied differentially expressed genes between PPBL and control memory B cells that encoded

membrane proteins. Eight genes were selected for further analyses based on the fold difference in gene expression and availability of monoclonal antibodies: CD1D, CD37, CD47, CD58, CD62L (SELL), CD73 (NT5E), CD74 and CD119 (IFNGR1) (Figure 3C). Flow cytometric analysis revealed that CD73 and CD62L expression levels were most discriminative between PPBL and control memory B cells (Figure 4A). While both markers showed a bimodal expression pattern on control memory B-cell subsets, their expression levels were uniformly low on all PPBL cells. The expression levels of CD1D, CD58 and CD119 were only slightly to moderately higher on PPBL than on control cells. Despite the significant differences in gene expression, no differences were observed in CD37, CD47 and CD74 membrane expression levels between PPBL and controls.

Due to the heterogeneous expression levels of CD73 and CD62L on control memory B cells, these markers could not be used independently to fully discriminate PPBL cells from control natural effector and IgM-only B-cell subsets. Therefore, we applied principal component analysis to study whether the combined information of CD62L, CD73, CD38 and IgD expression levels would be sufficient for discrimination of PPBL from controls.[35] Of four principal components, the 2D projection of the first and the third principal component (APS2), gave the best optical separation between all three subsets (Figure 4B). The marker that contributed the most to principal component 1 was CD73 (78%) and for principal component 3 this was IgD (76%). Concluding, we showed that PPBL cells and control IgM⁺ memory B cells can be separated based on a limited set of membrane markers: CD38, IgD and the newly identified CD62L and CD73.

Smoking does not induce downregulation of CD73 and CD62L
Heavy smoking can affect the immunophenotype of lymphocytes.[44-45] Since all five PPBL patients were heavy smokers, we wished to study whether the distinct CD73 and CD62L expression profiles were the result of smoking. Therefore, we analyzed the CD62L and CD73 expression levels on IgM⁺ memory B cells from healthy smoking and non-smoking women (age range 36-58). We found that CD73 expression was highly comparable between smokers and non-smokers, and clearly higher than in PPBL patients (data not shown). In contrast, CD62L expression was upregulated in smoking women as compared to non-smokers, but it was low in PPBL patients. Thus, the low levels of CD62L and CD73 in PPBL were not associated with smoking.

Low frequency of *BCL2-IGH* translocations in PPBL
The findings of splenomegaly, *BCL2-IGH* translocations, and development of a mature B-cell malignancy suggested that PPBL might be a pre-malignant condition.[2,4-9] We therefore studied typical molecular and phenotypic abnormalities of malignancies in PPBL cells and control B cells. First, we analyzed our patients for the presence of *BCL2-IGH* translocations involving either the MBR, the 3'MBR or the mcr of *BCL2* and one of the *IGHJ* genes (Figure 5A). *BCL2-IGH* rearrangements were detected in sorted PPBL cells in all 5 patients. Immunospectratyping of 4 patients revealed the presence of a single clone per patient (data not shown), and sequence analysis showed involvement of a breakpoint in the MBR, signs of Rag-mediated breaks in *IGH* and repair involving TdT (Figure 5B).[46] *BCL2-IGH* translocations were more frequent in PPBL cells, with a presence in 1 out of 1.3×10^3
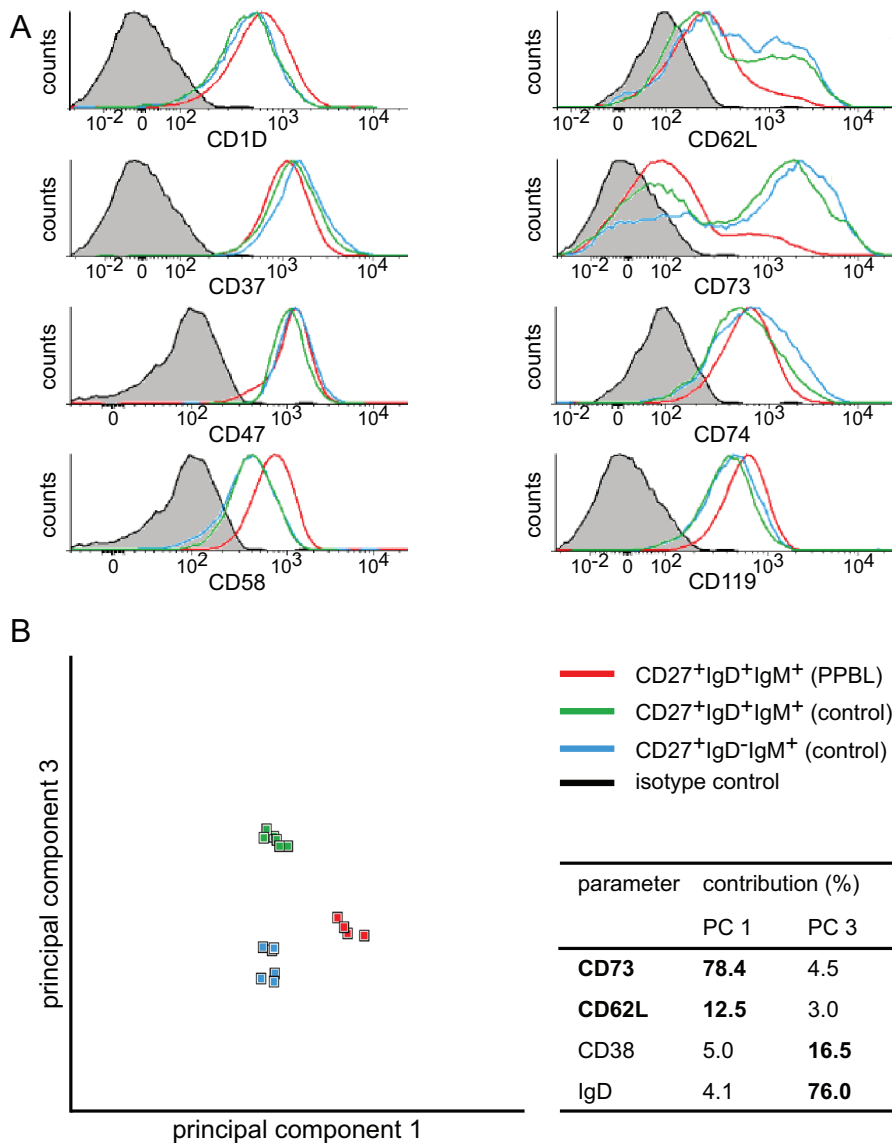
Figure 4. Multiparameter immunophenotyping of PPBL cells with newly identified markers.
(A) Expression levels of newly identified markers from gene expression profiling on PPBL cells and control IgM+ memory B-cell subsets. Each histogram represents merged data obtained for 4 PPBL patients or 6 healthy donors. Isotype controls are shown in grey. (B) Principal component analysis of flow cytometric data performed with INFINICYT software. Analyzed subsets were separated by an automatic population separator (APS) based on the expression levels of IgD, CD38, CD73 and CD62L. 2D projection of the first and the third principal component provided the best visual separation between the three subsets. Each dot represents a mean value for the analyzed subset in one of 4 patients or 6 healthy donors. The contributions of each of the markers to both the principal components are depicted with markers that contributed >10% indicated in bold. PC stands for the principal component.
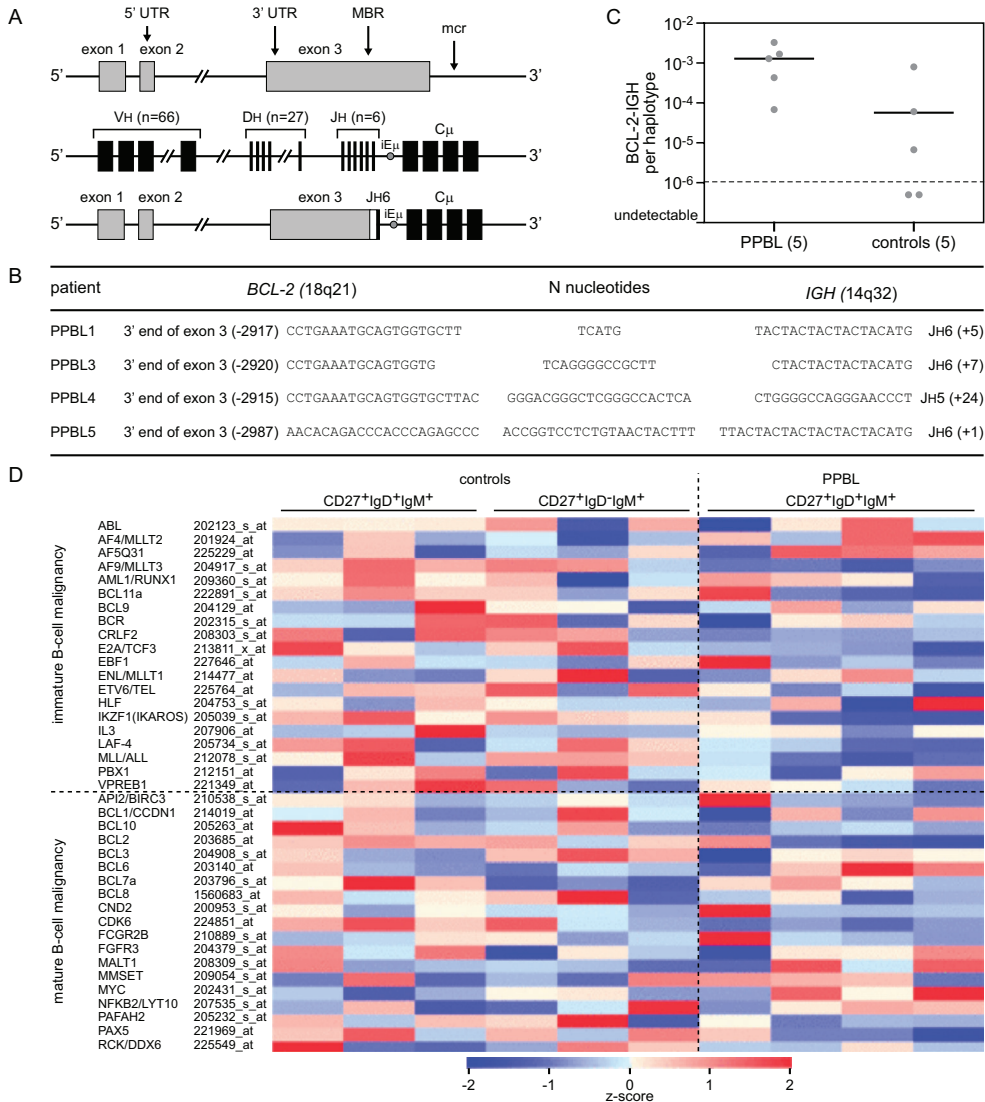
Figure 5. BCL2-IGH rearrangements and oncogene expression profiling of PPBL.
(A) Schematic representations of the *BCL2* gene (top), the *IGH* locus (middle) and a *BCL2-IGH* rearrangement (bottom panel). MBR denotes Major Breakpoint Region and mcr denotes microcluster region. (B) Sequence analysis of *BCL2-IGH* rearrangements that were amplified from 4 out of 5 patients. The position of breakpoint is indicated according to the 3' end of BCL2 exon 3 and the 5' end of the *IGHJ* gene. (C) Frequencies of *BCL2-IGH* rearrangements per haplotype as quantified with RQ-PCR in PPBL cells, natural effector cells from healthy donors and mature B-cell lines. In 2 out of 5 healthy donors, the frequency of rearrangements was below the detection limit of the assay indicated by dotted line ($<10^{-6}$ rearrangements per haplotype). PPBL and control rearrangement frequencies were not significantly different (Mann-Whitney test). Rearrangements were quantified relative to the t(14;18)-positive DoHH2 cell line. No rearrangements were found in 8 t(14;18)-negative mature B-cell lines. (D) Heat map with normalized expression levels of selected probe sets recognizing oncogenes involved in immature and mature B-cell malignancies. Z-scores were maximized to -2 and 2.

cells, than in controls (1 in 6.0×10^5 cells; Figure 5C). No signal was detected in mature B-cell lines, which were used as negative controls in this assay. Neither *BCL2* transcripts, nor BCL2 protein expression (not shown) were upregulated in PPBL cells, making it unlikely that these translocations contributed to the lymphocytosis.

Heterogeneous expression of oncogenes and tumor suppressor genes in PPBL

To study additional molecular processes that could drive the expansion of PPBL cells, we studied the gene expression levels of oncogenes that are typically involved in immature and mature B-cell malignancies in PPBL cells and control memory B cells. Individual PPBL patients showed upregulation of certain oncogenes as compared with natural effector and IgM only B cells from controls, but no single oncogene was upregulated in all of the patients. The most commonly upregulated oncogenes (z-score>1 in at least two patients) were *AF5Q31*, *AF9/MLLT1*, *BCL6, MATL1* and *MYC*, while the most commonly downregulated oncogenes (z-score <-1 in at least two patients) were *IKZF1*, *LAF-4*, *MLL/ALL*, *CDK6* and *BCL2*. Thus, it is unlikely that the same pathway was disrupted in all 5 PPBL patients. The expression levels of many reported tumor suppressor genes were not affected in PPBL: *TP53*, *TP73*, *RB1*, *MDM2*, *CDKN2A* (p16), *CDKN2B* (p15), *PTEN*, *ATM*, *PRDM1* (*BLIMP1*), *PHLPP1*, and *IRF4* (data not shown). Only *KLF4*, which functions as tumor suppressor in Hodgkin and non-Hodgkin lymphomas,[47] was downregulated in all of the patients and was among the most downregulated genes in PPBL (not shown).

Distinct phenotype of PPBL cells and mature B-cell malignancies

To study how closely the PPBL phenotype resembles that of a mature B-cell malignancy, we performed immunophenotyping in 4 PPBL cases with the B-CLPD antibody panel from the EU FP6 EuroFlow Consortium.[25] Multiparameter analysis was subsequently performed to compare the PPBL profile to those of 9 mature B-cell malignancies derived from various origins: the marginal zone, mantle zone, germinal center or memory B cells (Figure 6).

Principal component analysis revealed close clustering of all PPBL samples, implying that this is a truly unique biological entity. PPBL cells clustered separately from Burkitt lymphoma (BL), follicular lymphoma (FL), CD10+ DLBCL, hairy cell leukemia (HCL) and chronic lymphocytic leukemia (CLL). Still, in the automatic population separator view, the 1 standard deviation line in PPBL overlapped with lymphoplasmacytoid lymphoma (LPL) and CD10- DLBCL, and to a lesser extend with MZL and mantle cells lymphoma (MCL). The separation between PPBL and LPL was based mainly on the lower expression of CD200 and higher expression of CD305 (LAIR-1) in PPBL. Separation between PPBL and CD10- DLBCL was mainly based on the high expression levels of CD79b and IgM in PPBL. In contrast to healthy controls, CD62L contributed little to separation between PPBL and any of the analyzed malignancies (<10%). Thus, discrimination of PPBL from mature B cell malignancies is based on different markers than healthy controls and is possible with currently implemented EuroFlow immunophenotyping protocols.

DISCUSSION

Here we presented a detailed molecular and flow cytometric analysis of five PPBL patients. We showed that the persistent lymphocytosis was associated with intensive proliferation of CD27$^+$IgM$^+$IgD$^+$ cells that contained a broad and normally selected Ig repertoire with few SHM as compared to IgM$^+$ memory B-cell subsets in healthy donors. We demonstrated a unique gene expression profile in PPBL cells and identified cell surface markers to discriminate between PPBL cells, IgM$^+$ memory B cells from healthy donors, and mature B-cell malignancies.

We studied three processes that potentially contributed to the persistent B-cell lymphocytosis: proliferation, apoptosis and migration. In line with previous studies,[15] we found that PPBL cells were resting and lacked *MKI67* gene expression or Ki67 protein expression. We did observe a significantly higher replication history in PPBL cells than control IgM$^+$ memory B cells. Thus, although PPBL cells have undergone extensive proliferation, they have a resting phenotype. The hyperproliferation is likely to contribute to the B-cell expansion and potentially takes place in lymphoid tissue, analogous to current ideas about proliferation of tumor cells in chronic lymphocytic leukemia (CLL).[48] The high incidence of splenomegaly in PPBL patients mark the spleen as a likely site for this B-cell proliferation.

Our gene expression profiles analysis did not reveal deregulation of the TGFβ signaling pathway and the AP-1 complex, while multiple genes encoding Fas signaling proteins were upregulated. These findings do not support impaired apoptosis in PPBL and contrast observations from previous gene expression profiling.[16,43] This discrepancy is likely due to the fact that these studies performed on total blood mononuclear cells, while we analyzed purified B-cell subsets. Our approach allowed direct comparison of purified PPBL cells to the purified normal counterparts, providing a higher resolution to study differences in gene expression levels.

Expression analysis of adhesion molecule-encoding genes revealed downregulation of CD62L, CD31, CD18, ICAM-3 and CD73, but not CD11a, CD29 and CD49d. The results in part confirm previous findings,[15] and indicate deregulated adhesion and migration of PPBL cells.

PPBL cells had a broad and normally selected Ig repertoire. This clearly contrasts B-cell malignancies that carry monoclonal Ig genes in which often stereotypy is found between patients.[49-50] Benign B-cell expansions can be driven by infections, drug usage, cigarette smoking or genetic disorders and are polyclonal.[51-53] Infection-driven polyclonal B-cell expansions are often associated with Ig repertoire skewing: HBV infection promotes *IGHV1-3* gene usage, while the gp120 protein from HIV and *S. aureus* protein A both lead to increased *IGHV3* subgroup usage.[54-56] Other infectious microorganisms have properties of IgD superantigens and lead to B-cell expansion without bias in Ig repertoire, but with potential downregulation of IgD. These IgD superantigenic properties can be assigned to normal components of the human microflora, such as *M. catarrhalis*, *H. influenzae*, *E. coli* and *Streptococcus* group A.[57] Certain pathological conditions such as tobacco smoke exposure contribute to increased colonization of these microorganisms and higher incidence of infections.[58-59] Whereas these polyclonal expansions share characteristics of PPBL, they are usually transient and disappear when the infection or colonization
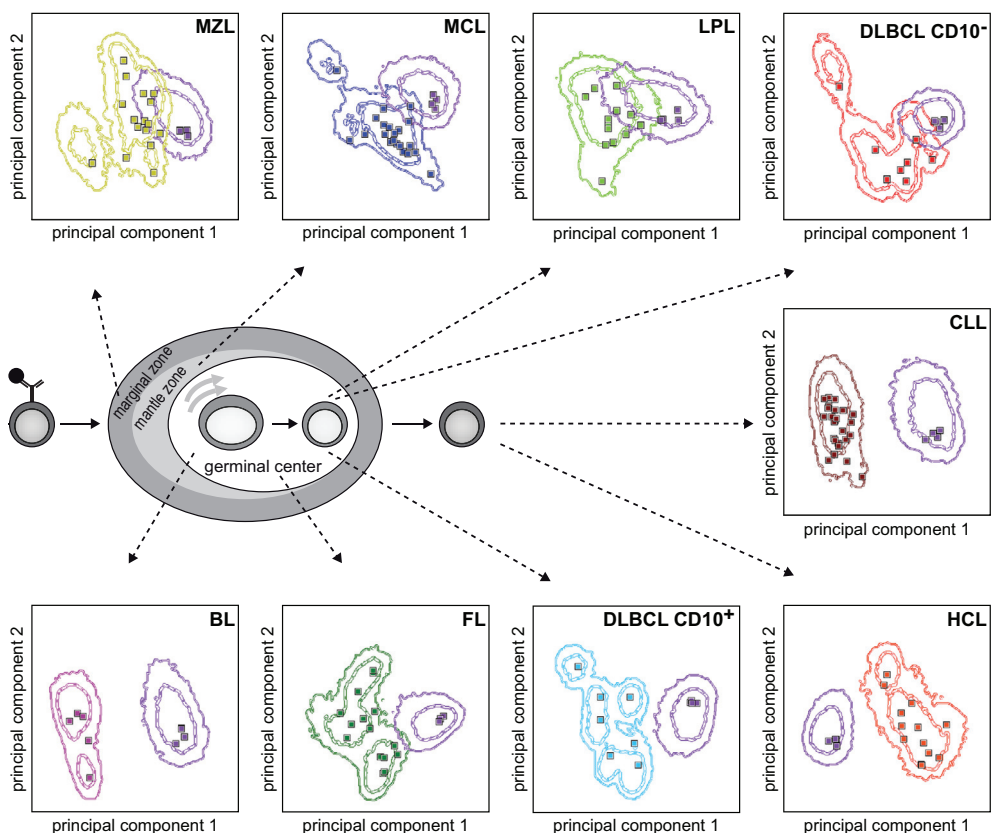
Figure 6. The immunoprofile of PPBL is distinct from mature B-cell malignancies.
PPBL cells were immunophenotyped with the previously published B-CLPD antibody panel designed to discriminate between mature B-cell malignancies.[25] Obtained data were analyzed with INFINICYT software and compared with the mature B-cell malignancies.[25] The presumed origins of the 9 mature B-cell malignancies are depicted in a schematic overview of B-cell maturation. The following abbreviations are used: MZL (marginal zone lymphoma), MCL (mantle cell lymphoma), LPL (lymphoplasmacytoid lymphoma), DLBCL (diffuse large B-cell lymphoma), CLL (chronic lymphocytic leukaemia), BL (Burkitt lymphoma), FL (follicular lymphoma), and HCL (hairy cell leukemia). PPBL and each of the analyzed malignancies were separated by an automatic population separator (APS) and visualized in 2D projections of the first and second principal components. Inner and outer continuous lines represent 1 and 2 standard deviations, respectively, of the indicated mature B-cell malignancy or PPBL.

is resolved. It is possible that foreign stimuli trigger the initial expansion, but this initial event might be followed by more changes in the cells that drive the persistency of PPBL.

We found that PPBL cells contained SHM in their rearranged Ig genes, but significantly less frequent than in IgM[+] memory B-cell subsets from healthy donors, particularly when the number of cell divisions in taken into account. In healthy adults, IgM-only cells originate from primary TD responses, while natural effector cells can be, at least in part, derived from TI responses.[19-20] Previous observations, such as the absence of proliferation in response to CD40L stimulation, functional T-cell anergy, and impaired IgG production upon anti-pneumococcal vaccinations, support the hypothesis of a TI origin of PPBL cells.[60-62] Our Ig

gene rearrangement and gene expression studies showed similar differences between PPBL and both IgM-only and natural effector B cells. In fact, natural effector and IgM-only B cells from controls were highly similar to each other. Thus, independent of their maturation pathways, their molecular characteristics as memory B cells are similar, while PPBL cells originate from a distinct and likely abnormal pathway as compared to natural effector and IgM-only memory B cells.

Our gene expression studies revealed 2 genes involved in Ig CSR, *BACH2* and CD73 that were downregulated in PPBL. We and others found reduced *BACH2* expression,[16] a transcription factor that was shown to be important for Ig CSR in mouse models.[63] The reduced CD73 gene expression results in very low CD73 surface expression in PPBL. CD73-deficient B cells were found capable to produce normal amounts of IgM, but were unable to synthesize IgG in response to either a TD or TI stimulators.[64] Thus, decreased *BACH2* and CD73 expression as compared to IgM$^+$ memory B-cell subsets from healthy controls potentially impairs terminal differentiation of these cells in PPBL.

Our detailed molecular studies did not reveal a clear relationship between PPBL and mature B-cell malignancies. For example, we found a low frequency of *BCL2-IGH* rearrangements and absence of stereotyped Ig genes. [49,65-67] Furthermore, the immunophenotype of PPBL cells was distinct from 9 analyzed mature B-cell malignances. Flow cytometric discrimination may be of value in distinction between PPBL and rare biclonal malignancies with a seemingly normal Igκ/Igλ ratio.[68-69] The separation of PPBL from LPL, CD10- DLBCL, MZL and MCL was not overt in all cases. This is most likely caused by the heterogeneous immunophenotypes of the LPL, DLBCL and MZL samples, a well-described phenomenon that underlies difficulties in differential diagnosis of these malignancies.[25,70-72] Moreover, some unconventional MCL cases can be difficult to distinguish from DLBCL.[25] Interestingly, in a few PPBL patients described so far, the diagnosis of PPBL was complicated by DLBCL and splenic MZL, but not any other haematological malignancy.[4-5] This, and the observed similarity between PPBL, DLBCL and MZL seem to indicate their origin from the same cell compartment and support the hypothesis that PPBL might precede B-cell malignancy development, albeit this is a rarely described event.

In this study, we showed for the first time that CD27$^+$IgM$^+$IgD$^+$ cells in PPBL have undergone extensive proliferation. Since, circulating B cells have a resting phenotype and gene expression profile, this proliferation seems to occur locally in tissue, preceding their appearance as expanded population in blood. The high Ig diversity with absence of stereotypes and the distinctive immunophenotype of PPBL is suggestive of a different pathophysiology than mature B-cell malignancies. Still, individual cases show some deregulated oncogene and tumor suppressor expression, and might be prone to develop into a malignancy. The newly identified cell surface markers can prove valuable for diagnosis of PPBL and might contribute to prognostic classification of patients at risk for developing a lymphoid malignancy.

IV

ACKNOWLEDGEMENTS

REFERENCES

1. Gordon DS, Jones BM, Browning SW, Spira TJ, Lawrence DN. Persistent polyclonal lymphocytosis of B lymphocytes. N Engl J Med. 1982;307:232-236.
2. Mossafa H, Malaure H, Maynadie M, et al. Persistent polyclonal B lymphocytosis with binucleated lymphocytes:a study of 25 cases. Groupe Francais d'Hematologie Cellulaire. Br J Haematol. 1999;104:486-493.
3. Himmelmann A, Gautschi O, Nawrath M, Bolliger U, Fehr J, Stahel RA. Persistent polyclonal B-cell lymphocytosis is an expansion of functional IgD(+)CD27(+) memory B cells. Br J Haematol. 2001;114:400-405.
4. Cornet E, Lesesve JF, Mossafa H, et al. Long-term follow-up of 111 patients with persistent polyclonal B-cell lymphocytosis with binucleated lymphocytes. Leukemia. 2009;23:419-422.
5. Roy J, Ryckman C, Bernier V, Whittom R, Delage R. Large cell lymphoma complicating persistent polyclonal B cell lymphocytosis. Leukemia. 1998;12:1026-1030.
6. Callet-Bauchu E, Renard N, Gazzo S, et al. Distribution of the cytogenetic abnormality +i(3)(q10) in persistent polyclonal B-cell lymphocytosis: a FICTION study in three cases. Br J Haematol. 1997;99:531-536.
7. Delage R, Jacques L, Massinga-Loembe M, et al. Persistent polyclonal B-cell lymphocytosis: further evidence for a genetic disorder associated with B-cell abnormalities. Br J Haematol. 2001;114:666-670.
8. Mossafa H, Tapia S, Flandrin G, Troussard X, Groupe Francais d'Hematologie C. Chromosomal instability and ATR amplification gene in patients with persistent and polyclonal B-cell lymphocytosis (PPBL). Leuk Lymphoma. 2004;45:1401-1406.
9. Delage R, Roy J, Jacques L, Darveau A. All patients with persistent polyclonal B cell lymphocytosis present Bcl-2/Ig gene rearrangements. Leuk Lymphoma. 1998;31:567-574.
10. Limpens J, Stad R, Vos C, et al. Lymphoma-associated translocation t(14;18) in blood B cells of normal individuals. Blood. 1995;85:2528-2536.
11. Liu Y, Hernandez AM, Shibata D, Cortopassi GA. BCL2 translocation frequency rises with age in humans. Proc Natl Acad Sci U S A. 1994;91:8910-8914.
12. Bell DA, Liu Y, Cortopassi GA. Occurrence of bcl-2 oncogene translocation with increased frequency in the peripheral blood of heavy smokers. J Natl Cancer Inst. 1995;87:223-224.
13. Troussard X, Flandrin G. Chronic B-cell lymphocytosis with binucleated lymphocytes (LWBL): a review of 38 cases. Leuk Lymphoma. 1996;20:275-279.
14. Larcher C, Fend F, Mitterer M, Prang N, Schwarzmann F, Huemer HP. Role of Epstein-Barr virus and soluble CD21 in persistent polyclonal B-cell lymphocytosis. Br J Haematol. 1995;90:532-540.
15. Feugier P, De March AK, Lesesve JF, et al. Intravascular bone marrow accumulation in persistent polyclonal lymphocytosis: a misleading feature for B-cell neoplasm. Mod Pathol. 2004;17:1087-1096.
16. Lawrie CH, Shilling R, Troussard X, et al. Expression profiling of persistent polyclonal B-cell lymphocytosis suggests constitutive expression of the AP-1 transcription complex and downregulation of Fas-apoptotic and TGFbeta signalling pathways. Leukemia. 2009;23:581-583.
17. Sims GP, Ettinger R, Shirota Y, Yarboro CH, Illei GG, Lipsky PE. Identification and characterization of circulating human transitional B cells. Blood. 2005;105:4390-4398.
18. Lee J, Kuchen S, Fischer R, Chang S, Lipsky PE. Identification and characterization of a human CD5+ pre-naive B cell population. J Immunol. 2009;182:4116-4126.
19. Berkowska MA, Driessen GJ, Bikos V, et al. Human memory B cells originate from three distinct germinal center-dependent and -independent maturation pathways. Blood. 2011.
20. Weller S, Braun MC, Tan BK, et al. Human blood IgM "memory" B cells are circulating splenic marginal zone B cells harboring a prediversified immunoglobulin repertoire. Blood. 2004;104:3647-3654.
21. Weller S, Faili A, Garcia C, et al. CD40-CD40L independent Ig gene hypermutation suggests a second B cell diversification pathway in humans. Proc Natl Acad Sci U S A. 2001;98:1166-1170.
22. Odegard VH, Schatz DG. Targeting of somatic hypermutation. Nat Rev Immunol. 2006;6:573-583.
23. Salcedo I, Campos-Caro A, Sampalo A, Reales E, Brieva JA. Persistent polyclonal B lymphocytosis: an expansion of cells showing IgVH gene mutations and phenotypic features of normal lymphocytes from the CD27+ marginal zone B-cell compartment. Br J Haematol. 2002;116:662-666.
24. Loembe MM, Neron S, Delage R, Darveau A. Analysis of expressed V(H) genes in persistent polyclonal

B cell lymphocytosis reveals absence of selection in CD27+IgM+IgD+ memory B cells. Eur J Immunol. 2002;32:3678-3688.

25. van Dongen JJ, Lhermitte L, Bottcher S, et al. EuroFlow antibody panels for standardized n-dimensional flow cytometric immunophenotyping of normal, reactive and malignant leukocytes. Leukemia. 2012.

26. van Zelm MC, Szczepanski T, van der Burg M, van Dongen JJ. Replication history of B lymphocytes reveals homeostatic proliferation and extensive antigen-induced B cell expansion. J Exp Med. 2007;204:645-655.

27. Andersen P, Permin H, Andersen V, et al. Deficiency of somatic hypermutation of the antibody light chain is associated with increased frequency of severe respiratory tract infection in common variable immunodeficiency. Blood. 2005;105:511-517.

28. van Dongen JJ, Langerak AW, Bruggemann M, et al. Design and standardization of PCR primers and protocols for detection of clonal immunoglobulin and T-cell receptor gene recombinations in suspect lymphoproliferations: report of the BIOMED-2 Concerted Action BMH4-CT98-3936. Leukemia. 2003;17:2257-2317.

29. Lefranc MP, Giudicelli V, Ginestoux C, et al. IMGT, the international ImMunoGeneTics information system. Nucleic Acids Res. 2009;37:D1006-1012.

30. Longo NS, Lugar PL, Yavuz S, et al. Analysis of somatic hypermutation in X-linked hyper-IgM syndrome shows specific deficiencies in mutational targeting. Blood. 2009;113:3706-3715.

31. Souto-Carneiro MM, Longo NS, Russ DE, Sun HW, Lipsky PE. Characterization of the human Ig heavy chain antigen binding complementarity determining region 3 using a newly developed software algorithm, JOINSOLVER. J Immunol. 2004;172:6790-6802.

32. van Zelm MC, van der Burg M, de Ridder D, et al. Ig gene rearrangement steps are initiated in early human precursor B cell subsets and correlate with specific transcription factor expression. J Immunol. 2005;175:5912-5922.

33. Nodland SE, Berkowska MA, Bajer AA, et al. IL-7R expression and IL-7 signaling confer a distinct phenotype on developing human B-lineage cells. Blood. 2011;118:2116-2127.

34. Pedreira CE, Costa ES, Barrena S, et al. Generation of flow cytometry data files with a potentially infinite number of dimensions. Cytometry A. 2008;73:834-846.

35. Costa ES, Pedreira CE, Barrena S, et al. Automated pattern-guided principal component analysis vs expert-based immunophenotypic classification of B-cell chronic lymphoproliferative disorders: a step forward in the standardization of clinical immunophenotyping. Leukemia. 2010;24:1927- 1933.

36. Verhagen OJ, Willemse MJ, Breunis WB, et al. Application of germline IGH probes in real-time quantitative PCR for the detection of minimal residual disease in acute lymphoblastic leukemia. Leukemia. 2000;14:1426-1435.

37. Korsmeyer SJ. BCL-2 gene family and the regulation of programmed cell death. Cancer Res. 1999;59:1693s-1700s.

38. Brezinschek HP, Brezinschek RI, Lipsky PE. Analysis of the heavy chain repertoire of human peripheral B cells using single-cell polymerase chain reaction. J Immunol. 1995;155:190-202.

39. Suzuki I, Pfister L, Glas A, Nottenburg C, Milner EC. Representation of rearranged VH gene segments in the human adult antibody repertoire. J Immunol. 1995;154:3902-3911.

40. Di Noia J, Neuberger MS. Altering the pathway of immunoglobulin hypermutation by inhibiting uracil-DNA glycosylase. Nature. 2002;419:43-48.

41. Meffre E, Schaefer A, Wardemann H, Wilson P, Davis E, Nussenzweig MC. Surrogate light chain expressing human peripheral B cells produce self-reactive antibodies. J Exp Med. 2004;199:145-150.

42. Good KL, Avery DT, Tangye SG. Resting human memory B cells are intrinsically programmed for enhanced survival and responsiveness to diverse stimuli compared to naive B cells. J Immunol. 2009;182:890-901.

43. Roussel M, Roue G, Sola B, Mossafa H, Troussard X. Dysfunction of the Fas apoptotic signaling pathway in persistent polyclonal B-cell lymphocytosis. Haematologica. 2003;88:239-240.

44. Pan F, Yang TL, Chen XD, et al. Impact of female cigarette smoking on circulating B cells in vivo: the suppressed ICOSLG, TCF3, and VCAM1 gene functional network may inhibit normal cell function. Immunogenetics. 2010;62:237-251.

45. Scott DA, Palmer RM. The influence of tobacco smoking on adhesion molecule profiles. Tob Induc Dis. 2002;1:7-25.

46. Kuppers R, Dalla-Favera R. Mechanisms of chromosomal translocations in B cell lymphomas. Oncogene. 2001;20:5580-5594.

IV

47. Guan H, Xie L, Leithauser F, et al. KLF4 is a tumor suppressor in B-cell non-Hodgkin lymphoma and in classic Hodgkin lymphoma. Blood. 2010;116:1469-1478.

48. Herishanu Y, Perez-Galan P, Liu D, et al. The lymph node microenvironment promotes B-cell receptor signaling, NF-kappaB activation, and tumor proliferation in chronic lymphocytic leukemia. Blood. 2011;117:563-574.

49. Bikos V, Darzentas N, Hadzidimitriou A, et al. Over 30% of patients with splenic marginal zone lymphoma express the same immunoglobulin heavy variable gene: ontogenetic implications. Leukemia. 2012.

50. Stamatopoulos K, Belessi C, Moreno C, et al. Over 20% of patients with chronic lymphocytic leukemia carry stereotyped receptors: Pathogenetic implications and clinical correlations. Blood. 2007;109:259-270.

51. Granados E, Llamas P, Pinilla I, et al. Persistent polyclonal B lymphocytosis with multiple bcl-2/IgH rearrangements: a benign disorder. Haematologica. 1998;83:369-375.

52. Corre F, Lellouch J, Schwartz D. Smoking and leucocyte-counts. Results of an epidemiological survey. Lancet. 1971;2:632-634.

53. Taylor RG. Smoking and the leucocyte count. Eur J Respir Dis. 1987;71:65-68.

54. Goodglick L, Braun J. Revenge of the microbes. Superantigens of the T and B cell lineage. Am J Pathol. 1994;144:623-636.

55. Farci P, Diaz G, Chen Z, et al. B cell gene signature with massive intrahepatic production of antibodies to hepatitis B core antigen in hepatitis B virus-associated acute liver failure. Proc Natl Acad Sci U S A. 2010;107:8766-8771.

56. Silverman GJ, Cary SP, Dwyer DC, Luo L, Wagenknecht R, Curtiss VE. A B cell superantigen-induced persistent "Hole" in the B-1 repertoire. J Exp Med. 2000;192:87-98.

57. Chen K, Cerutti A. New insights into the enigma of immunoglobulin D. Immunol Rev;237:160-179.

58. Bakhshaee M, Naderi HR, Ghazvini K, Sotoudeh K, Amali A, Ashtiani SJ. Passive smoking and nasopharyngeal colonization by Streptococcus pneumoniae, Haemophilus influenzae, and Moraxella catarrhalis in daycare children. Eur Arch Otorhinolaryngol. 2011.

59. Brook I. The impact of smoking on oral and nasopharyngeal bacterial flora. J Dent Res. 2011;90:704-710.

60. Loembe MM, Lamoureux J, Deslauriers N, Darveau A, Delage R. Lack of CD40-dependent B-cell proliferation in B lymphocytes isolated from patients with persistent polyclonal B-cell lymphocytosis. Br J Haematol. 2001;113:699-705.

61. Mitterer M, Lanthaler AJ, Irschick EU, Engelmann H, Larcher C, Huemer HP. Functional T-cell anergy in a case of persistent polyclonal B-cell lymphocytosis. Leuk Res. 2005;29:1479-1488.

62. Hafraoui K, Moutschen M, Smet J, Mascart F, Schaaf-Lafontaine N, Fillet G. Selective defect of anti-pneumococcal IgG in a patient with persistent polyclonal B cell lymphocytosis. Eur J Intern Med. 2009;20:e62-65.

63. Muto A, Ochiai K, Kimura Y, et al. Bach2 represses plasma cell gene regulatory network in B cells to promote antibody class switch. Embo J. 2010;29:4048-4061.

64. Thompson LF, Ruedi JM. Synthesis of immunoglobulin G by pokeweed mitogen- or Epstein-Barr virus-stimulated human B cells in vitro is restricted to the ecto-5'-nucleotidase positive subset. J Clin Invest. 1988;82:902-905.

65. Casassus P, Lortholary P, Komarover H, Lejeune F, Hors J. Cigarette smoking-related persistent polyclonal B lymphocytosis. A premalignant state. Arch Pathol Lab Med. 1987;111:1081.

66. Hadzidimitriou A, Agathangelidis A, Darzentas N, et al. Is there a role for antigen selection in mantle cell lymphoma? Immunogenetic support from a series of 807 cases. Blood. 2011;118:3088-3095.

67. Agathangelidis A, Hadzidimitriou A, Rosenquist R, Stamatopoulos K. Unlocking the secrets of immunoglobulin receptors in mantle cell lymphoma: implications for the origin and selection of the malignant cells. Semin Cancer Biol. 2011;21:299-307.

68. Hsi ED, Hoeltge G, Tubbs RR. Biclonal chronic lymphocytic leukemia. Am J Clin Pathol. 2000;113:798-804.

69. Chang H, Cerny J. Molecular characterization of chronic lymphocytic leukemia with two distinct cell populations: Evidence for separate clonal origins. Am J Clin Pathol. 2006;126:23-28.

70. Lin P, Molina TJ, Cook JR, Swerdlow SH. Lymphoplasmacytic lymphoma and other non-marginal zone lymphomas with plasmacytic differentiation. Am J Clin Pathol. 2011;136:195-210.

71. Molina TJ, Lin P, Swerdlow SH, Cook JR. Marginal zone lymphomas with plasmacytic differentiation and related disorders. Am J Clin Pathol. 2011;136:211-225.

72. A clinical evaluation of the International Lymphoma Study Group classification of non-Hodgkin's lymphoma.

The Non-Hodgkin's Lymphoma Classification Project. Blood. 1997;89:3909-3918.

73. Comans-Bitter WM, de Groot R, van den Beemd R, et al. Immunophenotyping of blood lymphocytes in childhood. Reference values for lymphocyte subpopulations. J Pediatr. 1997;130:388-393.

IV

V

Circulating human CD27-IgA+ memory B cells recognize bacteria with polyreactive immunoglobulins

Magdalena A. Berkowska[1], Jacques J.M. van Dongen[1], Dick de Ridder[2], Yen S. Ng[3], Eric R.F. Meffre[3],* and Menno C. van Zelm[1],*

[1]Dept. Immunology, Erasmus MC, Rotterdam, the Netherlands; [2]The Delft Bioinformatics Lab, Faculty of Electrical Engineering, Mathematics and Computer Science, Delft University of Technology, Delft, The Netherlands; [3]Department of Immunobiology, Yale University School of Medicine, New Haven, Connecticut, USA

*E.R.F.M. and M.C.v.Z. are joint senior authors of this study.

Manuscript in preparation

ABSTRACT

The vast majority of immunoglobulin (Ig)A production occurs in mucosal tissue following T-cell dependent and T-cell independent antigen responses. To study the nature of each of these responses, we analyzed the gene expression and Ig reactivity profiles of T-cell dependent CD27$^+$IgA$^+$ and T-cell independent CD27$^-$IgA$^+$ circulating memory B cells. Both CD27$^+$IgA$^+$ and CD27$^-$IgA$^+$ B cells showed a highly similar gene expression profile with IgG$^+$ memory B-cell subsets with typical upregulation of activation markers and downregulation of inhibitory receptors. Importantly, CD27$^-$IgA$^+$ B cells showed upregulated *CCR9* and *RUNX2* expression levels, which are associated with mucosal immune responses. In contrast, the Ig repertoire of CD27$^-$IgA$^+$ B cells differed from CD27$^+$IgA$^+$ B cells with respect to somatic hypermutation levels and prominent *IGLV3-1* gene use. Furthermore, CD27$^-$IgA$^+$ B cells were enriched in polyreactive antibodies that reacted with high affinity to common bacteria strains. Thus, T-cell independent IgA responses generate B-cell memory, but show a unique reactivity pattern with polyreactive recognition of bacteria.

INTRODUCTION

The mucosal surfaces of the oral cavity, lungs and intestinal tract are major sites of antibody production (1). This mainly concerns the secretory form of immunoglobulin S(Ig)A that is produced by terminally differentiated B cells: plasma cells.

Each human B cell carries surface (s)Ig that is generated through V(D)J recombination in the Ig heavy (IgH) and Igκ and Igλ light chain genes during stepwise differentiation in bone marrow (2-3). IgA responses involve affinity maturation by induction of somatic hypermutations (SHM) in the Ig variable domains and class-switch recombination from the IgM to the IgA isotype (4). Both SHM and CSR processes are mediated by the activation-induced cytidine deaminase (AID) enzyme (5), which is upregulated in activated B cells through CD40 signaling following interaction with CD40L on activated CD4⁺ T cells. Such a T-cell dependent (TD) response takes place in a germinal center reaction in lymphoid tissue and involves extensive proliferation and affinity maturation. Alternatively, AID expression can be induced in T-cell independent (TI) B-cell responses, which are associated with limited proliferation and affinity maturation to lipid or carbohydrate structures (4, 6-9). TI class-switching towards IgA is well-supported by the microenvironment of gut, especially by the dendritic cells (DC) in the gut-associated lymphoid tissue. These DCs secrete retinoic acid (RA) that activates circulating B cells to induce expression of the adhesion molecule α4β7 and the chemokine CCR9, which both mediate gut homing (10). Furthermore, upon activation via Toll-like receptors (TLR), DCs and monocytes secrete BAFF and APRIL, which bind to TACI on B cells and induces class-switching towards IgA in a CD40-independent manner (11-14). Finally, DC-derived TGFβ and RA act in concert with IL-5, IL-6 and IL-10 to induce differentiation of class-switched B cells into antibody secreting plasma cells (10, 14-16).

The microbiome of the human gastrointestinal tract contains large numbers of bacteria from up to 30,000 species (17-18). The majority of these bacteria are coated with Ig (19) that are generated in dynamic responses and require SHM (20-21). Although about 25% of IgA-producing plasmablasts are polyreactive, they show molecular signs of antigen-mediated selection (22). This suggests antigen-induced production rather than secretion of "natural antibodies" independent of antigen stimulation. It is tempting to speculate that TI IgA is directed against bacterial cell wall components of commensal bacteria to support the formation of a biofilm and disable translocation of bacterial flora through the epithelial layer (23-24). This would prevent priming of systemic high-affinity TD responses to beneficial gut microbiota as was observed in MyD88/TRIF knock-out mice deficient in TI IgA production, which spontaneously developed systemic responses against gut microbiota (25). Unfortunately, the lack of markers to distinguish IgA plasma cells in gut based on their origin from TI or TD responses prevents studies to address this issue.

Recently, we distinguished two circulating human IgA⁺ memory B-cell subsets based on differential CD27 expression. Detailed molecular analysis revealed that conventional CD27⁺IgA⁺ cells were generated from GC responses, whereas generation of unconventional CD27⁻IgA⁺ cells did not depend on cognate T cell help (26). In fact, the limited replication history, low levels of SHM and increased IgA2 use in CD27⁻IgA⁺ memory B cells were reminiscent of IgA⁺ B cells from the intestinal *lamina propria*. Therefore, we studied the CD27⁺IgA⁺ and CD27⁻IgA⁺ subsets to dissect the nature of IgA B-cell memory through gene

expression profiling and detailed immunophenotyping of three naive and six memory B-cell subsets. Furthermore, we assessed the reactivity patterns derived from TD and TI responses by analysis of monoclonal antibodies generated from single cell-sorted CD27$^+$IgA$^+$ and CD27$^-$IgA$^+$ memory B cells.

RESULTS

Gene expression profiling of naive and memory B-cell subsets
Circulating CD27$^+$IgA$^+$ and CD27$^-$IgA$^+$ B cells both display a memory B-cell phenotype (26). Still, their distinct degrees of molecular maturation suggest that they originate from different types of responses. To study whether the T-cell independent origin of CD27$^-$IgA$^+$ B cells results in a typical memory B-cell transcription program, we compared their gene expression profile with 3 naive and 5 other memory B-cell subsets.

Unbiased clustering analysis was performed based on probe sets that showed the greatest differential expression between any of the 9 analyzed B-cell subsets (Figure 1A). This analysis showed three main clusters. Cluster 1 comprised the three naive B cells (transitional, pre-naive and naive mature). The second cluster contained the IgM$^+$ memory B-cell subsets: natural effector and IgM-only B cells, and the Ig class-switched CD27$^+$IgA$^+$, CD27$^+$IgG$^+$, CD27$^-$IgA$^+$ and CD27$^-$IgG$^+$ memory B cells formed the third cluster (Figure 1A). Even though all class-switched memory B cells clustered closely together (distance ~0.1), CD27$^+$IgA$^+$ cells mostly resembled CD27$^+$IgG$^+$ cells, and CD27$^-$IgA$^+$ cells were most similar to CD27$^-$IgG$^+$ cells (Figure 1A). The expression patterns of these genes in CD27$^-$IgA$^+$ B cells correlated well with all Ig-class switched cells, showed medium correlation with the IgM$^+$ memory B-cell subsets and differed mostly from naive B cells (Figure 1B).

All 9 B-cell subsets showed high gene expression levels of pan-B markers CD19, CD20, BAFF-R, CD79A and CD79B (data not shown). The gene expression levels for markers that were used to define the subsets (CD5, CD38, IgM, IgD, IgA, IgG, CD27) correlated well with their protein expression levels (Figure 1C). All memory B-cell subsets showed increased expression levels of activation markers and co-stimulatory molecules, such as CD80, CD86, TACI, FAS and CD58, and downregulation of genes encoding inhibitory receptors CD22 and CD72 as compared to naive B-cell subsets (26-27). These expression patterns were confirmed on protein level with flowcytometry (Figure 2) (26) .

T cell-dependent and -independent response mediators
RUNX2 and *RUNX3* act downstream TGF-β and RA signaling pathways to induce TI class-switching towards IgA in gut (28). While *RUNX3*, *TGFBR* and *RARA* expression levels were similarly high in all analyzed subset, *RUNX2* was exclusively expressed by IgA$^+$ cells (Figure 1, data not shown). Remarkably, *RUNX2* expression was significantly higher in CD27$^-$IgA$^+$ than in CD27$^+$IgA$^+$ cells, corresponding with the TI origin of this subset.

TLR gene expression levels were highly comparable between IgA$^+$ and other memory B cells (not shown). However expression of *TLR1* was significantly lower and expression of *TLR10* was higher in CD27$^-$IgA$^+$ cells, than in naive mature B cells, TLR-1 and

TLR-10 protein expression levels were similarly low in both naive and memory B-cell subsets (Figure 2). Furthermore, there were no signs of deregulation of TLR-signaling pathway in IgA$^+$ cells.

Both IgA$^+$ B-cell subsets showed high expression of *IL6R* and *IL10RA*, which supports the role of IL-6 and IL-10 in IgA$^+$ memory B-cell differentiation, while their expression of *IL4R* was downregulated (not shown).

Expression of mucosa homing-related genes

Expression of chemokine receptors on lymphocytes determines their ability to respond to stimuli and to migrate to a certain anatomical location. All analyzed subsets expressed CXCR4 and CCR7 responsible for homing to lymph nodes, but their levels were significantly higher on naive than on class-switched memory B cells (data not shown). CCR7 protein was present on nearly all naive mature B cells, but only on a population of memory cells (Figure 2).

CD27$^-$IgA$^+$ cells, as the only of the analyzed subsets, expressed small-intestine homing receptor, CCR9 (not shown). Still, CCR9 protein expression was limited to a small population of cells (Figure 2). None of the analyzed subsets expressed CCR10.

Stimulation of chemokine receptors induces surface expression of diverse adhesion molecules. All analyzed subsets showed similarly high expression of genes encoding CD62L (*SELL*), α4β7 (*ITGA4/ITGB7*), and LFA-1 (*ITGAL/ITGB2*) involved in migration to lymph nodes (29-30), while memory B cells upregulated *ITGB1* encoding β1 subunit of α4β1, which is one of the adhesion molecules involved in migration to the mucosa (not shown).

Distinct Ig gene repertoires in CD27$^+$IgA$^+$ and CD27$^-$IgA$^+$ cells

The distinct maturation pathways of CD27$^+$IgA$^+$ and CD27$^-$IgA$^+$ memory B cells were hardly reflected in their transcription program. However, previous observations indicated that these pathways differentially impact IgH repertoire selection (26). Therefore, we studied the IgH and Ig light chain repertoires and gene features from purified single cells of both subsets.

The *IGHV* subgroup and *IGHJ* gene distributions in CD27$^+$IgA$^+$ and CD27$^-$IgA$^+$ memory B cells were similar to each other (Figure 3A), and to previously reported naive B cells (31). Over 50% of rearrangements utilized a member of the large *IGHV3* subgroup, followed by *IGHV4* (~20%) and *IGHV1* (~15%). In both IgA$^+$ subsets *IGHV3-23*, *IGHV3-30*, *IGHV3-48* were the most frequent *IGHV3* genes, and *IGHV4-59* was the most frequent *IGHV4* gene. The *IGHJ4* gene was mostly used *IGHJ* gene, followed by *IGHJ5* and *IGHJ6*. The IGH-CDR3 regions in rearrangements from both IgA$^+$ subsets showed similar length distributions with the majority regions being 10-14 amino acids in size (Figure 3B). The IGH-CDR3 regions did differ in the content of positively charged amino acids (arginine, lysine and histidine). There were fewer rearrangements with 2 positively charged amino acids in the IGH-CDR3 in CD27$^-$IgA$^+$ than in CD27$^+$IgA$^+$ memory B cells. (Figure 3B). In agreement with previous findings (26), CD27$^-$IgA$^+$ memory B cells carried fewer mutations in their *IGHV* genes than CD27$^+$IgA$^+$ cells. The median number of mutations in this subset was 10 and about 15% of sequences were unmutated. In contrast, nearly all *IGHV* genes of CD27$^+$IgA$^+$ memory B cells were mutated and the median mutation content was 19 (Figure 3B). Despite fewer SHM in *IGHV* of CD27$^-$IgA$^+$ than of CD27$^+$IgA$^+$ cells, these were normally selected in both subsets as reflected by a high ratio of replacement over
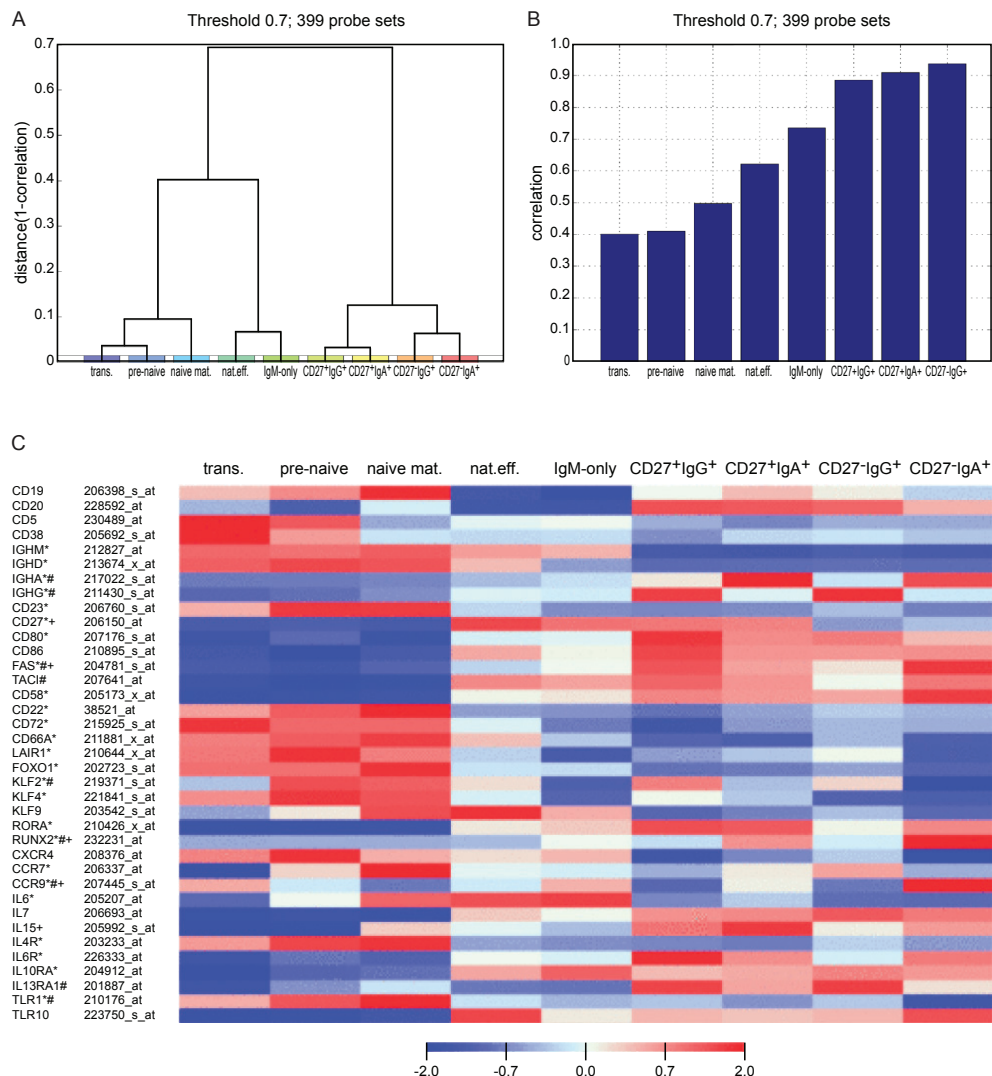
Figure 1. Gene expression profiling of naive and memory B-cell subsets.
(A) Hierarchical clustering (complete linkage) using 1-correlation as a distance measure based on the 399 probe sets that showed the most variation between any two samples (threshold at $\log_2$ value 0.7). Clustering analyses was performed without bias for known genes or subsets. (B) Correlation of the gene expression profiles of these 399 genes for CD27$^-$IgA$^+$ memory B cells as compared to the naive and memory B cell subsets. (C) Heat map with normalized expression levels of selected probe sets in naive and memory B-cell subsets. Z-scores were maximized to -2 and 2.

silent mutations (R/S ratio) of ~3 in their complementarity determining regions (CDR).

The *IGK* repertoire did not differ between the two IgA$^+$ memory B-cell subsets and was highly comparable with naive mature B cells showing predominant *IGKV1* and *IGKV3* subgroup and *IGKJ1* and *IGKJ4* gene use (Figure 4A) (31). In contrast to IgH and Igκ,

A
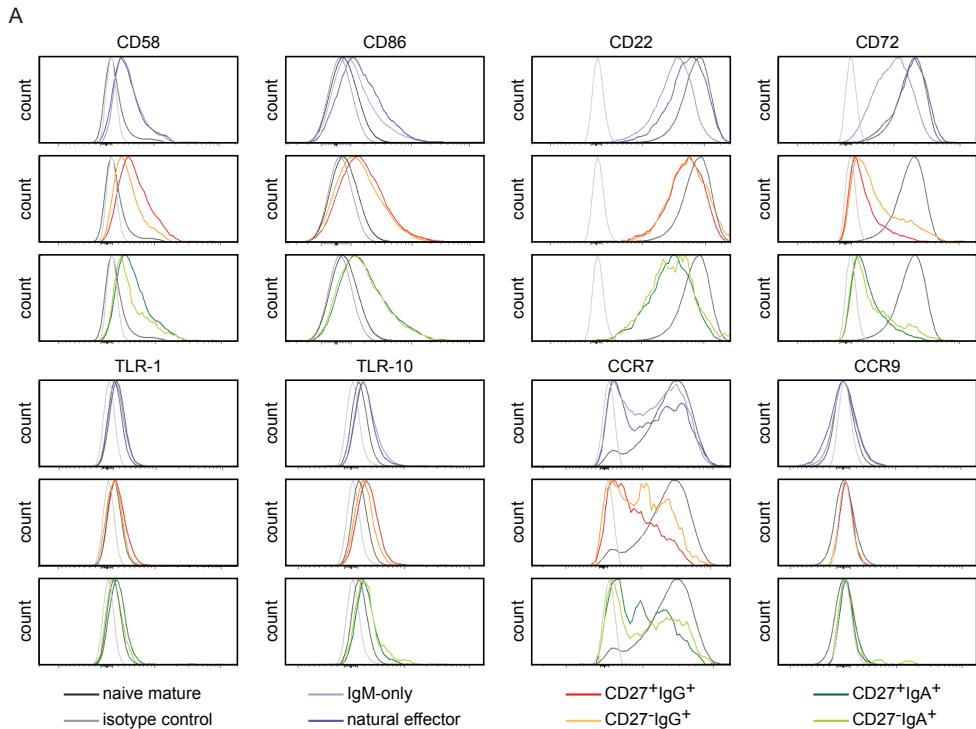
Figure 2. Expression levels of selected cell-surface markers on memory B-cell subsets.
Expression levels of selected co-stimulatory molecules (CD58, CD86), BCR-signaling inhibitors (CD22, CD72), Toll-like receptors (TLR-6, TLR-10) and chemokine receptors (CCR7, CCR9) were flow cytometrically analyzed on IgM⁺, IgG⁺ and IgA⁺ memory B-cell subsets. Each plot contains a light grey histogram representing the isotype control, and a dark grey histogram representing naive mature B cells.

the subsets differed in their Igλ repertoire. While almost 90% of *IGL* rearrangements in CD27⁺IgA⁺ cells involved the *IGLV1* or *IGLV2* subgroups, the rearrangements in CD27⁻IgA⁺ B cells reflected the pattern of naive mature cells with 29% *IGLV3* and 29% *IGLV2* subgroup use (Figure 4B). The increased *IGLV3* use in CD27⁻IgA⁺ B cells was mainly caused by abundant *IGLV3-1* gene use (20% vs 0%), while these cells contained fewer *IGLV2-8* genes than CD27⁺IgA⁺ cells (2% vs 18%; Figure 4C). The *IGLV2-8*, *IGLV3-1* nor any of the other *IGHV* genes showed preferential pairing with *IGHJ* genes (not shown). The *IGLJ* repertoire in CD27⁻IgA⁺ cells showed reduced *IGLJ1* and increased *IGHJ3* gene use as compared to CD27⁺IgA⁺ memory B cells.

Similar to *IGHV*, the rearranged *IGKV* and *IGLV* genes in CD27⁺IgA⁺ cells carried significantly more SHM than in CD27⁻IgA⁺ cells (Figure 4D). The SHM levels were in general lower than in *IGHV* with slightly more mutations in *IGLV* than *IGKV* in CD27⁺IgA⁺ memory B cells (15 vs 11). Similar to what was observed for *IGHV,* the *IGKV* and *IGLV* genes in CD27⁺IgA⁺ and CD27⁻IgA⁺ cells showed similarly high CDR R/S ratios ranging from 2.8 to 3.4. Interestingly, the *IGLV3-1* genes that were abundantly used in CD27⁻IgA⁺ cells were mostly unmutated. Together, these

Figure 3. Ig heavy chain repertoire and characteristics in CD27+IgA+ and CD27-IgA+ memory B cells.
(A) *IGHV* subgroup (upper panel) and *IGHJ* gene (lower panel) usage in IgA+ B-cell subsets. The numbers of analyzed sequences are indicated in the inner circles. (B) IGH-CDR3 length (upper panel) and charge (lower panel) distributions. (C) The number of SHM in rearranged *IGHV* genes. Each grey dot represents an individual sequence and black lines represent median values. Statistical analysis of the data was performed with the χ^2 test in (A) and (B) and with the Mann-Whitney test in (C); ****, p< .0001

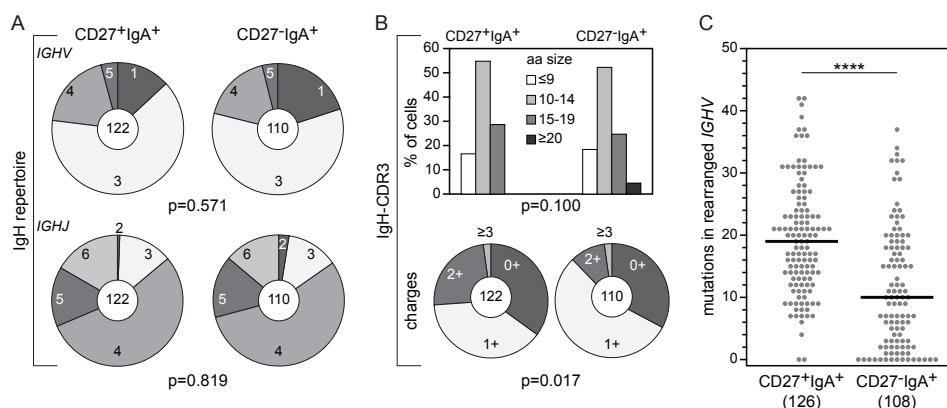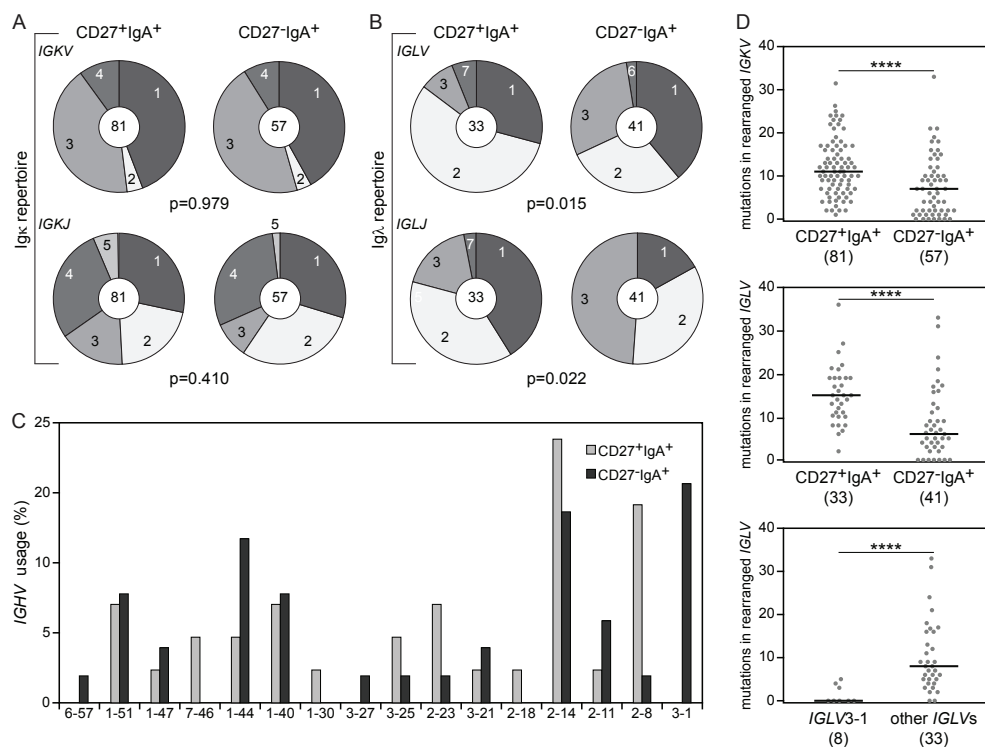**Figure 4. Igκ and Igλ light chain repertoire and characteristics in CD27+IgA+ and CD27-IgA+ memory B cells.**
(A) *IGKV* subgroup (upper panel) and *IGKJ* gene (lower panel) use in IgA+ memory B cell subsets. The numbers of analyzed sequences are indicated in the inner circles. (B) *IGLV* subgroup (upper panel) and *IGLJ* gene (lower panel)

use. (C) *IGLV* gene use. (D) The number of SHM in rearranged *IGKV* (upper panel) and *IGLV* (middle panel) in memory B-cell subsets, and in *IGLV3-1* and non-*IGLV3-1* genes of CD27$^-$IgA$^+$ memory B cells (bottom panel). Each grey dot represents an individual sequence and black lines represent median values. Statistical analysis of the data was performed with the χ^2 test in (A) and (B), and with the Mann-Whitney test in (C); ****, p< .0001

results indicate that CD27$^+$IgA$^+$ and CD27$^-$IgA$^+$ cells do not differ much regarding their Ig repertoires. Still, the higher SHM levels in CD27$^+$IgA$^+$ B cells and the distinct *IGL* gene usage reflect distinct degrees of maturation and different selection mechanisms.

High frequencies of autoreactive cells in IgA$^+$ memory B-cell subsets

To study whether the Ig repertoire differences between CD27$^+$IgA$^+$ and CD27$^-$IgA$^+$ memory B cells reflect distinct reactivity patterns, we cloned and expressed the amplified rearrangements as recombinant IgG antibodies. The frequencies of self-reactive antibodies in the IgA$^+$ memory B-cell subsets were determined with reactivity against the human Larynx carcinoma cell line HEp-2 (32). Human IgG$^+$ memory B cells were previously found to carry increased frequencies of autoreactive antibodies (47%) as compared to naive mature B cells (20%) (33). This increased self-reactivity was found to result from the introduction of SHM during memory B-cell formation (33). Using the same ELISA-based HEp-2 reactivity assay, we found that 31% of CD27$^+$IgA$^+$ and 26% CD27$^-$IgA$^+$ memory B cells were autoreactive (Figure 5A). These frequencies varied for individual donors, but were on average slightly higher than in naive mature B cells and lower than in IgG$^+$ memory B cells (Figure 5B). The autoreactive antibodies did not differ from non-autoreactive antibodies regarding their SHM levels or IGH-CDR3 size and composition (data not shown). Immunofluorescence analysis revealed that 12.5% (11/88) of CD27$^+$IgA$^+$ memory B cells reacted with cytoplasmic, nuclear or nuclear and cytoplasmic antigens, while only 4% (3/72) of CD27$^-$IgA$^+$ memory B cells were directed against cytoplasmic antigens, and none against nuclear antigens. Thus, both IgA$^+$ memory B cell subsets showed increased autoreactivity as compared with naive mature B cells, but these levels were clearly lower than in IgG$^+$ memory B cells.

Polyreactivity in CD27$^-$IgA$^+$ and in CD27$^+$IgA$^+$ memory B cells

To screen for polyreactivity, we determined the frequencies of the recombinant antibodies that recognized three structurally distinct antigens: dsDNA, insulin and LPS. Naive mature B cells (6%) and IgM$^+$ memory B cells (1%) hardly contain polyreactive antibodies, whereas these levels are increased in circulating IgG$^+$ memory B cells (23%) and intestinal IgG$^+$ and IgA$^+$ plasma cells (26%) (22, 33). The frequency of antibodies from CD27$^-$IgA$^+$ cells that recognized all three antigens (23%) was significantly higher than of CD27$^+$IgA$^+$ cells (12%; Figure 6,). These levels were clearly increased as compared to naive mature B cells. Interestingly, the frequencies of polyreactive antibodies in CD27$^-$IgA$^+$ memory B cells were similar to intestinal IgG$^+$ and IgA$^+$ plasma cells.

To study the nature of polyreactive antibodies in IgA$^+$ memory B cells, we compared their Ig repertoire with non-polyreactive antibodies. Significantly more polyreactive antibodies utilized members of the *IGHV1* subgroup at the expense of *IGHV3* and *IGHV4* (Figure 7A). Within *IGHV1*, *IGHV1-46* was mostly used and two of these antibodies derived from CD27$^+$IgA$^+$ were clonally related with identical Ig heavy and light chains, but different
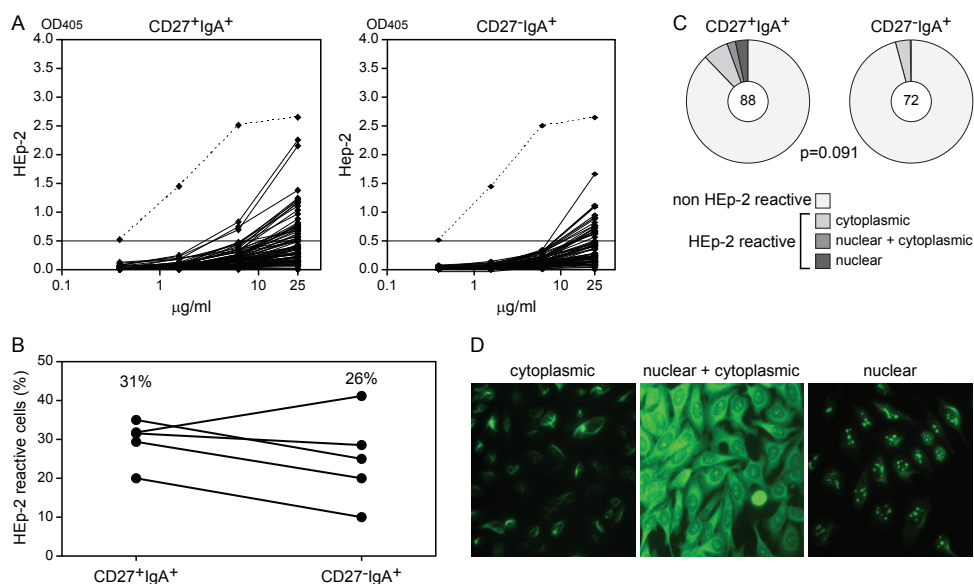
Figure 5. Autoreactivity in CD27$^+$IgA$^+$ and CD27$^-$IgA$^+$ memory B-cell subsets.
(A) Autoreactivity as measured by ELISA with HEp-2 cell lysates. In total, the reactivities of 88 antibodies from CD27$^+$IgA$^+$ cells and 72 antibodies from CD27$^-$IgA$^+$ cells, derived from 5 healthy donors were measured. The Dashed line represents the highly reactive ED45 positive control, and the red line represents a cut-off value of 0.5 above which antibodies were considered as HEp-2 reactive. (B) Frequencies of HEp-2 reactive CD27$^+$IgA$^+$ and CD27$^-$IgA$^+$ cells in 5 donors. Data points representing values for the same donor are connected with a black line. (C) Autoreactivity patterns of CD27$^+$IgA$^+$ and CD27$^-$IgA$^+$ cells as measured in an immunofluorescence assay (IFA) with HEp-2 cell–coated slides. The numbers of analyzed antibodies are indicated in the inner circles. (D) Representative pictures from IFA stainings; original magnification, 40x.

SHM levels. No differences were observed for the *IGHJ* gene use (Figure 7A). The presence of positively charged amino acids in IGH-CDR3 (Figure 7B) was not different, but the IGH-CDR3 length distribution was different between polyreactive and non-polyreactive antibodies. Non-polyreactive antibodies mainly contained IGH-CDR3 regions of 10-19 amino acids (85%), whereas polyreactive antibodies showed increased use of very short ($\leq$9 amino acids; 29%) or very long ($\geq$20 amino acids; 11%) IGH-CDR3s (Figure 7B).

The *IGHV* genes of polyreactive antibodies from CD27$^+$IgA$^+$ memory B cells carried similar SHM levels as non-polyreactive antibodies. In line with our observations on all *IGHV*, non-polyreactive antibodies from CD27$^-$IgA$^+$ memory B cells carried fewer SHM than antibodies from CD27$^+$IgA$^+$ B cells (Figure 7C). The polyreactive CD27$^-$IgA$^+$ clones, however, showed significantly increased *IGHV* SHM levels with a median of 19. Similar trends were seen for *IGKV* and *IGLV* mutation levels (not shown).

Thus, CD27$^-$IgA$^+$ memory B cells showed higher frequencies of polyreactive antibodies than CD27$^+$IgA$^+$ memory B cells, and these were similar to intestinal plasma cells. These antibodies were diverse, but showed distinct Ig repertoire and SHM properties than their non-polyreactive counterparts.
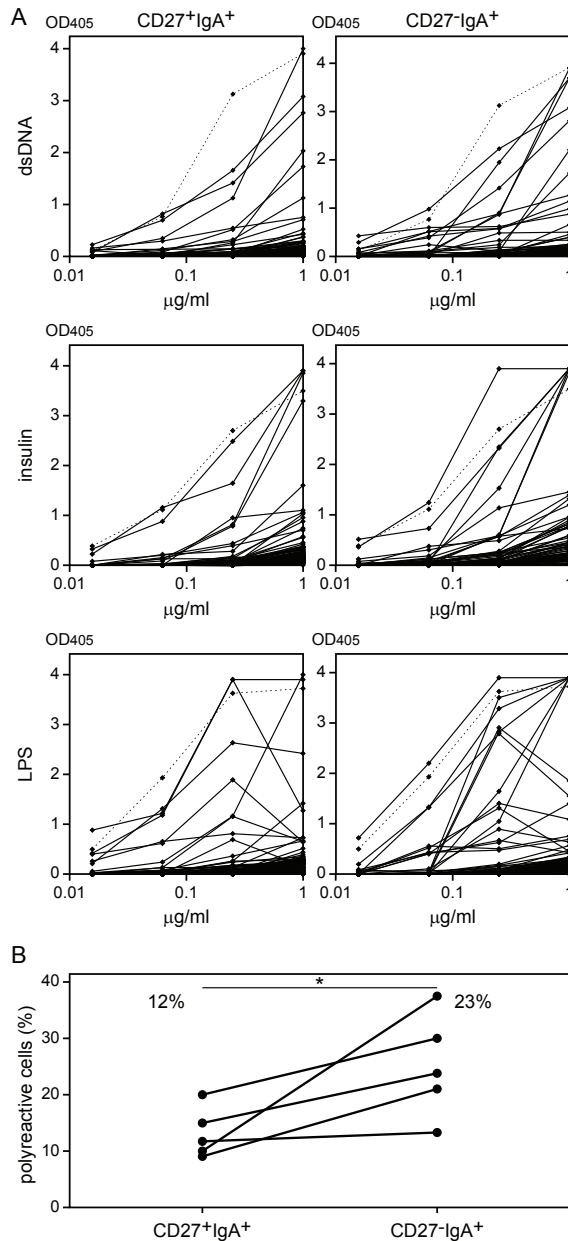
Figure 6. Polyreactivity in CD27⁺IgA⁺ and CD27⁻IgA⁺ memory B cell subsets.
(A) Antibodies triple-reactive against dsDNA (upper panel), insulin (middle panel), and LPS (lower panel) were defined as polyreactive. In total, 89 antibodies from CD27⁺IgA⁺ and 73 antibodies from CD27⁻IgA⁺ memory B cells were analyzed. Dashed lines represent the highly reactive ED45 positive control. (B) Frequencies of polyreactive CD27⁺IgA⁺ and CD27⁻IgA⁺ antibodies in 5 donors. Data points representing values for one donor are connected with a black line. Statistical analysis was performed with the two-tailed Student's t test for paired samples; *, $p < .05$
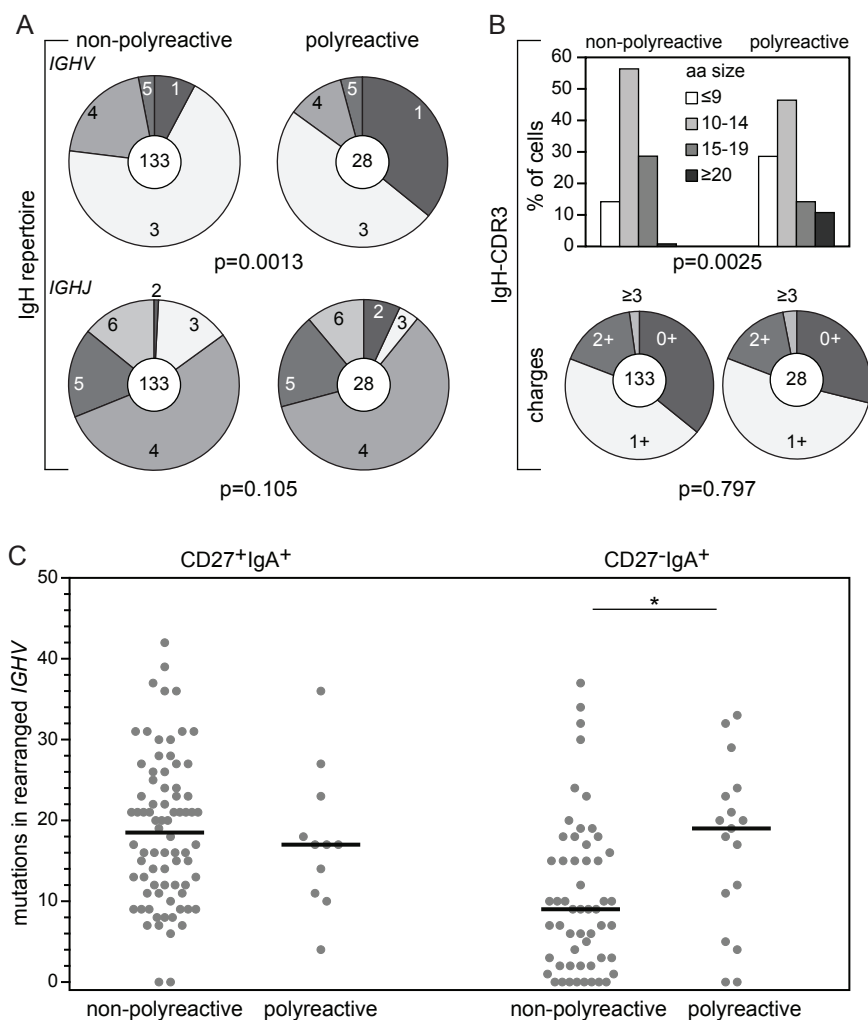
Figure 7. IgH repertoire and characteristics in polyreactive and non-polyreactive memory B cells.
(A) *IGHV* subgroup (upper panel) and *IGHJ* gene (lower panel) use in polyreactive and non-polyreactive IgA[+] memory B cells. The numbers of analyzed sequences are indicated in the inner circles. (B) IGH-CDR3 length (upper panel) and charge (lower panel) distributions. (C) The numbers of SHM in rearranged *IGHV* genes. Each grey dot represents an individual sequence and red lines represent median values. Statistical analysis of the data was performed with the χ^2 test in (A) and (B) and with the Mann-Whitney test in (C); [*], p< .0001

Bacteria reactivity in IgA^{+} memory B cells is associated with polyreactive cells

To study whether CD27^{+}IgA^{+} and CD27^{-}IgA^{+} memory B cells show distinct reactivities with specific microorganisms, we tested obtained antibodies for binding to flagellin, to representative commensal bacteria *Enterobacter cloacae* and *Enterococcus faecalis*, and to potentially pathogenic *Escherichia coli* and *Streptococcus aureus*. Irrespective of the tested antigen, the frequencies of reactive antibodies were higher in CD27^{-}IgA^{+}
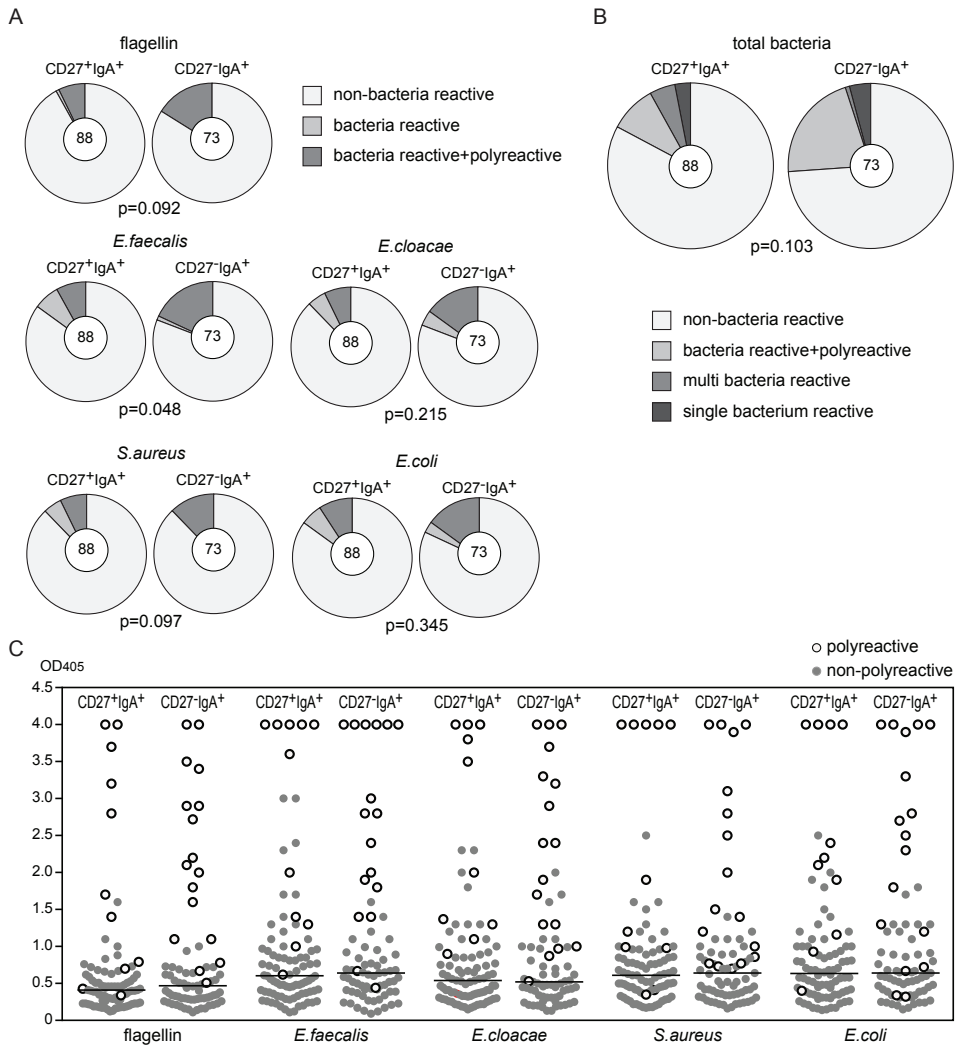
Figure 8. Reactivity of CD27+IgA+ and CD27-IgA+ memory B cells with commensal and potentiall pathogenic bacteria.
(A) Pie charts summarizing the frequencies of antibodies from CD27+IgA+ and CD27-IgA+ memory B cells with reactivities against flagellin, commensal bacteria (*E. cloacae*, *E. faecalis*) and potentially pathogenic bacteria (*E. coli*, *S. aureus*). The numbers of analyzed antibodies are indicated in the inner circles. (B) Overall bacteria reactivities of CD27+IgA+ and CD27-IgA+ memory B cells. (C) Reactivity levels against bacteria as measured by ELISA for antibodies from CD27+IgA+ and CD27-IgA+ memory B cells. Each grey dot represents a non-polyreactive antibody, and each white dot a polyreactive antibody. Red lines represent median values of all antibodies together. In (A) and (B), data were statistically analyzed with the χ^2 test.

than in CD27+IgA+ memory B cells (Figure 8A). CD27-IgA+ cells showed the highest binding frequencies for the commensal *E. cloacae* and *E. faecalis* strains, with lower *E. coli* and *S. aureus* specificities. CD27+IgA+ memory B cells were the least reactive

against flagellin (8.0%; 7/88) and the most reactive against *E. coli* (14.8%; 13/88).

Most of the bacteria-binding antibodies in IgA$^+$ memory B cells were polyreactive. Still, some bacteria-reactive non-polyreactive antibodies were identified and found to be more frequent in CD27$^+$IgA$^+$ than in CD27$^-$IgA$^+$ cells. Several of these antibodies bound to multiple bacteria (Figure 8B). Finally, all of the strongly bacteria-reactive Igs were polyreactive (Figure 8C). This implies that aspecific polyreactive interactions, rather than specific bacteria-targeted interactions play a role in maintaining the balance with commensal and pathogenic microorganisms in gut.

DISCUSSION

Here we showed that unconventional CD27$^-$IgA$^+$ memory B cells share a common gene expression profile with conventional CD27$^+$IgA$^+$ and CD27$^+$IgG$^+$ memory B cells. They showed a distinct Ig repertoire with fewer mutations and increased polyreactivity. This polyreactivity formed the basis for strong binding to mucosa-colonizing commensal and potentially pathogenic bacteria.

Despite their origin from unconventional TI immune responses, CD27$^-$IgA$^+$ memory B cells displayed a gene expression profile typical for all activated memory B cells, clearly distinct from naive B-cell subsets. The differences concerned upregulation of co-stimulatory molecules, downregulation of BCR-signaling inhibitors, and downregulation of naive B cells-pecific transcription factors in memory B cells (27, 34-35). All of these changes break the quiescence of naive cells and increase the B-cell responsiveness, crucial for fast and strong memory responses (27, 35). Thus, both TD and TI IgA responses generate B-cell memory with a common transcription profile.

The IgA memory B-cell maturation program was mainly characterized by increased expression of *RUNX2*. *RUNX2* acts together with *RUNX3* downstream of the TGF-β and RA signaling pathways to induce TI class-switching towards IgA in gut (28). *RUNX2* was expressed exclusively by IgA$^+$ cells, and its expression level was significantly higher in CD27$^-$IgA$^+$ than in CD27$^+$IgA$^+$ memory B-cell subset. Therefore, both subsets could have undergone class-switching in response to TGF-β and RA, but this was more common in CD27$^-$IgA$^+$ cells and corresponds with their TI origin. Furthermore, IgA$^+$ memory B cells showed increased expression of *IL6R* and *IL10R* as compared to naive mature B cells. Since *IL6/IL6R* and *IL10/IL10R* signaling act synergistically to sustain terminal B-cell differentiation, this suggests that both CD27$^+$IgA$^+$ and CD27$^-$IgA$^+$ subsets have the potential to develop into antibody-producing plasma cells (36-37). Still, *IL6R* and *IL10RA* were also highly expressed by other memory B cells, which reflects their role differentiation of IgM and IgG-expressing plasma cells (38-39).

CCR9 and CCR10 direct B-cell migration towards mucous membranes (40, 41 , 42). Still, we found no expression of *CCR10* and a limited expression of *CCR9* on CD27$^-$IgA$^+$ cells. It is important to realize, that in our experimental settings gut-derived CD27$^-$IgA$^+$ cells were analyzed in the peripheral blood, and the migration to blood requires downregulation of mucosa-homing receptors. A small population of CCR9 protein-expressing CD27$^-$IgA$^+$ cells is most probably composed of cells recently activated to migrate to the gastrointestinal tract. Such a recirculation of cells between distinct mucosal locations has been described,

and clonally related IgA+ B cells can be found at distant mucosal locations (43-44). Ig gene analysis in single-cell sorted CD27+IgA+ and CD27-IgA+ cells provided a simultaneous insight into the Ig heavy and light chain repertoires. While both subsets had highly comparable *IGH* and *IGK* repertoires, their *IGL* repertoires clearly differed. Broad *IGL* repertoire, commonly observed in gut, seems to be the result of ongoing receptor revision processes (45-46). Although receptor revision could potentially contribute to the observed repertoire differences between CD27+IgA+ and CD27-IgA+ cells, it is unlike to promote selective expansion of a one particular *IGHV* gene as we observed for *IGLV3-1* gene in CD27-IgA+ cells. Furthermore, the presence of non-templated nucleotides, which are introduced during rearrangements in bone marrow, but not during receptor revision, in rearrangements utilizing *IGLV3-1* gene, seems to oppose this concept.

CD27-IgA+ memory B cells had significantly less SHM in their Ig variable regions than CD27+IgA+ cells. This could be a direct consequence of their origin from TI responses associated with limited expression of AID (47-48). Still, not all IgA functions in gut seem to require intensive affinity maturation (49). It has been postulated, that a long co-evolution between host and microbiome favors genes that germline conformation can recognize conserved bacterial antigens (50). Furthermore, multiple studies have shown that IgA isolated from mice colonized with a single bacteria strain is frequently unmutated, but still can bind the antigen with a good affinity (20, 51-52). Since all amplified *IGLV3-1* genes in CD27-IgA+ cells were either in germline conformation or carried very few SHM, they may potentially have such an evolutionary conserved structure.

We here found that both CD27-IgA+ and CD27+IgA+ memory B cells showed increased autoreactivity and polyreactivity as compared to naive mature B cells (31). Previous studies demonstrated reduced autoreactivity and polyreactivity in IgM+ memory cells as compared to naive mature B cells (53), whereas these were increased in IgG+ memory B cells (33, 54). Thus, with respect to the reactivity patterns IgA+ memory B cells seemed more similar to IgG+ than to IgM+ memory B cells. Moreover, this distinctiveness of IgA+ and IgG+ memory B cells and IgM+ memory B cells was recently revealed by large-scale *IGH* repertoire analysis (55-56).

The frequency of polyreactive Igs in CD27-IgA+ cells was significantly higher than in CD27+IgA+ cells, but comparable with IgA+ and IgG+ plasmablasts (22). It has been previously suggested that the frequency of polyreactive cells may differ per physiological niche, e.g. IgG+ plasma cells in bone marrow present significantly lower polyreactivity than circulating IgG+ memory B cells (54). Thus, similar polyreactivity levels in CD27-IgA+ cells and in the intestinal plasmablasts support their common origin and suggest that this polyreactivity level may be beneficial for the responses in the gastrointestinal tract.

Polyreactive IgA+ memory B cells showed increased *IGHV1* usage as compared to nonpolyreactive cells, which was mainly due to increased frequencies of *IGHV1-46* genes. Since the *IGHV1-46* gene is frequently found in responses against rotavirus, this may suggest the origin of *IGHV1-46* –expressing cells from intestinal antiviral responses (57).

Molecular features of polyreactive Igs: increased SHM load in CD27-IgA+ cells, and less restricted IGH-CDR3 length distribution, suggested that different mechanisms are responsible for polyreactivity development in memory B cells than in naive cells (31). The role of SHM in the introduction of polyreactivity has been already well established by multiple studies in

V

mice and human, which have demonstrated that reversion of SHM in Ig genes to their germline conformation results in a significant decrease in frequency of polyreactive cells (33, 53, 58). Based on the current study, we can further conclude that this effect is even more prominent in memory cells with on overall low SHM load. Furthermore, since the introduction of SHM is statistically more likely to impair the structure of short than of long IGH-CDR3s, it can partially explain high frequency of polyreactive cells with short IGH-CDR3s.

Polyreactive Igs, with high SHM load, in CD27⁻IgA⁺ cells were highly reactive with commensal bacteria. It has been previously reported that IgA⁺ cells with SHM in their Ig genes are important to maintain the balance with gut microbiome (21). Mice carrying the mutated form of AID that allows CSR but not SHM, presented with severe intestinal lymphoid hyperplasia due to an abnormally strong microbial drive of the mucosal immune system (21). Thus, polyreactive interactions seem to be responsible for maintaining the balance with gut microbiome.

Summarizing, we showed that both TD and TI immune responses generate IgA⁺ memory B cells with highly similar transcription profiles. Still, the shape of the Ig repertoire and the reactivity of cells are highly dependent on their origin and reflect their physiological function with CD27⁻IgA⁺ memory B cells showing high-affinity binding to bacteria with polyreactive antibodies.

ACKNOWLEDGEMENTS

MATERIALS AND METHODS

Cell sorting and gene expression profiling

Human naive and memory B-cell subsets were defined as described previously (26), and purified from post-Ficoll mononuclear cells on a FACSAriaII cell sorter (BD Biosciences). RNA was isolated from each sorted subset with the RNeasy Mini Kit (Qiagen). Gene expression was quantified using Affymetrix HG-U133 Plus 2.0 GeneChip arrays (containing 54,675 probe sets), as previously described (3, 59). Expression profiles of the three naive and six memory B-cell subsets from 2-3 healthy donors were compared based on the perfect match probe intensity levels. RMA background removal and quantile normalization were performed, followed by a per-probe set two-way ANOVA (with factors probe and subset). This resulted in average expression levels for each probe set in each cell type, as well as p values for the significance of the difference between cell types. The p values were adjusted for multiple testing using Šidák stepdown adjustment (60), and all differences with adjusted p values < .05 were considered significant.

The maximum difference in expression between any two subsets was calculated for each probe set that showed a signal. Only probe sets that showed larger differences than a certain threshold were selected for clustering. These differences were subsequently set at $\log_2$ threshold values 0.4, 0.5, 0.6, 0.7, 0.8 and 0.9. Correlation ρ between samples was then

calculated based on only these selected probe sets, and the data were hierarchically clustered (complete linkage) using 1-ρ as a distance measure (59).

Single-cell sorting
Post-Ficoll mononuclear cells from healthy donors were enriched for B cells by magnetic separation with CD19 microbeads (Miltenyi Biotech) and stained with CD20-PE-Cy7, CD27-APC (both from Biolegend), CD38-FITC (BD Pharmingen), CD27-APC and IgA-PE (Southern Biotech) prior to purification. Single CD20$^+$CD38^{dim}CD27$^+$IgA$^+$ and CD20$^+$CD38^{dim}CD27$^-$ IgA$^+$ memory B cells were sorted on a FACSVantage (BD Biosciences) into 96-well PCR plates containing 4 μl lysis solution (0.5× PBS containing 10mM DTT, 8 U RNAsin [Promega], and 0.4 U 5′-3′ RNase Inhibitor [Eppendorf]) and immediately frozen on dry ice.

cDNA synthesis, Ig genes amplification, antibody production, and purification
RNA from single cells was reverse-transcribed in the original 96-well plate in 12.5-μl reactions containing 100 U Superscript II RT (Life Technologies) for 45 minutes at 42°C. RT-PCR reactions and primer sequences were as described previously (31, 61-62). An *IGHA*-specific primer (5'CTTTCGCTCCAGGTCACACTGAG 3') was used in the 1st PCR reaction. Cloning strategy, expression vectors, antibody expression, and purification were performed as described previously (31, 61). Ig sequences were analyzed by Ig BLAST comparison with GenBank. IgH-CDR3 was defined as the interval between the conserved arginine/lysine at position 94 in IGHV-FR3 and the conserved tryptophan at position 103 in the *IGHJ* gene.

ELISAs and immunofluorescence assays
Antibody reactivity analysis was performed as described previously with the highly polyreactive ED45 antibody as positive control in HEp-2 reactivity and polyreactivity ELISAs (31, 61), Antibodies were considered polyreactive when they recognized the 3 distinct antigens: dsDNA, insulin, and LPS. ELISA plates for bacteria-reactivity testing were coated with purified flagellin from *B. subtilis* (InvivoGen), or sonicated lysates from cultured *E.cloacae* (ATCC 13047), *E. faecalis* (ATCC 29212), *E. coli* or *S. aureus* at the concentration of 1ng/μl. For indirect immunofluorescence assays, HEp-2 cell-coated slides (Bion Enterprises Ltd.) were incubated in a moist chamber at room temperature with purified recombinant antibodies at 50-100 μg/ml according to the manufacturer's instructions. FITC-conjugated goat anti-human IgG was used as detection reagent.

Statistical analysis
Statistical analyses were performed with the two-tailed Student's t test, Mann-Whitney U test, or χ² test as indicated in details in the Figure legends. P values < .05 were considered statistically significant.

REFERENCES

1. Macpherson, A.J., K.D. McCoy, F.E. Johansen, and P. Brandtzaeg. 2008. The immune geography of IgA induction and function. *Mucosal immunology* 1:11-22.
2. Ghia, P., E. ten Boekel, E. Sanz, A. de la Hera, A. Rolink, and F. Melchers. 1996. Ordering of human bone

marrow B lymphocyte precursors by single-cell polymerase chain reaction analyses of the rearrangement status of the immunoglobulin H and L chain gene loci. *The Journal of experimental medicine* 184:2217-2229.

3. van Zelm, M.C., M. van der Burg, D. de Ridder, B.H. Barendregt, E.F. de Haas, M.J. Reinders, A.C. Lankester, T. Revesz, F.J. Staal, and J.J. van Dongen. 2005. Ig gene rearrangement steps are initiated in early human precursor B cell subsets and correlate with specific transcription factor expression. *J Immunol* 175:5912-5922.

4. Cerutti, A. 2008. The regulation of IgA class switching. *Nat Rev Immunol* 8:421-434.

5. Muramatsu, M., K. Kinoshita, S. Fagarasan, S. Yamada, Y. Shinkai, and T. Honjo. 2000. Class switch recombination and hypermutation require activation-induced cytidine deaminase (AID), a potential RNA editing enzyme. Cell 102:553-563.

6. Fagarasan, S., K. Kinoshita, M. Muramatsu, K. Ikuta, and T. Honjo. 2001. In situ class-switching and differentiation to IgA-producing cells in the gut lamina propria. *Nature* 413:639-643.

7. Fagarasan, S., and T. Honjo. 2000. T-Independent immune response: new aspects of B cell biology. *Science* 290:89-92.

8. Chorny, A., I. Puga, and A. Cerutti. 2010. Innate signaling networks in mucosal IgA class switching. *Adv Immunol* 107:31-69.

9. Macpherson, A.J., D. Gatto, E. Sainsbury, G.R. Harriman, H. Hengartner, and R.M. Zinkernagel. 2000. A primitive T cell-independent mechanism of intestinal mucosal IgA responses to commensal bacteria. *Science* 288:2222-2226.

10. Mora, J.R., M. Iwata, B. Eksteen, S.Y. Song, T. Junt, B. Senman, K.L. Otipoby, A. Yokota, H. Takeuchi, P. Ricciardi-Castagnoli, K. Rajewsky, D.H. Adams, and U.H. Andrian. 2006. Generation of gut-homing IgA-secreting B cells by intestinal dendritic cells. *Science* 314:1157-1160.

11. He, B., R. Santamaria, W. Xu, M. Cols, K. Chen, I. Puga, M. Shan, H. Xiong, J.B. Bussel, A. Chiu, A. Puel, J. Reichenbach, L. Marodi, R. Doffinger, J. Vasconcelos, A. Issekutz, J. Krause, G. Davies, X. Li, B. Grimbacher, A. Plebani, E. Meffre, C. Picard, C. Cunningham-Rundles, J.L. Casanova, and A. Cerutti. 2010. The transmembrane activator TACI triggers immunoglobulin class switching by activating B cells through the adaptor MyD88. *Nature immunology* 11:836-845.

12. Castigli, E., S. Scott, F. Dedeoglu, P. Bryce, H. Jabara, A.K. Bhan, E. Mizoguchi, and R.S. Geha. 2004. Impaired IgA class switching in APRIL-deficient mice. Proceedings of the National Academy of Sciences of the United States of America 101:3903-3908.

13. Castigli, E., S.A. Wilson, S. Scott, F. Dedeoglu, S. Xu, K.P. Lam, R.J. Bram, H. Jabara, and R.S. Geha. 2005. TACI and BAFF-R mediate isotype switching in B cells. *The Journal of experimental medicine* 201:35-39.

14. Litinskiy, M.B., B. Nardelli, D.M. Hilbert, B. He, A. Schaffer, P. Casali, and A. Cerutti. 2002. DCs induce CD40-independent immunoglobulin class switching through BLyS and APRIL. *Nature immunology* 3:822-829.

15. Borsutzky, S., B.B. Cazac, J. Roes, and C.A. Guzman. 2004. TGF-beta receptor signaling is critical for mucosal IgA responses. *J Immunol* 173:3305-3309.

16. Tokuyama, H., and Y. Tokuyama. 1995. Endogenous cytokine expression profiles in retinoic acid-induced IgA production by LPS-stimulated murine splenocytes. *Cellular immunology* 166:247-253.

17. Gill, S.R., M. Pop, R.T. Deboy, P.B. Eckburg, P.J. Turnbaugh, B.S. Samuel, J.I. Gordon, D.A. Relman, C.M. Fraser-Liggett, and K.E. Nelson. 2006. Metagenomic analysis of the human distal gut microbiome. *Science* 312:1355-1359.

18. Arumugam, M., J. Raes, E. Pelletier, D. Le Paslier, T. Yamada, D.R. Mende, G.R. Fernandes, J. Tap, T. Bruls, J.M. Batto, M. Bertalan, N. Borruel, F. Casellas, L. Fernandez, L. Gautier, T. Hansen, M. Hattori, T. Hayashi, M. Kleerebezem, K. Kurokawa, M. Leclerc, F. Levenez, C. Manichanh, H.B. Nielsen, T. Nielsen, N. Pons, J. Poulain, J. Qin, T. Sicheritz-Ponten, S. Tims, D. Torrents, E. Ugarte, E.G. Zoetendal, J. Wang, F. Guarner, O. Pedersen, W.M. de Vos, S. Brunak, J. Dore, H.I.T.C. Meta, M. Antolin, F. Artiguenave, H.M. Blottiere, M. Almeida, C. Brechot, C. Cara, C. Chervaux, A. Cultrone, C. Delorme, G. Denariaz, R. Dervyn, K.U. Foerstner, C. Friss, M. van de Guchte, E. Guedon, F. Haimet, W. Huber, J. van Hylckama-Vlieg, A. Jamet, C. Juste, G. Kaci, J. Knol, O. Lakhdari, S. Layec, K. Le Roux, E. Maguin, A. Merieux, R. Melo Minardi, C. M'Rini, J. Muller, R. Oozeer, J. Parkhill, P. Renault, M. Rescigno, N. Sanchez, S. Sunagawa, A. Torrejon, K. Turner, G. Vandemeulebrouck, E. Varela, Y. Winogradsky, G. Zeller, J. Weissenbach, S.D. Ehrlich, and P. Bork. 2011. Enterotypes of the human gut microbiome. *Nature* 473:174-180.

19. van der Waaij, L.A., P.C. Limburg, G. Mesander, and D. van der Waaij. 1996. In vivo IgA coating of anaerobic bacteria in human faeces. *Gut* 38:348-354.

20. Hapfelmeier, S., M.A. Lawson, E. Slack, J.K. Kirundi, M. Stoel, M. Heikenwalder, J. Cahenzli, Y. Velykoredko, M.L. Balmer, K. Endt, M.B. Geuking, R. Curtiss, 3rd, K.D. McCoy, and A.J. Macpherson. 2010. Reversible microbial colonization of germfree mice reveals the dynamics of IgA immune responses. *Science* 328:1705-1709.

21. Wei, M., R. Shinkura, Y. Doi, M. Maruya, S. Fagarasan, and T. Honjo. 2011. Mice carrying a knock-in mutation of Aicda resulting in a defect in somatic hypermutation have impaired gut homeostasis and compromised mucosal defense. *Nature immunology* 12:264-270.

22. Benckert, J., N. Schmolka, C. Kreschel, M.J. Zoller, A. Sturm, B. Wiedenmann, and H. Wardemann. 2011. The majority of intestinal IgA+ and IgG+ plasmablasts in the human gut are antigen-specific. *J Clin Invest* 121:1946-1955.

23. Macpherson, A.J., L. Hunziker, K. McCoy, and A. Lamarre. 2001. IgA responses in the intestinal mucosa against pathogenic and non-pathogenic microorganisms. *Microbes Infect* 3:1021-1035.

24. Bollinger, R.R., M.L. Everett, S.D. Wahl, Y.H. Lee, P.E. Orndorff, and W. Parker. 2006. Secretory IgA and mucin-mediated biofilm formation by environmental strains of Escherichia coli: role of type 1 pili. *Mol Immunol* 43:378-387.

25. Macpherson, A.J., M.B. Geuking, E. Slack, S. Hapfelmeier, and K.D. McCoy. 2012. The habitat, double life, citizenship, and forgetfulness of IgA. *Immunological reviews* 245:132-146.

26. Berkowska, M.A., G.J. Driessen, V. Bikos, C. Grosserichter-Wagener, K. Stamatopoulos, A. Cerutti, B. He, K. Biermann, J.F. Lange, M. van der Burg, J.J. van Dongen, and M.C. van Zelm. 2011. Human memory B cells originate from three distinct germinal center-dependent and -independent maturation pathways. *Blood* 118:2150-2158.

27. Good, K.L., D.T. Avery, and S.G. Tangye. 2009. Resting human memory B cells are intrinsically programmed for enhanced survival and responsiveness to diverse stimuli compared to naive B cells. *J Immunol* 182:890-901.

28. Watanabe, K., M. Sugai, Y. Nambu, M. Osato, T. Hayashi, M. Kawaguchi, T. Komori, Y. Ito, and A. Shimizu. 2010. Requirement for Runx proteins in IgA class switching acting downstream of TGF-beta 1 and retinoic acid signaling. *J Immunol* 184:2785-2792.

29. Warnock, R.A., S. Askari, E.C. Butcher, and U.H. von Andrian. 1998. Molecular mechanisms of lymphocyte homing to peripheral lymph nodes. *The Journal of experimental medicine* 187:205-216.

30. Bargatze, R.F., M.A. Jutila, and E.C. Butcher. 1995. Distinct roles of L-selectin and integrins alpha 4 beta 7 and LFA-1 in lymphocyte homing to Peyer's patch-HEV in situ: the multistep model confirmed and refined. *Immunity* 3:99-108.

31. Wardemann, H., S. Yurasov, A. Schaefer, J.W. Young, E. Meffre, and M.C. Nussenzweig. 2003. Predominant autoantibody production by early human B cell precursors. *Science* 301:1374-1377.

32. Egner, W. 2000. The use of laboratory tests in the diagnosis of SLE. *J Clin Pathol* 53:424-432.

33. Tiller, T., M. Tsuiji, S. Yurasov, K. Velinzon, M.C. Nussenzweig, and H. Wardemann. 2007. Autoreactivity in human IgG+ memory B cells. *Immunity* 26:205-213.

34. Pritchard, N.R., and K.G. Smith. 2003. B cell inhibitory receptors and autoimmunity. *Immunology* 108:263-273.

35. Hart, G.T., K.A. Hogquist, and S.C. Jameson. 2012. Kruppel-like factors in lymphocyte biology. *J Immunol* 188:521-526.

36. Zhang, Y., J.X. Lin, and J. Vilcek. 1988. Synthesis of interleukin 6 (interferon-beta2/B cell stimulatory factor 2) in human fibroblasts is triggered by an increase in intracellular cyclic AMP. *J Biol Chem* 263:6177-6182.

37. Burdin, N., F. Rousset, and J. Banchereau. 1997. B-cell-derived IL-10: production and function. *Methods* 11:98-111.38. Defrance, T., B. Vanbervliet, F. Briere, I. Durand, F. Rousset, and J. Banchereau. 1992. Interleukin 10 and transforming growth factor beta cooperate to induce anti- CD40-activated naive human B cells to secrete immunoglobulin A. *The Journal of experimental medicine* 175:671-682.

39. Yoshizaki, K., T. Nakagawa, K. Fukunaga, L.T. Tseng, Y. Yamamura, and T. Kishimoto. 1984. Isolation and characterization of B cell differentiation factor (BCDF) secreted from a human B lymphoblastoid cell line. *J Immunol* 132:2948-2954.

40. Hieshima, K., Y. Kawasaki, H. Hanamoto, T. Nakayama, D. Nagakubo, A. Kanamaru, and O. Yoshie. 2004. CC chemokine ligands 25 and 28 play essential roles in intestinal extravasation of IgA antibody-secreting cells. *J Immunol* 173:3668-3675.

41. Pabst, O., L. Ohl, M. Wendland, M.A. Wurbel, E. Kremmer, B. Malissen, and R. Forster. 2004. Chemokine receptor CCR9 contributes to the localization of plasma cells to the small intestine. *The Journal of experimental medicine* 199:411-416.

42. Kunkel, E.J., C.H. Kim, N.H. Lazarus, M.A. Vierra, D. Soler, E.P. Bowman, and E.C. Butcher. 2003. CCR10 expression is a common feature of circulating and mucosal epithelial tissue IgA Ab-secreting cells. *J Clin Invest* 111:1001-1010.

43. Holtmeier, W., A. Hennemann, and W.F. Caspary. 2000. IgA and IgM V(H) repertoires in human colon: evidence for clonally expanded B cells that are widely disseminated. *Gastroenterology* 119:1253-1266.

44. Dunn-Walters, D.K., L. Boursier, and J. Spencer. 1997. Hypermutation, diversity and dissemination of human intestinal lamina propria plasma cells. *European journal of immunology* 27:2959-2964.

45. Su, W., J.N. Gordon, F. Barone, L. Boursier, W. Turnbull, S. Mendis, D.K. Dunn-Walters, and J. Spencer. 2008. Lambda light chain revision in the human intestinal IgA response. *J Immunol* 181:1264-1271.

46. Su, W., L. Boursier, A. Padala, J.D. Sanderson, and J. Spencer. 2004. Biases in Ig lambda light chain rearrangements in human intestinal plasma cells. *J Immunol* 172:2360-2366.

47. Weller, S., C.A. Reynaud, and J.C. Weill. 2005. Splenic marginal zone B cells in humans: where do they mutate their Ig receptor? *European journal of immunology* 35:2789-2792.

48. He, B., W. Xu, and A. Cerutti. Comment on "Gut-associated lymphoid tissue contains the molecular machinery to support T-cell-dependent and T-cell-independent class switch recombination". *Mucosal immunology* 3:92-94; author reply 94-95.

49. Stoel, M., H.Q. Jiang, C.C. van Diemen, J.C. Bun, P.M. Dammers, M.C. Thurnheer, F.G. Kroese, J.J. Cebra, and N.A. Bos. 2005. Restricted IgA repertoire in both B-1 and B-2 cell-derived gut plasmablasts. *J Immunol* 174:1046-1054.

50. Slack, E., M.L. Balmer, J.H. Fritz, and S. Hapfelmeier. 2012. Functional flexibility of intestinal IgA - broadening the fine line. *Front Immunol* 3:100.

51. Bos, N.A., J.C. Bun, S.H. Popma, E.R. Cebra, G.J. Deenen, M.J. van der Cammen, F.G. Kroese, and J.J. Cebra. 1996. Monoclonal immunoglobulin A derived from peritoneal B cells is encoded by both germ line and somatically mutated VH genes and is reactive with commensal bacteria. *Infect Immun* 64:616-623.

52. Lindner, C., B. Wahl, L. Fohse, S. Suerbaum, A.J. Macpherson, I. Prinz, and O. Pabst. 2012. Age, microbiota, and T cells shape diverse individual IgA repertoires in the intestine. *The Journal of experimental medicine* 209:365-377.

53. Tsuiji, M., S. Yurasov, K. Velinzon, S. Thomas, M.C. Nussenzweig, and H. Wardemann. 2006. A checkpoint for autoreactivity in human IgM+ memory B cell development. *The Journal of experimental medicine* 203:393-400.

54. Scheid, J.F., H. Mouquet, J. Kofer, S. Yurasov, M.C. Nussenzweig, and H. Wardemann. 2011. Differential regulation of self-reactivity discriminates between IgG+ human circulating memory B cells and bone marrow plasma cells. *Proceedings of the National Academy of Sciences of the United States of America* 108:18044-18048.

55. Wu, Y.C., D. Kipling, H.S. Leong, V. Martin, A.A. Ademokun, and D.K. Dunn-Walters. 2010. High-throughput immunoglobulin repertoire analysis distinguishes between human IgM memory and switched memory B-cell populations. *Blood* 116:1070-1078.

56. Wu, Y.C., D. Kipling, and D.K. Dunn-Walters. 2011. The relationship between CD27 negative and positive B cell populations in human peripheral blood. *Front Immunol* 2:81.

57. Weitkamp, J.H., B.J. Lafleur, and J.E. Crowe, Jr. 2006. Rotavirus-specific CD5+ B cells in young children exhibit a distinct antibody repertoire compared with CD5- B cells. *Hum Immunol* 67:33-42.

58. Guo, W., D. Smith, K. Aviszus, T. Detanico, R.A. Heiser, and L.J. Wysocki. 2010. Somatic hypermutation as a generator of antinuclear antibodies in a murine model of systemic autoimmunity. *The Journal of experimental medicine* 207:2225-2237.

59. Nodland, S.E., M.A. Berkowska, A.A. Bajer, N. Shah, D. de Ridder, J.J. van Dongen, T.W. LeBien, and M.C. van Zelm. 2011. IL-7R expression and IL-7 signaling confer a distinct phenotype on developing human B-lineage cells. *Blood* 118:2116-2127.

60. Ludbrook, J. 1998. Multiple comparison procedures updated. *Clin Exp Pharmacol Physiol* 25:1032-1037.

61. Meffre, E., A. Schaefer, H. Wardemann, P. Wilson, E. Davis, and M.C. Nussenzweig. 2004. Surrogate light chain expressing human peripheral B cells produce self-reactive antibodies. *The Journal of experimental medicine* 199:145-150.

62. Tiller, T., E. Meffre, S. Yurasov, M. Tsuiji, M.C. Nussenzweig, and H. Wardemann. 2008. Efficient generation of monoclonal antibodies from single human B cells by single cell RT-PCR and expression vector cloning. *J Immunol Methods* 329:112-124.

VI

Human IgE^{+} plasma cells and memory B-cell subsets are derived from germinal center-dependent and –independent responses

Magdalena A. Berkowska[1], Jorn J. Heeringa[1], Enes Hajdarbegovic[2], H. Bing Thio[2], P. Martin van Hagen[3], Alberto Orfao[4], Jacques J.M. van Dongen[1] and Menno C. van Zelm[1]

[1]Dept. Immunology, [2]Dept. Dermatology, [3]Dept. Internal Medicine, Erasmus MC, Rotterdam, the Netherlands; [4]Centro de Investigación del Cáncer and Service of Cytometry, Dept. Medicine, University of Salamanca, Salamanca, Spain.

ABSTRACT

The prevalence of IgE-mediated diseases increases worldwide. Despite extensive studies, IgE-expressing B cells remain poorly characterized. We developed a reliable flow cytometric strategy to detect and purify IgE$^+$ plasma cells from tonsils and two IgE$^+$ memory B-cell subsets from blood. Detailed molecular characterization revealed germinal center-dependent origins of tonsil plasma cells and CD27$^+$IgE$^+$ memory B cells. However, CD27$^-$IgE$^+$ memory B cells can be derived independently from germinal centers and were specifically increased in atopic dermatitis patients. Our study sheds light on the development of IgE$^+$ cells in health, opens new possibilities to study the pathogenesis of IgE-mediated diseases in man, and can contribute to accurate monitoring of anti-IgE treatment in patients with severe allergic reactions.

INTRODUCTION

Asthma and allergy are very common immunological diseases that affect mainly children and young adults. The disease incidence has increased over the past decades in most Western countries.[1-2] It has been estimated that currently ~8% of adults in the United States suffers from asthma,[3] and 30-40% of the world population is affected by one or more allergic diseases.[4] Type I responses are mediated by an expansion of T helper type 2 (TH2) cells and isotype switching of B cells to generate allergen-specific immunoglobulin (Ig)E. IgE function and regulation is markedly different from the other Ig isotypes and thought to have evolved to function as defense against parasites, especially helminths and protozoa. Most IgE is bound to the high affinity receptor FcεRI on mast cells and basophils.[5] Antigen recognition and consequently cross-linking of IgE on these cells leads to the local release of molecules (inflammatory mediators, e.g. histamine and leukotrienes), enzymes and cytokines,[6-8] which together result in eosinophilia and the allergic hypersensitivity response.

Allergic patients show abnormal IgE responses and often increased total serum IgE levels. Their reactivity patterns towards harmless food- or airborne particles (allergens) underlie the disease and affect the type of complaints.[9-10] Despite the crucial role of IgE, little is known about the cellular aspects of responses. The three main reasons for this are: 1) the presumed scarcity of the IgE-expressing B cells,[11] 2) the poor expression of membrane (m)IgE due to suboptimal polyadenylation signals downstream of the exons encoding the cytoplasmic tail of IgE,[12] and 3) the presence of the low-affinity receptor FcεRII (CD23) on B cells that binds IgE and results in detection of IgE on non-IgE-expressing B cells.[13]

Class-switching towards IgE is primarily thought to take place in lymphoid germinal centers (GC), where it is mediated by IL-4, IL-13, and CD40L on activated TH2 cells.[7] In addition, co-stimulatory signals can be provided by the interaction between CD23 and CD21 on B cells, as well as signaling via CD86.[14-17] The resulting IgE-expressing cells migrate through the blood stream to local tissues as evidenced by the presence of IgE transcripts in blood and mucosa.[18-20] However, the respiratory mucosa and the gastrointestinal tract also show molecular signs of IgE class switching.[21-22] This is reminiscent of mucosal IgA responses that can take place independent of cognate T-cell help, possibly against non-peptide antigens.[23-24]

Recent studies have elucidated some cellular aspects of IgE responses in mice following immunization with haptenated proteins or infection with the helminth *Nippostrongylus brasiliensis*. IgE-producing plasma cells derived from GC reactions were consistently found in lymph nodes. These were mostly short-lived and their participation in GCs seemed transient, while long-term memory was present in the form of IgG1⁺ germinal center that were prone to switch to IgE upon subsequent antigen encounter.[25-26] Direct IgM→IgE classswitching was found,[27] but the generation of high-affinity IgE antibodies depended on indirect IgM→IgG1→IgE switching.[28] IgE⁺ memory B cells have only been observed by Talay *et al.*, which is potentially due to the manipulated IgE allele.[29] Some results were contradictory between these studies, most likely due to alternative methods to visualize IgE⁺ B cells: IgE staining following ice-cold acid wash,[25] knock-in with cytoplasmic reporter gene,[26] knock-in cytoplasmic reporter and a human IgE membrane region replacing the mouse sequence.[30] Therefore, these studies cannot be directly extrapolated to human IgE responses and

B-cell memory.

The B-cell compartment in human is quite distinct from mouse models: the continuous antigenic pressure results in the persistent presence of GCs in lymphoid tissue, and a large fraction of circulating B cells has a memory phenotype.[31] These features limit direct extrapolation from (manipulated) mouse models to human disease. B-cell differentiation and immune responses involve unique processes that leave permanent marks in their genomic DNA: V(D)J recombination for Ig repertoire development, somatic hypermutation (SHM) for affinity maturation, and Ig class switch recombination (CSR) for effector function.[32] We have recently delineated the human memory B cell compartment by direct *ex vivo* analysis of Ig genes in sorted B cell subsets. CD27-IgA+ B cells and CD27+IgM+IgD+ 'natural effector' B cells (at least in part) were derived from local and systemic GC-independent responses, respectively; CD27-IgG+ and CD27+IgM+IgD- 'IgM-only' B cells were derived from primary GC responses and CD27+IgG+ and CD27+IgA+ B cells (at least in part) from consecutive GC responses.

We now developed an 8-color flow cytometry-based strategy to reliably detect IgE+ plasma cells and CD27-IgE+ and CD27+IgE+ memory B-cell subsets following stepwise exclusion of IgM+, IgD+, IgG+ and IgA+ B cells. These IgE+ B cells lacked CD23 expression and carried IgE transcripts. We employed molecular analysis of their replication history, SHM, and CSR profiles and studies in CD40L-deficient and in atopic dermatitis patients to reveal new insights into their maturation pathways and involvement in allergic disease.

METHODS

Patients

Peripheral blood samples from 5 CD40L-deficient patients, 23 atopic dermatitis patients, 17 psoriasis patients and multiple healthy donors, and childhood tonsils were obtained with informed consent and according to the guidelines of the Medical Ethics Committee of Erasmus MC.

All CD40L-deficient patients lacked CD40L protein expression on activated T cells as measured after 5-hour stimulation with phorbol 12-myristate 13-acetate (Sigma-Aldrich) and calcium ionophore (Sigma-Aldrich). Mutations in *CD40L* gene were detected by exon sequencing. Two of these patients were described previously.[33]

Patients with atopic dermatitis and psoriasis vulgaris were selected from the outpatient clinic of Dermatology and Venereology at Erasmus Univeristy Hospital in Rotterdam. The diagnosis of psoriasis vulgaris was made by certified dermatologists by clinical examination only. Patients with atopic dermatitis fulfilled the criteria by Hanifin and Rajka.[43] At the time of inclusion a physician global assessment was scored for both groups by the attending physician. Total serum IgE and IgE against common inhalant allergens (Phadiatop) were measured with ImmunoCAP 250 (Phadia, AD Sweden) according to manufacturers manual.

Flow cytometric immunophenotyping and cell sorting

Absolute counts of blood CD3+ T cells, CD16+/56+ NK cells and CD19+ B cells were obtained

with a diagnostic lyse-no-wash protocol. 8-color flow cytometric immunophenotyping of memory B cells from peripheral blood and plasma cells from tonsils was performed using monoclonal antibodies against IgM- Hor V450 (G20-127), IgD-biotin (IA6-2) and CD27-BV421 (M-T271) (all from BD Pharmingen), IgG-FITC and IgG-PE (G18-145), CD19-PECy7 (SJ25C1), CD27-PerCP-Cy5.5 and CD27-APC (L128), CD38-PE and CD38-APC-H7 (HB7), CD21-APC (CR2) and CD23-APC (EBVCS-5) (all from BD Biosciences), IgMPerCP-Cy5.5 (MHM-88; BioLegend), IgD-FITC (goat polyclonal from SBA), IgA-FITC and IgA-PE (IS11-8E10; Miltenyi Biotec), IgE-FITC (Fc Sp.; Invitrogen), CD80-FITC (MAB104), CD86-PE (HA5.2B7) and CD95-FITC (UB2) (all from Beckman Coulter), CD180 (MHR73-11; eBioscience) and TACI-bio (G112; PeproTech). Biotinylated antibodies were detected with Streptavidin PO (Invitrogen) and unlabeled CD180 was detected with goat anti-mouse IgG-PE. Mouse IgG1-FITC and IgG1-PE (BD Biosciences) were used as isotype controls. Intracellular staining was performed upon fixation and permeabilization with the FIX&PERM® Kit (ADG) according to manufacturers manual.

Sorting experiments were performed on FACSAria cell sorter (BD Biosciences) with an >95% purity as determined by post-sort analysis. Post-ficoll mononuclear cells from healthy donors were enriched for B cells by magnetic separation with CD19 beads (Miltenyi Biotec) prior to purification of memory B cells. IgE⁺ memory B-cell subsets were defined as CD19⁺CD38dimCD27⁺IgD⁻IgM⁻IgE⁺ and CD19⁺CD38dimCD27⁻IgD⁻IgM-IgE⁺, and remaining memory B-cell subsets, plasma cells and centrocytes were defined as described previously.[33,40]

Sequence analysis of complete *IGH* gene rearrangements

RNA from CD19⁺CD38dimCD27⁺IgD⁻IgM⁻ and CD19⁺CD38dimCD27⁻IgD⁻IgM⁻ B cells and total plasma cells was isolated using the GeneElute Mammalian Total RNA Miniprep kit (Sigma-Aldrich) and reversely transcribed with random hexamers. Complete *IGH* gene rearrangements were amplified in a semi-nested approach with a previously described set of 4 L-VH forward primers and 5' CATCACCGGCTCCGGGAAGTAG 3' *IGHE* consensus reverse primer in first PCR and 5' GTTTTTGCAGCAGCGGGTCAAG 3' *IGHE* consensus reverse primer in nested PCR, or in a one-step PCR with either *IGHM* 5'GGGAATTCTCACAGGAGACGA 3' or *IGHA* 5′GTGGCATGTCACGGACTTG 3′ or *IGHG* 5′CACGCTGCTGAGGGAGTAG 3′ consensus reverse primer.[66]

Following amplification, PCR products were cloned into the pGEM T-easy vector (Promega, Madison, WI) and prepared for sequencing on the ABI Prism 3130 XL fluorescent sequencer (Applied Biosystems). Obtained sequences were analyzed with IMGT database (www.imgt.org) to assign the *IGHV*, *IGHD* and *IGHJ* gene, and to identify somatic mutations.[67] From each unique clone, the position and frequency of mutations was determined within the *IGHV* gene, as was the length of the IgH-CDR3.

Replication history analysis using the KREC assay

DNA was isolated from each sorted subset with the GenElute Mammalian Total DNA Miniprep Kit (Sigma-Aldrich). The replication history of sorted B-cell subsets was determined with the Kappa-deleting Recombination Excision Circles (KREC) assay as described previously.[40] Briefly, the amounts of coding and signal joints of the *IGK*-deleting rearrangement were measured by realtime-quantitative (RQ-)PCR in DNA from sorted B-cell

VI

populations on an ABI Prism 7000 (Applied Biosystems). Signal joints, but not coding joints are diluted two-fold with every cell division.[40] To measure the number of cell divisions undergone by each population, we calculated the ratio between the number of coding joints and signal joints. The previously established control cell line U698 DB01 (InVivoScribe) contains one coding and one signal joint per genome and was used to correct for minor differences in efficiency of both RQ-PCR assays.[40]

IgκREHMA

The frequency of mutated *IGK* alleles was determined with the Igκ restriction enzyme hotspot mutation assay (IgκREHMA) as described previously.[40, 68] The frequently used *IGKV3-20* gene contains a mutation hotspot in IGKV-CDR1, which can be cut by restriction enzyme Fnu4HI. IGKV3-20–IGKJ rearrangements were amplified with a HEX-labeled forward primer from genomic DNA of sorted B-cell subsets, subjected to restriction enzyme digestion with KpnI and Fnu4HI and run on the ABI Prism 3130 XL (Applied Biosystems). Unmutated gene products were cut by Fnu4HI and visualized as 244 or 247-bp HEX-coupled fragments. KpnI cuts all products in FR2 downstream of the Fnu4HI sites, resulting in a 262-bp HEX-coupled mutated fragment. The unmutated B-cell line CLL-1 was used as a positive control for complete digestion with Fnu4HI. The digests hardly contained undigested gene products of 481bp, indicating complete digestion by KpnI.

Ig switch region analysis

Hybrid Sμ-Sε regions were amplified from genomic DNA in a nested long range PCR (LR-PCR) using Expand Long Template PCR System Kit (Roche Diagnostics Corp.) according to manufacturer's instructions.[69-70] LR-PCR was run with annealing temperature of 61°C, and elongation time of 2' in first 20 cycles and 2' with 10" autoextension in the following 20 cycles. Sμ: 5'GAGGGTGGTAATGATTGGTAATGCTTTGGA 3' and Sε: 5'GGCCCTTCGCCCCTGGCCTGGAGTCCCAAG 3' primers were used in the first PCR reaction and Sμ: 5'CTGCAGGGAACTGGGGTATCAAGTAGAGGG 3' and Sε: 5'TTAGCTTGGTCTTGAAGTCTGCTCTAGGTA 3' primer in the nested PCR.[69-70] PCR products were prepared for sequencing on the ABI Prism 3130 XL and obtained sequences were aligned with the *IGH* reference sequence (NG_001019)

Statistical analysis

Statistical analyses were performed with the Mann-Whitney U test or χ^2 test as indicated in detail in Tables and Figure legends. p values < .05 were considered statistically significant.

RESULTS

Detection of IgE$^+$ plasma cells in childhood tonsils

The identification of IgE$^+$ B cells by flow cytometry has been controversial because of the scarcity of these cells, the low IgE expression levels and the contamination with cells that have captured IgE with their Fcε receptors.[11-13] We acknowledged these difficulties and tried to overcome these with an 8-color flow cytometric approach to detect
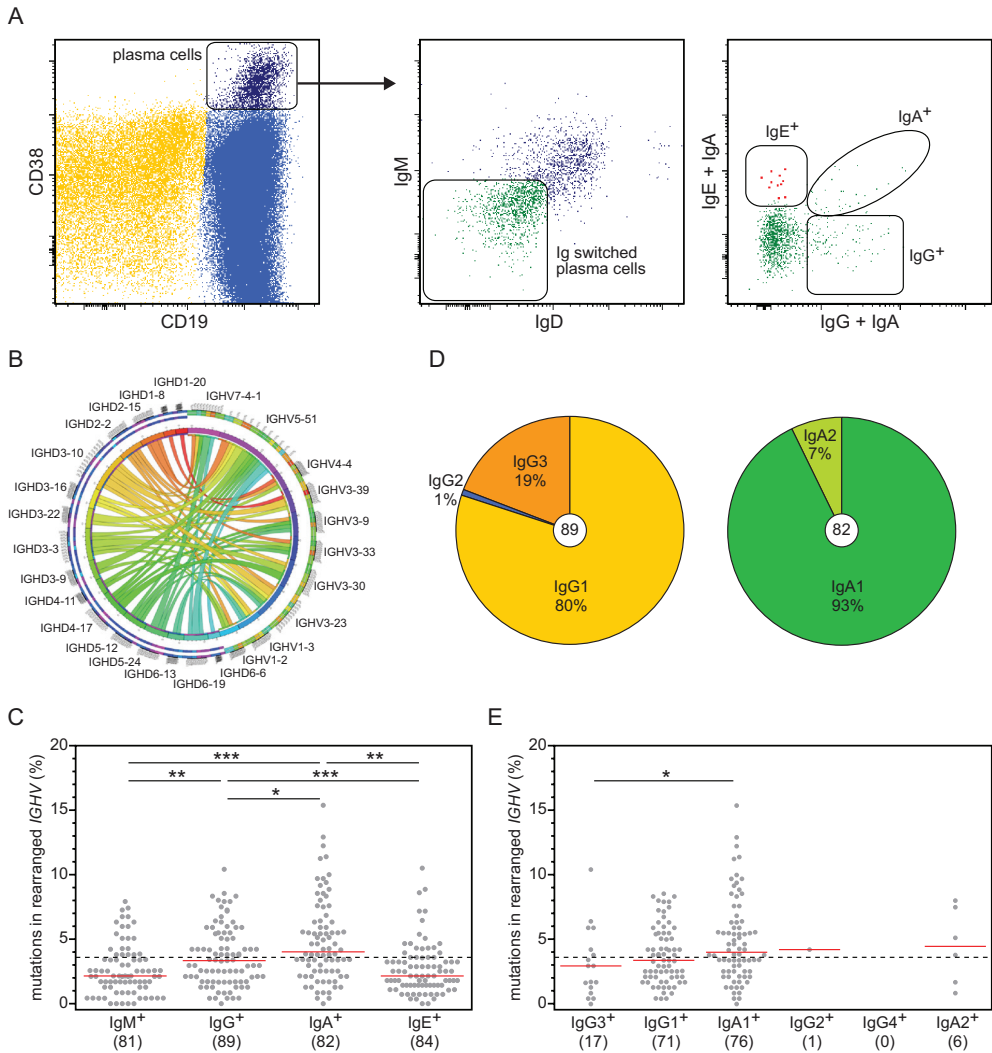
Figure 1 IgE^{+} plasma cells in childhood tonsils originate from primary GC responses.
(a) Representative images from flow cytometric analysis of plasma cell subsets in childhood tonsil. IgM^{-}IgD^{-} cells were gated with the total CD19^{+}CD38^{high} plasma cell fraction and analyzed for surface IgG, IgA and IgE expression. (b) Random pairing of the 10 most frequently used *IGHV* genes with diverse *IGHD* genes in IgE^{+} plasma cells as visualized with the Circos software package (http://mkweb.bcgsc.ca/circos). (c) SHM frequencies in rearranged *IGHV* genes in *IGHM*, *IGHG*, *IGHA* and *IGHE* transcripts. Each dot represents an individual sequence, red lines represent median values and the dashed line indicates the median SHM frequency in centrocytes. The numbers of analyzed sequences are indicated in brackets below the corresponding Ig isotypes. (d) Ig-subclass distribution in IgG[+] and IgA^{+} plasma cells. The total number of analyzed sequences is indicated in the inner circle. (e) SHM fequencies in rearranged *IGHV* genes of IgG[+] or IgA^{+} plasma cells. Data were statistically analyzed with the Mann-Whitney test. [*], p< .05, [**], p< .01, [***], p< .001;

IgE$^+$ plasma cells in childhood tonsil and IgE$^+$ memory B-cell subsets in blood (Fig. 1,2). In childhood tonsil, we identified plasma cells based on the CD19$^+$CD38^{high} phenotype (Fig. 1a). Subsequently, we selected IgM$^-$IgD$^-$ cells within the plasma cell gate, followed by analysis of monoclonal antibodies against IgE, IgA and IgG. By combining IgE and IgA in the FITC channel and IgG and IgA in the PE channel, we were able to identify IgE$^+$, IgA$^+$ and IgG$^+$ plasma cells with 2 fluorescent parameters. In childhood tonsil, CD19$^+$CD38^{high} plasma cells constituted ~4% of total CD19$^+$ cells. These plasma cells were mostly CD138$^-$, of which 66% co-expressed IgM and IgD. About 30% of the total plasma cells was surface Ig negative, but expressed cytoplasmic IgG (not shown). The remaining plasma cells either expressed IgG (2.6%), IgA (1.2%) or IgE (1.6%) on their membrane.

To study the nature of IgE$^+$ plasma cells in childhood tonsils, we analyzed IgH gene rearrangements in *IGHE* transcripts and compared these with *IGHM*, *IGHG* and *IGHA* transcripts. All transcripts were amplified using multiple primers recognizing all *IGHV* subgroups and a reverse primer specific for the constant region. *IGHE* transcripts were readily amplified from cDNA of plasma cells and yielded diverse clones (Fig. 1b). Nearly all of these contained SHM (Fig. 1c). The median SHM levels were the highest in IgA$^+$ plasma cells (4.4%), significantly lower in IgG$^+$ cells (3.3%), and the lowest in IgM$^+$ and IgE$^+$ cells (both 2.1%). We previously found that plasma cells in childhood tonsil proliferated ~8 cycles, similar to centrocytes. Therefore, the comparable SHM and replication history patterns suggest that in childhood tonsil most plasma cells are derived from a primary germinal center response. Further evidence for this was obtained by analysis of IgG and IgA subclass distribution. Nearly all transcripts showed use of *IGHM*-proximal *IGHG3*, *IGHG1* and *IGHA1* subclasses (Fig. 1d), and the frequency of SHM in *IGH* transcripts increased with their distance from *IGHM* (Fig. 1e), fitting with an origin from primary immune responses.

Germinal center-dependent and –independent IgE$^+$ memory B-cell subsets in blood

To study whether IgE$^+$ B memory cells could also be reliably detected, we first focused on the CD19$^+$CD38^{dim} B lymphocyte population in childhood tonsil. However, this analysis yielded too few events to confirm the presence of IgE$^+$ memory B cells (data not shown). Then, we focused on blood of healthy adult donors, who carry large numbers of circulating memory B cells from distinct origins and maturation pathways.[33] We first gated on the CD19$^+$CD38^{dim} B lymphocyte population, followed by selection of IgM$^-$IgD$^-$ class switched memory B cells (Fig. 2a). Within this population we detected IgE$^+$ B cells that could be distinguished into two subsets: CD27$^+$IgE$^+$ and CD27$^-$IgE$^+$ B cells. While low numbers of circulating CD19$^+$CD38^{high} plasma cells can be detected in blood, we could not reliably detect an IgE$^+$ plasma cell subset.

To study the kinetics of the IgE$^+$ B-cell subsets with age, we analyzed their frequencies in multiple healthy children and adult donors. In young children (0-5 years), CD27$^+$IgE$^+$ cells were scarce with a median frequency of 0.03% of total CD19$^+$ B cells (Fig. 2b). This frequency increased with age and reached 0.1% of total B cells in adults of 31-40 years. In contrast, CD27$^-$IgE$^+$ cells were more abundant in children than in adults, with the highest frequency of 0.12% of total B cells in children of 6-15 year. Thus, two subsets of IgE$^+$ B cells can be reproducibly detected in blood of healthy individuals and show distinct kinetics with age.

Of the six previously defined memory B cell subsets, natural effector and CD27⁻IgA⁺ B cells can be generated independently of cognate T cell help. To study whether one or both of the IgE⁺ B cell subsets could be generated in a T-cell independent manner, we analyzed these cells in blood of 5 CD40L-deficient patients (Fig. 2c). In agreement with previous observations, these patients lacked IgG⁺ memory B cells and had strongly reduced IgM⁺ and IgA⁺ memory B cells. Still, we were able to detect small numbers of both CD27⁺IgE⁺ and CD27⁻IgE⁺ B-cell subsets. The CD27⁺IgE⁺ events were on the borderline of detection level. CD27⁻IgE⁺ B cells were reliably detected with about 30% reduced frequencies as compared to healthy age-matched controls (Fig. 2d). From this, we concluded that IgE⁺ B cells can be formed in absence of cognate T cell help and these cells are nearly all CD27⁻.

Memory B cells have a typical immunophenotype characteristic for activated cells.[33-34] To study whether CD27⁺IgE⁺ and CD27⁻IgE⁺ B cells shared these features, we compared their immunophenotype with naive mature B cells and the 6 previously defined memory subsets: natural effector, CD27⁺IgM-only, CD27⁺IgG⁺, CD27⁻IgG⁺, CD27⁺IgA⁺ and CD27⁻IgA⁺ B cells.[35] All analyzed B-cell subsets had high expression of CD21 (Fig. 2e). A minor fraction of CD27⁻IgA⁺ and CD27⁻IgG⁺ cells lacked CD21 expression, confirming previous observations that part of the CD21^low B cell subset is negative for IgM and IgD.[36] CD23 was highly expressed on naive B cells, but not on memory B cells confirming previous observations.[37-39] The detection of IgE on CD27⁺ and CD27⁻ memory B cells subsets is therefore not the result of FcεR-bound molecules. Furthermore, CD27⁺IgE⁺ and CD27⁻IgE⁺ B cells showed an immunophenotype that was characteristic for activated cells; with increased expression of the B7 family members CD80 and CD86, and TNF receptor superfamily member TACI as compared to naive mature B cells. In contrast to IgM⁺, IgA⁺ and IgG⁺ memory B cells, IgE⁺ B cells did not show upregulation of TLR-related CD180.[9] Still, CD27⁺IgE⁺ and CD27⁻IgE⁺ B cells carry a typical memory B-cell immunophenotype with absence of CD23, presence of CD21 and upregulation of activation markers.

Distinct degrees of replication history and SHMs in CD27⁺IgE⁺ and CD27⁻IgE⁺ memory B cells

The presence of CD27⁻IgE⁺ memory B cells in CD40L-deficient patients suggests that analogous to CD27⁻IgA⁺ B cells, these cells can be generated independently from cognate T-cell help. To study whether CD27⁺IgE⁺ and CD27⁻IgE⁺ memory B cells in healthy individuals are derived from distinct pathways, we purified these cells to analyze their Ig gene rearrangements and to quantify in vivo replication history and SHM levels. Despite the low cell numbers and low levels of *IGHE* transcripts,[12] this yielded multiple unique sequences that displayed diverse use of *IGHV*, *IGHD* and *IGHJ* genes (Fig. 3a).

IgM⁺, IgG⁺ and IgA⁺ memory B-cell subsets in human have undergone selection against long IgH-CDR3 regions.[33] To study whether this feature is shared by IgE⁺ memory B-cell subsets, we analyzed the length of IgH-CDR3 regions in amplified *IGHE* transcripts. The median IgH-CDR3 region lengths in both CD27⁺IgE⁺ and CD27⁻IgE⁺ memory B cells were 16 amino acids, which was similar to centrocytes, but more than the 14-15 amino acids found in other memory B-cell subsets. Thus, selection mechanisms for IgE⁺ memory B cells seem different than for other memory B-cell subsets.

CD27⁺IgE⁺ memory B cells showed a replication history of ~9 cell divisions (Fig. 3c).

VI
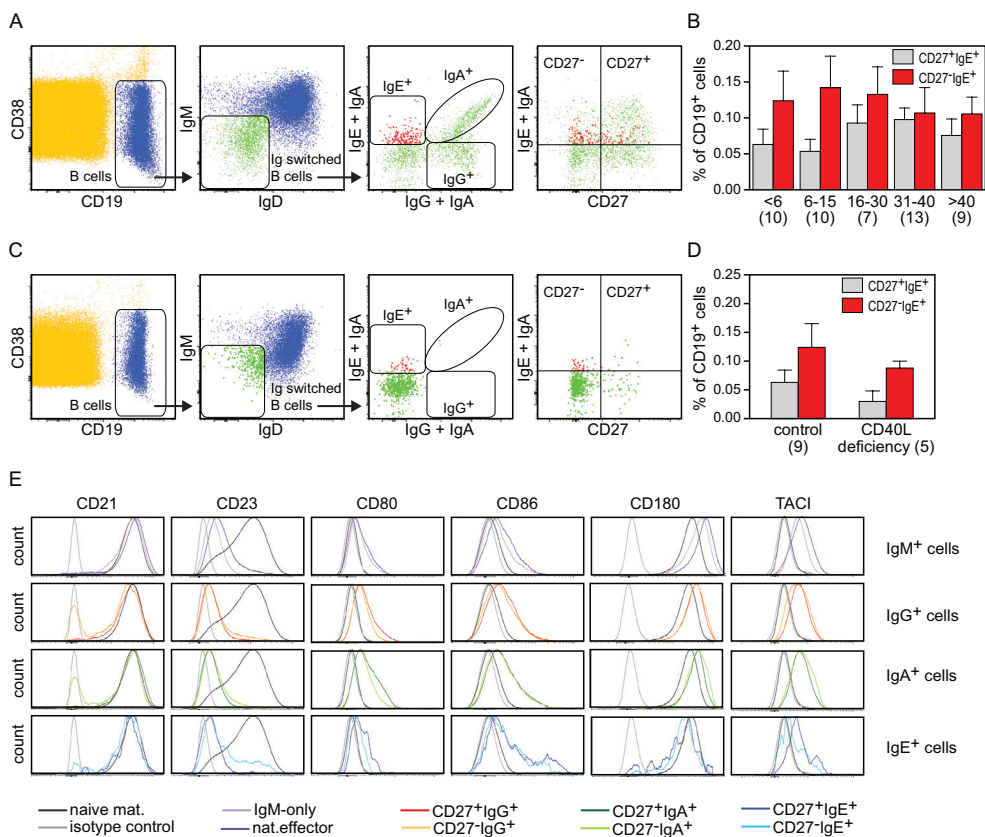
Figure 2 Germinal center-dependent and –independent IgE⁺ memory B-cell subsets in blood.

(a) Representative images of flow cytometric analysis of circulating memory B-cell subsets in healthy donors; IgM⁻ IgD⁻ cells were selected from total CD19⁺CD38^dim B cells, analyzed for IgG, IgA and IgE expression, and subdivided into CD27⁺ and CD27⁻ subsets. (b) CD27⁺IgE⁺ and CD27⁻IgE⁺ B cell frequencies in healthy children and adults. Bars represent mean values with SEM. The numbers of analyzed healthy donors are indicated in brackets below the corresponding age categories. (c) Representative images of flow cytometric analysis of circulating memory B-cell subsets in CD40L-deficient patients. (d) CD27⁺IgE⁺ and CD27⁻IgE⁺ B cell frequencies in CD40L-deficient patients and healthy age-matched donors (0-3y).(e) Expression levels of CD21, CD23, CD80, CD86, CD180 and TACI on IgM⁺, IgG⁺, IgA⁺ memory B cell subsets and the two IgE⁺ B cell subsets. Each plot contains a light grey histogram representing the isotype control, and a dark grey histogram representing naive mature B cells.

This was similar to CD27⁺IgM-only and CD27⁻IgG⁺ B cells and only slightly more than 8 cell divisions of centrocytes in childhood tonsil. In contrast, CD27⁻IgE⁺ B cells had a limited replication history of ~4 cell divisions, which was significantly lower than in CD27⁺IgE⁺ B cells and centrocytes, but similar to CD27⁻IgA⁺ memory B cells. This supports the idea that CD27⁻IgE⁺ and CD27⁻IgA⁺ memory B cells are not derived from germinal center responses, while their CD27⁺ counterparts are. In agreement with the replication history, the SHM levels in rearranged *IGHV* genes and the frequency of mutated *IGKV3-20* alleles of CD27⁺IgE⁺ B cells were similar to CD27⁺IgM-only and CD27⁻IgG⁺ B cells, and slightly higher than
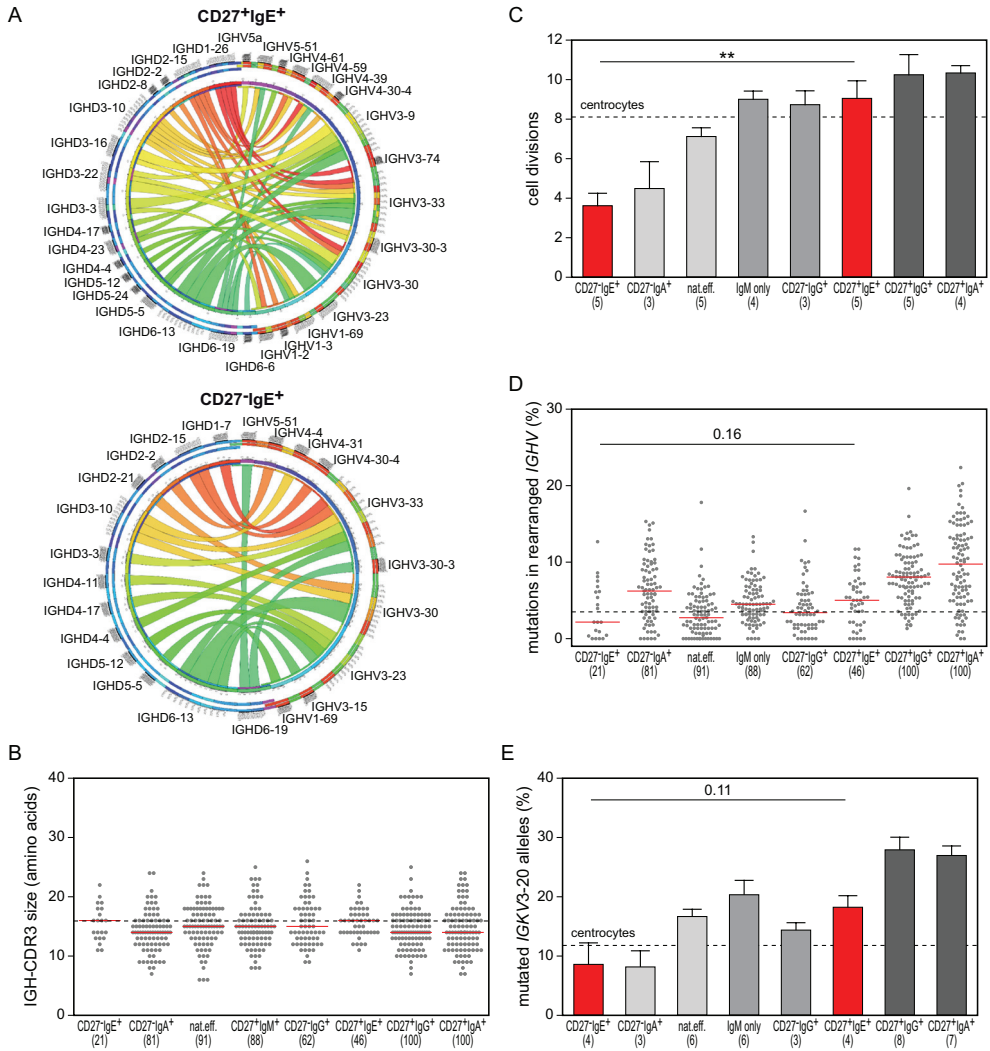
Figure 3. Distinct levels of molecular maturation in CD27+IgE+ and CD27-IgE+ memory B cells.
(a) Diverse use and pairing of *IGHV* and *IGHD* genes in *IGHE* transcripts of CD27+IgE+ and CD27-IgE+ memory B cells. Visualized with the Circos software package (http://mkweb.bcgsc.ca/circos); (b) IgH-CDR3 size distributions in memory B-cell subsets. Each grey dot represents a unique rearrangement, and red lines indicate median values. The dashed black line represents the median IgH-CDR3 size of centrocytes (n=55).[33, 40] (c) Replication histories of memory B-cell subsets as measured with the KREC assay [33, 40]. Bars represent mean values with SEM. IgE+ B-cell subsets are depicted in red, germinal centerindependent B-cell subsets in light grey, and memory B cells derived from primary and consecutive germinal center responses in middle and dark grey, respectively. The number of for centrocytes. (d) Frequencies of mutated nucleotides in rearranged *IGHV* genes. (e) Frequencies of mutated *IGKV3-20* genes as measured with the IgκREHMA assay. Differences between CD27+IgE+ and CD27-IgE+ cells were statistically analyzed with the Mann-Whitney test. **, p< .01

in centrocytes (Fig. 3d,e). The median frequency of SHM in *IGHV* of CD27$^-$IgE$^+$ B cells was lower than that of centrocytes and similar to natural effector B cells. The *IGHV* SHM levels of both IgE$^+$ memory B cells subsets were significantly lower than what was found for their IgA$^+$ counterparts (Fig. 3d). Still, analysis of the SHM distribution revealed high ratios of replacement versus silent mutations (R/S) in IGHV-CDRs of CD27$^+$IgE$^+$ (2.7) and CD27$^-$IgE$^+$ (4.2) memory B cells. These were comparable with other memory B-cell subsets (range: 2.3-4.0),[33] and are a molecular sign of affinity maturation. Finally, the frequencies of *IGKV3-20* alleles with a mutation in a CDR1 hotspot were similarly low in CD27$^-$IgE$^+$ and CD27$^-$IgA$^+$ memory B cells (Fig. 3e). Both these subsets seem to lack selection for mutations in this hotspot region.[40]

Thus, the replication history and SHM levels of the CD27$^+$IgE$^+$ memory B population suggest that most of these cells are derived from primary germinal center responses, while CD27$^-$IgE$^+$ and CD27$^-$IgA$^+$ B cells share an origin from local T-cell independent responses.

Direct *IGHM-IGHE* class switching dominant in IgE$^+$ cells formation

The *IGHE* constant region is located distally from *IGHM* in the *IGH* locus with multiple constant genes in between. Therefore, class switching to IgE can occur directly in naive cells, but also indirectly in cells that have previously switched to IgA or IgG. (Fig. 4a). To study the frequencies of indirect switching, we analyzed hybrid Sμ-Sε switch regions in genomic DNA of purified IgE$^+$ memory B cells. The majority of amplified Sμ-Sε switch regions in both CD27$^+$IgE$^+$ and CD27$^-$IgE$^+$ B cells revealed direct joining of Sμ with Sε (Fig. 4b). Still, a minor fraction of Sμ-Sε switch regions contained remnants of an Sγ (mainly Sγ1) region,[11] indicative of an indirect CSR. Sμ-Sε switch regions containing Sγ remnants were significantly more frequent in CD27$^+$IgE$^+$ (32%) than in CD27$^-$IgE$^+$ (5%) memory B cells (Fig. 4c). Thus, while CD27$^-$IgE$^+$ cells seem to be almost exclusively generated directly from IgM$^+$ cells, IgE class switching of CD27$^+$IgE$^+$ memory B cells can be preceded by formation of IgG$^+$ cells.

Increased circulating CD27$^-$IgE$^+$ memory B cells in patients with atopic dermatitis

We exploited the reliable detection of IgE$^+$ memory B cell subsets in blood to study these in 23 patients with atopic dermatitis, an allergic response often characterized by increased IgE serum levels.[41] In addition to 16 age-matched healthy controls, we included a cohort of 14 patients with psoriasis, which is also an immune-mediated skin disease, but mainly mediated by T$_H$1 and T$_H$17 cells, rather than T$_H$2 responses.[42] The frequencies of total IgE$^+$ memory B cells within the CD19$^+$ B-cell fraction were not significantly different between healthy donors (median of 0.15%), atopic dermatitis patients (0.19%) and psoriasis patients (0.11%; Fig. 5a). Consistent with this, the frequencies of CD27$^+$IgE$^+$ memory B cells were similarly low in all study groups (0.07% of CD19$^+$ cells). However, the median frequency of CD27$^-$IgE$^+$ cells in atopic patients (0.12%) was significantly higher than in healthy donors (0.08%; p< .05) and psoriasis patients (0.05%; p< .05).

To study a relation with disease severity, patients were scored for disease activity according to the criteria by Hanifin and Rajka.[43] Patients with a 'high' disease severity had more CD27$^+$IgE$^+$ and CD27$^-$IgE$^+$ cells than patients with the 'mild' or 'moderate' manifestation of the disease (data not shown). Due to low numbers of patients per group, these

differences did not reach statistical significance. The frequencies of IgE+ memory B cells did not correlate with total or allergen-specific IgE serum levels (Fig. 5b).[12]

Patients with atopic dermatitis display constant immune response activity. Repetitive B cell exposure to allergen in the course of an allergic disease triggers antibody affinity maturation. To study the effects of repetitive antigen triggers on the IgE responses, we analyzed SHM in *IGHE* transcripts amplified from 5 patients with a selective increase in CD27-IgE+ memory B cells (6-fold more CD27-IgE+ than CD27+IgE+ B cells). The frequency of SHM in *IGHV* genes of atopic dermatitis patients was significantly higher than in control CD27-IgE+ memory B cells, but similar to CD27+IgE+ B cells. Patient's transcripts showed molecular signs of affinity maturation with a high IGHV-CDR R/S ratio (2.8). Thus, patients with atopic dermatitis show increased levels of circulating CD27-IgE+ memory B cells that show molecular signs of extensive antibody maturation.

Model of IgE+ plasma cell and memory B-cell formation in human

To recapitulate our findings, we propose a model of IgE+ plasma cell and memory B cell formation in human (Fig.6) Based on the distinct molecular features and similarity to previously characterized memory B-cell subsets, we distinguish CD27+IgE+ memory B cells derived from TD responses in the germinal center and CD27-IgE+ memory B cells from local responses in local (mucosal) tissue. IgE+ plasma cells can be derived from both TD and TI maturation pathways. In non-allergic donors, the majority of IgE+ memory B cells and plasma cells is derived from primary immune responses.

DISCUSSION

Using a novel 8-color flow-cytometric strategy, we reliably detected IgE+ plasma cells in childhood tonsils, and circulating CD27+IgE+ and CD27-IgE+ memory B-cell subsets. Purification of these subsets and comparative analysis with IgM+, IgG+ and IgA+ B cells allowed us to dissect their origins from germinal center responses (IgE+ plasma cells and CD27+IgE+ memory B cells) and germinal center-independent responses (CD27-IgE+). The germinal center-dependent responses generated more SHM and frequently underwent Ig CSR via IgG1, whereas both processes were reduced in CD27-IgE+ memory B cells. These CD27-IgE+ cells were increased in patients with atopic dermatitis and showed extensive SHM.

Prior to selection of IgE+ B cells, we performed a stepwise exclusion of IgM+, IgD+, IgG+ and IgA+ cells. This approach increased the specificity of detection of rare IgE+ B cells with weak IgE signals due to the suboptimal polyadenylation signals in the membrane IgE splice variant.[12] Moreover, with this strategy, we excluded CD23+ naive B cells that stained positively for IgE due to CD23-mediated capture from serum (not shown).[38, 44] Thus far, the detection of IgE+ B cells has been problematic,[45] and often depended on cold acid wash to disrupt CD23-IgE binding,[46] which can be very damaging to the cells. Our direct flow cytometric approach on otherwise untreated cells allowed detailed immunophenotyping and molecular analyses. Thus, we could show that these cells were antigen-experienced IgE-switched B cells with SHM-containing IgE transcripts, extensive replication history and an activated immunophenotype.
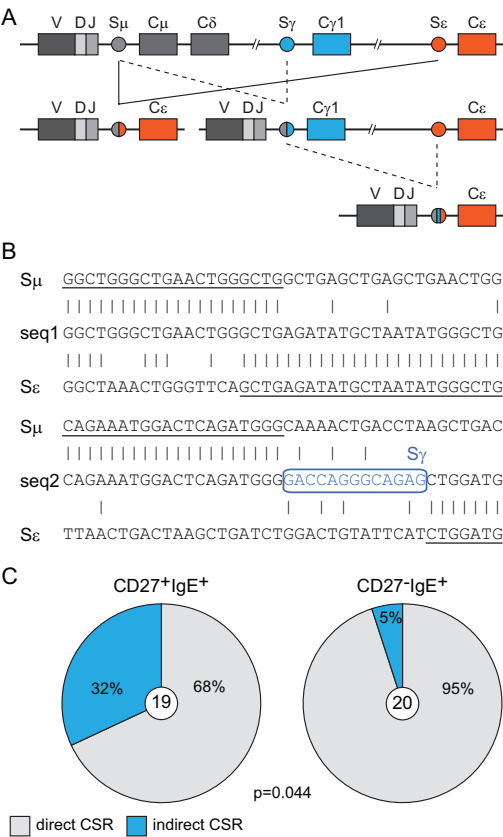
VI

A

V DJ Sμ Cμ Cδ Sγ Cγ1 Sε Cε

V DJ Cε V DJ Cγ1 Cε

V DJ Cε

A

total IgE$^+$ B cells   CD27$^+$IgE$^+$ CD27$^-$IgE$^+$

% of CD19$^+$ B cells

ctrl (n=16) AD (n=23) psor (n=14) ctrl (n=16) AD (n=23) psor (n=14) ctrl (n=16) AD (n=23) psor (n=14)

B

Sμ GGCTGGGCTGAACTGGGCTGGCTGAGCTGAGCTGAACTGG

seq1 GGCTGGGCTGAACTGGGCTGAGATATGCTAATATGGGCTG

Sε GGCTAAACTGGGTTCAGCTGAGATATGCTAATATGGGCTG

Sμ CAGAAATGGACTCAGATGGGCAAAACTGACCTAAGCTGAC

Sγ

seq2 CAGAAATGGACTCAGATGGG GACCAGGGCAGAG CTGGATG

Sε TTAACTGACTAAGCTGATCTGGACTGTATTCATCTGGATG

B

IgE$^+$ B-cells (cells/µl)

CD27$^+$IgE$^+$
CD27$^-$IgE$^+$

IgE$^+$ antibodies in serum (U/ml)

C

CD27$^+$IgE$^+$ CD27$^-$IgE$^+$

32%   68%   (19)   5%   95%   (20)

p=0.044

direct CSR   indirect CSR

C

Mutations in rearranged *IGHV* (%)

*

CD27$^+$IgE$^+$ (46)   CD27$^-$IgE$^+$ (21)   CD27$^-$IgE$^+$ (58)

controls   AD patients

Figure 4 Molecular analysis of Ig class switching in CD27$^+$IgE$^+$ and CD27$^-$IgE$^+$ memory B cells.

(a) Schematic representation of direct (left side) and indirect (right side; via IgG1) class-switching towards *IGHE* constant region in the human *IGH* locus.(b) Examples of hybrid Sμ-Sε switch regions generated in direct (top panel) and sequential (bottom panel) class-switching towards *IGHE*; remnants of Sγ1 in the Sμ-Sε junction are boxed and indicated in blue font (c) Frequencies of direct and indirect class switching in CD27$^+$IgE$^+$ and CD27$^-$IgE$^+$ memory B cells. The numbers of analyzed sequences are indicated in the inner circles. Data were statistically analyzed with the χ^2 test.
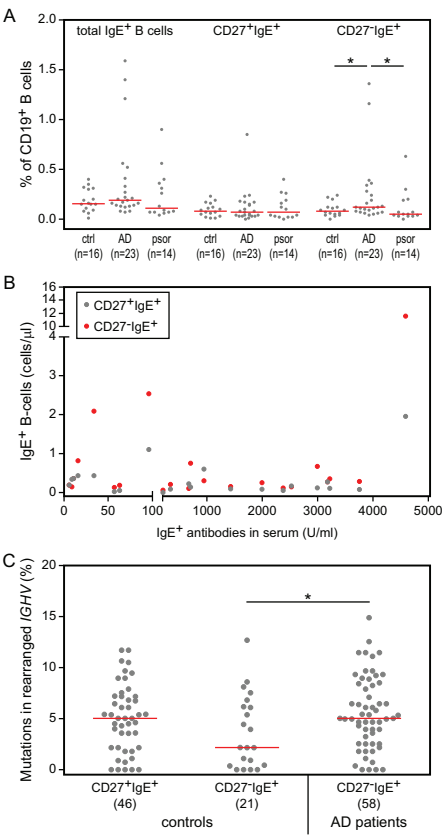
Figure 5 Increased frequencies of CD27$^-$IgE$^+$ memory B cells in atopic dermatitis patients are independent of IgE levels in serum.

(a) Frequencies of total IgE$^+$, CD27$^+$IgE$^+$ and CD27$^-$IgE$^+$ memory B cells in atopic dermatitis (AD) patients, psoriasis (psor) patients and healthy age-matched donors (ctrl). Individual data points are shown as grey dots with red lines indicating median values. The number of analyzed individuals is indicated in brackets. Data were statistically analyzed with the Man-Whitney test; *, p< .05. (b) Correlation between CD27$^+$IgE$^+$ and CD27$^-$IgE$^+$ memory B-cell numbers, and IgE serum levels in 23 patients with atopic dermatitis. (c) Frequencies of mutated nucleotides in rearranged *IGHV* genes. Each grey dot represents an individual sequence. *IGHE* transcripts in atopic dermatitis were amplified from peripheral blood mononuclear cells in patients with a specific increase of CD27$^-$IgE$^+$ memory B cells (at least 6-fold more CD27$^-$IgE$^+$ than CD27$^+$IgE$^+$ B cells).

Figure 6. Model of generation of human IgE[+] plasma cell and memory B cells from GC-dependent and GC-independent maturation pathways.

Upon maturation from recent bone marrow emigrants (transitional B cells), naive mature B cells scavenge the peripheral lymphoid system for antigens.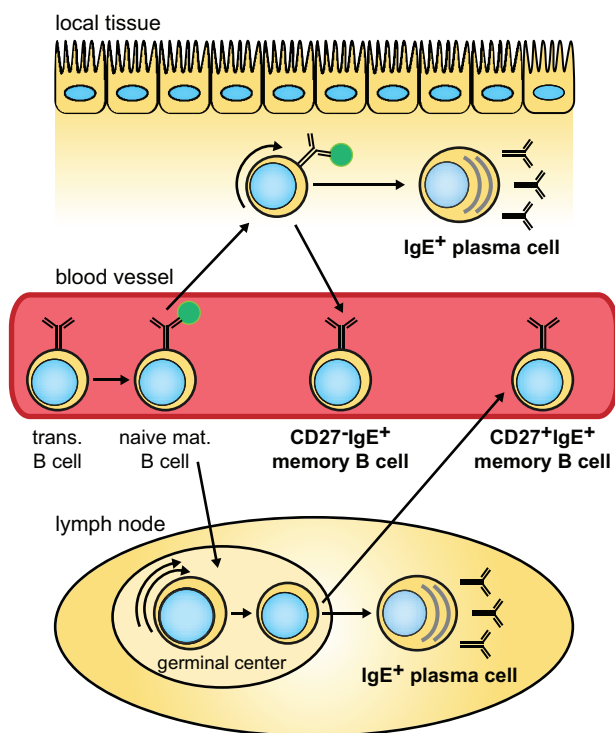 Those cells that recognize peptide allergens in specialized lymphoid structures (lymph nodes) receive co-stimulation from T cells and form GCs. Intensive proliferation and affinity maturation in GCs result in the formation of IgE^{+} plasma cells and circulating CD27^{+}IgE^{+} memory B cells. Those naive mature B cells that recognize antigens independent from T-cell help in local tissue (e.g. mucosa, skin), undergo limited proliferation and SHM, and develop locally into plasma cells or circulating CD27^{-}IgE^{+} memory B cells.

The majority of plasma cells in childhood tonsils had an immature phenotype with surface Ig and low CD138 expression, which is commonly seen in plasma cells in lymph nodes, but not in blood and bone marrow,[47-48] and likely reflects recent generation. Interestingly, the majority of plasma cells in tonsil expressed surface IgM or cytoplasmic IgG, with only a few IgA and IgE expressing cells. Recently, circulating plasma cells were reported to frequently express IgA and to be derived from local responses in mucosa.[48-49] Apparently, despite the close proximity to the nasopharyngeal mucosa, tonsils do not necessarily host mucosal immune responses. The *IGH* transcripts from tonsil plasma cells showed similar SHM frequencies as centrocytes, and *IGHA* and *IGHG* class switching to *IGHM*-proximal *IGHA1*, *IGHG1* and *IGHG3*. Together with our previous observations that these cells also showed similar replication histories, suggests their origin from primary immune responses.[33, 40]

In blood, we identified circulating IgE^{+} B cells that could be separated into a CD27^{+} and a CD27^{-} subset. Both subsets showed immunophenotypic and molecular signs of B-cell memory: (1) high expression of activation and costimulatory molecules; (2) extensive replication history; and (3) SHM levels with high R/S ratios in IGHV-CDRs. The existence of IgE[+] B-cell memory has been disputed, although some indirect evidence exists from the kinetics of allergic responses.[50-51] Moreover, several studies report the detection of low numbers of circulating IgE^{+} B cells displaying a plasma cell-like phenotype.[52-53] The IgE^{+} B cells we identified showed a memory B cell phenotype with low CD38 expression and upregulation of CD80, CD86, CD95 and TACI. Moreover, sort purified cells expressed IgE-switched transcripts with SHM. Thus, IgE[+] memory B cells can be formed in healthy individuals and can be detected in peripheral blood.

We separated the circulating IgE^{+} memory B cells into CD27^{+} and CD27^{-} subsets. These cells did not merely differ in their phenotype: the replication history, SHM levels and frequency of indirect class switching were significantly higher for CD27^{+}IgE^{+} than for CD27^{-}IgE^{+} memory B cells. The replication history and SHM levels of CD27^{+}IgE^{+} memory B cells were slightly higher than in centrocytes, but lower than in CD27^{+}IgG^{+} and CD27^{+}IgA^{+} memory B cells, indicating that the majority of CD27^{+}IgE^{+} B cells in healthy adults are derived from primary GC responses. This is probably different in allergic patients, in whom higher levels of SHM were found.[54] These highly mutated clones are potentially generated upon repeated allergen contact.

The low frequencies of hybrid Sμ-Sε regions with Sγ remnants are suggestive of direct class switching of activate naive B cells to IgE. For the CD27^{-}IgE^{+} memory B-cell subset, this would fit with the low replication history and SHM levels. Moreover, these patterns are highly comparable to CD27^{-}IgA^{+} memory B cells that show frequent direct switching to *IGHA2*, which is genomically close to *IGHE*. The high frequency of direct switching and the replication history of ~9 cell divisions indicate that the vast majority of CD27^{+}IgE^{+} memory B cells in healthy controls is generated from a primary GC response. The generation of high affinity IgE antibodies in the mouse depends on CSR via an IgG1 intermediate.[55] From our results, it remains unclear whether the cells directly and indirectly switched to IgE differ in reactivity. Still, this would not be suggestive of unique maturation pathways for IgE^{+} memory cells, because it is to be expected that a secondary response results in higher SHM levels and antigen affinity. Moreover, IgG[+] memory B cells express increased *IL13R* transcripts as compared to naive, IgM[+] and IgA[+] memory B cells. Thus, these cells are more susceptible to IL-13-induced IgE CSR (unpublished observation). Finally, it is to be expected that healthy individuals do not contain large numbers of memory B cells that express high affinity IgE. It would therefore be interesting to study these processes in patients with allergies.

CD27^{-}IgE^{+} memory B cells had limited replication history and SHM levels, and were normally present in CD40L-deficient patients, indicating their origin from a TI pathway. Until recently, CD27 was considered a pan memory B-cell marker,[56-57] but there is growing evidence that also CD27- Ig-class switched cells display memory B-cell characteristics.[33, 58-59] Importantly, the replication history, SHM levels and Ig CSR profile of CD27^{-}IgE^{+} memory B cells is similar to CD27^{-}IgA^{+} memory B cells, suggestive of their common origin from local mucosal responses.[33] Indeed, multiple studies demonstrated local IgE production in the respiratory tract of patients with atopic rhinitis and asthma,[18, 22, 60-61] and gastrointestinal tract

of patients with food allergy,[21] and showed increased local IL-4 and IL-13 production in these pathological conditions.[62-63] Unlike CD27⁺IgE⁺ cells, CD27⁻IgE⁺ memory B cells reached the highest frequencies in childhood. Since GC-dependent responses remain underdeveloped in young children, involvement of CD27⁻IgE⁺ cells in local responses could possibly explain early onset of some allergic diseases.[64]

We found increased CD27⁻IgE⁺ memory B-cell numbers in atopic dermatitis patients. While this increase was not found in psoriasis, the nature of these cells in atopic dermatitis remains unclear. The CD27⁻IgE⁺ phenotype could reflect the mainly local manifestation of this allergic disease. These cells would then be abnormally expanded with increased levels of SHM as compared to healthy controls. Alternatively, the CD27⁻IgE⁺ memory B cells in these patients are derived from a GC response with normal SHM levels, but display an abnormal phenotype. Still, our findings of increased CD27⁻IgE⁺ memory B cell levels in a subset of atopic dermatitis patients suggest that analysis of CD27⁻IgE⁺ memory B-cell numbers can contribute to diagnosis of these patients, especially in cases with low IgE serum levels.[41]

On top of diagnostics, IgE⁺ memory B cell measurements could prove valuable in monitoring of patients undergoing immunotherapy or anti-IgE antibody therapy (e.g. with omalizumab). A recent study indicated that the beneficial effect of omalizumab is the result of reduced IgE production.[65] Therefore, the kinetics of disappearance of IgE⁺ memory B cells could be an early marker to predict therapy outcome for patients with severe allergies.

Thus, by implementing a new strategy to reliably detect IgE-expressing B cells, we provided new insights into the biology of human IgE⁺ plasma cells and delineated memory B-cell subsets from TD and TI responses. These insights open new possibilities to study the mechanisms underlying IgE-mediated diseases, which can be directly translated into patient care.

ACKNOWLEDGEMENTS

REFERENCES

1. Asher, M.I. et al. Worldwide time trends in the prevalence of symptoms of asthma, allergic rhinoconjunctivitis, and eczema in childhood: ISAAC Phases One and Three repeat multicountry cross-sectional surveys. *Lancet* 368, 733-743 (2006).
2. Devereux, G. The increase in the prevalence of asthma and allergy: food for thought. *Nat Rev Immunol* 6, 869-874 (2006).
3. Akinbami, L.J., Moorman, J.E. & Liu, X. Asthma prevalence, health care use, and mortality: United States, 2005-2009. Natl Health Stat Report, 1-14 (2011).
4. Pawankar, R., Canonica, G., Holgate, S. & Lockey, R. WAO White Book on Allergy 2011-2012: Executive Summary. (2011).
5. Poole, J.A., Matangkasombut, P. & Rosenwasser, L.J. Targeting the IgE molecule in allergic and asthmatic diseases: review of the IgE molecule and clinical efficacy. *J Allergy Clin Immunol* 115, S376-385 (2005).
6. Chang, T.W., Wu, P.C., Hsu, C.L. & Hung, A.F. Anti-IgE antibodies for the treatment of IgE-mediated allergic diseases. *Adv Immunol* 93, 63-119 (2007).

VI

7. Geha, R.S., Jabara, H.H. & Brodeur, S.R. The regulation of immunoglobulin E classswitch recombination. *Nat Rev Immunol* 3, 721-732 (2003).
8. Schroeder, H.W., Jr. & Cavacini, L. Structure and function of immunoglobulins. *J Allergy Clin Immunol* 125, S41-52 (2010).
9. Ramesh, S. Food allergy overview in children. *Clin Rev Allergy Immunol* 34, 217-230 (2008).
10. Waserman, S. & Watson, W. Food allergy. *Allergy Asthma Clin Immunol* 7 Suppl 1, S7 (2011).
11. Stone, K.D., Prussin, C. & Metcalfe, D.D. IgE, mast cells, basophils, and eosinophils. *J Allergy Clin Immunol* 125, S73-80 (2010).
12. Karnowski, A., Achatz-Straussberger, G., Klockenbusch, C., Achatz, G. & Lamers, M.C. Inefficient processing of mRNA for the membrane form of IgE is a genetic mechanism to limit recruitment of IgE-secreting cells. *Eur J Immunol* 36, 1917-1925 (2006).
13. Acharya, M. et al. CD23/FcepsilonRII: molecular multi-tasking. *Clin Exp Immunol* 162, 12-23 (2010).
14. Gauchat, J.F., Lebman, D.A., Coffman, R.L., Gascan, H. & de Vries, J.E. Structure and expression of germline epsilon transcripts in human B cells induced by interleukin 4 to switch to IgE production. *J Exp Med* 172, 463-473 (1990).
15. Punnonen, J. et al. Interleukin 13 induces interleukin 4-independent IgG4 and IgE synthesis and CD23 expression by human B cells. *Proc Natl Acad Sci U S A* 90, 3730- 3734 (1993).
16. Hibbert, R.G. et al. The structure of human CD23 and its interactions with IgE and CD21. *J Exp Med* 202, 751-760 (2005).
17. Jeannin, P. et al. CD86 (B7-2) on human B cells. A functional role in proliferation and selective differentiation into IgE- and IgG4-producing cells. *J Biol Chem* 272, 15613- 15619 (1997).
18. Coker, H.A., Durham, S.R. & Gould, H.J. Local somatic hypermutation and class switch recombination in the nasal mucosa of allergic rhinitis patients. *J Immunol* 171, 5602-5610 (2003).
19. KleinJan, A., Vinke, J.G., Severijnen, L.W. & Fokkens, W.J. Local production and detection of (specific) IgE in nasal B-cells and plasma cells of allergic rhinitis patients. *Eur Respir J* 15, 491-497 (2000).
20. Snow, R.E., Chapman, C.J., Holgate, S.T. & Stevenson, F.K. Clonally related IgE and IgG4 transcripts in blood lymphocytes of patients with asthma reveal differing patterns of somatic mutation. *Eur J Immunol* 28, 3354-3361 (1998).
21. Coeffier, M., Lorentz, A., Manns, M.P. & Bischoff, S.C. Epsilon germ-line and IL-4 transcripts are expressed in human intestinal mucosa and enhanced in patients with food allergy. *Allergy* 60, 822-827 (2005).
22. Takhar, P. et al. Class switch recombination to IgE in the bronchial mucosa of atopic and nonatopic patients with asthma. *J Allergy Clin Immunol* 119, 213-218 (2007).
23. Fagarasan, S., Kinoshita, K., Muramatsu, M., Ikuta, K. & Honjo, T. In situ class switching and differentiation to IgA-producing cells in the gut lamina propria. *Nature* 413, 639-643 (2001).
24. He, B. et al. Intestinal bacteria trigger T cell-independent immunoglobulin A(2) class switching by inducing epithelial-cell secretion of the cytokine APRIL. *Immunity* 26, 812-826 (2007).
25. Erazo, A. et al. Unique maturation program of the IgE response in vivo. *Immunity* 26, 191-203 (2007).
26. Yang, Z., Sullivan, B.M. & Allen, C.D. Fluorescent In Vivo Detection Reveals that IgE(+) B Cells Are Restrained by an Intrinsic Cell Fate Predisposition. *Immunity* 36, 857-872 (2012).
27. Wesemann, D.R. et al. Immature B cells preferentially switch to IgE with increased direct Smu to Sepsilon recombination. *J Exp Med* 208, 2733-2746 (2011).
28. Xiong, H., Dolpady, J., Wabl, M., Curotto de Lafaille, M.A. & Lafaille, J.J. Sequential class switching is required for the generation of high affinity IgE antibodies. *J Exp Med* 209, 353-364 (2012).
29. Lafaille, J.J., Xiong, H. & Curotto de Lafaille, M.A. On the differentiation of mouse IgE(+) cells. *Nat Immunol* 13, 623 (2012).
30. Talay, O. et al. IgE(+) memory B cells and plasma cells generated through a germinalcenter pathway. *Nat Immunol* 13, 396-404 (2012).
31. Ahmed, R. & Gray, D. Immunological memory and protective immunity: understanding their relation. *Science* 272, 54-60 (1996).
32. MacLennan, I.C. Germinal centers. *Annual review of immunology* 12, 117-139 (1994).
33. Berkowska, M.A. et al. Human memory B cells originate from three distinct germinal center-dependent and -independent maturation pathways. *Blood* 118, 2150-2158 (2011).
34. Good, K.L., Avery, D.T. & Tangye, S.G. Resting human memory B cells are intrinsically programmed for

enhanced survival and responsiveness to diverse stimuli compared to naive B cells. *J Immunol* 182, 890-901 (2009).

35. Berkowska, M.A., van der Burg, M., van Dongen, J.J. & van Zelm, M.C. Checkpoints of B cell differentiation: Visualizing Ig-centric processes. *Ann NY Acad of Sci* in press (2011).

36. Isnardi, I. et al. Complement receptor 2/CD21- human naive B cells contain mostly autoreactive unresponsive clones. *Blood* 115, 5026-5036 (2010).

37. Klein, U., Kuppers, R. & Rajewsky, K. Evidence for a large compartment of IgM-expressing memory B cells in humans. *Blood* 89, 1288-1298 (1997).

38. Kikutani, H. et al. Fc epsilon receptor, a specific differentiation marker transiently expressed on mature B cells before isotype switching. *J Exp Med* 164, 1455-1469 (1986).

39. Weller, S. et al. Human blood IgM "memory" B cells are circulating splenic marginal zone B cells harboring a prediversified immunoglobulin repertoire. *Blood* 104, 3647-3654 (2004).

40. van Zelm, M.C., Szczepanski, T., van der Burg, M. & van Dongen, J.J. Replication history of B lymphocytes reveals homeostatic proliferation and extensive antigeninduced B cell expansion. *J Exp Med* 204, 645-655 (2007).

41. Novak, N. & Bieber, T. Allergic and nonallergic forms of atopic diseases. *J Allergy Clin Immunol* 112, 252-262 (2003).

42. Mak, R.K., Hundhausen, C. & Nestle, F.O. Progress in understanding the immunopathogenesis of psoriasis. *Actas Dermosifiliogr* 100 Suppl 2, 2-13 (2009).

43. Hanifin, J.M. & Rajka, G. Diagnostic features of atopic dermatitis. *Acta Derm Venereol* 92, 44-47 (1980).

44. Veneri, D. et al. Expression of CD27 and CD23 on peripheral blood B lymphocytes in humans of different ages. *Blood Transfus* 7, 29-34 (2009).

45. Horst, A. et al. Detection and characterization of plasma cells in peripheral blood: correlation of IgE+ plasma cell frequency with IgE serum titre. *Clin Exp Immunol* 130, 370-378 (2002).

46. Kumagai, K., Abo, T., Sekizawa, T. & Sasaki, M. Studies of surface immunoglobulins on human B lymphocytes. I. Dissociation of cell-bound immunoglobulins with acid pH or at 37 degrees C. *J Immunol* 115, 982-987 (1975).

47. Medina, F., Segundo, C., Campos-Caro, A., Gonzalez-Garcia, I. & Brieva, J.A. The heterogeneity shown by human plasma cells from tonsil, blood, and bone marrow reveals graded stages of increasing maturity, but local profiles of adhesion molecule expression. *Blood* 99, 2154-2161 (2002).

48. Caraux, A. et al. Circulating human B and plasma cells. Age-associated changes in counts and detailed characterization of circulating normal CD138- and CD138+ plasma cells. *Haematologica* 95, 1016-1020 (2010).

49. Mei, H.E. et al. Blood-borne human plasma cells in steady state are derived from mucosal immune responses. *Blood* 113, 2461-2469 (2009).

50. Takahama, H., Furusawa, S. & Ovary, Z. IgE memory B cells identified by the polymerase chain reaction. *Cell Immunol* 176, 34-40 (1997).

51. Niederberger, V. et al. Antigens drive memory IgE responses in human allergy via the nasal mucosa. *Int Arch Allergy Immunol* 142, 133-144 (2007).

52. Donohoe, P.J. et al. IgE+ cells in the peripheral blood of atopic, nonatopic, and bee venom-hypersensitive individuals exhibit the phenotype of highly differentiated B cells. *J Allergy Clin Immunol* 95, 587-596 (1995).

53. Dullaers, M. et al. The who, where, and when of IgE in allergic airway disease. *J Allergy Clin Immunol* 129, 635-645 (2012).

54. Dahlke, I., Nott, D.J., Ruhno, J., Sewell, W.A. & Collins, A.M. Antigen selection in the IgE response of allergic and nonallergic individuals. *J Allergy Clin Immunol* 117, 1477-1483 (2006).

55. Jung, S., Siebenkotten, G. & Radbruch, A. Frequency of immunoglobulin E class switching is autonomously determined and independent of prior switching to other classes. *J Exp Med* 179, 2023-2026 (1994).

56. Agematsu, K. et al. B cell subpopulations separated by CD27 and crucial collaboration of CD27+ B cells and helper T cells in immunoglobulin production. *European journal of immunology* 27, 2073-2079 (1997).

57. Tangye, S.G., Liu, Y.J., Aversa, G., Phillips, J.H. & de Vries, J.E. Identification of functional human splenic memory B cells by expression of CD148 and CD27. *The Journal of experimental medicine* 188, 1691-1703 (1998).

58. Fecteau, J.F., Cote, G. & Neron, S. A new memory CD27-IgG+ B cell population inperipheral blood expressing VH genes with low frequency of somatic mutation. *J Immunol* 177, 3728-3736 (2006).

59. Wei, C. et al. A new population of cells lacking expression of CD27 represents a notable component of the B cell memory compartment in systemic lupus erythematosus. *J Immunol* 178, 6624-6633 (2007).

VI

60. Takhar, P. et al. Allergen drives class switching to IgE in the nasal mucosa in allergic rhinitis. *J Immunol* 174, 5024-5032 (2005).

61. Ying, S. et al. Local expression of epsilon germline gene transcripts and RNA for the epsilon heavy chain of IgE in the bronchial mucosa in atopic and nonatopic asthma. *J Allergy Clin Immunol* 107, 686-692 (2001).

62. Cameron, L.A. et al. Expression of IL-4, Cepsilon RNA, and Iepsilon RNA in the nasal mucosa of patients with seasonal rhinitis: effect of topical corticosteroids. *J Allergy Clin Immunol* 101, 330-336 (1998).

63. Humbert, M. et al. Elevated expression of messenger ribonucleic acid encoding IL-13 in the bronchial mucosa of atopic and nonatopic subjects with asthma. *J Allergy Clin Immunol* 99, 657-665 (1997).

64. Roduit, C. et al. Development of atopic dermatitis according to age of onset and association with early-life exposures. *J Allergy Clin Immunol* 130, 130-136 e135 (2012).

65. Lowe, P.J. & Renard, D. Omalizumab decreases IgE production in patients with allergic (IgE-mediated) asthma; PKPD analysis of a biomarker, total IgE. *Br J Clin Pharmacol* 72, 306-320 (2011).

66. Tiller, T. et al. Efficient generation of monoclonal antibodies from single human B cells by single cell RT-PCR and expression vector cloning. *J Immunol Methods* 329, 112-124 (2008).

67. Lefranc, M.P. et al. IMGT, the international ImMunoGeneTics information system. *Nucleic Acids Res* 37, D1006-1012 (2009).

68. Andersen, P. et al. Deficiency of somatic hypermutation of the antibody light chain is associated with increased frequency of severe respiratory tract infection in common variable immunodeficiency. *Blood* 105, 511-517 (2005).

69. Shapira, S.K. et al. Deletional switch recombination occurs in interleukin-4-induced isotype switching to IgE expression by human B cells. *Proc Natl Acad Sci U S A* 88, 7528-7532 (1991).

70. Shapira, S.K., Vercelli, D., Jabara, H.H., Fu, S.M. & Geha, R.S. Molecular analysis of the induction of immunoglobulin E synthesis in human B cells by interleukin 4 and engagement of CD40 antigen. *J Exp Med* 175, 289-292 (1992).

VII

General discussion

Healthy vertebrates are immunocompetent, i.e. they carry an immune system that provides adequate immune responses and subsequent immunity to a broad spectrum of antigens. Immunocompetence requires a tight balance between the production of a large repertoire of cells with unique receptors and a strong immune response of groups of cells with an antigen-specific repertoire. The research described in this thesis was started with the ultimate goal to determine how a broad B-cell repertoire is formed in human bone marrow, and how it is specified upon antigen encounter in the peripheral lymphoid system.

By studying the Ig gene rearrangements in cells cultured from human cord blood and displaying differential IL-7Rα expression, it was demonstrated that the IL-7 /IL-7R signaling pathway plays a crucial role in ordered Ig gene rearrangements. IL-7R signaling suppresses the Ig light chain rearrangements before the completion of a functional IgH (**Chapter II**). Furthermore, it was shown that, similar to mice, the human *IGH* locus undergoes contraction prior to V(D)J recombination in bone marrow.

Analysis of antigen-experienced B-cell compartment in peripheral blood revealed that this is composed of multiple phenotypically distinct subsets (**Chapters III and VI**). The molecular features of these subsets indicated that $CD27^+IgG^+$, $CD27^+IgA^+$, $CD27^+IgE^+$, $CD27^-IgG^+$ and $CD27^+IgM^+$ cells originate from T-cell dependent (TD) immune responses, while $CD27^+IgM^+IgD^+$, $CD27^-IgA^+$ and $CD27^-IgE^+$ cells are derived from T-cell independent (TI) responses. Irrespective of their origin all memory B-cell subsets showed similar upregulation of co-stimulatory molecules and downregulation of BCR-signaling inhibitors (**Chapters III, V and VI**). Still, gene expression profiles of IgA^+ and IgG^+ memory B cells were more related to each other than to IgM^+ memory B cells (**Chapter V**).

The gene expression profile of $CD27^+IgM^+IgD^+$ B cells in patients with persistent polyclonal B-cell lymphocytosis was highly similar to IgM^+ memory B cells of healthy controls (**Chapter IV**). Still, these cells displayed abnormally low SHM frequencies despite hyperproliferation. Moreover, their low expression levels of CD73 and CD62L can facilitate the diagnostic process of this disorder.

The studies described in this thesis resulted in identification and characterization of 3 novel memory B-cells subsets. Circulating $CD27^-IgA^+$ B cells were found to be derived from TI responses in the intestinal *lamina propria*. These cells presented with a distinct reactivity pattern from conventional $CD27^+IgA^+$ B cells, which was visualized by analysis of monoclonal antibodies generated from single-cell sorted IgA^+ cells (**Chapter V**). Moreover, for the first time cellular components of IgE responses, IgE-secreting plasma cells, and $CD27^+IgE^+$ and $CD27^-IgE^+$ memory B cells, were identified and assigned to the distinct maturation pathways (**Chapter VI**).

Regulation of Ig locus contraction: implications for the B-cell repertoire

Murine precursor B cells undergo Ig loci contraction prior to rearrangements in the bone marrow.[1-3] This contraction ensures a close spatial proximity between genomically distant V, (D) and J genes, thereby enabling their random pairing during V(D)J recombination to generate a broad B-cell antigen receptor (BCR) repertoire. In **Chapter II** of this thesis, it was shown that the human *IGH* locus undergoes similar contraction in human pro-B cells when it is poised to rearrange. Multiple proteins have been identified to be implicated in the *IGH* locus contraction, and control this process at different levels, such as formation of multi-loop

chromatin subcompartments, contraction of Ig loci, and formation of a synapse between two rearrangeable elements. Among these proteins are B-cell specific transcription factors, such as E2A, EBF, and Pax5,[1,3-5] but also Rag proteins,[6] ubiquitously expressed YY1,[7] cohesins and CTCF.[8-10] Still, it remains unclear how these factors act together and which of these are directly involved in the regulation of the *IGH* conformation. The role of candidate proteins in the Ig loci contraction can be studied by siRNA-mediated knockdown of these proteins in the developing B cells, followed by analysis of the spatial proximity between V, (D) and J genes using 3D fluorescent in situ hybridization.

The random pairing between V, (D), and J genes seems to be hampered early in the ontogeny. B cells isolated from fetal liver, fetal bone marrow and umbilical cord blood display a restricted Ig repertoire with dominant usage of DJ-proximal V genes in *IGH* rearrangements.[11-12] Moreover, these cells have short IGH-CDR3 regions with limited numbers of N-nucleotides (**Chapter II**),[13] which can result in altered recognition of antigens.[14] Since human precursor B cells from umbilical cord blood, and potentially fetal bone marrow, can be used in hematopoietic stem cell transplantations (reviewed in [15]), it is crucial to understand whether they can reconstitute a broad postnatally immunocompetent repertoire in adults.

In addition to intrinsic factors (expression of protein regulating Ig loci contraction), B-cell repertoire formation can be modulated by environmental factors (e.g. production of cytokines by stromal cells). It has been reported that B cells developing from lymphoid progenitors seeding the thymus, have a restricted B-cell repertoire, with increased usage of J-proximal V genes, similar to B cells in fetal development.[16-18] In mice the development of these cells seems to be blocked due to low IL-7 production by thymic stroma.[19] If impaired fetal B-cell development is mainly due to immaturity of the stromal cells, they could still generate a broad immunocompetent repertoire in the environment of adult stroma upon transplantation.

IL-7/IL-7R signaling in human B-cell development: directions for further studies
IL-7/IL-7R signaling is crucial for murine precursor B-cell proliferation and survival,[20-22] suppression of *IGK* gene rearrangements prior to complete *IGH* rearrangements,[23] and controlling chromatin accessibility at the *IGH* locus via induction of histone acetylation at distal V genes.[24-27] Still, the importance of IL-7R signaling in man remains unclear, because it is redundant for the generation of circulating mature B cells.[28-30] The work presented in this thesis demonstrated that in the absence of IL-7R signaling, human precursor B cells rearrange their Ig light chains regardless of the presence of a functional IgH. (**Chapter II**). Thus, in both man and mouse IL-7/IL-7R signaling has a non-redundant function to suppress premature Ig light chain rearrangements.

IL-7R is composed of two subunits: common γ chain and IL-7Rα. Patients with genetic defects in genes encoding these subunits (IL2RG, IL-7RA) lack T cells and NK cells, but have normal numbers of circulating B cells.[28-30] Still, the function of these B cells seems defective, [31] and the defects cannot be simply explained by the lack of normal T-cell/B-cell interactions. In a recent publication, Recher *et al*. demonstrated that IL-21 is the primary common γ chain-binding cytokine required for human B-cell differentiation, and in *in vitro* cultures IL2RG-deficient B cells fail to proliferate and differentiate in response to CD40/IL-21 stimulation.[32] Still, additional B-cell defects in IL2RG-deficient patients can be related to the role of IL-7/IL-7R signaling. Premature Ig light chain rearrangements in the absence

VII

of a functional IgH *in vivo* can lead to increased B-cell death, limited B-cell repertoire in the periphery, and consequently to, impaired B-cell responses.

The role of IL-7/IL-7R signaling in the generation of a diverse Ig repertoire can be studied in patients with IL2RG or IL-7RA-deficiency. Specifically, the comparison between these two deficiencies will be interesting, because common γ chain is involved in signaling pathways of multiple cytokines, while IL-7Rα recognizes TSLP independent of IL2RG. Furthermore, deficiency in the JAK3, which signals downstream common γ chain, can result in a similar phenotype to IL2RG deficiency. Still, patients with mutation in JAK3 selectively hampering IL-7 signaling have been described,[30] and these would be of a special interest for studies on the role of IL-7R-signaling in man.

Distinct maturation pathways trigger a universal memory B-cell transcription profile
Multiple phenotypically distinct memory B-cell subsets have been identified in humans. The studies presented in **Chapters III and VI** of this thesis distinguished 8 memory B-cell subsets based on differential expression of CD27 and IgH isotypes. Subsequent molecular characterization of their replication history, Ig somatic hypermutation, and class-switch profiles demonstrated that these subsets originate from 3 different maturation pathways: (1) primary and consecutive germinal center responses ($CD27^+IgM^+$, $CD27^-IgG^+$ and $CD27^+IgE^+$ B cells, and $CD27^+IgA^+$ and $CD27^+IgG^+$ B cells, respectively), (2) systemic germinal center-independent responses in the marginal zone of spleen ($CD27^+IgM^+IgD^+$ B cells), and local germinal center independent responses ($CD27^-IgA^+$ and $CD27^-IgE^+$ B cells; Figure 1). Still, irrespective of their distinct origins, IgM^+, IgA^+, IgG^+ memory B cell showed similar upregulation of co-stimulatory molecules and downregulation of BCR-signaling inhibitors (**Chapter V**). However, it remains unclear, whether and to what extent, different memory B-cell maturation pathways influence the function and reactivity of individual cells.

The memory B-cell repertoire is shaped by the encounter of individual naive B cells with their cognate antigen. Therefore, responses in anatomical locations such as the mucous membrane, local tissue or spleen can exert different selection pressure than systemic immune responses in lymph nodes. Still, recently, Wu *et al*. performed large-scale *IGH* repertoire analysis in naive and memory B-cell subsets, and demonstrated highly comparable Ig gene usage in $CD27^+$ and $CD27^-$ class-switched memory B cells. Thus, the *IGH* repertoire seemed to reflect the similarity of transcription profiles in these cells rather than their origin from different maturation pathways.[33] However, this study was limited by the lack of separation between IgG^+ and IgA^+ cells, and the lack of Ig light chain analysis. Indeed, the studies presented in this thesis revealed that IgA^+ memory cells from local TI responses differed from IgA^+ cells from TD responses mainly with respect to the *IGL* repertoire, and an increased frequency of polyreactive Igs (**Chapter V**). Since so far, no major differences have been observed in the transcription profiles and *IGH* repertoires in IgG^+ and IgA^+ cells, additional studies on differentially expressed genes and reactivity patterns of IgG^+ cells should contribute to better understanding of their physiological functions.

Gene expression profiles in IgM^+ memory B cells differed from class-switched subsets, and more resembled naive B cells (**Chapter VI**). This distinctiveness of IgM B-cell memory was also demonstrated by the analysis of their *IGH* repertoires,[33-34] and reactivity patterns[35] which were clearly different than in class-switched B cells (**Chapter V**).[36] All of these imply
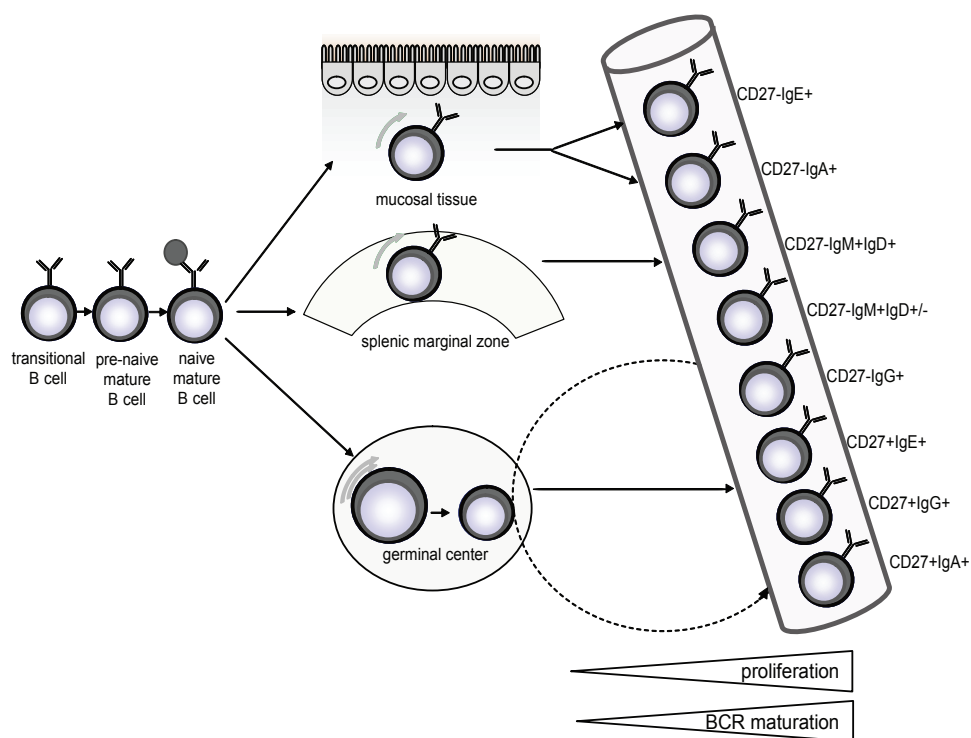
Figure 1. B-cell maturation pathways.
Naive mature B cells can undergo T cell–independent (TI) or T cell–dependent (TD) immune responses. TI responses occur locally in the mucosal tissue or systemically in the splenic marginal zone, and are characterized by low proliferation and SHM levels as compared with TD responses in germinal ceter structures. Secondary responses induce further proliferation and SHM. Despite distinct levels of BCR maturation, all memory B cells display selection against inherently autoreactive *IGHV4–34* genes and long IGH-CDR3 regions.

that IgM[+] memory B cells are derived from unique, but rather primitive immune responses, which is consistent with the fact that IgM is the first immunoglobulin to arise during the primary immune response.

The similarity between CD27^{+}IgM^{+}IgD^{+} and CD27^{+}IgM^{+}IgD^{-} cells can imply that despite their distinct origins both subsets are involved in responses against similar antigens. Still, so far, the only specific reactivity assigned to IgM^{+} memory B cells is against capsular polysaccharides,[37] and it is unclear whether it applies to both subsets or only to CD27^{+}IgM^{+}IgD^{+} cells. Alternatively, the similarity between IgM^{+} memory B-cell subsets may be related to the fact that part of the circulating CD27^{+}IgM^{+}IgD^{+} subsets is derived from TD responses.

How to dissect CD27^{+}IgM^{+}IgD^{+} cells from different origins
Limited replication history of CD27^{+}IgM^{+}IgD^{+} cells as compared to germinal center B cells, and their presence in CD40L-deficient patients (**Chapter III**)[38-39] trace back their origin to TI responses in the marginal zone of spleen. However, the CD27^{+}IgM^{+}IgD^{+} subset is reduced in numbers in CD40L-deficiency as compared to healthy age-matched controls and therefore

VII

is believed to partially originate from TD response (**Chapter III**).[38-39] Moreover, in healthy donors CD27+IgM+IgD+ B cells can carry mutations in the *BCL6* gene, which is mutated during germinal center reaction.[40] Still, so far, no cell surface markers have been identified to distinguish between CD27+IgM+IgD+ cells from different origins, and it remains one of the main struggles of the current memory B-cell research. Identification of such markers would not only contribute to the basic knowledge about the process of the memory B-cell formation, but could also contribute to the monitoring of the function of splenic marginal zone.

Two potential markers to discriminate between TD and TI origins of CD27+IgD+IgM+ cells were identified during immunophenotyping of the expanded population in persistent polyclonal B-cell lymphocytosis (PPBL; **Chapter IV**). Expression of CD62L and CD73 was low on CD27+IgD+IgM+ cells in PPBL, but bimodal in healthy controls. Based on this, it is tempting to hypothesize that CD62L and CD73 define two distinct subpopulations in health, only one of which is expanded in PPBL patients. It is also possible that CD27+IgM+IgD+ cells derived from TD and TI responses cannot be described by an individual marker, but rather by a combination of multiple markers. These additional markers could be revealed by comparative gene expression profiling of CD27+IgM+IgD+ cells in patients with defect in TD and TI memory B-cell responses.

CD27+IgM+IgD+ cells from TI responses in spleen are absent in patients with congenital or acquired asplenia. It has been demonstrated that splenectomized patients present with a gradual loss of IgM+ memory B cells,[41] which stabilizes after 6 months, and have impaired immune responses against capsular polysaccharides.[42-43] On the contrary, CD40 and CD40L-deficient patients, have only CD27+IgD+IgM+ cells derived from TI responses. Thus, cell surface markers differentially expressed between CD27+IgM+IgD+ cells in these two models could be used to dissect cell from different origins in healthy individuals. These different origins should be confirmed by analysis of their replication history, somatic hypermutations (SHM) in the Ig genes, and mutations in *BCL6*.

Recently, Griffin *et al*.[44] claimed to identify a human counterpart of murine B1 cells. These cells were defined as CD20+CD27+CD43+, carried mutated Ig genes and were capable of spontaneous IgM production. The relatively high frequency of these cells (20-80% of CD20+CD27+ cells) suggested that they should constitute a major part of the CD27+IgD+IgM+ subset. Still, later publications pointed at multiple sources of contamination in this study.[45-46] The majority of CD20+CD27+CD43+ cells defined by Griffin *et al*. seemed to be B-T cell doublets co-expressing CD3, and a substantial fraction of the remaining B cells expressed CD38, which is a marker of plasma cells.[45-46] Consequently, on average CD27+CD43+ cells constitute <1% of total B cells. Thus, if human B1 cells exist, their contribution to the CD27+IgM+IgD+ B-cell subset is minor.

Reactivity of IgA B-cell memory and beyond

IgA is the most abundantly produced Ig in man. Only part of this IgA production occurs systemically, whereas the majority is generated locally in mucous membranes. IgA+ memory B cells derived from both systemic and local responses can be identified in blood. As demonstrated in **Chapter III**, CD27+IgA+ cells present with high replication history and SHM levels, reminiscent of their germinal center origin from systemic responses, while CD27-IgA+ cells with limited replication history, increased IgA2 and Igλ usage seem derived from local

TI responses in the *lamina propria* of gut. The different origins of these two IgA^{+} memory B-cell subsets are further reflected by their distinct reactivity patterns (**Chapter V**). CD27^{-}IgA^{+} cells show higher frequency of polyreactive clones, and more aspecific interactions with bacteria, as compared to CD27^{+}IgA^{+} cells. Still, the frequency of cells with unidentified BCR reactivity in both IgA^{+} memory B-cell subsets and in previously described intestinal plasmablasts remains high.[47] Thus, identification of the full IgA reactivity spectrum would require additional studies.

Thousands of human commensal[48] and pathogenic bacteria strains have been identified so far. Although ELISA-based assays or recently developed live bacterial FACS are convenient techniques to determine Ig reactivity against individual bacteria strains,[47,49-50] they are difficult to apply in a large-scale screening. Therefore, alternatively IgA reactivity could be tested not against individual bacteria species, but against their common structural groups. The cell wall of Gram-positive and Gram-negative bacteria contains peptidoglycan, a polymer in which short peptides are cross-linked with polysaccharides.[51] These surface polysaccharides are more diverse and considerably different than in human,[52] and often contain antigenic determinants that trigger an immunogenic response.[53] The reactivity of human IgA against bacterial glycans can be tested using glycan arrays, which contain various immobilized oligosaccharides and/or polysaccharides (reviewed in [54]). Since certain glycans are specific for selective bacterial groups, these analyses can also provide some indication about the recognized bacterial species.[52] An analogical approach can be used to identify antibodies specifically recognizing bacterial peptides. It has been previously demonstrated that the bacterial proteome is clearly different from these in human,[55] and peptide arrays designed for certain bacteria species are already in development.

Several unresolved issues remain for subsequent studies on IgA B-cell memory. Although based on their origin from TD responses, CD27^{+}IgA^{+} cells are expected to mainly recognize peptide antigens, and TI CD27^{-}IgA^{+} cells could display non-peptide reactivity, this requires further investigation. Another open question is whether there is a difference in the IgA responses to virulent and non-virulent strains of the same bacteria species. Possibly, virulent strains are the ones which cannot be successfully removed in the local responses and trigger responses at the systemic level. Finally, it remains unknown whether increased occurrence of IgA2 in the lower gastrointestinal tract is associated with its particular reactivity or is solely caused by its increased resistance against digestion by bacterial proteases in this environment.[56]

The knowledge about IgA B-cell memory can be applied to studies on the mechanisms of inflammatory bowel disease (IBD). IBD is associated with diverse defects in the innate immune system (reviewed in [57]), and patients present with increased systemic antibody responses to the components of commensal microflora,[49] suggestive of defects in local IgA responses.

Controversies over IgG^{+} B-cell memory

One of the first studies describing CD27^{-}IgG^{+} cells reported their increased frequency in systemic lupus erythematosus (SLE).[58-59] Although the work presented in this thesis largely contributed to unraveling the origin of CD27^{-}IgG^{+} subset in health (**Chapter III**), its involvement in the autoimmunity remains unknown. In a recent study, Tiller *et al*.

VII

demonstrated that in healthy adults >40% of IgG^{+} cells can recognize autoantigens.[36] Still, it is unclear, why these autoreactive Igs do not lead to disease development. One of the potential explanations could lie in the Ig subclass usage. Approximately 50% of CD27^{+}IgG^{+} cells utilize IgG2 and IgG4 (**Chapter III**), which in contrast to IgG1 and IgG3, cannot efficiently activate complement to induce antibody-dependent cell-mediated cytotoxicity.[60] Thus, autoreactive IgG2 and IgG4 could be less harmful than autoreactive IgG1 or IgG3. In contrast to CD27^{+}IgG^{+} cells, CD27^{-}IgG^{+} cells almost exclusively utilize IgG1 or IgG3. Still, nothing is known about the frequency of autoreactive cells in this subset.

IgG2 (and IgG4) transcripts contained higher SHM levels than IgG1 and IgG3 transcripts, suggesting that at least partially these cells are derived from consecutive immune responses (**Chapter III**). This origin seems to be supported by the increased IgG2 levels observed after secondary as compared to primary immunization,[61] and increased IgG2 responses in elderly people.[62] Still, in a recent study Wu *et al*. demonstrated that the repertoire of IgG2^{+} cells shares common features with these in IgM^{+} cells, and suggested that both types of cells can respond to TI antigens.[33] This issue could be also addressed by the studies on the reactivity of IgG subclasses.

IgE^{+} B cells – from identification to application

The prevalence of IgE-mediated diseases increases worldwide.[63] Still, IgE-expressing B cells are scarce and until recently remained undetectable in man.[64] In studies presented in **Chapter VI**, a novel flow cytometric approach was implemented to reliably identify IgE^{+} plasma cells and two IgE[+] memory B-cells subsets. Detailed molecular characterization of these cells revealed germinal center-dependent origins of IgE^{+} tonsil plasma cells and CD27^{+}IgE^{+} memory B cells. In contrast, CD27^{-}IgE^{+} memory B cells showed fewer SHM and limited proliferation, and were present in patients who lacked functional germinal centers. Moreover, patients with atopic dermatitis showed increased frequencies of CD27^{-}IgE^{+}, but not CD27^{+}IgE^{+} memory B cells. This studies opened new possibilities to study the pathogenesis of IgE-mediated diseases in man, and can contribute to accurate monitoring of anti-IgE treatment in patients with severe allergic reactions.

Majority of the IgE-mediated diseases has a local manifestation with immune response to allergen developing in skin, mucous membranes, lung or gastrointestinal tract. This could suggest that their development is associated with increased formation of CD27^{-}IgE^{+} memory B cells. If this association is confirmed by additional studies, the levels of circulating CD27^{-}IgE^{+} memory B cells can be used as a marker of ongoing local allergic reaction.

Interestingly, under certain physiological conditions, the same allergens, which can cause local immune responses, lead to a systemic response in a form of an anaphylactic shock. It has been estimated that the lifetime prevalence of anaphylaxis from diverse triggers is as high as 0.05% to 2%.[65] Still, the mechanisms discriminating between the development of local and systemic IgE responses are poorly understood. Based on the model presented in this thesis, it is tempting to speculate that systemic IgE-mediated responses occur in case of insufficient local responses, and lead to formation of CD27^{+}IgE^{+} memory B cells. This would be in analogy to what is observed for IgA^{+} cells in responses to commensal microorganisms: once the local response is impaired, commensal bacteria-specific IgA is produced systematically.[66] If this hypothesis is confirmed, the level of CD27^{+}IgE^{+} cells can be used in monitoring of

patients prone to development of anaphylactic reactions.

It remains unclear why certain individuals are more prone to develop allergy than others. The process of class-switching is driven by cytokines with IL-4 and IL-13 being important for switching to IgE.[67-70] Thus, increased class-switching towards IgE could be caused by elevated levels of these cytokines in the environment, and/or increased expression of cytokine receptors on B cells. Microarray analysis revealed that *IL4R* was expressed in all B-cell subsets (with higher expression on naive cells), whereas *IL13RA* expression was low on naive and IgM[+] memory B cells, intermediate on IgA[+] memory B cells, and the highest on IgG[+] memory B cells (**Chapter V**). The majority of IgE[+] memory B cells is generated directly from naive mature cells, as demonstrated by their SHM levels and the low frequencies of hybrid Sμ-Sε switch regions that contain Sγ remnants (**Chapter VI**). Therefore, IL-13R expression on naive B cells could be a limiting factor for class-switching towards IgE in health.[71]

Therapy of IgE-mediated diseases includes desensitization with specific immunotherapy (SIT) (reviewed in [72]) and omalizumab treatment.[73] Desensitization therapy involves exposure of the patient to gradually increasing doses of allergen, which results in generation of IgG4 ather than IgE responses. Thus, the ratio between antigen-specific IgG4^{+} and IgE^{+} B cells could be used as a measure of therapy efficacy.

Omalizumab neutralizes IgE by blocking its receptor-binding site.[73] While many patients respond well to the treatment, it is ineffective in approximately 40% of cases.[74] Thus, identification of markers which could predict outcome of the therapy, seems crucial to minimize its costs. Even though omalizumab–bound serum IgE cannot be easily measured, several studies reported persistently low IgE serum levels following omalizumab treatment cessation. This suggests that the production of IgE has been halted by the treatment and that targeting of IgE[+] memory B cells and plasma cells might be the main reason for therapy success.[75-76] A novel anti-IgE antibody has been generated that only targets membrane IgE on IgE-expressing cells.[77] This antibody does not bind serum IgE or IgE bound to Fc receptors and potentially targets IgE-expressing B cells more effectively than omalizumab. Thus, analysis of IgE[+] memory B-cell levels can be used to monitor the effectiveness of anti-IgE treatment in severe allergic patients.

Concluding remarks

Diversification of the B-cell antigen receptor in bone marrow results in the formation of a broad B-cell repertoire. In the peripheral lymphoid system, this repertoire is further shaped upon antigen encounter to generate immunological memory (Figure 2). Since the diverse tissue environments and types of antigens support B-cell responses differently, memory B cells vary in their replication history, effector functions, reactivity patterns and phenotypes. Multiple immunological diseases are associated with aberrant responses to certain types of antigens. Thus, the knowledge about the origins of memory B cells can result in dissection of individual subsets mediating the pathology in these diseases. Consequently, these subsets can become targets for a therapy. Moreover, since memory B-cell subsets are circulating in blood, analysis of their levels can be used to monitor the treatment efficacy.
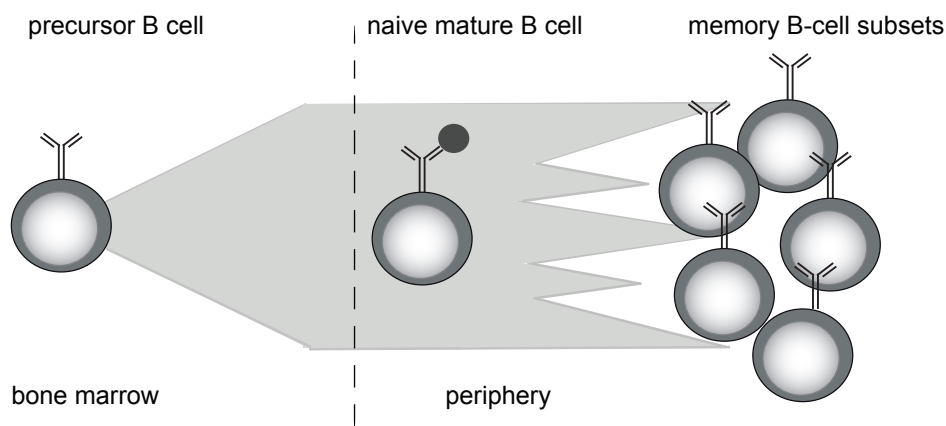
VII

Figure 2. Generation of an immunocompetent B-cell repertoire.
Human precursor B cells in the bone marrow rearrange their Ig genes to create a broad naive B-cell repertoire. Of all the naive B cells in the peripheral lymphoid system, only these which recognize antigen can futher specifiy to form immunological memory. Memory B cells generated in response to various types of antigens form subsets, with different phenotypes, molecular features and reactivity patterns.

REFERENCES

1.   Sayegh C, Jhunjhunwala S, Riblet R, Murre C. Visualization of looping involving the immunoglobulin heavy-chain locus in developing B cells. *Genes Dev*. 2005;19:322-327.
2.   Roldan E, Fuxa M, Chong W, et al. Locus 'decontraction' and centromeric recruitment contribute to allelic exclusion of the immunoglobulin heavy-chain gene. *Nat Immunol*. 2005;6:31-41.
3.   Fuxa M, Skok J, Souabni A, Salvagiotto G, Roldan E, Busslinger M. Pax5 induces V-to-DJ rearrangements and locus contraction of the immunoglobulin heavy-chain gene. *Genes Dev*. 2004;18:411-422.
4.   Bain G, Maandag EC, Izon DJ, et al. E2A proteins are required for proper B cell development and initiation of immunoglobulin gene rearrangements. *Cell*. 1994;79:885-892.
5.   Lin H, Grosschedl R. Failure of B-cell differentiation in mice lacking the transcription factor EBF. *Nature*. 1995;376:263-267.
6.   Hewitt SL, Yin B, Ji Y, et al. RAG-1 and ATM coordinate monoallelic recombination and nuclear positioning of immunoglobulin loci. *Nat Immunol*. 2009;10:655-664.
7.   Liu H, Schmidt-Supprian M, Shi Y, et al. Yin Yang 1 is a critical regulator of B-cell development. *Genes Dev*. 2007;21:1179-1189.
8.   Degner SC, Verma-Gaur J, Wong TP, et al. CCCTC-binding factor (CTCF) and cohesin influence the genomic architecture of the Igh locus and antisense transcription in pro-B cells. *Proc Natl Acad Sci U S A*. 2011;108:9566-9571.
9.   Degner SC, Wong TP, Jankevicius G, Feeney AJ. Cutting edge: developmental stage-specific recruitment of cohesin to CTCF sites throughout immunoglobulin loci during B lymphocyte development. *J Immunol*. 2009;182:44-48.
10. Hou C, Dale R, Dean A. Cell type specificity of chromatin organization mediated by CTCF and cohesin. *Proc Natl Acad Sci U S A*. 2010;107:3651-3656.
11. Cuisinier AM, Guigou V, Boubli L, Fougereau M, Tonnelle C. Preferential expression of VH5 and VH6 immunoglobulin genes in early human B-cell ontogeny. *Scand J Immunol*. 1989;30:493-497.
12. Van Es JH, Raaphorst FM, van Tol MJ, Meyling FH, Logtenberg T. Expression pattern of the most JH-proximal human VH gene segment (VH6) in the B cell and antibody repertoire suggests a role of VH6-encoded IgM antibodies in early ontogeny. *J Immunol*. 1993;150:161-168.

13. Schroeder HW, Jr., Zhang L, Philips JB, 3rd. Slow, programmed maturation of the immunoglobulin HCDR3 repertoire during the third trimester of fetal life. *Blood*. 2001;98:2745-2751.

14. Schelonka RL, Ivanov, II, Vale AM, Dimmitt RA, Khaled M, Schroeder HW, Jr. Absence of N addition facilitates B cell development, but impairs immune responses. *Immunogenetics*. 2011;63:599-609.

15. Gluckman E, Rocha V. Cord blood transplantation: state of the art. *Haematologica*. 2009;94:451-454.

16. Dunn-Walters DK, Howe CJ, Isaacson PG, Spencer J. Location and sequence of rearranged immunoglobulin genes in human thymus. *Eur J Immunol*. 1995;25:513-519.

17. Akashi K, Richie LI, Miyamoto T, Carr WH, Weissman IL. B lymphopoiesis in the thymus. *J Immunol*. 2000;164:5221-5226.

18. Weerkamp F, Baert MR, Brugman MH, et al. Human thymus contains multipotent progenitors with T/B lymphoid, myeloid, and erythroid lineage potential. *Blood*. 2006;107:3131-3137.

19. Hashimoto Y, Montecino-Rodriguez E, Leathers H, Stephan RP, Dorshkind K. B-cell development in the thymus is limited by inhibitory signals from the thymic microenvironment. *Blood*. 2002;100:3504-3511.

20. Namen AE, Lupton S, Hjerrild K, et al. Stimulation of B-cell progenitors by cloned murine interleukin-7. *Nature*. 1988;333:571-573.

21. Goodwin RG, Lupton S, Schmierer A, et al. Human interleukin 7: molecular cloning and growth factor activity on human and murine B-lineage cells. *Proc Natl Acad Sci U S A*. 1989;86:302-306.

22. Lee G, Namen AE, Gillis S, Kincade PW. Recombinant interleukin-7 supports the growth of normal B lymphocyte precursors. *Curr Top Microbiol Immunol*. 1988;141:16-18.

23. Malin S, McManus S, Cobaleda C, et al. Role of STAT5 in controlling cell survival and immunoglobulin gene recombination during pro-B cell development. *Nat Immunol*. 2010;11:171-179.

24. Corcoran AE, Riddell A, Krooshoop D, Venkitaraman AR. Impaired immunoglobulin gene rearrangement in mice lacking the IL-7 receptor. *Nature*. 1998;391:904-907.

25. Bertolino E, Reddy K, Medina KL, Parganas E, Ihle J, Singh H. Regulation of interleukin 7-dependent immunoglobulin heavy-chain variable gene rearrangements by transcription factor STAT5. *Nat Immunol*. 2005;6:836-843.

26. Stanton ML, Brodeur PH. Stat5 mediates the IL-7-induced accessibility of a representative D-Distal VH gene. *J Immunol*. 2005;174:3164-3168.

27. Chowdhury D, Sen R. Stepwise activation of the immunoglobulin mu heavy chain gene locus. *Embo J*. 2001;20:6394-6403.

28. Buckley RH. Molecular defects in human severe combined immunodeficiency and approaches to immune reconstitution. *Annu Rev Immunol*. 2004;22:625-655.

29. Giliani S, Mori L, de Saint Basile G, et al. Interleukin-7 receptor alpha (IL-7Ralpha) deficiency: cellular and molecular bases. Analysis of clinical, immunological, and molecular features in 16 novel patients. *Immunol Rev*. 2005;203:110-126.

30. Li J, Nara H, Rahman M, Juliana FM, Araki A, Asao H. Impaired IL-7 signaling may explain a case of atypical JAK3-SCID. *Cytokine*. 2010;49:221-228.

31. Railey MD, Lokhnygina Y, Buckley RH. Long-term clinical outcome of patients with severe combined immunodeficiency who received related donor bone marrow transplants without pretransplant chemotherapy or post-transplant GVHD prophylaxis. *J Pediatr*. 2009;155:834-840 e831.

32. Recher M, Berglund LJ, Avery DT, et al. IL-21 is the primary common gamma chain-binding cytokine required for human B-cell differentiation in vivo. *Blood*. 2011;118:6824-6835.

33. Wu YC, Kipling D, Dunn-Walters DK. The relationship between CD27 negative and positive B cell populations in human peripheral blood. *Front Immunol*. 2011;2:81.

34. Wu YC, Kipling D, Leong HS, Martin V, Ademokun AA, Dunn-Walters DK. High-throughput immunoglobulin repertoire analysis distinguishes between human IgM memory and switched memory B-cell populations. *Blood*. 2010;116:1070-1078.

35. Tsuiji M, Yurasov S, Velinzon K, Thomas S, Nussenzweig MC, Wardemann H. A checkpoint for autoreactivity in human IgM+ memory B cell development. *J Exp Med*. 2006;203:393-400.

36. Tiller T, Tsuiji M, Yurasov S, Velinzon K, Nussenzweig MC, Wardemann H. Autoreactivity in human IgG+ memory B cells. *Immunity*. 2007;26:205-213.

37. Moens L, Wuyts M, Meyts I, De Boeck K, Bossuyt X. Human memory B lymphocyte subsets fulfill distinct roles in the anti-polysaccharide and anti-protein immune response. *J Immunol*. 2008;181:5306-5312.

VII

38. Weller S, Faili A, Garcia C, et al. CD40-CD40L independent Ig gene hypermutation suggests a second B cell diversification pathway in humans. *Proc Natl Acad Sci U S A*. 2001;98:1166-1170.

39. Weller S, Braun MC, Tan BK, et al. Human blood IgM "memory" B cells are circulating splenic marginal zone B cells harboring a prediversified immunoglobulin repertoire. *Blood*. 2004;104:3647-3654.

40. Seifert M, Kuppers R. Molecular footprints of a germinal center derivation of human IgM+(IgD+)CD27+ B cells and the dynamics of memory B cell generation. *J Exp Med*. 2009;206:2659-2669.

41. Cameron PU, Jones P, Gorniak M, et al. Splenectomy associated changes in IgM memory B cells in an adult spleen registry cohort. *PLoS One*. 2011;6:e23164.

42. Hosea SW, Burch CG, Brown EJ, Berg RA, Frank MM. Impaired immune response of splenectomised patients to polyvalent pneumococcal vaccine. *Lancet.* 1981;1:804-807.

43. Giebink GS, Le CT, Schiffman G. Decline of serum antibody in splenectomized children after vaccination with pneumococcal capsular polysaccharides. *J Pediatr*. 1984;105:576-582.

44. Griffin DO, Holodick NE, Rothstein TL. Human B1 cells in umbilical cord and adult peripheral blood express the novel phenotype CD20+ CD27+ CD43+ CD70. J Exp Med. 2011;208:67-80.

45. Descatoire M, Weill JC, Reynaud CA, Weller S. A human equivalent of mouse B-1 cells? *J Exp Med*. 2011;208:2563-2564

46. Perez-Andres M, Grosserichter-Wagener C, Teodosio C, van Dongen JJ, Orfao A, van Zelm MC. The nature of circulating CD27+CD43+ B cells. *J Exp Med*. 2011;208:2565-2566

47. Benckert J, Schmolka N, Kreschel C, et al. The majority of intestinal IgA+ and IgG+ plasmablasts in the human gut are antigen-specific. *J Clin Invest*. 2011;121:1946-1955.

48. Arumugam M, Raes J, Pelletier E, et al. Enterotypes of the human gut microbiome. *Nature*. 2011;473:174-180.

49. Haas A, Zimmermann K, Graw F, et al. Systemic antibody responses to gut commensal bacteria during chronic HIV-1 infection. *Gut*. 2011;60:1506-1519.

50. Slack E, Hapfelmeier S, Stecher B, et al. Innate and adaptive immunity cooperate flexibly to maintain host-microbiota mutualism. *Science*. 2009;325:617-620.

51. Vollmer W, Blanot D, de Pedro MA. Peptidoglycan structure and architecture. *FEMS Microbiol Rev.* 2008;32:149-167.

52. Herget S, Toukach PV, Ranzinger R, Hull WE, Knirel YA, von der Lieth CW. Statistical analysis of the Bacterial Carbohydrate Structure Data Base (BCSDB): characteristics and diversity of bacterial carbohydrates in comparison with mammalian glycans. *BMC Struct Biol*. 2008;8:35.

53. Zheng LL, Li YX, Ding J, et al. A comparison of computational methods for identifying virulence factors. *PLoS One*. 2012;7:e42517.

54. Oyelaran O, Gildersleeve JC. Glycan arrays: recent advances and future challenges. *Curr Opin Chem Biol*. 2009;13:406-413.

55. Trost B, Pajon R, Jayaprakash T, Kusalik A. Comparing the similarity of different groups of bacteria to the human proteome. *PLoS One*. 2012;7:e34007.

56. Plaut AG, Wistar R, Jr., Capra JD. Differential susceptibility of human IgA immunoglobulins to streptococcal IgA protease. *J Clin Invest*. 1974;54:1295-1300.

57. Gersemann M, Wehkamp J, Stange EF. Innate immune dysfunction in inflammatory bowel disease. *J Intern Med*. 2012;271:421-428.

58. Wei C, Anolik J, Cappione A, et al. A new population of cells lacking expression of CD27 represents a notable component of the B cell memory compartment in systemic lupus erythematosus. *J Immunol*. 2007;178:6624-6633.

59. Fecteau JF, Cote G, Neron S. A new memory CD27-IgG+ B cell population in peripheral blood expressing VH genes with low frequency of somatic mutation. *J Immunol.* 2006;177:3728-3736.

60. Bruggemann M, Williams GT, Bindon CI, et al. Comparison of the effector functions of human immunoglobulins using a matched set of chimeric antibodies. *J Exp Med.* 1987;166:1351-1361.

61. de Voer RM, van der Klis FR, Engels CW, et al. Kinetics of antibody responses after primary immunization with meningococcal serogroup C conjugate vaccine or secondary immunization with either conjugate or polysaccharide vaccine in adults. *Vaccine*. 2009;27:6974-6982.

62. Wu YC, Kipling D, Dunn-Walters DK. Age-Related Changes in Human Peripheral Blood IGH Repertoire Following Vaccination. *Front Immunol*. 2012;3:193.

63. Pawankar R, Canonica G, Holgate S, Lockey R. WAO White Book on Allergy 2011-2012: Executive Summary.

2011.

64. Stone KD, Prussin C, Metcalfe DD. IgE, mast cells, basophils, and eosinophils. *J Allergy Clin Immunol*. 2010;125:S73-80.

65. Lieberman P, Camargo CA, Jr., Bohlke K, et al. Epidemiology of anaphylaxis: findings of the American College of Allergy, Asthma and Immunology Epidemiology of Anaphylaxis Working Group. *Ann Allergy Asthma Immunol*. 2006;97:596-602.

66. Macpherson AJ, Geuking MB, Slack E, Hapfelmeier S, McCoy KD. The habitat, double life, citizenship, and forgetfulness of IgA. *Immunol Rev*. 2012;245:132-146.

67. Cocks BG, de Waal Malefyt R, Galizzi JP, de Vries JE, Aversa G. IL-13 induces proliferation and differentiation of human B cells activated by the CD40 ligand. *Int Immunol*. 1993;5:657-663.

68. Gascan H, Gauchat JF, de Waal Malefyt R, Schneider P, Yssel H, de Vries JE. Regulation of human IgE synthesis. *Clin Exp Allergy*. 1991;21 Suppl 1:162-166.

69. Gascan H, Gauchat JF, Roncarolo MG, Yssel H, Spits H, de Vries JE. Human B cell clones can be induced to proliferate and to switch to IgE and IgG4 synthesis by interleukin 4 and a signal provided by activated CD4+ T cell clones. *J Exp Med*. 1991;173:747-750.

70. Punnonen J, Aversa G, Cocks BG, et al. Interleukin 13 induces interleukin 4-independent IgG4 and IgE synthesis and CD23 expression by human B cells. *Proc Natl Acad Sci U S A*. 1993;90:3730-3734.

71. Hajoui O, Zheng H, Guay J, Letuve S, Fawaz LM, Mazer BD. Regulation of IL-13 receptor alpha 1 expression and signaling on human tonsillar B-lymphocyte subsets. *J Allergy Clin Immunol*. 2007;120:1425-1432.

72. Krishna MT, Huissoon AP. Clinical immunology review series: an approach to desensitization. *Clin Exp Immunol*. 2011;163:131-146.

73. Belliveau PP. Omalizumab: a monoclonal anti-IgE antibody. *MedGenMed*. 2005;7:27.

74. Bousquet J, Rabe K, Humbert M, et al. Predicting and evaluating response to omalizumab in patients with severe allergic asthma. *Respir Med*. 2007;101:1483-1492.

75. Lowe PJ, Renard D. Omalizumab decreases IgE production in patients with allergic (IgE-mediated) asthma; PKPD analysis of a biomarker, total IgE. *Br J Clin Pharmacol*. 2011;72:306-320.

76. Lanier BQ. Unanswered questions and warnings involving anti-immunoglobulin E therapy based on 2-year observation of clinical experience. *Allergy Asthma Proc*. 2005;26:435-439.

77. Brightbill HD, Jeet S, Lin Z, et al. Antibodies specific for a segment of human membrane IgE deplete IgE-producing B cells in humanized mice. *J Clin Invest*. 2010;120:2218-2229.

VII

Summary
Samenvatting

SUMMARY

B lymphocytes are critical components of the adaptive immune system. They are generated throughout life from hematopoietic stem cells in bone marrow. B cells differentiate in bone marrow to form a unique B-cell antigen receptor (BCR) by V(D)J recombination of the genes encoding the Ig heavy (IgH) and Ig light chains. This process involves random rearrangement of V, D and J genes independent of antigen. Upon formation of a functional BCR, B cells migrate to the periphery. Because every precursor B cell creates a unique BCR, the total peripheral B-cell pool contains a broad repertoire of antigen receptors.

Circulating naive B cells only start further maturation following antigen encounter. Naive mature B cells that recognize antigens are selected to undergo enormous clonal proliferation and generate a huge number of daughter cells with the potential to recognize the same pathogen. This clonal expansion generates long-lived memory B cells and antibody-producing plasma cells.

Healthy vertebrates are immunocompetent, i.e. they carry an immune system that provides adequate immune responses and subsequent immunity to a broad spectrum of antigens. Immunocompetence requires a tight balance between the production of a large repertoire of cells with unique receptors and a strong immune response of groups of cells with an antigen-specific repertoire. The research described in this thesis was set out to determine how a broad B-cell repertoire is formed in human bone marrow, and how it is specified upon encounter of different types of antigens in the peripheral lymphoid system.

IL-7/IL-7R signaling is crucial for murine precursor B-cell development. Still, it was believed to be redundant for B-cell differentiation in man, because patients with genetic defects in genes encoding IL-7R subunits have normal numbers of circulating B cells. In **Chapter II** we studied Ig gene rearrangements in cultured human B-lineage cells with and without expression of IL-7R. IL-7R$^+$ cells were more blastic than IL7R- cells and their gene expression profile resembled these of pro-B cells and large pre-B cells, while IL-7R$^-$ cells mainly resembled small pre-B cells. Even though pre-B cells should have a functional IgH, in both cultured subsets complete IgH rearrangement were scarce. Interestingly, in contrast to IL-7R$^+$ cells, IL-7R$^-$ cells rearranged Ig light chain genes in the absence of a functional IgH. This implies that in man IL-7/IL-7R signaling has a non-redundant function to suppress premature Ig light chain rearrangements.

Multiple distinct memory B-cell subsets have been identified in humans, but it remained unclear how their phenotypic diversity corresponds to the type of responses from which they originate. Especially the contribution of germinal center-independent responses was controversial. In **Chapter III** we presented the results of a detailed molecular and flow cytometric analysis of 6 memory B-cell subsets defined based on the differential expression of CD27 and IgH isotypes. Replication history and somatic hypermutation (SHM) levels in Ig genes of CD27$^-$IgG$^+$ and CD27$^+$IgM$^+$ cells resembled those of germinal center cells, suggestive of their origin from germinal center responses. Furthermore, the high replication history and SHM levels revealed that CD27$^+$IgA$^+$ and CD27$^+$IgG$^+$ cells are at least partially derived from consecutive germinal center reactions. In contrast, natural effector and CD27$^-$IgA$^+$ memory B cells had limited proliferation and were present in CD40L-deficient patients, reflecting a germinal center-independent origin. Natural effector cells at least in part

originate from systemic T-cell independent responses in the splenic marginal zone. CD27$^-$IgA$^+$ cells share low replication history and dominant Igλ and IgA2 use with gut *lamina propria* IgA$^+$ B cells, suggesting their common origin from local germinal center-independent responses. Thus, we showed that circulating memory B cells originate from 3 distinct maturation pathways: (1) primary and consecutive germinal center-dependent responses, and (2) systemic and (3) local germinal center independent responses. Our findings provide new opportunities to study these processes in immunological diseases.

Persistent polyclonal B-cell lymphocytosis (PPBL) is a rare benign disorder characterized by an expansion of CD27$^+$IgM$^+$IgD$^+$ cells. Despite an increasing number of described cases, the nature of this condition remained poorly understood. In **Chapter IV** we demonstrated that CD27$^+$IgM$^+$IgD$^+$ cells in PPBL are hyperproliferated memory B cells with a broad BCR repertoire that contain limited SHM in Ig genes. PPBL cells could be discriminated from healthy IgM$^+$ memory B cells with a limited set of cell surface markers: IgD, CD38, CD73 and CD62L. Despite heterogenous deregulation of oncogenes, PPBL cells from different patients showed a homogenous immunophenotype, distinct from mature B-cell malignancies. These new insights can prove valuable for diagnosis of PPBL and prognostic classification of patients at risk for developing a lymphoid malignancy.

The vast majority of IgA is produced in mucosal tissue following T-cell dependent and T-cell independent antigen responses. We studied the nature of each of these responses in **Chapter V** by analysis of the gene expression and Ig reactivity profiles of T-cell dependent CD27$^+$IgA$^+$ and T-cell independent CD27$^-$IgA$^+$ circulating memory B cells. We found similar gene expression profiles for both IgA$^+$ and CD27$^+$IgG$^+$ and CD27$^-$IgG$^+$ memory B-cell subsets. Still, CD27$^-$IgA$^+$ B cells showed unique expression of homing receptors and transcription factors, reminiscent of their mucosal origin. CD27$^-$IgA$^+$ memory B cells carried fewer SHM in rearranged Ig genes and showed increased *IGLV3-1* gene use as compared to CD27$^+$IgA$^+$ cells. Furthermore, CD27$^-$IgA$^+$ B cells were enriched in polyreactive antibodies that reacted with high affinity to common bacteria strains. Thus, T-cell independent IgA responses generate B-cell memory, but show a unique reactivity pattern with polyreactive recognition of bacteria.

The prevalence of IgE-mediated diseases increases worldwide. Despite extensive studies, IgE-expressing B cells remained poorly characterized. In **Chapter VI** we developed a reliable flow cytometric strategy to detect and purify IgE$^+$ plasma cells from tonsils and two IgE$^+$ memory B-cell subsets from blood. Detailed molecular characterization revealed germinal center-dependent origins of tonsil plasma cells and CD27$^+$IgE$^+$ memory B cells. The replication history and SHM levels in CD27$^+$IgE$^+$ memory B cells in healthy donors were higher than in germinal center cells, and similar to memory B cells from primary immune responses. However, limited replication history and SHM levels in CD27$^-$IgE$^+$ memory B cells, similar to CD27$^-$IgA$^+$ cells and their presence in CD40L-deficiency suggested their origin from local germinal center-independent responses. Moreover, CD27$^-$IgE$^+$ cells were specifically increased in atopic dermatitis patients. Our study sheds light on the development of IgE$^+$ cells in health, opens new possibilities to study the pathogenesis of IgE-mediated diseases, and can contribute to accurate monitoring of anti-IgE treatment in patients with severe allergic reactions.

Defects in B-cell repertoire can result in impaired B-cell responses and lead to multiple immunological diseases such as immmunodeficiency, autoimmunity, allergy, leukemia and

lymphoma. Thus, understanding of the processes involved in B-cell repertoire formation and shaping seems critical to unravel the mechanisms underlying these diseases. The studies presented in this thesis shed new light on the role of IL-7/IL-7R signaling in the human precursor B-cell development and demonstrated the complexity of human memory B-cell responses. We demonstrated that this knowledge can be applied to unraveling the mechanisms of lymphoproliferative disorders such as PPBL. Furthermore, understanding of the components of an immunocompetent repertoire can contribute to identification of defects in the immunodeficiencies. Dissection of individual B-cell subsets mediating immunological diseases can improve their diagnosing and result in development of new therapeutic approaches.

SAMENVATTING

B cellen spelen een belangrijke rol in het immuunsysteem, omdat ze antistoffen produceren. Gedurende het hele leven worden B cellen gevormd vanuit bloedstamcellen in het beenmerg. Tijdens de ontwikkeling in het beenmerg creëren voorloper B cellen ieder een uniek antistof molecuul, ook wel immunglobuline (Ig) genoemd, dat ze als receptor op het celmembraan tot expressie brengen. Deze Ig's zijn in staat om specifieke structuren op een pathogeen te herkennen, een specifiek antigeen. Het Ig, bestaande uit twee identieke zware eiwitketens (IgH) en twee identieke lichte eiwitketens (Igκ of Igλ), wordt gevormd door middel van relatief willekeurige herschikking van de DNA segmenten die coderen voor deze Ig's: 'variable' (V), 'diversity' (D) en 'joining' (J) gensegmenten. Dit proces wordt ook wel V(D)J recombinatie genoemd en gebeurt volledig onafhankelijk van antigenen aanwezig in de omgeving. Zodra een voorloper B cel een functioneel Ig heeft gevormd, migreert deze naar de bloedbaan waar de B cel gaat circuleren tussen verschillende lymfoïde organen, zoals de milt en lymfeklieren, op zoek naar antigeen. Aangezien elke B cel een uniek Ig creëert, bevat het menselijk lichaam een breed repertoire aan Ig's en kan hierdoor bescherming bieden tegen een groot aantal antigenen in de omgeving.

B cellen die vanuit het beenmerg migreren naar de bloedbaan hebben nog geen antigeen gezien en worden naïeve B cellen genoemd. Zodra naïeve B cellen hun specifieke antigeen hebben herkend, worden deze geactiveerd en ontwikkelen ze verder. Vervolgens ondergaan naïeve B cellen meerdere celdelingen en genereren hiermee veel dochtercellen die allemaal hetzelfde antigeen kunnen herkennen. Deze dochtercellen brengen kleine veranderingen aan in het DNA dat codeert voor het Ig, waardoor de bindingscapaciteit van het Ig molecuul voor zijn antigeen verandert. B cellen met een sterkere bindingscapaciteit voor hetzelfde antigeen worden positief geselecteerd, waardoor de immuunreactie sterker en specifieker wordt. Dit proces van optimaliseren van de bindingscapaciteit van het Ig molecuul heet somatische hypermutatie (SHM) en gebeurt in een kiemcentrum ('germinal center'). Deze germinal center is een gespecialiseerde structuur in lymfeklieren en andere lymfoïde organen waar B cellen onder andere hulp krijgen van T cellen in hun ontwikkeling. De dochtercellen rijpen vervolgens uit tot plasmacellen, die antistoffen produceren, of langlevende B geheugencellen, die snel kunnen reageren als hetzelfde antigeen nog een keer herkend wordt.

Gezonde mensen zijn immunocompetent. Dit houdt in dat het immuunsysteem adequaat reageert op contact met antigeen en hierdoor immuniteit biedt voor een breed spectrum van antigenen. Voor immunocompetentie is het belangrijk dat er een optimale balans is tussen het vormen van een breed repertoire aan Ig's en het starten van sterke immuunreacties door groepen cellen die specifiek hetzelfde antigeen herkennen. Het onderzoek beschreven in dit proefschrift had tot doel om te bepalen hoe in beenmerg een breed B cel repertoire wordt gevormd, en hoe dit repertoire wordt gespecificeerd in perifere lymfoïde organen na contact met verschillende typen antigenen.

Stimulatie van de interleukine 7 receptor (IL-7R) door IL-7, een signaalmolecuul geproduceerd door omliggende cellen, is cruciaal voor voorloper B cel ontwikkeling in muizen. Aangezien mensen met een defect in de genen die coderen voor onderdelen van de IL-7R, een normaal aantal circulerende B cellen ontwikkelen, is er in de mens altijd aangenomen dat signalering via IL-7/IL-7R niet essentieel is. In **Hoofdstuk II** hebben we

de Ig genherschikkingen bestudeerd in gekweekte humane B cellen met en zonder expressie van IL-7R. IL-7R$^+$ cellen waren meer blastvormig dan IL-7R$^-$ cellen. Daarnaast leek de set genen die IL-7R$^+$ cellen tot expressie brachten sterk op die van twee typen vroege voorloper B cellen: de 'pro-B'-cellen en 'large pre-B'-cellen. De set genen die de IL-7R$^-$ cellen tot expressie brachten daarentegen kwam vooral overeen met de 'small pre-B'-cellen, voorloper B cellen in een later stadium van de ontwikkeling. Hoewel pre-B cellen een functionele IgH herschikking zouden moeten hebben, vonden we maar heel weinig volledige herschikking van de IgH keten in beide kweken. Een interessante bevinding is dat in tegenstelling tot IL-7R$^+$ cellen, de IL-7R- cellen een herschikte lichte keten hadden zonder de aanwezigheid van een functionele zware keten. Dit impliceert dat in de mens, IL-7/IL-7R signalering een onmisbare functie heeft in het onderdrukken van vroegtijdige herschikking van de lichte keten.

Meerdere verschillende B geheugencel populaties zijn geïdentificeerd in humaan bloed, maar het is nog onduidelijk hoe de verschillende fenotypes van deze cellen correleren met het type immuunreacties waar ze door zijn ontstaan. Vooral over het bestaan van germinal center-onafhankelijke B cel populaties bestaat nog veel controversie. In **Hoofdstuk III** presenteren we de resultaten van een gedetailleerde moleculaire en flowcytometrische analyse van 6 B geheugencel populaties, gedefinieerd aan de hand van de expressie van CD27 en de verschillende IgH isotypes (IgM, IgA of IgG). De CD27$^-$IgG$^+$ en CD27$^+$IgM$^+$ cellen hadden evenveel celdelingen doorgemaakt en eenzelfde mate van SHM als cellen in de germinal center, wat suggereert dat ze een germinal center-afhankelijke oorsprong hebben. Daarnaast wijzen een hoog aantal celdelingen en hoge SHM frequentie er op dat een deel van de CD27$^-$IgA$^+$ en CD27$^+$IgG$^+$ populaties meerdere achtereenvolgende germinal center-reacties hebben doorgemaakt. CD27$^-$IgA$^+$ en CD27$^+$IgM$^+$IgD$^+$ 'natural effector' B geheugencellen, daarentegen, hadden minder celdelingen ondergaan dan de germinal center cellen. Verder waren deze twee subsets aanwezig in patiënten die geen germinal centers kunnen vormen door een deficiëntie in het gen voor CD40L, wat suggereert dat deze twee subsets zijn ontstaan in een germinal center-onafhankelijke reactie. Natural effector cellen komen tenminste gedeeltelijk voort uit een systemische T cel onafhankelijke reactie in de marginale zone van de milt. CD27$^-$IgA$^+$ cellen tonen overeenkomsten met darm lamina propria IgA+ B cellen in het lage aantal doorgemaakte celdelingen en verhoogd gebruik van Igλ en het IgA2 isotype. Alle data samen, laat zien dat circulerende B geheugencellen ontstaan in 3 verschillende maturatie routes: (1) primaire en opvolgende germinal center-afhankelijke reacties, (2) systemische en (3) locale germinal center-onafhankelijke reacties. Onze bevindingen bieden nieuwe mogelijkheden om deze processen in immunologische ziektes te bestuderen.

Persistente Polyklonale B cel Lymfocytose (PPBL) is een zeldzame, goedaardige aandoening die wordt gekarakteriseerd door een expansie van CD27$^+$IgM$^+$IgD$^+$ 'natural effector' B cellen. Hoewel het aantal beschreven patiënten groter wordt, is de aard van de aandoening nog slecht begrepen. In **Hoofdstuk IV** demonstreren we dat natural effector cellen in PPBL veel celdelingen hebben ondergaan en een B geheugencel fenotype hebben met een breed Ig repertoire en een lage frequentie aantal SHM. PPBL cellen konden worden onderscheiden van gezonde IgM$^+$ B geheugencellen door middel van een set van celmembraan eiwitten: IgD, CD38, CD73 en CD62L. Ondanks heterogene deregulatie van oncogenen, hadden PPBL cellen van verschillende patiënten een homogeen immuunfenotype, dat niet overeen kwam met monoklonale, rijpe B cel maligniteiten. Deze nieuwe inzichten

kunnen een waardevolle bijdrage leveren in de diagnose van PPBL en de prognostische classificatie van patiënten voor het risico op het ontwikkelen van een lymfoïde maligniteit.

IgA wordt vooral geproduceerd in mucosale weefsels tijdens T cel-afhankelijke en T cel-onafhankelijke antigeen reacties. In **Hoofdstuk V** hebben wij beide typen reacties bestudeerd door CD27+IgA+ T cel-afhankelijke en CD27-IgA+ T cel-onafhankelijke circulerende B geheugencellen te vergelijken met betrekking tot de genen die ze tot expressie brengen en de reactiviteit van hun Ig moleculen. We vonden een vergelijkbaar genexpressie profiel voor beide IgA+, CD27-IgG+ en CD27+IgG+ B geheugencel populaties. Wel toonde de CD27-IgA+ B cel populatie unieke expressie van 'homing' receptoren en transcriptie factoren die wijzen op een mucosale oorsprong. CD27-IgA+ B geheugencellen toonden minder SHM in herschikte Ig genen en toonden verhoogd gebruik van het *IGLV3-1* gen in vergelijking met CD27+IgA+ cellen. Verder waren CD27-IgA+ B cellen verrijkt in polyreactieve antistoffen die met hoge bindingssterkte reageerden op meerdere bacteriestammen. Dit betekent dat T cel-onafhankelijke IgA reacties wel B cel geheugen produceren, maar een unieke reactiviteit tonen met polyreactieve herkenning van bacteriën.

Wereldwijd komen IgE-gemedieerde allergieën steeds vaker voor. Ondanks uitgebreide studies zijn IgE-positieve B cellen nog slecht gekarakteriseerd. In **Hoofdstuk VI** ontwikkelden we een betrouwbare flowcytometrische methode om IgE+ plasmacellen in tonsillen en twee IgE+ B geheugencel subsets in bloed te detecteren en isoleren. Gedetailleerde moleculaire analyses illustreerden een germinal center-afhankelijke oorsprong voor de IgE+ plasmacellen in tonsillen en CD27+IgE+ B geheugencellen in bloed. Het aantal doorgemaakte celdelingen en de mate van SHM in CD27+IgE+ B geheugencellen in gezonden donoren waren hoger dan cellen in de germinal center en vergelijkbaar met B geheugencellen van primaire immuun reacties. CD27-IgE+ B geheugencellen daarentegen, toonden een beperkt aantal celdelingen en beperkte mate van SHM, vergelijkbaar met CD27-IgA+ cellen. Deze observaties, samen met de aanwezigheid van deze CD27-IgE+ cellen in CD40L deficiënte patiënten, suggereert dat ze van locale germinal center-onafhankelijke reacties afkomstig zijn. Verder was het aantal CD27-IgE+ cellen specifiek verhoogd in patiënten met atopisch eczeem. Onze studie heeft meer inzicht gegeven in de ontwikkeling van IgE+ cellen in gezonde personen, biedt nieuwe mogelijkheden om de pathogenese van IgE-gemedieerde ziektes te bestuderen en kan bijdragen aan het nauwkeurig volgen van een anti-IgE behandeling in patiënten met ernstige allergische reacties.

Defecten in het B cel repertoire kunnen resulteren in verzwakte B cel afweer en daardoor leiden tot verschillende immunologische ziektes, waaronder immunodeficiënties, autoimmuniteit, allergie, leukemie en lymfomen. Daarom is begrip in het proces dat betrokken is bij het vormen en optimaliseren van het B cel repertoire essentieel voor het ontrafelen van de mechanismen die ten grondslag liggen aan deze ziektes. De gepresenteerde studies in dit proefschrift geven inzicht in de rol van IL-7/IL-7R signalering in de humane voorloper B cel ontwikkeling en illustreren de complexiteit van humane B geheugencel reacties. We hebben gedemonstreerd dat deze kennis kan worden toegepast op het ontrafelen van lymfoproliferatieve aandoeningen zoals PPBL. Daarnaast kan begrip over de componenten van een immunocompetent repertoire bijdragen aan de identificatie van defecten in immunodeficiënties. Opsplitsen van individuele B cel subsets betrokken bij immunologische ziektes, kan het stellen van de diagnose verbeteren en mogelijk resulteren in nieuwe behandelingmethodes.

ABBREVIATIONS

AD	atopic dermatitis
AID	activation-induced ctidine deaminase
APRIL	a proliferation-inducing ligand
APS	automatic population separator
BAFF	B-cell activating factor
BCMA	B-cell maturation antigen
BCR	B-cell antigen receptor
BER	base-excision repair
BL	Burkitt lymphoma
BM	bone marrow
C	constant
CB	cord blood
CDR	complementarity determining region
CLL	chronic lymphocytic leukemia
CSR	class-switch recombination
D	diversity
DC	dendritic cell
DLBCL	diffuse large B-cell lymphoma
ds	double-stranded
EBF	early B-cell factor
FISH	fluorescence in situ hybridization
FL	follicular lymphoma
FR	framework
GC	germinal center
HCL	hairy cell leukemia
HSC	hematopoietic stem cell
IG	immunoglobulin
IGH	Ig heavy chain
IGK	Ig kappa light chain
IGKREHMA	Igκ restriction enzyme hot-spot mutation assay
IGλ	Ig lambda light chain
J	joining
Kde	kappa-deleting element
KLF	Krüppel-like factor
KREC	kappa-deleting recombintaion excision circle
LP	lamina propria
LPL	lymphoplasmacytoid lymphoma
LPS	lipopolysaccharide
MCL	mantle cell lymphoma
MMR	mismatch repair
MZ	marginal zone
MZL	marginal zone lymphoma

NHEJ	nonhomologous end joining
NLR	nucleotide oligomerization domain-like receptor
N-nucleotide	non-templated nucleotide
PC	principal component
P-nucleotide	palindromic nucleotide
Pol	polymerase
PPBL	persistent polyclonal B-cell lymphocytosis
RAG	recombinase activating gene
RQ-PCR	real-time quantitative PCR
RSS	recombination signal sequence
S	Ig switch region
SCID	severe combined immunodeficiency
SHM	somatic hypermutation
SIT	specific immunotherapy
STAT5	signal transducer and activator of transcription 5
TACI	transmembrane activator and CAML interactor
TCR	T-cell receptor
TD	T-cell dependent
TdT	deoxynucleotidyl transferase
TI	T-cell independent
TLR	Toll-like receptor
TNF	tumor necrosis factor
UNG	uracil-N-glycosylase
V	variable

Acknowledgements

So this is it. After over four years of intensive work the book is almost ready. And as good as it feels to see all of these chapters finally finished and printed, it feels even better to look back and to realize how many great and inspiring people were involved in the individual studies. Therefore, I am happy to have this opportunity to express my gratitude towards all of the people who were an important part of my professional, but also private life over the past years.

I am not sure if good things happen "by accident". But I am sure that it is important to get a chance to make good things happen. I got this chance over six years ago from dr. M. van der Burg, when I first came into a contact with the department of Immunology at the Erasmus MC. Dear Mirjam, thank You for giving me an opportunity to start the research adventure, but, more importantly, thank You for all Your support over the past years.

In the same place I would also like to thank prof. T. Szczepański, with whom I had my first job interview over six years ago, and who is now a member of the PhD committee. Za zdrowe podejście do zmagań naukowych i za wszelkie wsparcie okazane na przestrzeni lat, dziękuję Tomku!

Some acknowledgements are challenging to write because there are simply too many things to be grateful for. The person that I owe the most is dr. Menno van Zelm. Menno, although You had just obtained Your PhD yourself, You took the risk of supervising me and my (originally non-existing) project. Thank You for Your courage, enthusiasm and unlimited scientific curiosity. With these and a lot of hard work on both sides we achieved more than I ever hoped for.

I would also like to express my gratitude to my promoter, prof. J.J.M. van Dongen. Dear Jacques, when I look back at of all the things I have learnt from You at least two seem to stand out: the conviction that "good is the biggest enemy of the best" and the necessity to search for a broader context of all the things. I hope that these will guide me through the rest of my professional life.

I would like to thank all of the colleagues over the past 5 years, especially the current and the former members of the PID and the BCD groups. Dear Barbara, Ingrid and Sandra, thank You for Your positive attitude and willingness to share Your knowledge and skills. Hanna, Diana, Magda, Jorn, Benjamin, Bob and Halima, it was encouraging to see how quickly You gained new skills and grew up into science. Thank You all for Your help, but even more, thank You for Your friendship.

I was lucky to have great fellow PhD students, with whom I could share the ups and downs of the past time. My thoughts especially come back to Nicole, Hanna, Leendert and Kim with whom I worked the longest. Good luck with Your future careers! Hanna and Diana, You were perfect roommates over the last years. Thanks for all the scientific and non-scientific conversations! Thank You also for the nice Dutch summary of this thesis. I am looking forward to see Your books in the near future.

I would also like to express my gratitude to prof. E. Meffre and all the members of the Meffre laboratory in New Haven. Thank You for giving me the opportunity to learn how to generate monoclonal antibodies from single cells from real experts. Dear all, it was not "super-fast and super-easy", but it was absolutely worth it.

I am grateful to the co-authors to all of the studies for smooth and fruitful collaboration, and to Sandra de Bruin - Versteeg for patience with preparing nice and professional figures. It was a pleasure to work with all of You.

Many thanks to the PhD committee members for their time and involvement, and to my paranimphs, Diana and Benjamin, for all Your support over the past years, and during the last days.

Finally, I am grateful to all of the people who made me feel at home in the Netherlands: to all the 'Friends' friends, especially to Ching, Nebojsha, Elsa, Elisa, Diana, and Jackie, and to all the 'non-Fiends' friends: Juan, Maru, Arjan, Dorieke and many others. Thank You for Your presence in my life! Dziękuję też tym znanym od dawien dawna, którzy wpadali z wizytami. Basiu, dzięki za spotkania przy kawie w różnych dziwnych miejscach świata. To…gdzie planujemy kolejne? Mysza, nie wiem, za co mam Ci dziękować w pierwszej kolejności… Więc po prostu podziękuję za to, co najbardziej deficytowe, a czego dostałam od Ciebie dużo w ciągu ostatnich lat: za Twój czas, i za Twoją obecność!

Last but not least, I am grateful that I always had a good reason to come back to Poland. Rodzicom i rodzinie dziękuję za to, że pozwolili mi wyjechać i rozwijać się, ale i za to , że zawsze mnie przyjmowali z otwartymi ramionami w trakcie powrotów.

<div style="text-align: right">

Thank You,
Magda

</div>

About the author

CURRICULUM VITAE

Personal details

Name: Magdalena Agnieszka Berkowska
Place of birth: Jaworzno, Poland
Nationality: Polish
Date of birth: 24-10-1983

Education

2008-2012	PhD studentship at Department of Immunology, Erasmus University Medical Center (Erasmus MC),Rotterdam, the Netherlands
July-Dec. 2011	Research visit at the Department of Immunobiology, Yale University, CT, USA;'What is your gut feeling? Reactivity of local and systemic IgA B-cell memory against commensal and pathogenic bacteria' Scientific supervisor: dr. E.R.F. Meffre
2007-2008	employment as a research technician at the Department of Immunology, Erasmus Medical Center, Rotterdam, the Netherlands
July-Sept. 2006	Internship at the Department of Immunology, Erasmus MC, Rotterdam, the Netherlands,'Composition of junctions formed during V(D)J recombination in bone marrow precursor B-cells with Artemis, NBS and XLF defects' Scientific supervisor: dr. M. van der Burg
2002-2007	Master of Biotechnology, specialization Medical Biotechnology, Jagiellonian University, Cracow, Poland master thesis: 'Percentage changes in monocytes' subpopulations in the course of rheumatoid arthritis and coronary artery disease' Scientific supervisor: prof. J.Pryjma
2005-2007	First two years of medical studies at Jagiellonian University Medical College, Cracow, Poland
1998-2002	Secondary School No.4 in Sosnowiec, Poland

List of publications

Berkowska MA, van der Burg M, van Dongen JJ, van Zelm MC. Checkpoints of B cell differentiation: visualizing Ig-centric processes. Ann N Y Acad Sci. 2011;1246:11-25.

Berkowska MA, Driessen GJ, Bikos V, et al. Human memory B cells originate from three distinct germinal center-dependent and -independent maturation pathways. Blood. 2011;118:2150-2158.

Nodland SE, Berkowska MA, Bajer AA, et al. IL-7R expression and IL-7 signaling confer a distinct phenotype on developing human B-lineage cells. Blood. 2011;118:2116-2127.

van der Burg M, Pac M, Berkowska MA, et al. Loss of juxtaposition of RAG-induced immunoglobulin DNA ends is implicated in the precursor B-cell differentiation defect in NBS patients. Blood. 2010;115:4770-4777.

PhD PORTFOLIO

ERASMUS UNIVERSITEIT ROTTERDAM

Name PhD student: Magdalena Agnieszka Berkowska

Erasmus MC Department: Immunology
Research School: Molecular Medicine
PhD period: August 2008-August 2012
Promoter: Prof. dr. J.J.M. van Dongen
Copromoter: Dr. M.C. van Zelm

PhD training

In-depth courses

2008   Molecular Medicine
2008   Practical Introduction to Laser Scanning Microscopy
2009   Molecular Immunology
2009   Vaccine Symposium
2010   Biomedical English Writing and Communication
2010   High resolution/deconvolution workshop
2010   Euroflow Educational Workshop
2011   Mucosal Immunology Symposium
2012   Regulatory B-cell Symposium
2012   Basic Introduction Course on SPSS

Other

2008-2011   Journal club; Department of Immunology
2008-2012   Seminars and minisymposia; Department of Immunology

Teaching

Supervising practicals
2010-2012   Practicum Immunology
2009   Bachelor thesis supervision
2009-2011   3x Master thesis supervision

National Conferences

2008	Dutch Society for Immunology (NVVI) Annual Meeting; *Poster presentation*
2009	13th Molecular Medicine Day, Rotterdam, The Netherlands; *Poster presentation*
2009	Workgroup Immunodeficiency meeting, Leiden, The Netherlands; *Oral presentation*
2010	14th Molecular Medicine Day, Rotterdam, The Netherlands; *Poster presentation*
2010	Dutch Society for Immunology (NVVI) Annual Meeting; *Poster presentation*
2010	Mini-Symposium 'From Stem Cell to Lymphocyte', Rotterdam, The Netherlands; *Oral presentation*
2011	15th Molecular Medicine Day, Rotterdam, The Netherlands; *Poster presentation*
2012	16th Molecular Medicine Day, Rotterdam, The Netherlands; *Oral presentation*

International Conferences

2009	'B cells in Context' Conference from the Keystone Symposia Series, Taos, NM, USA; *Oral presentation*
2010	European Mucosal Immunology Group Meeting, Amsterdam, The Netherlands; *Poster presentation*
2011	'B Cells: new Insights into Normal versus Dysregulated Function' Conference from the Keystone Symposia Series, Whistler, Canada; *Oral presentation*
2012	15th Biennal Meeting of the European Society for Immunodeficiencies, Florence, Italy; *Poster presentation*

Awards and funds

2011	Fund for conference attendance from the Trust Fund Association Erasmus University Rotterdam
2011	Ter Meulen Fund from the Royal Netherlands Academy of Arts and Sciences (KNAW) for a working visit in the department of Immunobiology, Yale University, USA
2012	Best publication award from the Molecular Medicine Postgraduate School, Erasmus MC, Rotterdam, the Netherlands for the publication 'Human memory B cells originate from three distinct germinal center-dependent and -independent maturation pathways.'